

**Lodz University of Technology**  
**Faculty of Civil Engineering, Architecture and Environmental Engineering**  
**Institute of Environmental Engineering and Building Installations**

**ANNA DOMINIKA BOCHENEK MSC. ENG.**

**THE INFLUENCE OF URBAN FORMS  
AND ADAPTATION STRATEGIES ON MICROCLIMATE  
AND HUMAN THERMAL COMFORT**

The doctoral thesis written under the supervision of :  
**prof. TUL, dr hab. Katarzyna Klemm**  
**PhD Eng. Konrad Witczak**

**Łódź, 2021**

## ACKNOWLEDGEMENTS

*I would like to express my profound gratitude to my supervisor, prof. TUL dr hab.*

*Katarzyna Klemm for all help provided during the preparation of the doctoral dissertation. It was you who inspired me to explore scientific field related to the adaptation of cities to changing climatic conditions.*

*You spent a lot of time discussing emerging research problems, refining the methodology, and consulting the results of the research.*

*You have shown me a lot of patience. When I doubted you gave me hope that I would be able to achieve success.*

*I would like to express my sincere thanks to PhD Eng. Konrad Witczak. Thank you for the fruitful cooperation, which ended with the extension of the dissertation to issues connected with the internal environment. Thanks to you, I have broadened my scientific knowledge, which I hope will be able to be used in further stages of scientific development.*

*Expressions of gratitude to the employees of the Faculty of Civil Engineering, Architecture and Environmental Engineering, in particular the Institute of Environmental Engineering and Building Installations, Lodz University of Technology. You supported me at every step of my scientific activity.*

*I would like to thank my family and friends in particular. It is you who stand by my side every day. It is you who put up with my 'expressive' temperament. When necessary, you bring me to the right level. When necessary you carry me on your shoulders.*

*'The most difficult thing is the decision to act, the rest is merely tenacity. The fears are paper tigers. You can do anything you decide to do. You can act to change and control your life; and the procedure, the process is its own reward.'*

*- Amelia Earhart -*

## SUMMARY

The implementation of adaptation strategies is considered as one of measures for adapting cities to changing climatic conditions. Making appropriate planning decisions, taking into account the specificity of a given area, requires having access to reliable data on the effectiveness of adaptation measures. It is necessary to determine the impact of planned projects on climatic conditions as well as on the thermal comfort of people living in urban spaces. However, the complexity of this issue requires knowledge of architecture and urban planning, construction, environmental engineering and climatology. As a result, it is possible to describe the complex processes occurring in urban areas.

The present dissertation is part of the current research on urban physics. The paper is divided into eleven chapters. The first part is the introduction. It justifies the necessity of undertaking research on the given issue. Research thesis has been defined, which assumes the existence of relation between the form of buildings and the effectiveness of introduced adaptation strategies. It also defines **the main objective of this study, i.e. the evaluation of (1) the influence of characteristic forms of urban development, (2) selected adaptation strategies on microclimatic conditions, as well as human thermal comfort.** The study delimits the geographical research area - the Metropolitan Area of Lodz, which is a key area for the city's identity and of interest to planners and municipal authorities. It defines the research methodology, which involves the use of available archival information sources, digital data resources, and computer-aided tools.

The second chapter is the theoretical foundation of the doctoral dissertation. It describes the characteristic microclimatic conditions prevailing in cities, which are the result of spatial development, i.e. the compact nature of development structure, the large percentage of impermeable surfaces, and the reduction of environmental components. The description addresses potential adaptation strategies to counteract negative climate change that can be implemented in the inner city. It discusses the research on human thermal comfort in the outdoor environment.

The third chapter presents the tool used, from the field of Computational Fluid Dynamics (CFD) to perform numerical simulations. Currently, the ENVI-met is one of the widely used applications for the assessment of complex climatic phenomena occurring in urban areas. It allows to create models that can be used for estimation of climatic conditions in public spaces. Finally, it is possible to determine the thermal comfort prevailing in the outdoor environment.

The fourth chapter is a description of the author's method of determining typical development structures in the Metropolitan Area of Lodz. The analyses were based on archival data resources (from the National Archive, the City Conservation Officer, and the Regional Conservation Officer) and information from digital databases of public institutions (Lodz Geodesy Centre). The information was processed using Geographic Information System tools. As a result, geometric models of typical development forms in the Metropolitan Area were created.

The fifth chapter covers the climatic conditions in the city of Lodz. The analyses were carried out for the basic parameters prevailing during a Typical Meteorological Year. Taking into account the fact that the information is obtained from the suburban zone - Lodz-Lublinek station, the author's approach has been proposed based on combining the conditions of the suburban and inner city zones. As a result, it was possible to calculate the air flow velocity in the city center. Data were used in numerical simulation processes.

The main part of this dissertation, related to numerical simulations, is the analysis of microclimatic conditions and thermal comfort. The sixth chapter discusses scenarios related to the influence of development forms of the Metropolitan Area on microclimatic conditions and external thermal comfort. The seventh chapter investigates the effectiveness of selected adaptation strategies, involving the introduction of green roofs, walls, tree rows, and water elements, in relation to the thermal conditions prevailing in the areas of typical forms of the Metropolitan Area of Lodz. An extensive discussion is also presented, including the research results, in relation to the effectiveness of adaptation strategies implemented in cities. The eighth chapter presents the potential impact of green solutions on the thermal conditions inside buildings located in the Metropolitan Area of Lodz.

The ninth chapter presents a comparison of obtained results with the literature studies conducted. The description concerns both studies on the influence of development form on the external microclimate conditions and the effectiveness of adaptation strategies in relation to the internal thermal conditions. It is concluded with recommendation cards that refer to selected solutions that can potentially be implemented in the Metropolitan Area of Lodz.

The last part is a summary of conducted research. It confirms the research thesis that there is a relationship between the development structure and the effectiveness of adaptation strategies in cities. It presents conclusions of a general nature as well as discusses further directions of research.

# TABLE OF CONTENTS

## SUMMARY

<b>CHAPTER I. INTRODUCTION</b> .....	<b>- 1 -</b>
1.1. Necessity of present study .....	- 1 -
1.2. Aims and objectives .....	- 3 -
1.3. Methodology .....	- 4 -
1.4. Structure of the thesis .....	- 5 -
<b>CHAPTER II. LITERATURE REVIEW</b> .....	<b>- 7 -</b>
2.1. Characteristic features of urban climate .....	- 7 -
2.2. Climate change adaptation strategies in urban environment.....	- 13 -
2.3. Outdoor thermal comfort.....	- 19 -
2.3.1. Heat exchange between a human body and the outdoor environment .....	- 20 -
2.3.2. Thermal comfort indices.....	- 23 -
<b>CHAPTER III. THE NUMERICAL MODEL</b> .....	<b>- 34 -</b>
3.1. Numerical modelling of an urban microclimate.....	- 34 -
3.2. The general structure of ENVI-met application .....	- 35 -
3.3. Boundary conditions.....	- 38 -
3.4. Governing equations of the atmospheric model.....	- 39 -
3.5. The human-biometeorological dimension.....	- 50 -
3.6. Model validation.....	- 50 -
<b>CHAPTER IV. SELECTION OF URBAN FORMS</b> .....	<b>- 54 -</b>
4.1. Street canyon .....	- 54 -
4.2. Forecourt .....	- 61 -
<b>CHAPTER V. CITY'S MICROCLIMATIC CONDITIONS</b> .....	<b>- 66 -</b>

<b>CHAPTER VI. NUMERICAL SIMULATION OF MICROCLIMATIC AND THERMAL CONDITIONS.....</b>	<b>- 76 -</b>
6.1. Canyons .....	- 78 -
6.2. Forecourts .....	- 86 -
<b>CHAPTER VII. INFLUENCE OF ADAPTATION STRATEGIES ON EXTERNAL ENVIRONMENT .....</b>	<b>- 93 -</b>
7.1. The role of greenery .....	- 93 -
7.2. The impact of blue infrastructure .....	- 117 -
7.3. The effectiveness of climate change adaptation strategies within the context of analyzed urban form .....	- 129 -
<b>CHAPTER VIII. INDOOR THERMAL CONDITIONS.....</b>	<b>- 145 -</b>
<b>CHAPTER IX. DISCUSSION .....</b>	<b>- 157 -</b>
9.1. The influence of urban form on microclimatic conditions and outdoor thermal comfort.....	- 157 -
9.2. The influence of external environment on indoor thermal comfort .....	- 163 -
9.3. Recommendation for planners.....	- 166 -
<b>CHAPTER X. CONCLUSIONS AND RECOMMENDATIONS.....</b>	<b>- 157 -</b>
10.1. Conclusions.....	- 157 -
10.2. Recommendations for future research.....	- 163 -
Literature .....	- 174 -
List of figure captions.....	- 200 -
List of table captions .....	- 206 -
Appendixes .....	- 208 -

## Symbols

$a_{bldg}$	building footprint	[m <sup>2</sup> ]
$a_f$	albedo of leaf surface	
$a_g$	shortwave albedo of the ground	
$a_s$	albedo of ground surface	
$a_{site}$	reference area	[m <sup>2</sup> ]
$\bar{a}$	averaged albedo for walls and ground surfaces in the model area	
$A$	the coefficient dependent on the airflow velocity	
$A_{Du}$	DuBois area	[m <sup>2</sup> ]
Af	Tropical rainforest climate (Köppen climate classification)	
Am	Tropical monsoon climate (Köppen climate classification)	
Aw	Tropical wet and dry climate (Köppen climate classification)	
BSh	Hot semi-arid climate (Köppen climate classification)	
BSk	Cold semi-arid climate (Köppen climate classification)	
BWh	Hot desert climate (Köppen climate classification)	
$c_{df}$	drag coefficient at the plant foliage (= 0.2)	
$c_p$	specific heat of air at constant pressure (= 1847)	[Jkg <sup>-1</sup> K <sup>-1</sup> ]
$c_1, c_2, c_3$	standard values for calibrating $\varepsilon$ -equation, available from lit.	
$c_\mu, \sigma_E, \sigma_\varepsilon$	constants for the turbulence model: $c_\mu = 0.09, \sigma_E = 1, \sigma_\varepsilon = 1.3$	
$C$	convective heat flow	[W]
$C_f$	bulk heat transfer coefficient	

$C_{fa}$	Humid subtropical climate (Köppen climate classification)	
$C_{fb}$	Temperate oceanic climate (Köppen climate classification)	
$C_h^g$	sensible heat flux bulk transfer coefficient at ground layer	
$C_{sa}$	Hot-summer Mediterranean climate (Köppen climate classification)	
$C_h^s$	bulk coefficient	
$C_{wa}$	Monsoon-influenced humid subtropical climate (Köppen climate classification)	
$D$	leaf diameter	[m]
$D_t$	total short-wave diffuse radiation flux absorbed by a human body	[Wm <sup>-2</sup> ]
$D_\eta$	hydraulic diffusivity	
$E$	turbulent kinetic energy	[m <sup>2</sup> s <sup>-2</sup> ]
$E_D$	latent heat flow to evaporate water into water vapour diffusing through the skin	[W]
$E_{RE}$	sum of heat flows for heating and humidifying the inspired air	
$E_{SW}$	heat flow due to evaporation of sweat	
$E_t$	total long-wave radiation flux absorbed by a human body	[Wm <sup>-2</sup> ]
$f$	Coriolis Parameter (= 10 <sup>-4</sup> )	[s <sup>-1</sup> ]
$f_{cl}$	ratio of the surface area of the clothed body to the surface area of the nude body	
$f_p$	surface projection factor	
$f_w$	fraction of wet leaves	



$F$	extinction coefficient	
$F(p, y, m, i)$	cumulative distribution function of the daily meteorological means within each calendar month	
$F_s(p, y, m)$	Finkelstein-Schafer statistics	
$g$	acceleration due to gravity (= 9.81)	$[\text{ms}^{-2}]$
$G$	coefficient of mean temperature of ambient radiation in heat perception	
$G_0$	substrate heat ( $0$ : ground)	$[\text{Wm}^{-2}]$
$h_{avg}$	average building height	$[\text{m}]$
$h_{bldg}$	average building height in a reference area	$[\text{m}]$
$h_c$	heat convection coefficient	$[\text{Wm}^{-2}\text{K}^{-1}]$
$h_1, h_2$	height of view obscuration by building constructions at the selected point	$[\text{m}]$
$H_f$	heat sensible flux	$[\text{Wm}^{-2}]$
$H_g$	ground sensible heat flux	$[\text{Wm}^{-2}]$
$H_{max}$	the maximum height	$[\text{m}]$
$H_{o,w,r}$	turbulent sensible heat (for ground $o$ , wall $w$ or roof $r$ surface)	$[\text{Wm}^{-2}]$
$I_{ir}$	total infrared irradiance	$[\text{Wm}^{-2}]$
$I_s$	total solar irradiance	$[\text{Wm}^{-2}]$
$I_t$	total short-wave direct irradiance absorbed by a human body	$[\text{Wm}^{-2}]$
$J_{f, evap}$	evaporative heat flux between plant and surroundings	$[\text{Wm}^{-2}]$
$J_{f,h}$	direct heat flux between plant and surroundings	$[\text{Wm}^{-2}]$
$J_{f,trans}$	transpiration heat flux between plant and surroundings	$[\text{Wm}^{-2}]$
$J_i$	the rank of $i$ -th daily meteorological mean values within a given month and year	

$k$	heat transmission coefficient	$[\text{Wm}^{-2}\text{K}^{-1}]$
$K$	von Kármán constant (0.4)	
$K$	ground thermal conductivity	
$K_E, K_\epsilon$	diffusion coefficients for local turbulence (production & dissipation)	$[\text{m}^2\text{s}^{-1}]$
$K_h^{(0,w)}$	exchange coefficient for heat at ground $\theta$ or wall surface $w$	$[\text{m}^2\text{s}^{-1}]$
$K_i$	the rank of i-th daily mean meteorological value for the calendar month in the entire dataset	
$K_m^{(0,w)}$	exchange coefficient for momentum at ground $\theta$ or wall surface $w$	$[\text{m}^2\text{s}^{-1}]$
$K_q^{(0,w)}$	exchange coefficient for vapour at ground $\theta$ or wall surface $w$	$[\text{m}^2\text{s}^{-1}]$
$K_s$	thermal diffusivity	$[\text{m}^2\text{s}^{-1}]$
$l_f$	latent heat of vaporization at ground temperature	$[\text{Jkg}^{-1}]$
$L$	latent heat of vaporization	$[\text{Jkg}^{-1}]$
$L_f$	foliage latent heat flux	$[\text{Wm}^{-2}]$
$L_g$	ground latent heat flux	$[\text{Wm}^{-2}]$
$LAD$	Leaf Area Density	$[\text{m}^2\text{m}^{-3}]$
$LAI$	Leaf Area Index	$[\text{m}^3\text{m}^{-3}]$
$m_{trans}$	total transpiration in plant element	
$M$	metabolic rate	$[\text{Wm}^{-2}]$
$n$	number of measurements	
$Offset$	deviation of air temperature	
$p_a$	water vapour pressure	$[\text{Pa}]$
$\bar{p}$	daily mean value of meteorological parameter	
$p'$	local pressure perturbation	$[\text{Pa}]$

$P_{bldg}$	building perimeter	[m]
$Pr$	production of turbulence energy due to wind shearing	
$q$	specific humidity ( $q_0$ at the surface)	[Kgkg <sup>-1</sup> ]
$q_{af}$	mixing ratio for air within foliage canopy	
$q_{f,sat}$	saturation mixing ratio at foliage temperature	
$q_g$	mixing ratio at ground temperature	
$\Delta q$	leaf-to-air humidity deficit	[Kgkg <sup>-1</sup> ]
$Q_E$	latent heat flux density	[Wm <sup>-2</sup> ]
$Q_E$	additional turbulence produced by vegetation	[s <sup>-1</sup> ]
$Q_h$	sink/source terms due to heat	[ms <sup>-2</sup> ]
$Q_q$	sink/source terms due to vapour	[ms <sup>-2</sup> ]
$Q_{(wr)}$	heat flux through wall or roof	[Wm <sup>-2</sup> ]
$Q_c$	additional turbulence dissipated by vegetation	[s <sup>-1</sup> ]
$r_a$	aerodynamic resistance of the leaf	[sm <sup>-1</sup> ]
$r_s$	stomatal resistance at leaf surface	[sm <sup>-1</sup> ]
$r''$	surface wetness factor	
$R$	net radiation of the body	
$R_{lw}^{\downarrow(0)}$	atmospheric long-wave radiation flux density ( $\theta$ : at model boundary)	[Wm <sup>-2</sup> ]
$R_{lw}^{\uparrow}$	long-wave radiation flux density from ground	[Wm <sup>-2</sup> ]
$R_{lw}^{\leftrightarrow}$	long-wave radiation flux density from walls	[Wm <sup>-2</sup> ]
$R_{lw,net}^{(s,us)}$	net long-wave radiation (fraction shielded/unshielded by buildings)	[Wm <sup>-2</sup> ]
$R_{n,lw}$	divergence of long-wave radiation flux density	[Wm <sup>-2</sup> ]
$R_{sw,dif}^0$	diffuse short-wave radiation flux density ( $\theta$ : at model boundary)	[Wm <sup>-2</sup> ]

$R_{sw,dir}^0$	direct short-wave radiation flux density ( $\theta$ : at model boundary)	[Wm <sup>-2</sup> ]
$R_{sw,net}$	net short-wave radiation density	[Wm <sup>-2</sup> ]
$RAD$	Root Area Density	[m <sup>2</sup> m <sup>-3</sup> ]
$S$	storage heat flows for heating or cooling the body mass	
$S_u, S_v, S_z$	sink/source terms due to wind drag	[ms <sup>-2</sup> ]
$SVF$	Sky View Factor	
$S_{\eta,0}$	sink term connected with the surface evaporation	
$t$	time	[s]
$t_a, T_a$	air temperature	[°C]
$t_{cl}$	clothed surface temperature	[°C]
$t_{mrt}$	mean radiant temperature	[K or °C]
$t_{rf}$	transmission factor (= 0.3)	
$T$	absolute temperature	[K]
$T_a$	air temperature	[K or °C]
$T_{af}$	air temperature within the canopy	[°C]
$T_{ag}$	air temperature within the canopy	[K]
$T_{a,i}$	air temperature inside the buildings	[K]
$T_{f(+,-)}$	leaf temperature (+ overlying side, - underlying side of the leaf)	[K]
$Th$	dissipation of turbulence energy due thermal stratification	
$T_o$	ground surface temperature	[K or °C]
$T_w$	wall temperature	[K]
$u, v, w$	wind speed in the x, y, and z directions	[ms <sup>-1</sup> ]
$u_i, x_i$	i.e. $u, v, w$ and to x, y, z with $i = 1, 2, 3$ (Einstein summation)	

$u_*$	frictional velocity	[ms <sup>-1</sup> ]
$U$	heat transfer coefficient	[Wm <sup>-2</sup> K <sup>-1</sup> ]
$\bar{U}_{(z)}$	average wind speed at 10 m height	[ms <sup>-1</sup> ]
$v_a$	wind speed	[ms <sup>-1</sup> ]
$VH$	side wall area of buildings	[m <sup>2</sup> ]
$w_1, w_2$	distances of vertical obscuring planes from the selected point	[m]
$W$	physical work output	
$W$	mean wind speed at height $z$ ( $w = u^2 + v^2 + w^2$ ) <sup>0.5</sup>	[ms <sup>-1</sup> ]
$W_{af}$	wind speed within the canopy	[ms <sup>-1</sup> ]
$W_{dew}$	dew on leaf surfaces	[kgm <sup>-2</sup> ]
$x, y, z$	cartesian coordinates	[m]
$\Delta x, \Delta y, \Delta z$	grid resolution of the model in the 3 directions	[m]
$X, Y, Z$	horizontal and vertical dimensions of the core model	[m]
$y_i$	reference value	
$\hat{y}_i$	simulation output value	
$z_d$	displacement of the zero plane	[m]
$z_p$	vegetation height	[m]
$z_r$	root depth	[m]
$z_0$	roughness coefficient	[m]
$(z - z_d)$	effective height	[m]
$\alpha$	constant (0.8)	
$\alpha_f$	shortwave albedo of the foliage layer	
$\alpha_k$	body absorption coefficient for short-wave radiation ( $\approx 0.7$ )	
$\beta$	angle of incident direct beam/normal to surface	°

$\eta$	volumetric soil water content in the first soil layer ( $\eta_{fc}$ - at field capacity)	$[\text{m}^3\text{m}^{-3}]$
$\eta$	external mechanical efficiency heat exchange (usually is set to zero)	
$\theta$	potential temperature	[K]
$\theta_c$	optimal operative temperature	[°C]
$\theta_{ed-1}$	the daily mean external temperature for the previous day	[°C]
$\theta_{ref}$	average temperature over all grids at height z	[K]
$\theta_{rm}$	running mean temperature for today	[°C]
$\sigma_B$	Stefan-Boltzmann constant ( $= 5.664 \cdot 10^{-8}$ )	$[\text{Wm}^{-2}\text{K}^{-4}]$
$\sigma_f$	foliage fraction coverage	
$\sigma_{lw}^{\downarrow}$	modification factor for downwards long-wave radiation	
$\sigma_{lw}^{\uparrow}$	modification factor for upwards long-wave radiation	
$\sigma_{svf}$	Sky View Factor	
$\sigma_{sw,dif}$	modification factor for diffuse short-wave radiation	
$\sigma_{sw,dir}$	modification factor for direct short-wave radiation	
$\varepsilon$	dissipation of turbulence	
$\varepsilon_f$	emissivity of foliage	
$\varepsilon_p$	emissivity of the human body ( $\approx 0.97$ )	
$\varepsilon_s, \varepsilon_w$	emissivity of ground and wall surface	
$\rho$	air density ( $\rho_0 = 1.29$ )	$[\text{kgm}^{-3}]$
$\rho_{af}$	density of air at foliage temperature	$[\text{kgm}^{-3}]$
$\rho_{ag}$	density of air near the soil surface	$[\text{kgm}^{-3}]$
$\rho_{urb}$	site coverage ratio	
$\rho_w$	water density	$[\text{kgm}^{-3}]$

$\delta c$	factor depending on evaporation and transpiration probability	
$\lambda_s$	heat conductivity	[Wm <sup>-1</sup> K <sup>-1</sup> ]
$\varphi$	sun position	°
$\varphi(p, m, i)$	cumulative distribution function of the daily meteorological means over all years in the data set	
$\omega$	vertical angle of an obstacle	°
$\pi$	azimuth angle	°

### Acronyms

1D	one-dimensional domain
2D	two-dimensional domain
3D	three-dimensional domain
ADI	Alternating Directions Implicit Method
AR	Aspect Ratio
ASHRAE	American Society of Heating, Refrigeration and Air Conditioning Engineers
ASV	Air Temperature Sensation Vote
CFD	Computational Fluid Dynamics
CSV	Cloud Cover Sensation Vote
EPA	Environmental Protection Agency
EPS	Expandable Polystyrene
ET	Effective Temperature
EU	European Union
FASST	the Fast All Season Soil Strength Model
GIS	Geographic Information System
HSV	Humid Sensation Vote
InterSIT	Internet Terrain Information System for Lodz

IMiGW	Institute of Meteorology and Water Management of the National Research Institute
LAD	Leaf Angle Distribution
LAI	Leaf Area Index
MAPE	Mean Absolute Percentage Error
MEMI	Munich Energy-Balance Model for individuals
PBL	Planetary Boundary Layer
PDD	Predicted Percentage Dissatisfied
PET	Physiological Equivalent Temperature
PMV	Predicted Mean Vote
RAD	Root Area Density
REALCOOL	Really Cooling Water Bodies in Cities
RL	Friction Layer
RMSE	Root Mean Square Error
SET	Standard Effective Temperature
SL	Surface Layer
SSV	Sun Sensation Vote
SVF	Sky View Factor
TMY	Typical Meteorological Year
T <sub>op</sub>	Operative Temperature
TSV	Thermal Sensation Vote
UBL	Urban Boundary Layer
UCL	Urban Canopy Layer
UHI	Urban Heat Island
UTCI	Universal Thermal Climate Index
WSV	Wind Sensation Vote



### **Abbreviations connected with numerical simulations**

E-WA - the measurement point above the street in the east-west oriented canyon

E-WN - the northern measurement point in the east-west oriented urban form

E-WN-T - the northern measurement point nearby the tree in the east-west oriented urban form

E-WS - the southern measurement point in the east-west oriented urban form

E-WS-T - the southern measurement point nearby the tree in the east-west oriented urban form

N-SA - the measurement point above the street in the north-south oriented canyon

N-SE - the eastern measurement point in the north-south oriented urban form

N-SE-T - the eastern measurement point nearby the tree in the north-south oriented urban form

N-SW - the western measurement point in the north-south oriented urban form

N-SW-T - the western measurement point nearby the tree in the north-south oriented urban form

### Chapter VI.

HF - High Forecourt - the scenario connected with the highest building structure of the forecourt (21m)

HR - High Ratio - the scenario connected with the highest building structure in the canyon (21m)

LF - Low Forecourt - the scenario connected with the lowest building structure of the forecourt (7m)

LR - Low Ratio - the scenario connected with the lowest building structure in the canyon (7m)

MF - Mean Forecourt - the scenario connected with the typical building structure of the forecourt (14m)

MR - Mean Ratio - the scenario connected with the typical building structure in the canyon (14m)

## Chapter VII.

BC - Base Case - the reference scenario for the canyon

BP - Bioretention Planters - the scenario connected with an addition of four bioretention planters in the canyon (128 m<sup>2</sup>)

BP2 - Bioretention Planters 2 - the scenario connected with an addition of twelve bioretention planters in the canyon (384 m<sup>2</sup>)

FGR - Forecourt Green Roof - the scenario connected with an addition of green roof in the forecourt (25%)

FGR2 - Forecourt Green Roof 2 - the scenario connected with an addition of green roof in the forecourt (51%)

FGR3 - Forecourt Green Roof 3 - the scenario connected with an addition of green roof in the forecourt (100%)

FW - Forecourt Green Wall - the scenario connected with an addition of green wall in the forecourt (26%)

FW2 - Forecourt Green Wall 2 - the scenario connected with an addition of green wall in the forecourt (51%)

FW3 - Forecourt Green Wall 3 - the scenario connected with an addition of green wall in the forecourt (100%)

GR - Green Roof - the scenario connected with an addition of green roof in the canyon (43%)

GR2 - Green Roof 2 - the scenario connected with an addition of green roof in the canyon (57%)

GR3 - Green Roof 3 - the scenario connected with an addition of green roof in the canyon (100%)

T - Tree Case - the scenario connected with an addition of trees in the canyon (6%)

T2 - Tree Case 2 - the scenario connected with an addition of trees in the canyon (10%)

T3 - Tree Case 3 - the scenario connected with an addition of trees in the canyon (19%)

W - Green Wall - the scenario connected with an addition of green wall in the canyon (47%)

W2 - Green Wall 2 - the scenario connected with an addition of green wall in the canyon (60%)

W3 - Green Wall 3 - the scenario connected with an addition of green wall in the canyon (100%)

WR - Water Reservoir - the scenario connected with an addition of water reservoir in the forecourt (42m<sup>2</sup>)

WR2 - Water Reservoir 2 - the scenario connected with an addition of water reservoir in the forecourt (84m<sup>2</sup>)

#### Chapter VIII.

LF - Last Floor - the scenario for rooms located at the height of the last floor in the Metropolitan Area of Lodz

LZ - Living Zone - the scenario for rooms located at the residential level in the Metropolitan Area of Lodz

GR - Green Roof - the scenario connected with an addition of green roof on the building

GW - Green Wall - the scenario connected with an addition of green wall on the building

RTR2021 - Roof Technical Requirements 2021 - the scenario, to meet technical requirements, connected with an addition of insulation layer on the building

RTR2021/GR - Roof Technical Requirements 2021/Green Roof - the scenario connected with an addition of the insulation layer and the extensive green roof on the building

WTR2021 - Wall Technical Requirements 2021 - the scenario, to meet technical requirements, connected with an addition of insulation layer on the building

WTR2021/GW - Wall Technical Requirements 2021/Green Wall - the scenario connected with an addition of the insulation layer and the living façade on the building

**THE INFLUENCE OF URBAN FORMS  
AND ADAPTATION STRATEGIES ON MICROCLIMATE  
AND HUMAN THERMAL COMFORT**

PhD Thesis

## CHAPTER I. INTRODUCTION

### 1.1. Necessity of present study

Currently, more than half of the world's population lives in highly urbanized areas. Within Europe, this percentage, which is one of the highest in the world, is 77%. It is expected to increase to 85% by 2100 ([The United Nations Population Division, 2018](#)). There is no doubt that cities have become 'hotspots' characterized by specific climatic conditions. Their modification is caused by (1) transformations of building layouts, including the creation of large impervious surfaces, (2) reduction of green areas, which are responsible for regulating water management, (3) emission of waste heat or heat lost in technological processes and energy devices as well as heat used for heating buildings, (4) and also intensive emission of pollutants into the atmosphere. In the light of progressing global changes, climate modification on a local scale will intensify the negative phenomena that occur in highly urbanized areas. These include the Urban Heat Island phenomenon, heat waves, heavy rainfall and hailstorms, local flooding, strong winds, and the formation of superstorm cells. They constitute a serious problem from the point of view of human comfort and health, especially in relation to disadvantaged groups (elderly and sick people)([Goggins et al., 2012](#), [Kováts & Hajat, 2008](#), [Arsenović et al., 2019](#)). Due to global warming, it is very likely that the frequency and intensity of these climate phenomena will increase in the future ([Kotharkar et al., 2018](#), [Elghonaimy & Mohammed, 2019](#), [Ramírez-Aguilar et al., 2019](#), [Geletič et al., 2020](#), [Martilli et al., 2020](#), [Veena et al., 2020](#)).

Adaptation and adjustment of urban areas to climate change can be ensured through the implementation of adaptation strategies. In 2008, the Environmental Protection Agency (EPA) published a set of mitigation actions. Among the proposed solutions, special emphasis was placed on the implementation of blue-green infrastructure elements, which are possible to introduce in the strict city centers, in particular vegetation in the form of horizontal (green roofs), as well as vertical (living facades, tall greenery in the form of trees)([EPA, 2008](#)).

Many cities have already started to implement adaptation strategies to improve the urban thermal environment and pedestrian thermal comfort. These include changing the geometry of buildings, reducing impervious surfaces, introducing specialized building materials that allow rainwater to be stored and even infiltrate and soak into the ground, and using blue-

green infrastructure. These actions are extremely important because anthropogenic changes are constantly progressing in urban areas. This also applies to the strict city centers, where as a result of pressure from developers, the whole complexes of multi-storey buildings are implemented. This leads, among others, to strong transformations of the climate conditions and disturbances of the surface infiltration properties. However, the transformations of urban layouts oriented towards the improvement of climatic conditions can translate into a higher quality of life for people in cities.

In order to meet the needs of cities in adapting to changing climatic conditions, an attempt has been made to develop a method for assessing the effectiveness of selected solutions with respect to the external as well as internal environment.

Literature studies indicate that the effectiveness of individual strategies varies greatly. This is due to both the characteristics of buildings for each city, geographical location, climate zone, as well as the level of economic development affecting, among others, the technical infrastructure of the city. In case of thermal comfort perceived by the users of urban space, the situation is even more complex. Thermal sensations depend on physical parameters of people, the type of performed activity, the duration of exposure, as well as the ability to adapt to conditions in the external environment.

Therefore, the implementation of one specific scheme is impossible. In order to fully assess the effectiveness of adaptive solutions, it is necessary to know in detail the conditions of individual locations.

The present study was limited to the city of Lodz, which is the fourth largest and third most populated city in Poland. The research covered the Metropolitan Area of Lodz, which has become a point of interest for planners and municipal authorities. The area is inhabited by more than one fifth of the population. It was considered to be the most degraded space in the city. It is a priority area in terms of transformations. In accordance with the provisions of the 2026+ Metropolitan Revitalization Programme for Lodz, planning measures are to contribute to 'the revitalization of the residential area' by transforming buildings along with their functionally connected surroundings. With regard to the revitalized space, it is also postulated that the technical standard of buildings will be improved. Activities will include, among others, thermo-modernization of buildings, improvement of energy efficiency, and introduction of power supply from renewable sources. It is extremely important because the city's core is constituted by historic 19th century buildings. The compact, dense structure is the cause of Urban Heat Island in Lodz. As shown by Kłysik research (1998), the intensity of this phenomenon is enormous, especially in the period of unfavorable weather conditions.

Therefore, an increasing attention is being paid to the implementation of adaptation measures which will allow to limit this unfavorable phenomenon and improve the inhabitants' quality of life.

## 1.2. Aims and objectives

This study can be considered as a 'bridge' between the research sphere dealing with complex physical phenomena occurring in highly urbanized areas, and the practical activity allowing the translation of previous achievements into guidelines for professionals involved in the design of urban structures.

The formulated **research thesis** assumes the existence of a relationship between the form of development and the effectiveness of the introduced adaptation strategies. Therefore, **the main aim** of this study was to evaluate (1) **the influence of characteristic urban forms**, (2) **selected adaptation strategies on the microclimatic conditions, as well as on the thermal comfort of humans**. The work includes cognitive, methodological and application aspects.

**The cognitive aim** is to determine the typical building structures of the Metropolitan Area of Lodz and to assess the meteorological conditions in the city center of Lodz.

**The methodological goal** is an attempt to develop a research procedure aimed at assessing the effectiveness of the application of adaptation strategies in specific, characteristic building layouts.

**The application objective** includes the development of recommendation cards, i.e. planning guidelines, referring to the indication of the most effective adaptation solutions that can be implemented within the characteristic forms of the Metropolitan Area of Lodz.

In order to achieve the above assumptions, **objectives** were formulated:

- characterization of typical forms in the Metropolitan Area of Lodz using computer techniques (Geographic Information Systems),
- development of an updated database of meteorological conditions for Metropolitan Area of Lodz (Typical Meteorological Year),
- assessment of microclimatic conditions in the areas of typical forms of the Metropolitan Area of Lodz using numerical methods (ENVI-met application),
- assessment of the impact of adaptation strategies, connected with the introduction of blue-green elements, on the microclimatic conditions, as well as the human thermal comfort in the external environment of Lodz,

- determination of the impact of adaptation strategies on the thermal comfort prevailing inside the buildings of the Metropolitan Area of Lodz.

### **1.3. Methodology**

In recent years, there has been a growing interest in the issues of shaping microclimate and thermal comfort within urban spaces. Usually the studies are conducted in the inner-city areas, where the land use has a great influence on the prevailing environmental conditions. However, the results are often incomparable. The reasons for this can be found in the varied geographical location (climate zone), external environmental conditions (year seasons), study areas (selected public spaces), survey method (measurement campaigns, computer simulations), statistical indicators, and the form of result presentation.

In the field of urban climatology, the most commonly used method is field research, referred to as measurement campaigns, during which meteorological parameters are measured, including air temperature, radiation temperature, relative humidity, wind direction and speed at a height of 10m above the ground level. They are extremely tedious studies, which should be conducted on an hourly basis. They are associated with numerous organizational problems involving the proper selection of measuring equipment, as well as the research supervision. In the era of computer technology development, numerical simulations become an alternative. They allow to carry out analyses taking into account complex physical processes occurring in external environment in a relatively short time. One application that is considered to be the most widely used in the field of urban climatology is ENVI-met. The program in the field of computational fluid dynamics (CFD) requires entering information on basic meteorological parameters only. On their basis, a comprehensive analysis of microclimatic conditions is carried out taking into account the complex ground-plant-air relationships occurring in urbanized environments. The program enables also to assess the thermal comfort of humans residing in urban spaces. The ENVI-met environment can be integrated with software for calculation of energy efficiency of buildings. This allows to estimate the impact of external weather conditions on the thermal comfort inside residential buildings.

In this study, the author's concept, which is a multi-track approach to the assessment of microclimatic conditions prevailing in the outdoor environment, has been applied. First, analyses were carried out to determine the parameters of urban layout of the Lodz Metropolitan Area. The research was necessary due to the specific character of this area (19th century historical building structure). Detailed information was obtained from state



institutions, i.e. the City Conservator of Monuments, the Regional Conservator of Monuments, and the Municipal Surveying Centre. Computer methods using Geographic Information System (GIS) were applied. This comprehensive approach allowed for the selection of characteristic building forms occurring in the Metropolitan Area of Lodz - the street canyon and the urban forecourt.

The next step was to assess the influence of selected adaptation strategies on the microclimate in the areas of characteristic forms of development. The implementation of blue-green infrastructure that could be applied in the area of the Metropolitan Area of Lodz was considered. The analyzes were carried out using the ENVI-met tool. Simulation studies were also carried out with regard to the thermal comfort of people residing within the previously determined characteristic building forms.

Then, studies were carried out on the impact of selected adaptation strategies on thermal conditions in residential buildings located in the Metropolitan Area of Lodz. The analysis of the effectiveness of the adopted solutions, such as green roofs and green walls, was carried out using the DesignBuilder program. The implementation of selected strategies with regard to existing and modernized buildings was considered.

The author's research results were used to create recommendation sheets, which are planning guidelines for characteristic forms occurring in the Metropolitan Area of Lodz. They were prepared for each case, i.e. (1) east-west oriented canyons, (2) north-south oriented canyons, (3) east-west oriented urban forecourts, and (4) north-south oriented forecourts.

#### **1.4. Structure of the thesis**

The paper, which is divided into eleven chapters, contains information on the previous research achievements in the field of urban climatology, as well as the author's own research results for characteristic urban forms of the Metropolitan Area of Lodz. The individual chapters of this paper focus on the following issues:

- **Chapter II** - specificity of the climate of highly urbanized areas, adaptation strategies possible to implement in inner-city areas, and thermal sensations experienced by humans in the external environment.
- **Chapter III** - methods of climatic studies using numerical simulations of computer fluid dynamics (CFD).
- **Chapter IV** - determination of characteristic urban forms occurring in the Metropolitan Area of Lodz (street canyons, and urban forecourts).

- **Chapter V** - the creation of the Typical Meteorological Year in accordance with [ISO 15927-4:2005 - Hygrothermal performance of buildings - Calculation and presentation of climatic data - Part 4: Hourly data for assessing the annual energy use for heating and cooling \(2005\)](#).
- **Chapter VI** - evaluation of the influence of building form on microclimatic conditions, as well as thermal comfort of humans living in an outdoor environment.
- **Chapter VII** - assessment of the impact of selected adaptation strategies consisting in the implementation of blue-green infrastructure elements in the areas of characteristic urban forms of the Metropolitan Area of Lodz.
- **Chapter VIII** - analysis of the impact of chosen adaptation strategies on human thermal comfort inside the buildings.
- **Chapter IX** - determination of planning guidelines for each case study of (1) east-west oriented canyons, (2) north-south oriented canyons, (3) east-west oriented urban forecourts, and (4) north-south oriented urban forecourts.
- **Chapter X** - conclusions and further research directions.

## CHAPTER II. LITERATURE REVIEW

### 2.1. Characteristic features of urban climate

The dynamic rate of civilizational development is reflected in strong transformations of settlement systems. In particular, anthropogenic modifications affect the way of land use, i.e. the structure of urban layout (including building arrangement, structure density), type of development (understood as the type - multi-family, single-family), functions located in the buildings (including residential, service, industrial), as well as components of natural environment (Laskowski, 1987). These transformations negatively affect the living comfort of residents.

The changes taking place are observable on a mesoscale covering units of several tens of kilometers. The subject of this study covers the areas of whole cities or separate fragments of fairly homogeneous areas. Next, the research is conducted within the Urban Boundary Layer (UBL)(Figure 2.1. a-b). In the case of detailed studies - in microscale - the analyses include isolated structures (e.g. single objects, groups of buildings). The studies are carried out within the vertical scale of Urban Canopy Layer (UCL)(Figure 2.1. c), which constitutes the lower part of the roughness sub-layer (approximately from the ground to the rooftops of buildings)(Martinelli & Matzarakis, 2017). It is believed that urban climatic events are most strongly felt within the Urban Canopy Layer. At this level, the most intense influence of environmental parameters on the human comfort residing in the outdoor environment is observed (Zielonko-Jung, 2013).

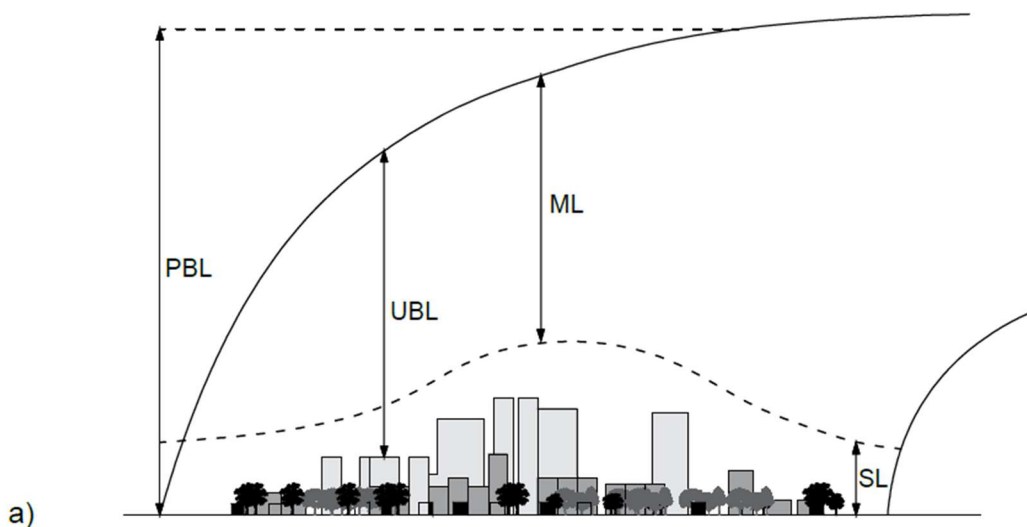


**Figure 2.1. a.** Structure of the atmospheric boundary layer over the city (a) mesoscale; abbreviations: PBL - planetary boundary layer, UBL - urban boundary layer, SL - surface layer, source: based on Oke (2000)).

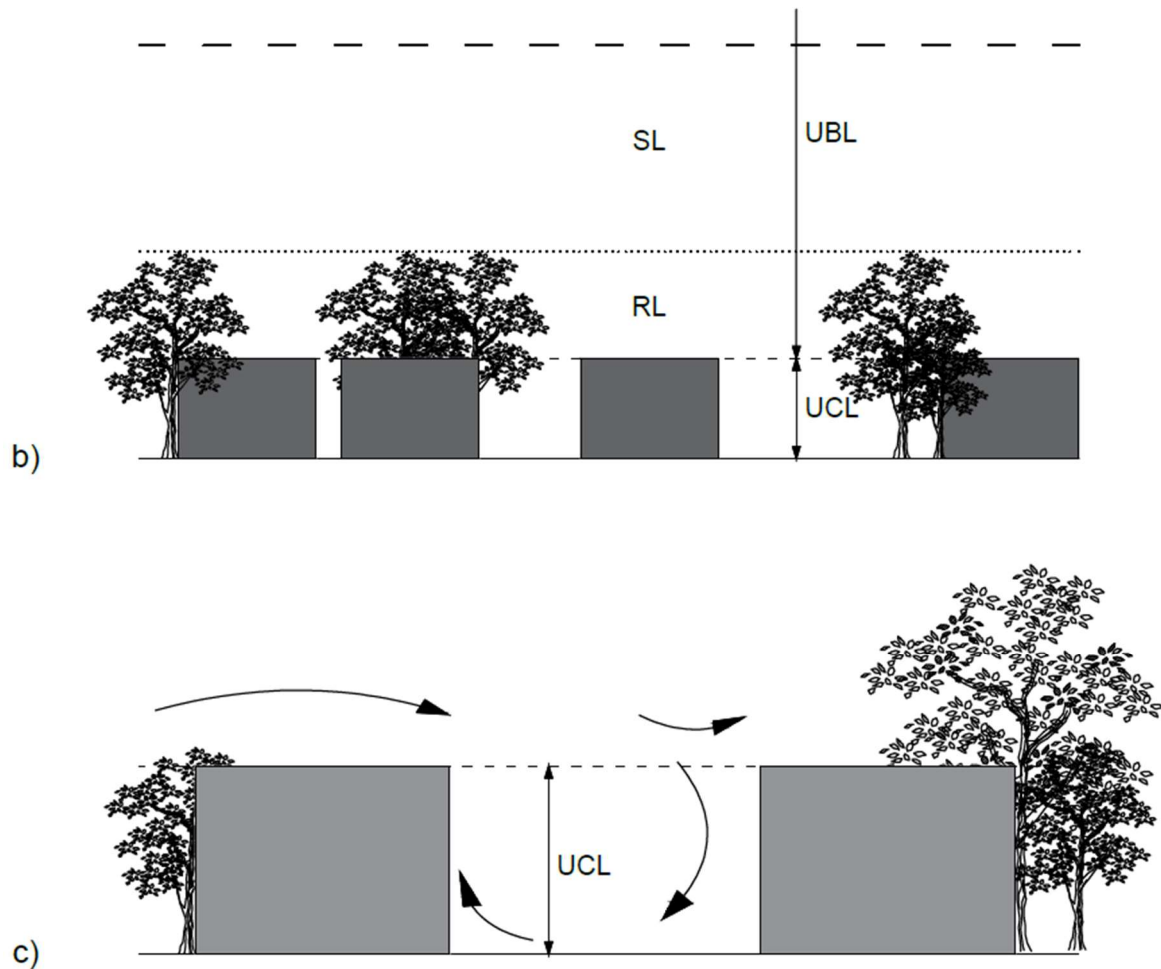


**Figure 2.1. b-c.** Structure of the atmospheric boundary layer over the city (b) local scale; c) microscale; abbreviations: UBL - urban boundary layer, SL - surface layer, RL - friction layer, UCL - roof layer; source: own elaboration based on [Oke \(2000\)](#)).

### Thermal conditions

Air temperature is considered one of the most significant parameters shaping thermal conditions of the biosphere. Its spatial diversity is the greatest in urbanized areas, which is due to the complex nature of urban layout. What is more, recorded values of air temperature, despite smaller amount of solar radiation reaching the earth surface, are much higher in urban areas. This results in the phenomenon of Urban Heat Island, defined as the difference in temperature between downtown areas and areas surrounding the city. It is noticeable in settlement units with more than 5000 inhabitants ([Dian et al., 2020](#)). Due to the scale of occurrence, it is one of the most frequently addressed issues in the scientific sphere. Research on UHI has been conducted extensively in Europe ([Ketter & Matzarakis, 2015](#), [Nastran et al., 2019](#), [Rodríguez et al., 2020](#), [Ferrari et al., 2020](#)), Asia ([Wang et al., 2016](#), [Kotharkar et al., 2018](#), [Hong et al., 2019](#), [Yang et al., 2020](#)), North America ([Silva & Fillpot,](#)

2018, Bauer, 2020, Equere et al, 2020), South America (Wu et al., 2019, Umezaki & Ribeiro, 2020), and Africa (Shahraiyni et al., 2016, Bahi et al., 2016, Simwanda et al., 2019, Aboleata et al., 2020). According to Hart & Sailor (2009), the intensity of Urban Heat Island phenomenon is closely related to the spatial development. The center-periphery temperature difference can vary from 1-2°C during the daytime, while 3-6°C during the nighttime. According to Akbari et al. (2016), the temperature difference can reach 6-10°C. In extreme cases it can reach 12°C (Poland, Czech Republic, India)(Szymanowski & Kryza, 2012, Geletič et al., 2019, Veena et al., 2020). Undoubtedly, the phenomenon affects deterioration in the quality of urban conditions. It contributes significantly to an increase in the number of hot days, and an increase in heat waves. It causes a weakening of air flow, as well as an increase in pollution levels (Hogrefe et al., 2004). It directly affects the prevailing microclimatic conditions and human thermal comfort. It translates into economic issues related to expanded energy costs and extra cooling consumptions (Akbari et al. 2001). As a result heat-stress associated mortality and illnesses (impaires public health)(Knowlton et al., 2004).

### **Solar conditions**

Solar radiation is a determinant of the physical phenomena occurring in ground level of the atmosphere. The amount of solar radiation reaching the earth's surface is significantly modified, especially in urban areas. It is related to (1) insolation time (covering the horizon) resulting from the shape of urban structure, (2) properties of horizontal and vertical surfaces (materials of buildings, artificial surfaces of the ground), as well as (3) changes in the state of atmosphere (cloudiness, pollution)(Lewińska, 2000). The results of literature studies show that solar radiation reaching the ground surface can be reduced by 40% in urban areas of temperate climate zone. The maximum values are observed in June-July, while the minimum in December (Kicińska & Wawer, 2010). It is estimated that the value of total solar radiation is reduced on average by 5-8% in urban areas. It is lower on average by 2-6% in summer, and 10-15% in winter (in extreme cases a reduction of 40% was observed). The opposite trend is observed for diffuse radiation, which is much stronger compared to suburban areas (Hess et al., 1980).

Radiation absorption is related to the urban layout of the city (anthropogenic elements and environmental components). It is determined by a dimensionless coefficient - albedo, which is the ratio of the amount of radiation reflected in all directions to the amount of radiation on a given surface. Its value varies from 0 (radiation is completely absorbed) to 1

(total reflection). According to Oke (1981), the albedo of urbanized areas is usually lower than that of suburban areas (Table 2.1.). This is caused by urban arrangement, which affects the level of radiation absorption by pavements. Fortuniak & Pawlak (2003) showed that the geometric factor can lower the albedo by several tens of percent. Also the physical properties of building materials (e.g. density, porosity, and heat capacity) contribute significantly to changes in radiation conditions. The average albedo value in urbanized areas is 10-27%. This is 10-20% less than for open areas.

**Table 2.1.** Albedo of city element.

BUILDING STRUCTURE	ALBEDO	
	MORNING	DAY
<b>Sapporo</b>		
residential	0.18	0.13
low rise	0.16	0.13
high rise	0.16	0.12
<b>Tokyo</b>	0.12	
<b>ARTIFICIAL STRUCTURES</b>		
roof (tiles)	0.19	
street (asphalt)	0.05 - 0.24	
pavement	0.30 - 0.40	
<b>NATURAL STRUCTURES</b>		
<b>grass</b>	0.30	
<b>forest</b>	0.20	0.16

**Source:** own elaboration based on Santamouris, 2000, Sugawara H. et al., 2014, Chatzidimitriou & Yannas, 2015.

The study of Chatzidimitriou & Yannas (2015) confirms that the albedo value of materials in urban areas is much lower. The authors conducted a study investigating the influence of construction materials on microclimatic conditions in Thessaloniki, in the northern Greece. The study areas were public spaces (parks, squares and forecourt) with different spatial development. The first stage of study consisted of field measurements. Analyses focused on the influence of building materials on microclimatic conditions. Also the components of natural environment were taken into consideration (surfaces like grass, high greenery). The second stage was to estimate the influence of construction and natural elements on thermal comfort. The authors showed that there is an inverse relationship between the temperature of pavement and the albedo value of material used. The darker the

color of pavement, the higher the air temperature. It should be emphasized that the use of materials with light shades positively influences the microclimatic conditions, but contributes to a negative impact on human thermal comfort (reflected solar radiation from the ground causes higher mean radiant temperature). In complex urban structures the physical properties of building materials (porosity, thermal capacity) should be taken into account. The right choice of pavement will influence the microclimatic conditions and ultimately the perceived thermal comfort.

### Wind conditions

The change in atmospheric flows is most evident in the Atmospheric Boundary Layer (Figure 2.2.). Then, the anemometric conditions depend on the land use. Modification of wind structure is caused by natural environmental components (terrain, exposure and slope, valley depth) and anthropogenic factors (structure of buildings). It is estimated that the average annual value of wind speed decreases by 20-30% in urban areas. The greatest slowdown is observed in the near-surface layer. Compact structure of buildings (high roughness of ground) causes that the air flow takes place above the buildings. At the ground surface the wind speed is minimal. Then, an important role in shaping the climatic conditions is played by the area' thermics. The opposite situation is observed above the friction layer. As the height increases, the wind speed increases. It can be even six times higher at the level of 300 m above sea level compared to the bottom wind (Lewińska J., 2000).

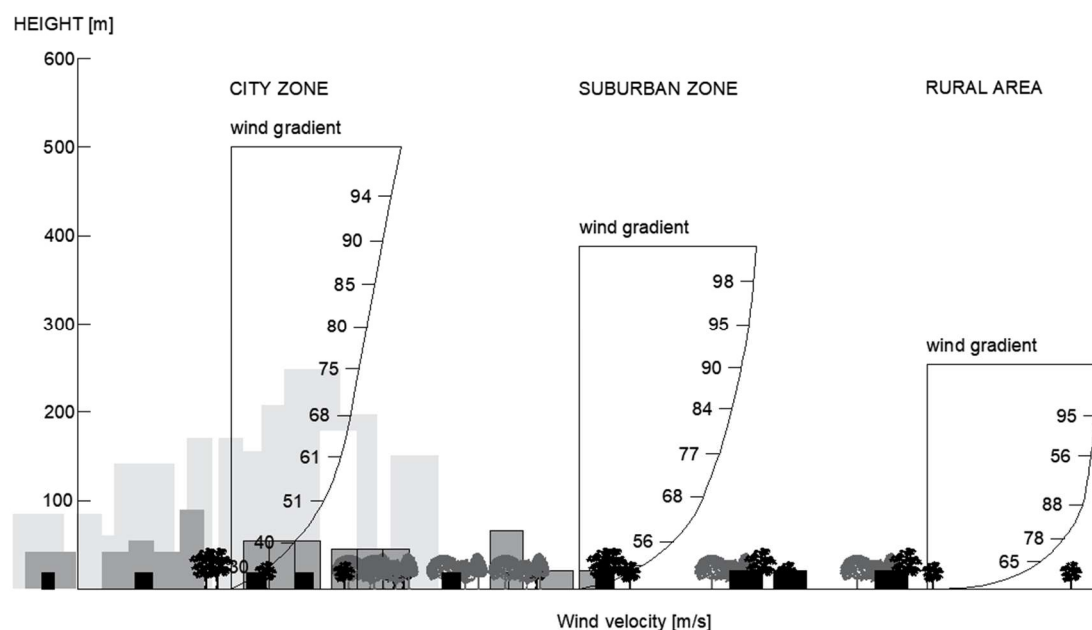
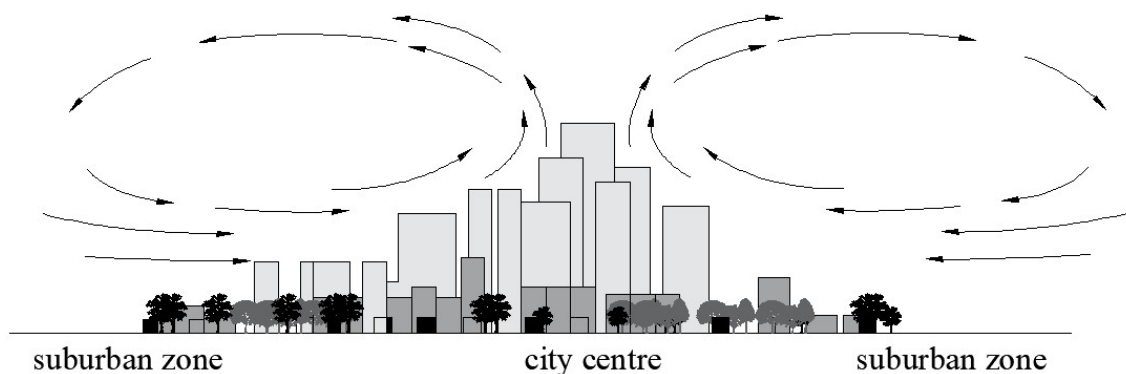


Figure 2.2. Wind profiles (source: own elaboration based on Lewińska J., 2000).

The mosaic form of urban layout contributes to varying thermal conditions within the city. The highest temperature is observed in the inner city zone, which is usually characterized by the highest ground roughness. This structure causes the formation of convergence zones, which force vertical air movements. Then the wind speed is accelerated. Different thermal conditions may intensify air flow in calm atmospheric conditions - the so-called breeze circulation (Figure 2.3.). This is when cool air from suburban areas flows onto heated up inner city areas with lower atmospheric pressure. The opposite trend, an anti-breeze, occurs over buildings. Air moves from heated up inner-city areas to outer zones. Moreover, it causes air changes in the direction of air flow by 10-20° especially in areas of dense urban development.



**Figure 2.3.** Breeze circulation over the city (source: own elaboration based on Hegger M. et al., 2008).

Forecasts show that the transformation dynamics of highly urbanized areas will increase. Intensive urbanization will lead to densification and expansion of the urban area. Settlement units will be characterized by an increasing proportion of impermeable surfaces, and thus a smaller amount of greenery. As a result, specific climatic conditions will be formed with distinctly different radiation, thermal, humidity, wind and aerosanitary parameters. In the first case - radiation flows there will be a reduction of direct solar radiation reaching the ground surface. However, a much greater proportion of diffuse radiation will be observed. There will be energy interception by building materials, which will heat up much more strongly than natural surfaces (e.g., the ground). Thermal changes will cause an increase in maximum air temperature as well as more frequent occurrence of heat waves and heat days. Changes in the sphere of natural water circulation will translate into prolonged rainless periods combined with temperatures above 25°C and occurrence of sudden local floods resulting from strong, short-lived precipitation. Changes in aerosanitary conditions (an increase in concentration of air pollutants) will also be significant. As a consequence, a less



favourable environment for human life will be created. Undoubtedly, progressive changes in climate conditions will cause a serious problem from the human comfort and health point of view (Goggins et al., 2012, Kováts & Hajat, 2008, Arsenović et al., 2019).

## 2.2. Climate change adaptation strategies in urban environment

Climate change is described as one of the greatest threats to humanity that will significantly affect both people and elements of the environment. As a result, the European Union has set the goal of being the first carbon-neutral continent in the world by 2050. According to the Paris Agreement on Climate Change, countries aim to keep global warming well below 2°C compared to pre-industrial temperatures. Unfortunately, projections show that this will be extremely difficult, as temperatures are already higher compared to the pre-industrial era. Moreover, it could increase by as much as 3°C by the end of this century (The EU, The JRC PESETA IV). The superimposition of global transformations as well as characteristic changes in urban climate conditions makes it necessary to take immediate action.

Undoubtedly, **adaptation measures** are one of the possibilities to counteract environmental changes. The currently implemented strategies are the result of arrangements at the EU level, i.e. provisions of the White Paper and the Green Paper from the Commission to the Council, the European Parliament, the European Economic and Social Committee and the Committee of the Regions (White Paper, 1985, Green Paper from the Commission to the Council, 2007). The implemented actions result from national and regional strategies, as well as local communities' initiatives. They are taken in relation to the existing phenomena, as well as possible future ones. Measures are introduced in sectors such as construction, energy, water management, mining, forestry, **urban areas**, agriculture, biodiversity, coastal zone, transport, tourism and health. They refer to components of the natural environment, as well as those transformed by human activity. Ultimately, they are intended to result in the adaptation of urban areas to changing climatic conditions (Ministry of the Environment, CLIMADA).

A compendium of adaptation measures has been published by the Environmental Protection Agency (EPA, 2008). It addresses solutions such as: (1) trees and vegetation, (2) green roofs, (3) cool roofs, (4) cool pavements, (5) water elements, (6) reduction activities enabling mitigation of anthropogenic impacts in urban areas. The description of adaptation strategies was made for selected solutions. In the further part of this paper, the strategies

were used as elements shaping the microclimatic conditions, as well as the residents' thermal comfort.

### **Trees and Vegetation**

The introduction of vegetation is one of the most widely used passive methods to counteract the Urban Heat Island effect (Ng et al., 2012). It contributes to the modification of microclimatic conditions through shading. It causes the reduction of solar radiation reaching the earth's surface. During summer, only 10% to 30% of solar energy penetrates through the tree canopy. A significant part is used in photosynthesis. In winter, the amount of energy reaching the ground surface varies from 10% to 80%. Greenery causes a change in thermal conditions. An example is the effect of vegetation on pavement heating. Dense tree crowns, by limiting solar radiation, contribute to the reduction of ground temperature. They affect the heat absorption of building materials. Modification of climatic conditions through evapotranspiration is mentioned as another advantage of vegetation (Zhang et al., 2017). Greenery absorbs water through the root system. Transpiration occurs in the above-ground parts of plants. The result is a change in moisture conditions. The use of passive technologies is one of the least invasive transformation forms of urban spaces, thus it does not violate the status quo of existing buildings, especially historic buildings in strict city centers.

The impact of green technologies varies due to local conditions of settlement units. The scale of impact depends on the amount of greenery introduced (Ng et al., 2012, Srivanit & Hokao, 2013, Rui et al., 2019, Ouyang et al., 2020, Teshnehdel et al., 2020), spatial arrangement of trees (Wu & Chen, 2017, Tsoka et al., 2021, Lee & Mayer, 2021) and the species of greenery (Takács et al., 2016, Karimi Afshar et al., 2018). An increase in green coverage can reduce air temperature by 0.12°C (China, Yan et al., 2018), 0.22°C (China, Wu & Chen, 2017), 0.43°C (Japan, Hamada & Ohta, 2010). The distribution of greenery modifies microclimatic conditions. A 10% increase in tree canopy results in a 0.22 °C decrease in temperature (Wu & Chen, 2017). Intensification of greenery to 25% results in a day time cooling benefit of up to 2°C (Middel et al., 2015). Green cover of 33% can result in a temperature drop of up to 1°C (Ng et al., 2012). The introduction of 20-30% natural area in urban environments is considered optimal (Ouyang et al., 2020). In practice, the use of more vegetation is difficult for practical reasons.

## Green roofs

Green roofs are a passive solution contributing to the increase of biologically active surface in built-up areas. They become increasingly popular, as they optimize the use of urban space (there is no need to designate new land for the solution). They are used as an element installed on service facilities: administration, large-format shopping, science and culture, as well as residential buildings.

Intensive green roofs are considered to be the most effective solution (Figure 2.4). The basis is vegetation, which is planted in a thick layer of vegetative substrate (up to 125 cm) on the building roofs. This type of passive technology contributes to the increase of tall greenery. Stable construction allows even for planting trees. The second implemented solution are extensive roofs (Figure 2.5). In this case, buildings are covered with low vegetation, which is not very demanding.


	<b>Intensive green roof</b>	
	implementation cost:	from 150 euro/m <sup>2</sup>
	maintenance cost:	3.5-15 euro/m <sup>2</sup>
	<b>Space requirements</b>	
	roof slope angle:	max 5°
	substrate thickness:	max 125 cm
	burden:	max 570 kg/m <sup>2</sup>
water retention:	up to 160 l/m <sup>2</sup>	

**Figure 2.4.** ASROS center in Fukuoka (source: <https://www.floornature.com>).

Undoubtedly, green roofs influence climatic conditions in cities. Various mitigating effects of living roofs are observed under different climates and urban densities. In a hot-dry climate, the temperature reduction is 1.4 °C (Cairo), the temperate climate is 0.3 °C in Paris (Morakinyo et al., 2017), 0.5 °C in Rome (Battista et al., 2016), and 1.5 °C in Germany (Köhler & Kaiser, 2019). The effect is to mitigate the Urban Heat Island phenomenon.

Green roofs allow rainfall to be captured and held in the environment for longer periods of time. They reduce surface runoff by about 90%. As a result, it is possible to reduce the cost of maintaining the natural system, as well as relieve the sewer system during heavy rainfall.

Green infrastructure influences the energy efficiency of buildings. It is a kind of natural insulation, especially in summer. The effect is a lower temperature inside the buildings. This translates into lower energy demand associated with cooling of rooms. In winter, it reduces heat loss through roofing.

	<b>Extensive green roof</b>	
	implementation cost:	from 50-255 euro/m <sup>2</sup>
	maintenance cost:	0.5-3 euro/m <sup>2</sup>
	<b>Space requirements</b>	
	roof slope angle:	even 45°
	substrate thickness:	from 7 cm
	burden:	from 80 kg/m <sup>2</sup>
water retention:	from 25 l/m <sup>2</sup>	

**Figure 2.5.** Green roof, Lake Toxaway, NC  
(source: <https://greenroofs.org>).

## Green walls

Another adaptation strategy is the implementation of green walls in urban areas (Figure 2.6.). Vertical surfaces of buildings are covered entirely or partially with vegetation. The least demanding form involves the introduction of plantings directly into the ground. Climbing vegetation adjacent directly to the walls of buildings is used. More complex cases involve the use of supporting structures. Then, systems of ropes or trusses are used to keep plants in a certain position.

Green wall systems contribute to the quality of urban environment. Alexandri & Johnes (2008) showed that living facades provide a more efficient adaptive solution than green roofs. They have the effect of modifying climatic conditions to the roof level. According to Herath et al. (2018) the introduction of 50% living facades into a highly urbanized environment reduces air temperature by 1.86°C. Studies by Srivanit et al. (2013)(Japan) confirm that microclimatic conditions undergo changes. The air temperature can be decreased by up to 2.27°C. Furthermore, the use of green walls affects the surface temperature, which is reduced by 6 to 10°C (Singapore)(2010). However, the impact of changes can be observed as the temperature increases. The warmer the climate, the greater the importance of introducing green technologies in urban areas. Green walls have an impact not only on microclimatic conditions. Passive technology can improve atmospheric air

quality. The concentration of pollutants can be 30% lower in areas where vegetation has been implemented (Rui et al., 2019).



**Figure 2.6.** Green wall systems (left - Residential Green Wall, Canaletto, 259 City Road, London (source: <https://www.biotechure.uk.com>); right - Cairo, Egypt (source: <http://www.greenprophet.com>)).

## Water elements

Blue infrastructure is considered as a part of adaptation efforts. Solutions that are under consideration include water retention ponds, bioretention basins, infiltration trenches, and bioretention planters (description provided below, [Figures 2.7. - 2.10.](#)). They can be introduced as a supplementary component with a considerable surface area in green areas. They can also be implemented within road infrastructure in highly urbanized environments (city centers).

Blue infrastructure contributes to the modification of environmental conditions, in particular the regulation of water management. It protects urban areas from flooding, reduces surface runoff from catchments, treats rainwater, provides habitat for flora and fauna, and has aesthetic value ([Iwaszuk et al., 2019](#)).

Blue-net elements cause a reduction in air temperature during the day. An example is water bodies at least half a meter deep, which absorb a significant part of solar radiation due to their high thermal capacity. However, numerous studies show that they increase the air temperature at night. This is due to thermal exchange along the atmosphere-surface pathway. At night, the water temperature is higher than the air temperature. Then, heat transfer occurs to the environment. To prevent a significant temperature increase, mitigation measures (e.g. proper natural ventilation) are taken ([Steenefeld et al., 2014](#), [Van Hove et al., 2015](#)).



© Christian Kruppa

**Water retention ponds** - can be created on the basis of natural terrain or artificially made. They are used as reservoirs for retaining and purifying water. They are also the habitat of flora and fauna occurring in urban areas.

**Figure 2.7.** Potsdamer Platz retention pond (source: <https://www.facebook.com/potsdamer.platz>).



**Bioretention basins** - implemented in heavily sealed areas. They are used to collect and purify rainwater. As a result, they reduce the surface runoff from the catchment area.

**Figure 2.8.** Bioretention basin at Water Street in Plymouth Center, Massachusetts (source: <http://capecodgreenguide.wordpress.com>).



**Infiltration trenches** - implemented in the form of roadside ditches as elements of road infrastructure. Depressions are filled with gravel or stone. During heavy rains they stop surface runoff. In addition, they treat water that is drained from sealed, asphalt pavements.

**Figure 2.9.** Infiltration trench in Paso Robles, United States (source: <http://www.svrdesign.com>).

---



**Figure 2.10.** Bioretention planters in El Cerrito, United States (source: <http://www.madrono.org>).

**Bioretention planters** - elements artificially implemented into the urban environment. The objects, in the form of concrete tanks, allow to collect and purify water. As a result, they influence water conditions.

Their undoubted advantage is the ease of implementation in cities. They can be installed in the strict centers, i.e. within the forecourt development, in street canyons, as well as in public squares. It should be noted that they bring aesthetic benefits, affecting the appearance of urban spaces.

---

There are ongoing projects to determine the impact of adaptation scenarios on urban climate. An example is **REALCOOL (Really Cooling Water Bodies in Cities) conducted in Dutch cities**. Research is carried out on the impact of blue as well as green strategies on environmental parameters. The key issue is the use of blue-green combinations. Then, thermal discomfort can be reduced by 1-10°C ([Jacobs et al., 2020](#)).

### 2.3. Outdoor thermal comfort

There are many definitions of thermal comfort. One of the best known, created by the American Society of Heating, Refrigeration and Air Conditioning Engineers, defines thermal comfort as a state of mind that expresses satisfaction with the thermal environment ([ASHRAE 55, 2014](#)). According to [the Polish standard ISO 7730 \(2006\)](#), comfortable conditions prevail when people express satisfaction with the prevailing thermal environment ([PN-EN ISO 7730, 2006](#)). A more rational definition explains thermal comfort as a state of thermal balance. This means that it is felt when the amount of heat generated in the body (through metabolic processes) is balanced with the amount of heat released to the environment (through convection, radiation and conduction). This is when the human physical parameters, i.e. skin temperature, sweat rate and/or core temperature are in thermal equilibrium ([Fanger, 1970](#)).

Assessment of thermal comfort can be carried out by using thermal comfort indices. Literature research shows that there are currently many international, national standards,

guidelines, and advisories for the assessment of thermal conditions. These are used for both indoor and outdoor environment evaluation. The comfort of indoor environment has been well documented in previous decades. This was due to the possibility of performing tests in a relatively stable environment and the possibility of its mechanical control (with respect to climatic parameters). In the second case, the assessment of thermal comfort was and still is more complex. This is due to the highly dynamic nature of external environment, which is caused by sudden changes in meteorological parameters, in particular solar radiation and wind speed (Coccolo et al., 2013). Moreover, the assessment of thermal comfort depends on the duration of human exposure to microclimatic parameters, which can last from a few minutes to several hours. Depending on the time spent in the outdoor environment, people have the ability to acclimatize, which is related to the modification of clothing and physical activity performed. This allows them to modify the perceived thermal conditions. Assessment of thermal comfort is a result of physical and psychological conditions. Satisfaction with the thermal environment is also a result of expectations, choices and previous experiences with exposure to environmental factors (Auliciems, 1998).

Thermal environment and its effects on humans cannot be described as a function of single variable. The human body (through receptors) experiences all microclimatic parameters simultaneously. Models used to assess thermal comfort are based on the same assumption - they are functions of multiple variables. According to international studies (ASHRAE 55, 2014) as well as national standards (PN-EN ISO 7730, 2006), four meteorological parameters (temperature, solar radiation, relative humidity and wind speed) and two physical parameters (metabolism and thermal insulation of clothing) are listed as the main factors affecting thermal comfort. In this way, the models take into account the physical conditions and effects of the external environment on humans. These parameters are the components of models to assess thermal comfort for both indoor and outdoor research (Fang et al., 2018).

### **2.3.1. Heat exchange between a human body and the outdoor environment**

#### **The Fanger's model**

A breakthrough in the history of thermal comfort research was the publication of a book entitled "Thermal Comfort" by Ole Fanger (1970). It was the culmination of research conducted on a group of students at the Technical University of Denmark and at Kansas State University, United States. Fanger was the first to identify the environmental and



physical parameters that directly affect thermal conditions. The human thermal balance equation was described by four basic meteorological parameters (air temperature, mean radiant temperature, humidity and air velocity) as well as thermal insulation of clothing and physical activity (Equation 2.1).

$$\begin{aligned} & (M/A_{Du})(1-\eta) - 0.35[43 - 0.061(M/A_{Du})(1-\eta) - p_a] - 0.42[(M/A_{Du})(1-\eta) - 50] - 0.0023(M \\ & /A_{Du})(44 - p_a) - 0.0014(M/A_{Du})(34 - t_a) \\ & = 3.4 \times 10^{-8} f_{cl} [(t_{cl} + 273)^4 - (t_{mrt} + 273)^4] + f_{cl} h_c (t_{cl} - t_a) \end{aligned}$$

**Equation 2.1.** Energy balance.

where:  $M$ : metabolic rate ( $\text{W}/\text{m}^2$ ),  $A_{Du}$ : DuBois area [ $\text{m}^2$ ],  $\eta$ : external mechanical efficiency heat exchange (usually is set to zero),  $p_a$ : water vapour pressure [Pa],  $t_a$ : air temperature [ $^{\circ}\text{C}$ ],  $t_{mrt}$ : mean radiant temperature,  $f_{cl}$ : ratio of the surface area of the clothed body to the surface area of the nude body,  $t_{cl}$ : clothed surface temperature [ $^{\circ}\text{C}$ ],  $h_c$ : heat convection coefficient [ $\text{W}/\text{m}^2\cdot\text{K}$ ].

Fanger's equation was applicable only to determine the thermal comfort of a human in an energy balance condition. It allowed obtaining satisfactory thermal conditions only for specific combination of variables in the equation. As is well known, not all space users will express satisfaction with the prevailing thermal conditions. Therefore, the author used the created energy balance equation to evaluate the dissatisfaction level with specific thermal conditions. Currently, the Fanger equation is used in the PMV (Predicted Mean Vote) and PDD (Predicted Percentage Dissatisfied) index of individuals expressing dissatisfaction with the prevailing thermal environment.

### The MEMI model

The Munich Energy-Balance Model for individuals (MEMI - Equation 2.2.) defines human energy balance as a component of meteorological parameters (air and ground temperature, humidity, shortwave radiation and airflow velocity), physiological factors (metabolic heat production, skin temperature), and information about thermal insulation properties of clothing (Sikora, 2008).

$$M + W + R + C + E_D + E_{RE} + E_{SW} + S = 0$$

**Equation 2.2.**

where:  $M$ : metabolic activity,  $W$ : physical work output,  $R$ : net radiation of the body,  $C$ : convective heat flow,  $E_D$ : latent heat flow to evaporate water into water vapour diffusing through the skin,  $E_{RE}$ : sum of heat flows for heating and humidifying the inspired air,  $E_{SW}$ : heat flow due to evaporation of sweat,  $S$ : storage heat flows for heating or cooling the body mass.

The unit of all parameters is Watt [W]. Parameters have positive signs if they cause heat gain for the body. Otherwise (heat losses), the parameters have negative signs. Additionally, the values of individual parameters in the equation depend on meteorological factors (Table 2.2.).

**Table 2.2.** Relationship of meteorological parameters and physical factors according to MEMI model.

MEMI PARAMETERS	METEOROLOGICAL PARAMETERS
the net radiation of the body ( $R$ )	mean radiant temperature
the convective heat flow ( $C$ )	air temperature, wind velocity
the latent heat flow to evaporate water diffusing through the skin (imperceptible perspiration)( $E_D$ )	air humidity
the sum of heat flows for heating and humidifying the inspired air ( $E_{RE}$ )	air temperature, air humidity
the heat flow due to evaporation of sweat ( $E_{SW}$ )	air humidity, wind velocity

**Source:** own elaboration.

### The Fiala's model

Fiala's heat transfer model was developed in 1999. It assumed the existence of a passive system to regulate heat exchange between 19 basic body parts. Each component was further divided into 5 layers (bone, muscle, adipose tissue, subcutaneous tissue, and skin), two to three segments (anterior, posterior, and inferior), and the circulatory system divided into three components (central blood pool, counter current heat exchanger, and pathways to individual tissue nodes). Each component was represented by one node in the model (over 300 nodes in total). The active system was responsible for physiological thermoregulatory

processes that altered the amount of heat exchange in the body. It was developed using an experimental method that measured the responses of subjects exposed to varying heat conditions (cold stress, cold, moderate, warm and hot stress conditions) and conducting specific physical activity. The model provided information on the magnitudes of individual physiological body parameters and heat flows. Currently, Fiala's heat balance equation is used as a component of the UTCI index - one of the most widely used to assess human thermal comfort in the outdoor environment.

### **2.3.2. Thermal comfort indices**

Literature research shows an increase in interest in the subject of thermal comfort assessment in the outdoor environment. According to de Freitas & Grigorieva (2017), there are 165 indices used to estimate human thermal sensations. Such a large number of indices may be confounding at first; however, they share common characteristics that allow them to be divided into two categories: empirical and rational indices. In the case of empirical indices, thermal comfort is assessed based on the thermal sensations of people who express their satisfaction or dissatisfaction with the prevailing meteorological conditions. Unfortunately, this form of assessment does not allow studying the influence of individual parameters on human thermal sensations. It is a component of the effects of temperature, humidity, and airflow on the human body. The assessment is made for sedentary activity. Moreover, various physical factors (gender, age, height and weight), psychological factors and clothing are not taken into account. The latter - rational indices are commonly used to assess thermal comfort in the outdoor environment. This is closely related to the development of computer techniques which enable the implementation of their heat balance equations in simulators. Finally, they allow simultaneous estimation of meteorological parameters in the outdoor environment as well as estimation of thermal conditions for different combinations of human physical parameters (Parsons, 2003).

Among the most commonly used empirical indices are Effective Temperature (ET) and Operative Temperature ( $T_{op}$ ). The most popular rational indices for estimating thermal comfort in outdoor environments include - Standard Effective Temperature (SET), Predicted Mean Vote (PMV), Physiological Equivalent Temperature (PET) and Universal Thermal Climate Index (UTCI)(Potchter et al., 2018). Comparison of the listed indices is presented in Table 2.3.

**Table 2.3.** Thermal comfort indices used in environment studies.

<b>TITLE</b>				
<b>AUTHORS</b>	<b>CITY, COUNTRY</b>	<b>CLIMATE</b>	<b>INDEX</b>	<b>NO. OF VOTES</b>
<b>EMPIRICAL INDICES - EFFECTIVE TEMPERATURE (ET)</b>				
1. <a href="#">Spagnolo and de Dear, 2003</a>	Sydney, Australia	Humid subtropical (Cfa)	T <sub>op</sub> PET, SET	1018
2. <a href="#">Yahia and Johansson, 2012</a>	Damascus, Syria	Dry, steppe (BSk)	PMV, PET, SET	920
<b>EMPIRICAL INDICES - OPERATIVE TEMPERATURE (T<sub>op</sub>)</b>				
1. <a href="#">Hwang et al., 2010</a>	Taichung, Taiwan	Humid subtropical (Cwa)	T <sub>op</sub>	3837
2. <a href="#">Yang et al., 2013</a>	Singapore	Tropical rainforest (Af)	T <sub>op</sub>	2036
3. <a href="#">Wang et al., 2017</a>	Groningen, Netherlands	Oceanic (Cfb)	T <sub>op</sub> PET	389
4. <a href="#">Fang et al., 2018</a>	Guangzhou, China	Humid subtropical (Cfa)	T <sub>op</sub> PET and UTCI	2007
<b>RATIONAL INDICES - STANDARD EFFECTIVE TEMPERATURE (SET)</b>				
1. <a href="#">Lin et al., 2011</a>	Taichung, Yunlin, Chiayi, Taiwan	Humid subtropical (Cwa)	SET	1644
2. <a href="#">Xi et al., 2012</a>	Guangzhou, China	Humid subtropical (Cfa)	SET	114
3. <a href="#">Zhou et al., 2013</a>	Wuhan, China	Humid subtropical (Cfa)	SET	386
4. <a href="#">Zhao et al., 2016</a>	Guangzhou, China	Humid subtropical (Cfa)	SET	1582
<b>RATIONAL INDICES - PREDICTED MEAN VOTE (PMV)</b>				
1. <a href="#">Nikolopoulou et al., 2001</a>	Cambridge, UK	Maritime temperate (Oceanic)(Cfb)	PMV	1431
2. <a href="#">Becker et al., 2003</a>	Yotvata, Israel	Desert arid (BWh)	PMV	288
3. <a href="#">Thorsson et al., 2004</a>	Göteborg, Sweden	Maritime temperate (Oceanic)(Cfb)	PMV	285
4. <a href="#">Kántor et al., 2007</a>	Szeged, Hungary	Maritime temperate (Oceanic)(Cfb)	PMV	844
5. <a href="#">Metje et al., 2008</a>	Birmingham, UK	Maritime temperate (Oceanic)(Cfb)	PMV	451
6. <a href="#">Aljawabra and Nikolopoulou, 2010</a>	Marakech, Morocco Phoenix, Ar. USA	Hot semi-arid (BSh) Desert (BWh)	PMV	303 126
7. <a href="#">Sangkertadi and Syafriny, 2014</a>	Manado, Indonesia	Tropical wet (Af)	PMV	300
8. <a href="#">Hashim et al., 2016</a>	Kota Damansara, Malaysia	Tropical rainforest (Af)	PMV	30
9. <a href="#">Salata et al., 2016</a>	Rome, Italy	Subtropical (Csa)	PMV	1565
<b>RATIONAL INDICES - PHYSIOLOGICALLY EQUIVALENT TEMPERATURE (PET)</b>				
1. <a href="#">Knez and Thorsson, 2006</a>	Tokyo, Japan Göteborg, Sweden	Humid subtropical (Cfa) Maritime temperate (Oceanic)(Cfb)	PET	63 43

**Table 2.3.** Continuation.

<b>RATIONAL INDICES - PHYSIOLOGICALLY EQUIVALENT TEMPERATURE (PET)</b>					
2.	<a href="#">Eliasson et al., 2007</a>	Göteborg,, Sweden	Maritime temperate (Oceanic)(Cfb)	PET	1379
3.	<a href="#">Oliveira and Andrade, 2007</a>	Lisbon, Portugal	Mediterranean (Csa)	PET	91
4.	<a href="#">Thorsson et al., 2007</a>	Tokyo, Japan	Humid subtropical (Cfa)	PET	1142
5.	<a href="#">Lin and Matzarakis, 2008</a>	Sun Moon Lake, Taiwan	Humid subtropical (Cwa)	PET	1644
6.	<a href="#">Lin, 2009</a>	Taichung, Taiwan	Humid subtropical (Cwa)	PET	505
7.	<a href="#">Mahmoud, 2011</a>	Cairo, Egypt	Desert arid (BWh)	PET	300
8.	<a href="#">Kántor et al., 2012</a>	Szeged, Hungary	Maritime temperate (Oceanic)(Cfb)	PET	967
9.	<a href="#">Makaremi et al., 2012</a>	Putrajaya, Malaysia	Tropical rainforest (Af)	PET	200
10.	<a href="#">Ng et al., 2012</a>	Hong Kong, China	Humid subtropical (Cwa)	PET	2702
11.	<a href="#">Schnell et al., 2012</a>	Tel Aviv, Israel	Subtropical (Csa)	PET	1457
12.	<a href="#">Cohen et al., 2013</a>	Tel Aviv, Israel	Subtropical (Csa)	PET	1731
13.	<a href="#">Yang et al., 2013</a>	Singapore, Singapore Changsha, China	Tropical rainforest (Af) Humid subtropical (Cfa)	PET	2020 2052
14.	<a href="#">Krüger et al., 2014</a>	Glasgow, UK	Maritime temperate (Oceanic)(Cfb)	PET	567
15.	<a href="#">Tung et al., 2014</a>	Taichung, Yunlin, Chiayi, Taiwan	Humid subtropical (Cwa)	PET	1644
16.	<a href="#">Chen et al., 2015</a>	Shanghai, China	Humid subtropical (Cfa)	PET	596
17.	<a href="#">Da Silva and De Alvarez, 2015</a>	Vitoria, Brazil	Humid tropical (Af)	PET	841
18.	<a href="#">Lin et al., 2015</a>	Keelung, Taichung, Tainan Taiwan	Humid subtropical (Cwa)	PET	2071
19.	<a href="#">Zeng and Dong, 2015</a>	Chengdu, China	Humid subtropical (Cwa)	PET	255
20.	<a href="#">Elnabawi et al., 2016</a>	Cairo, Egypt	Desert arid (BWh)	PET	320
21.	<a href="#">Hirashima et al., 2016</a>	Belo Horizonte, Brazil	Tropical wet and dry (Aw)	PET	1693
22.	<a href="#">Kántor et al., 2016</a>	Szeged, Hungary	Maritime temperate (Oceanic)(Cfb)	PET	5805
23.	<a href="#">Kovács et al., 2016</a>	Szeged, Hungary	Maritime temperate (Oceanic)(Cfb)	PET	5128
24.	<a href="#">Li et al., 2016</a>	Guangzhou, China	Humid subtropical (Cfa)	PET	1005
25.	<a href="#">Liu et al., 2016</a>	Changsha, China	Humid subtropical (Cfa)	PET	7851
26.	<a href="#">Shooshtarian and Ridley, 2016</a>	Melbourne, Australia	Temperate oceanic (Cfb)	PET	1023
27.	<a href="#">Louafi et al., 2017</a>	Constantine, Algeria,	Mediterranean (Csa)	PET	2220

**Table 2.3.** Continuation.

<b>RATIONAL INDICES - PHYSIOLOGICALLY EQUIVALENT TEMPERATURE (PET)</b>				
28. <a href="#">Middel et al., 2017</a>	Tempe, Ar, USA	Desert (BWh)	PET	1284
29. <a href="#">Shooshtarian and Rajagopalan, 2017</a>	Melbourne, Australia	Temperate oceanic (Cfb)	PET	1059
<b>RATIONAL INDICES - UNIVERSAL THERMAL CLIMATE INDEX (UTCI)</b>				
1. <a href="#">Rutty and Scott, 2015</a>	Barbados, Saint Lucia, Tobago, The Caribbean Islands	Tropical (Aw) maritime tropical (Am)	UTCI	472
2. <a href="#">Huang et al., 2016</a>	Wuhan, China	Warm and temperate (Cfa)	UTCI	1460
3. <a href="#">Lam et al., 2018</a>	Melbourne, Australia	Temperate oceanic (Cfb)	UTCI	3320
4. <a href="#">Maras et al., 2016</a>	Aachen, Germany	Temperate (Cfb)	UTCI	138
5. <a href="#">Krüger et al., 2017</a>	Curitiba, Brazil	Mesothermic humid subtropical (Cfb)	UTCI	1685

**Source:** own elaboration.

### Operative temperature ( $T_{op}$ )

According to Hwang et al. (2010), estimation of the thermal comfort prevailing in the outdoor environment is possible with simple indicators. One of them is the operative temperature. According to Appendix C of ASHRAE-55 standard (2014), it is defined as the uniform room temperature at which a person will exchange the same amount of heat by radiation and convection as in a non-uniform temperature environment. It is dependent on the air temperature, the average radiant temperature and the airflow velocity (Equation 2.3.).

$T_{op} = AT_a + (1 - A)T_{mrt}$	<b>Equation 2.3.</b>
----------------------------------	----------------------

In the equation, the coefficient  $A$  depends only on the airflow velocity. When  $v_a$  is less than 0.2 m/s, then  $A = 0.5$ , when  $v_a$  varies from 0.2 to 0.6 m/s then  $A = 0.6$ , when  $v_a$  exceeds 0.7 then  $A = 0.7$  (ASHRAE 55, 2014). According to Wang et al. (2017), this index can only be used to estimate the effect of microclimate parameters on thermal comfort. However, by comparing TSVs (obtained through surveys) with  $T_{op}$ , it is possible to determine the neutral temperature and the temperature preferred by users of public spaces. As shown in numerous studies (Hwang et al., 2010, Yang et al., 2013, Wang et al., 2017, Fang et al., 2018) their value will depend on local microclimatic conditions.

Operative temperature is used to determine internal thermal comfort. Then, the air temperature as well as the average ambient radiation temperature is taken into account

during the evaluation. Other meteorological variables including relative humidity or air velocity are ignored (Equation 2.4)(Lis, 2015).

$T_{op} = GT_{mrt} + (1 - G)T_a$	<b>Equation 2.4.</b>
----------------------------------	----------------------

where:  $T_{mrt}$  - mean temperature of ambient radiation [°C],  $T_a$  - air temperature [°C],  $G$  - coefficient of mean temperature of ambient radiation in heat perception.

The operative temperature was used in this study as an index for evaluating thermal comfort inside buildings located in the Metropolitan Area of Lodz.

### Predicted Mean Vote (PMV)

The Predicted Mean Vote is an index commonly used to estimate thermal comfort in outdoor environments. Initially, it was used in studies of indoor environments. A modification of the Fanger thermal balance equation used in the model by Jednritzky and Nübler made it adaptable for outdoor environment studies. The current modified model version is called “Klima-Michel-Modell,” which takes into account the influence of meteorological parameters, long- and short-wave radiation flows, typical physical activity, and human clothing (Jendritzky & Nübler, 1981).

According to the Polish standard EN-ISO 7730 (2006), the PMV index is defined as the average rating of a group of people expressing their thermal sensations on a seven-point rating scale. The index values usually range from [-3] to [+3]. Neutral conditions are defined as sensations that are assigned a value between [-0.5] and [0.5](Table 2.4.). In case of conducting research in an outdoor environment, the values of index are significantly beyond the scale of [-3], [+3]. This is due to the calculation of index on the basis of varying weather conditions and the average ratings of people expressing their satisfaction with the thermal environment. Discrepancy between the theoretical (seven-point scale) and empirical studies is due to the lack of restrictions on the minimum/maximum values of PMV in the case of studies conducted in the outdoor environment. Moreover, the values of index are dependent on the local climate and thus on the climatic zone in which the research is carried out.

**Table. 2.4.** PMV scale.

cold	cool	slightly cool	slightly warm	warm	hot	
-3	-2	-1	neutral conditions	+1	+2	+3

**Source:** own elaboration.

This fact is confirmed by the study conducted by Jihad and Tahiri for subtropical/tropical climate (Morocco). The authors showed that the value of PMV was dependent on the local climate, season, and the way of urban planning, in particular the ratio of building height forming a street canyon to street width. The value of index varied from [-4] to [11] throughout the year (Jihad & Tahiri, 2016). The study conducted by Thorsson et al. (2004) showed that the value of index ranged from [-11] to [+11] when the study was conducted in temperate zone. Also they showed that there is a discrepancy between PMV values obtained from simulation of atmospheric processes and surveys (40% discrepancy).

### Physiologically Equivalent Temperature (PET)

Literature studies show that the most commonly used index to assess thermal comfort in outdoor environments is Physiological Equivalent Temperature (PET; Table 2.5.). It is defined as air temperature at which, in a typical indoor setting (without wind and solar radiation), the heat budget of the human body is balanced with the same core and skin temperature as under the complex outdoor conditions to be assessed (Höppe, 1999). This approach allows a person to make an assessment of outdoor conditions based on previous experience gained in the indoor environment. In this case, the MEMI model is used to describe the human heat balance (see Chapter 2.3.1. for a detailed description).

**Table 2.5.** PET index scale.

PET °C	Thermal Perception	Grade Of Physiological Stress
4 °C	very cold	extreme cold stress
8 °C	cold	strong cold stress
13 °C	cool	moderate cold stress
18 °C	slightly cool	slight cold stress
23 °C	comfortable	no thermal stress
29 °C	slightly warm	slight heat stress
35 °C	warm	moderate heat stress
41 °C	hot	strong heat stress
	very hot	extreme heat stress

**Source:** own elaboration.

The value of PET index is dependent on the climatic zone. Potchter et al. (2018) conducted a literature analysis of 110 papers that were published between 2001 and 2017. Their main aim was to review methods for assessing thermal comfort in the outdoor environment, to identify the most commonly used thermal comfort indices, and to evaluate human thermal sensations depending on the climatic zone. In the case of PET index, the



variation of values depending on the prevailing climatic conditions was evident. The authors showed that its value ranged from 19 to 31°C for tropical climate, from 19 to 33°C for dry climate, from 10 to 31°C for warm temperate climate and from 6 to 24°C for continental climate. The neutral value of index ranged from 24 to 26°C for hot climates and 15 to 20°C for cold climates (Potchter et al., 2018).

### **Universal Thermal Climate Index (UTCI)**

The International Society for Biometeorology established an interdisciplinary group of experts (from thermo-physiology, occupational medicine, physics, meteorology, biometeorology and environmental science) under the European COST Action 730 (Cooperation in Science and Technical Development) program. Their aim was to invent a new universal index for the assessment of bioclimatic conditions. This index was to take into account information about complex thermophysical processes. It was also supposed to have universal applicability for different climatic conditions (taking into account seasonality of climate), as well as scale and research objective.

Several years of cooperation of the expert group resulted in an invention of new universal index for evaluation of thermal comfort in the outdoor environment (1999). The Universal Thermal Climate Index is defined as the equivalent air temperature at which, under reference conditions, the basic physiological parameters of the body take the same values as under real conditions. It means that the heat exchange between a person and the environment depends on the air temperature assuming unchanged level of other meteorological parameters (Equation 2.5). In order to determine the equivalent air temperature it is first necessary to calculate the human energy balance in real conditions. This is possible by using Fiala's model. Then the air temperature at which physiological parameters take the same values as in real conditions should be estimated. In the case of UTCI calculation, the following parameters were taken as reference meteorological conditions: mean radiant temperature equal to air temperature, water vapor pressure equal to 50% relative humidity (at temperature <29°C) and equal to 20 hPa at temperature higher than 29°C, wind speed at 10 meters above ground level equal to 0.5 m/s and relative air flow velocity associated with movement equal to 1.1 m/s. Metabolic heat production of 135 W/m<sup>2</sup> and clothed thermal insulation proportional to actual thermal conditions were assumed as physiological parameters (Błażejczyk et al., 2009). The Universal Thermal Climate Index equation takes a general form:

$UTCI(T_a, T_{mrt}, v_a, p_a) = T_a + \text{Offset}(T_a, T_{mrt}, v_a, p_a)$	<b>Equation 2.5.</b>
--	----------------------

where:  $T_a$  - air temperature (°C),  $T_{mrt}$  - mean radiant temperature (°C),  $v_a$  - air flow velocity (m/s),  $p_a$  - water vapour pressure, Offset - deviation of air temperature.

This indicator has a 10-point rating scale. The values range from [-40] to [+46](Table 2.6.). In many studies it is emphasized that neutral conditions are felt for values between [+9] and [+26]. This fact was confirmed by Lai et al. (2014), Pantavou et al. (2014), Huang et al. (2016), and Krüger et al. (2017).

**Table 2.6.** UTCI index scale.

UTCI °C	Grade Of Physiological Stress
above +46 °C	extreme heat stress
+38 °C TO +46 °C	very strong heat stress
+32 °C TO +38 °C	strong heat stress
+26 °C TO +32 °C	moderate heat stress
+9 °C TO +26 °C	no thermal stress
0 °C TO +9 °C	slight cold stress
-13 °C TO 0 °C	moderate cold stress
-27 °C TO -13 °C	strong cold stress
-40 °C TO -27 °C	very strong cold stress
below -40 °C	extreme cold stress

**Source:** own elaboration.

### Subjective evaluation of comfort conditions

Thermal comfort assessments can be carried out based on the subjective evaluations of people describing their thermal sensations. The information is obtained by means of surveys conducted in the outdoor environment (usually in the areas of selected public spaces, which are the research subject). Most often, the survey questionnaire is divided into three parts. The first is aimed at obtaining data on physical characteristics (e.g. age, gender, weight, height), as well as the respondent’s current thermal status (physical activity performed and clothing). In addition, the questionnaire can be supplemented with questions about socio-economic conditions (education level, occupational status, financial situation; Aljawabra & Nikolopoulou, 2010). Next, thermal impressions of the prevailing microclimatic conditions are determined. In this case, the thermal sensation scale (TSV) is used. According to ASHRAE-55 guidelines (2014), it has a 7-point scale (Table 2.7.). In many studies, the scale used is a 9-point scale (it has been expanded to include extreme conditions such as: “very cold” and “very hot”)(Table 2.8.). Impressions can be specified for each microclimate

parameter, i.e. air temperature (ASV - Air Temperature Sensation Vote), solar radiation (SSV - Sun Sensation Vote), humidity (HSV - Humid Sensation Vote), wind speed (WSV - Wind Sensation Vote), and cloud cover (CSV - Cloud Cover Sensation Vote). The last part of the questionnaire addresses preferred conditions determined by the McIntyre scale, as well as acceptable conditions estimated by a binary item (“acceptable” or “unacceptable”).

**Table 2.7.** ASHRAE-55 Thermal Sensation Vote scale (TSV).

	cold	cool	slightly cool	neutral conditions	slightly warm	warm	hot
	-3	-2	-1		+1	+2	+3

**Source:** own elaboration.

**Table 2.8.** Broadened Thermal Sensation Vote scale (TSV).

	very cold	cold	cool	slightly cool	neutral conditions	slightly warm	warm	hot	very hot
	-4	-3	-2	-1		+1	+2	+3	+4

**Source:** own elaboration.

Preferences can be expressed for each of the microclimatic parameters, i.e., air temperature (I prefer a warm condition, I have no preferences, I prefer a cool condition), solar radiation (prefer more sun, no preference and prefer less sun), humidity (prefer humid, no preference and prefer dryness), wind speed (prefer more wind, no preference and prefer less wind), cloudiness (prefer more cloud, no preference and prefer less cloud), and precipitation (prefer more precipitation, no preference and prefer less precipitation).

Field measurements of microclimatic parameters are carried out in parallel to the survey. They take place directly in the vicinity of a respondent filling out the questionnaire. Based on the comparison of obtained data it is possible to determine neutral, preferred, and acceptable conditions. Neutral conditions; the conditions which people feel neither cool nor warm (Fanger, 1970) are determined on the basis of linear regression curve between thermal feelings of respondents (according to the ordinal scale) and calculated thermal comfort index. Preferred conditions; the thermal environmental condition under which individuals prefer neither warmer nor cooler temperature are determined from the relationships described by two curves, i.e. (1) representing the relationship between air temperature and the percentage of individuals preferring higher air temperature, and (2) representing the relationship between air temperature and the percentage of individuals preferring lower

temperature (Fanger, 1973). Intersection of curves (point at which percentage of people preferring lower and higher temperature is the same) determines the preferred temperature. Conditions are considered acceptable if they are recognized as such by a minimum of 80% of respondents (threshold is defined in the ASHRAE-55, 2014).

### **Thermal comfort research - a critical view**

A thorough literature review leads to the conclusion that the current state of research on thermal comfort in the outdoor environment is not sufficient. Usually the studies are carried out for selected days of the year, which may reflect extreme or semi-extreme conditions, especially in summer. Few authors conduct comprehensive studies considering different microclimatic conditions for each season (Lin et al., 2011, Nikolopoulou et al., 2001, Lin & Matzarakis, 2008, Lin et al., 2015, Liu et al., 2016, Middel et al., 2017, Huang et al., 2016). This means that the research does not allow the development of practical guidelines for urban designers. This is caused by the lack of determination of average conditions in the given areas. In order to estimate them, it is necessary to use the provisions of international standards, which indicate how to determine the so-called Typical Meteorological Year. Their determination will allow to describe the averaged conditions in the external environment. The Author has not found in any of the studies subject to the analysis even a mention of the necessity to apply this type of approach - calculation of conditions for the Typical Meteorological Year.

Most often the studies are conducted in the areas of public urban or semi-public spaces (green areas, city squares, street canyons, yards of multi-family buildings). Unfortunately, the selection of diverse types of spaces results in a qualitative nature of the research. The choice of strictly defined types of public spaces would allow to determine the relationship between thermal comfort and the way of spatial development. Numerous authors emphasize the influence of development structure (determined by SVF and AR) on microclimatic conditions (Xi et al., 2012, Yang et al., 2013, Cohen et al., 2013, Louafi et al., 2017, Krüger et al., 2017).

The research is based on international standards (ISO 7726 - Ergonomics of the thermal environment - Instruments for measuring physical quantities, 1998). At first, field studies are carried out in selected areas of public spaces. They concern basic microclimatic parameters (temperature, average solar radiation temperature, relative humidity, air flow velocity). The studies require huge amounts of funds for research equipment. An example is the equipment used to determine the temperature of solar radiation. This problem is most

often solved by using an equation to calculate the average solar radiation temperature from the temperature, humidity, and wind values (Kántor et al., 2016, Middel et al., 2017, Wang et al., 2017, Fang et al., 2018). The method is presented in ISO 7726 (2001). In addition, field measurements are related to organizational problems (e.g., time for taking measurements). Simulation analyses are an alternative solution. Few authors use computer simulators to estimate microclimate parameters. The most commonly used are ENVI-met, Rayman and Bioklima applications (Kántor et al., 2007, Cohen et al., 2013, Salata et al., 2016, Louafi et al., 2017).

Surveys on thermal sensations, acceptable conditions and users' preferences of public spaces are carried out in parallel with field studies. Respondents usually represent two groups of people, i.e. local residents using a given space for recreational purposes, and people randomly appearing in a given area (moving from point A to B in the city). According to the author, an interesting solution would be to include a representative group of inhabitants in the research on thermal comfort. This is possible by determining the population structure of a given city on the basis of information contained in the databases of state institutions (statistical offices). Then, surveys should be carried out distinguishing particular groups of people in the survey (age groups). Finally, it would be possible to determine the average thermal impressions of the inhabitants of a given area.

Another problematic issue is the selection of an index to assess thermal comfort in the outdoor environment. The literature review showed that empirical indices, i.e. PMV, PET and UTCI are the most commonly used to determine thermal sensations of respondents. They take into account the influence of both microclimatic and psycho-physical factors on perceived thermal comfort. However, many authors emphasize the fact that the research results are not comparable. This is due to the inhabitant's adaptation of different climate zones to local conditions. Moreover, many authors point out that there are different thermal sensations within one climate zone (Eludoyin & Adelekan, 2013). Therefore, making an evaluation of thermal comfort requires both estimating the value of comfort index and performing surveys. The obtained survey results should then be compared in order to determine the thermal sensations of individuals within the area of specific microclimatic conditions.

## CHAPTER III. THE NUMERICAL MODEL

### 3.1. Numerical modelling of an urban microclimate

In the era of growing technological advances, it has become possible to conduct complex analyses of phenomena occurring in highly urbanized areas. The development of computer techniques allowed to conduct climatic studies, the results of which can be obtained in a relatively short time. In this case, computer simulations are the leading method. They are considered more efficient in comparison with time-consuming measurement campaigns supplemented with qualitative research (e.g. surveys, interviews). Thus, they become an increasingly common tool used in the field of urban climatology. The RayMan application modeling the mean radiant temperature and human thermal environment, BioKlima for the assessment of bioclimatic conditions, and the ENVI-met numerical fluid mechanics software are mentioned as the most commonly used for the assessment of the influence of building structure on climate and thermal comfort.

Currently, the last mentioned - ENVI-met application becomes commonly used for studies that deal with climatic conditions in urban areas. This is due to the characteristics of software which allows to create three-dimensional urban layouts taking into account building materials used which are characteristic for a given area. Thus, it is possible to transfer the real world to the virtual model. According to Lee & Mayer (2016), the tool predicts the effect of building form on microclimatic conditions with acceptable accuracy in the outdoor environment. Hourly parameter values can be read at selected grid points (depending on the set model resolution). Simulations performed take into account airflow between buildings, heat transfer processes of horizontal and vertical surfaces, turbulence, vegetation parameters, and dispersion of pollutants. According to Lenzholer & Kohl (2010), ENVI-met is one of the tools that take into account parameters that determine thermal comfort in the outdoor environment such as air temperature, direction, wind speed, relative humidity, and mean radiant temperature to estimate values of thermal comfort indices.

This paper uses the ENVI-met application due to its ability to assess both the impact of building form and adaptation strategies on microclimatic conditions and human thermal comfort in the outdoor environment. Moreover, the obtained simulation output data were used to calculate the thermal comfort perceived by the users of building structures located in the Metropolitan Area of Lodz.

### 3.2. The general structure of ENVI-met application

The ENVI-met application was developed by Prof. Bruse's team at Mainz University, Germany. It is used in the field of urban planning to simulate the influence of building form on climatic parameters, as well as to assess the thermal comfort of humans residing in a highly urbanized environment. It is successfully applied to research in the field of urban climatology.

The CFD (Computational Fluid Dynamics) software tool is used to conduct analyses and simulations in the field of numerical fluid mechanics. It is used to create three-dimensional non-hydrostatic microclimate models, taking into account the finite difference method (Hien et al., 2012). It estimates substrate-plant-air relationships over a diurnal cycle (typically 24 to 48 hours)(Huttner et al., 2008).

Four modules of the application are used in the climatic studies, i.e. SPACES allowing to create a three-dimensional terrain model, ConfigWizard in which the input meteorological parameters are defined, ENVI-met (core) responsible for the simulation of atmospheric processes, as well as LEONARDO allowing to graphically present the distribution of weather parameters and to read their values at the location points of measuring stations at a selected height.

Changes in urbanized environment are forecasted based on 3D core model (created in SPACES module) and 1D border model (meteorological parameters are defined in ConfigWizard module). The main task of 3D core model is to simulate changes in well-defined structure of buildings. Location of the model is determined based on geographical coordinates of the terrain (longitude and latitude).

Parameters of 3D model X, Y and Z as well as resolution of individual cells can be modified depending on the scope of conducted research. In case of grid structure determination there are two methods: equidistant and telescoping grid generation. The first one is based on model division into cells of equal size in each direction  $\Delta x = \Delta y = \Delta z$  (with the reservation that the height of the first five cells above the ground surface is  $\Delta z_g = 0.2\Delta z$ , in order to increase the accuracy of calculations related to microclimatic processes occurring near the ground surface). Second method - telescoping technique is used in case of investigations carried out in the strict city centers, where high objects are involved. Then, the telescoping factor is applied, which is defined as a percentage growth factor for the vertical parameter of the model. The maximum dimensions X, Y can be selected within a wide range. The vertical dimension of model Z is estimated from the parameters of the

highest object created in the model ( $Z \geq 2H_{max}$ ). The resolution of each model element can vary from 0.5 m to 10 m (Huttner et al., 2008).

Creation of objects is possible in 2D as well as 3D format. The application provides the necessary tools to model building constructions, diverse ground surfaces (natural, artificial), as well as vegetation. Individual elements of the real world are created based on components found in the ENVI-met database (Table 3.1.).

**Table 3.1.** Chosen model components.

<b>Materials</b>
<ul style="list-style-type: none"> <li>• cement and concrete (heavyweight, lightweight, hollow, filled block, cast dense, photoactive),</li> <li>• glass (heat protection, plexiglass, foamed, clear float glass, glass brick surface, shading plexiglass),</li> <li>• metal (aluminium, iron, steel),</li> <li>• misc (good, moderate, without insulation, PCV),</li> <li>• natural (masonry, air),</li> <li>• stone (aerated, burned, reinforced brick),</li> <li>• tile (tile, terracotta);</li> </ul>
<b>Soil</b>
<ul style="list-style-type: none"> <li>• natural (sand, loamy sand, sandy loam, silt loam, loam, sandy clay loam, silty clay loam, clay loam, sandy clay, clay, peat, wood planks, water),</li> <li>• artificial (smashed brick, cement concrete, mineral concrete, asphalt, granite, basalt, brick, styrofoam);</li> </ul>
<b>Greenings</b>
<ul style="list-style-type: none"> <li>• wall and roof greenings (with/without air gap),</li> <li>• high vegetation (by tree species, i.e. deciduous, coniferous; selected for Leaf Area Density, i.e. low, medium, high).</li> </ul>

**Source:** own elaboration.

The user can create a model using the elements from the database. In case of the lack of suitable solutions it is possible to modify/add materials, building partitions, types of surface and natural elements (vegetation). Then, it is necessary to determine their parameters (Table 3.2.).

The user then defines the meteorological conditions (1D model). Initially, the simulation date is chosen, resulting in the automatic generation of selected parameters (e.g. insolation). The test start time should be set at least two hours before sunrise. This is to ensure the stability of simulation process. Data are entered as meteorological boundary conditions. Wind speed at height of 10 m above ground level [m/s], direction of air inflow [deg], roughness length at measurement site [m] are defined. In case of temperature and humidity



it is possible to implement hourly values. The program automatically determines maximum and minimum values of the parameter during a day. In advanced settings the user has a possibility to make a correction of solar radiation based on adjustment factor. This is very useful function, because the parameters are overestimated by the application. The solar radiation value needs to be adjusted in order to ensure correct input data. Settings related to parameters inside buildings, soil conditions, type and concentration of air pollutants, as well as the degree of cloud cover can be used in broader urban climatology studies (Hien et al., 2012).

**Table 3.2.** Material parameters.

<b>Materials</b>	<b>Soils</b>	<b>Greenings (wall and roof)</b>
<ul style="list-style-type: none"> <li>• thickness,</li> <li>• absorption,</li> <li>• transmission,</li> <li>• reflection,</li> <li>• emissivity,</li> <li>• specific heat,</li> <li>• thermal conductivity,</li> <li>• density.</li> </ul>	<ul style="list-style-type: none"> <li>• water content at saturation,</li> <li>• water content at field capacity,</li> <li>• water content at wilting point,</li> <li>• hydraulic conductivity,</li> <li>• volumetric heat capacity,</li> <li>• heat conductivity.</li> </ul>	<p>Greening properties:</p> <ul style="list-style-type: none"> <li>• plant thickness,</li> <li>• Leaf Area Index (LAI),</li> <li>• Leaf Angle Distribution (LAD).</li> </ul> <p>Substrate properties:</p> <ul style="list-style-type: none"> <li>• substrate thickness,</li> <li>• emissivity of substrate,</li> <li>• albedo of substrate,</li> <li>• water coefficient of substrate for plants,</li> <li>• air gap between substrate and wall.</li> </ul>

**Source:** own elaboration.

The upper horizontal boundary and the vertical windward boundary act as an interface between the 1D boundary model and the 3D core model (Figure 3.1.). The 1D model extends the area of 3D structure to  $H = 2\ 500$  m (an average depth of a boundary layer). It enables to use microclimatic parameters as input data to the model - their transfer as start values to the upper boundary of prognostic 3D core model. Moreover, 1D soil model allows entering the information on temperature and relative humidity at the ground surface into the 3D model (excluding the cells forming the surface of urban structure in the 3D model to ensure homogeneity). Additionally, buffer zone called ‘nesting zone’ has been introduced. It causes model boundary area shift in order to eliminate numerical disturbances - boundary effects. It extends to dimensions that are at least twice the height of the highest building created in 3D model ( $2H_{max}$ ). Dimensions of individual nesting grids gets progressively larger as

distance from core model increases. The user defines the roughness of nesting grids by specifying the surface material - two soil types. In this way it is possible to adapt entered parameters as 1D model for airflow to 3D core model (Wu & Chen, 2017).

The simulation of atmospheric processes depends on the available computer components. Moreover, the larger the area to be simulated, the more tedious the simulation (in this study, 1 simulation for typical urban forms = 2 days; selected case of street canyon between intersections of Jaracza/Piotrkowska and Jaracza/Wschodnia streets = 5 days, selected case of urban forecourt at 50 Piotrkowska Street = 1 day).

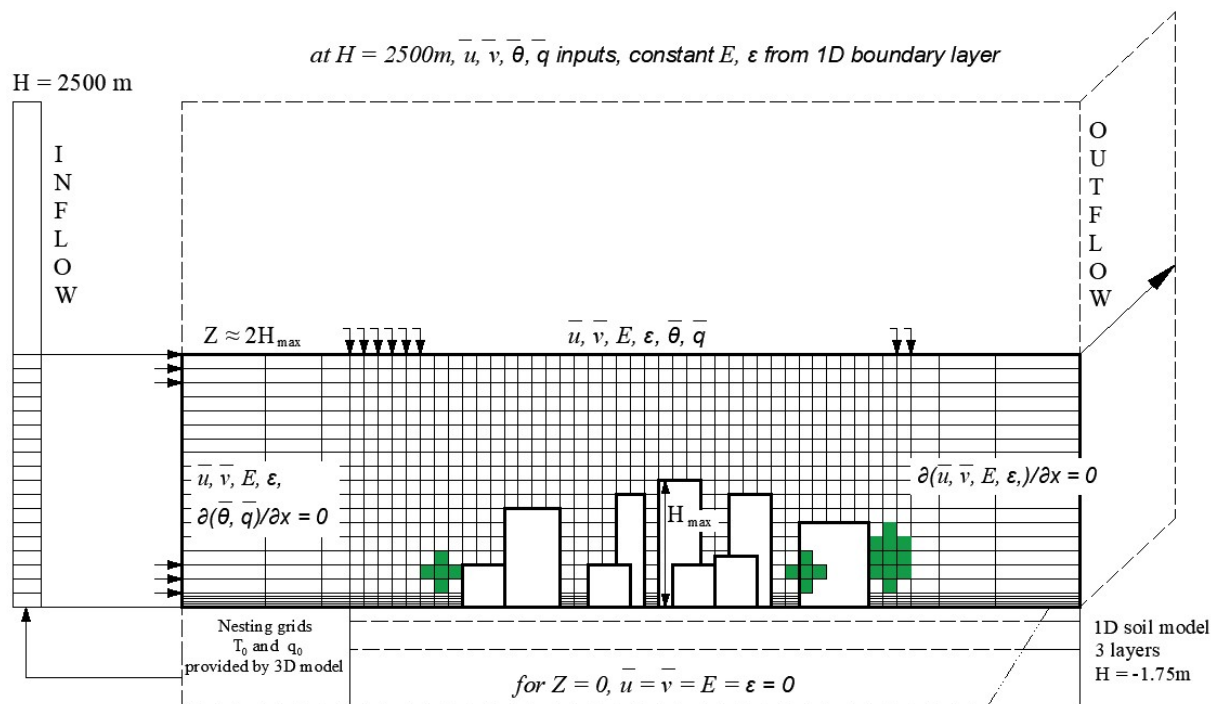


**Figure 3.1.** Model domain in the ENVI-met application (source: own elaboration based on Toudert F. A., 2005).

### 3.3. Boundary conditions

Three-dimensional models are treated as simplified representations of real-world conditions. In the modeler, objects are created based on a rectangular grid of cells. Consequently, they have the character of block models. The horizontal structure is defined by specifying the number of cells forming the grid, as well as their resolution. The terrain dimension can be more than 50 x 50 cells. Its resolution can vary from 0.5 m to 10 m (dimensions of a single cell). ‘Nesting grids’ are used for stability. They are additional cells at the edges of model that allow input to the created inhomogeneous urban environment. It is necessary to determine the level of roughness of the buffer zone (nesting grids) by

indicating the dominant pavement type found around the modeled structure. The vertical dimension of the model should be at least  $Z \geq 2H_{max}$  (Deng & Wong, 2020).

The application allows to create simulations of atmospheric processes for selected fragments of the urban structure. Therefore, it is required to determine the boundary conditions of a 3D model. The simplified forced lateral boundary conditions used in this study consist in entering hourly values for temperature and humidity. The defined parameters are forced at the height of 2 m in the simulation process. It is important to note that the method can be used to run tests on a 24 hour cycle. The initialization time of the 1D model is related to the computer hardware parameters. It runs until interaction between all start values reach stationary state ( $\bar{u}$ ,  $\bar{v}$ ,  $\bar{\Theta}$ ,  $\bar{q}$ ,  $E$ ,  $\varepsilon$  and the exchange coefficients  $K_m$ ,  $K_h$  and  $K_q$ ). The equations used in the 3D core model simulation process are described in detail in [Chapter 3.4. Governing equations of the atmospheric model](#). Their equivalents in the form of 1D equations are used as boundary conditions. Sometimes a parameterization is made to simplify the model. The vertical inflow profile extends to a height of 2 500 m. The temperature and humidity value for the top of the three dimensional model are calculated linearly on the basis of implemented values at 2 m height. The wind profile is determined based on logarithmic law. Then, the value of air flow at the height of 10 meters above the ground level is taken into account, as well as the roughness of the ground. Surface temperature is influenced by soil sub-model parameters. Temperature and moisture of the ground is defined at four heights, i.e., upper layer (0-20 cm), middle layer (20-50 cm), deep layer (50-200 cm) and bedrock layer (below 200 cm). Based on these, the tool determines the surface temperature.

Numerical aspect of the simulation are connected with the usage of finite difference method for all differential equations. The time steps depend on the calculated parameter. For airflow it is 10 minutes. The solar radiation time step is set by the user. For E- $\varepsilon$  system a 3-minutes time interval is used to ensure numerically stable solution. Alternating Directions Implicit Method (ADI) in combination with an upstream advection scheme is used to solve the advection-diffusion equations (Forouzandeh, 2018).

### **3.4. Governing equations of the atmospheric model**

The atmospheric sub-model is mainly based on fundamental laws of computational fluid dynamics, i.e., equation of conservation of mass, momentum, heat and moisture. It predicts the evolution of wind flow (speed and direction), turbulence, air temperature, relative

humidity. It takes into account absorption and emission of short-wave and long-wave radiation fluxes (Bruse & Fler, 1998).

Due to the fact that the tool used contains numerous equations, only those considered crucial in assessing the impact of adaptation strategies introduced in highly urbanized areas on microclimatic conditions, as well as human thermal comfort, are described in this paper.

### Mean air flow

The basic concept to describe a spatial and temporal evolution of the three-dimensional turbulent wind flow is given by the Navier-Stokes equations. In the application, the non-hydrostatic incompressible form is used (Equation 3.1-a - 3.1-c)(Bruse & Fler, 1998):

$$\frac{\partial u}{\partial t} + u_i \frac{\partial u}{\partial x_i} = - \frac{\partial p'}{\partial x} + K_m \left( \frac{\partial^2 u}{\partial x_i^2} \right) + f(v - v_g) - S_u \quad (\text{Equation 3.1-a.})$$

$$\frac{\partial v}{\partial t} + u_i \frac{\partial v}{\partial x_i} = - \frac{\partial p'}{\partial y} + K_m \left( \frac{\partial^2 v}{\partial x_i^2} \right) - f(u - u_g) - S_v \quad (\text{Equation 3.1-b.})$$

$$\frac{\partial w}{\partial t} + u_i \frac{\partial w}{\partial x_i} = - \frac{\partial p'}{\partial z} + K_m \left( \frac{\partial^2 w}{\partial x_i^2} \right) + g \left( \frac{\theta(z)}{\theta_{ref}(z)} \right) - S_w \quad (\text{Equation 3.1-c.})$$

$$\frac{\partial u}{\partial x} + \frac{\partial v}{\partial y} + \frac{\partial w}{\partial z} = 0 \quad (\text{Equation 3.1-d.})$$

where  $f$  ( $= 10^4 \text{ sec}^{-1}$ ) is the Coriolis parameter,  $p'$  is the local pressure perturbation,  $\theta$  is the potential temperature at level  $z$  and  $\theta_{ref}$  is an average temperature over all grid cells of height  $z$ , excluding those occupied by buildings.

The air density  $\rho$  was removed from the original compressible Navier-Stokes equations using the *Boussinesq Approximation*. It gave the opportunity of implementing one additional source terms in the w-equation to include thermal forced vertical motion. Finally, one continuity Equation (1-d) which has to be satisfied for each time step in order to keep the flow field mass conserving was reached. It should be taken into consideration that all three-dimensional advection and diffusion terms are written in the Einstein summation ( $u_i = u, v, w$ ;  $x_i = x, y, z$  for  $i = 1, 2, 3$  to save place).

$S_u, S_v$  and  $S_w$  are the local source/sink terms which describe the loss of wind speed due to drag forces connected with vegetation elements. This effect can be parametrized by Yamada (1982) and Liu et al. (1996) dependency as:

$$S_{u(i)} = \frac{\partial p'}{\partial x_i} = c_{d,f} LAD(z) \cdot W \cdot u_i \quad (\text{Equation 3.2.})$$

$W = (u^2 + v^2 + w^2)^{0.5}$  is the mean wind speed at height  $z$ ,  $LAD(z)$  is the leaf area density in  $[\text{m}^2 \text{m}^{-3}]$  of the vegetation in this height. The mechanical drag coefficient at plant elements  $c_{d,f}$  is set to 0.2.

## Temperature and humidity

In the sub-atmospheric model, the distribution of temperature  $\theta$  and specific humidity  $q$  is based on the combined advection-diffusion equation with internal source/sinks (Bruse & Fleer, 1998):

$$\frac{\partial \theta}{\partial t} + u_i \frac{\partial \theta}{\partial x_i} = K_h \left( \frac{\partial^2 \theta}{\partial x_i^2} \right) + \frac{1}{c_p \rho} \frac{\partial R_{n.lw}}{\partial z} + Q_h \quad (\text{Equation 3.3.})$$

$$\frac{\partial q}{\partial t} + u_i \frac{\partial q}{\partial x_i} = K_q \left( \frac{\partial^2 q}{\partial x_i^2} \right) + Q_q \quad (\text{Equation 3.4.})$$

Similar to the momentum equations,  $Q_h$  and  $Q_q$  are used to include heat and vapour exchange at vegetation in the sub-atmospheric model. The vegetation model, which is described later on, gives the possibility of quantifying  $Q_h$  and  $Q_q$  parameters.  $\partial R_{n.lw}/\partial z$  is the vertical divergence of longwave radiation taking into account the cooling and heating effect of radiative fluxes.

## Atmospheric turbulence

Estimation of basic meteorological parameters requires consideration of turbulent air movement. Turbulence is created by disturbance of laminar flow of air masses. It is associated with the presence of anthropogenic obstacles (buildings), as well as natural elements (vegetation). Depending on the weather conditions, the phenomenon scale is variable. Under the windy conditions, local turbulence production surpasses its dissipation. Turbulent eddies may be transported by the mean flow, which leads to increased turbulent exchange away from the original source. In the present case, turbulence processes are determined by approximated values from definable quantities (closure problem). The 1.5 turbulence closure model is used to describe the turbulence processes in the ENVI-met application.

In the atmospheric model, two additional equations are implemented for the local turbulence ( $E$ ) and its dissipation rate ( $\varepsilon$ ). They are based on the work of Mellor & Yamada (1975) as follows:

$$\frac{\partial E}{\partial t} + u_i \frac{\partial E}{\partial x_i} = K_E \left( \frac{\partial^2 E}{\partial x_i^2} \right) + Pr + Th + Q_E - \varepsilon \quad (\text{Equation 3.5.})$$

$$\frac{\partial \varepsilon}{\partial t} + u_i \frac{\partial \varepsilon}{\partial x_i} = K_\varepsilon \left( \frac{\partial^2 \varepsilon}{\partial x_i^2} \right) + c_1 \frac{\varepsilon}{E} Pr + c_3 \frac{\varepsilon}{E} Th - c_2 \frac{\varepsilon^2}{E} + Q_\varepsilon \quad (\text{Equation 3.6.})$$

The variables  $Pr$  and  $Th$  describe respectively the production and the dissipation of turbulent energy on account of wind shearing and thermal stratification. The former, can be

parameterized by the usage of the three dimensional deformation tensor of the local wind field.

$$Pr = 2K_m \left( \frac{\partial u}{\partial x} \right)^2 + K_m \left( \frac{\partial u}{\partial y} + \frac{\partial v}{\partial x} \right)^2 + K_m \left( \frac{\partial u}{\partial z} + \frac{\partial w}{\partial x} \right)^2 + 2K_m \left( \frac{\partial v}{\partial y} \right)^2 + K_m \left( \frac{\partial v}{\partial z} + \frac{\partial w}{\partial y} \right)^2 + 2K_m \left( \frac{\partial w}{\partial z} \right)^2$$

**(Equation 3.7.)**

The buoyancy production is given by:

$$Th = \frac{g}{\theta_{ref(z)}} K_h \frac{\partial \theta}{\partial z}$$

**(Equation 3.8.)**

The Th parameter is neglected under stable weather condition ( $Th > 0$ ). Depending on the complexity of the flow problem, different  $c_1, c_2, c_3$  values might be used. To calibrate the  $\varepsilon$ -equation in the atmospheric model standard values  $c_1 = 1.44, c_2 = 1.92, c_3 = 1.44$  given by Launder & Spalding (1974) are applied.

The influence of natural obstacles is taken into consideration. The additional emerged turbulence produced by the vegetation elements as well as the accelerated cascades of turbulence energy from large to small scale nearby plant foliage are described by two extra source terms added to the  $E - \varepsilon$  equation (Liu et al., 1996, Wilson, 1988).

$$Q_E = c_{d,f} LAD_{(z)} \cdot W^3 - 4c_{d,f} LAD_{(z)} \cdot |W| \cdot E$$

**(Equation 3.9.)**

$$Q_\varepsilon = 1.5c_{d,f} LAD_{(z)} \cdot W^3 - 6c_{d,f} LAD_{(z)} \cdot |W| \cdot \varepsilon$$

**(Equation 3.10.)**

where  $c_{d,f}$  is a drag coefficient at the plant foliage and  $W$  is the mean wind speed at a considered height ( $z$ ). The source term ( $\varepsilon$ ) in the letter equation is found on the basis of Kolmogorov relation ( $\varepsilon = 0.16E^{3/2}/l$ ). While the  $E - \varepsilon$  field is calculated, the turbulent exchange coefficients are calculated on the grounds of the assumption of the local turbulence isotropy:

$$K_m = c_\mu \frac{E^2}{\varepsilon}$$

**(Equation 3.11.)**

$$K_h = K_q = 1.35K_m$$

**(Equation 3.12.)**

$$K_E = \frac{K_m}{\sigma_E}$$

**(Equation 3.13.)**

$$K_\varepsilon = \frac{K_m}{\sigma_\varepsilon}$$

**(Equation 3.14.)**

with  $c_\mu = 0.09, \sigma_E = 1, \sigma_\varepsilon = 1.3$ . When it comes to the simulation of boundary layer flows, the additional scaling function is added to adjust diffusion coefficients to thermal stratification following Sievers et al. (1987) and Businger et al. (1971).

## Radiative fluxes

As a top boundary conditions, there are included the incoming shortwave and longwave fluxes. In the application the two stream radiative flux approximation for the longwave fluxes and the set of empirical equations for the shortwave wavelength spectra are used.

In the urban environment model, radiative fluxes are altered by artificial and natural obstacles. The five reduction coefficients are implemented to estimate their effect on radiative conditions. Their values can ranged from 1 for the undisturbed fluxes to 0 for total absorption (Bruse, 1995).

The radiative environment partially blocked by the hindrances is expressed by the usage of the Sky View Factor ( $SVF$ ). It defines the ratio of unobstructed sky hemisphere which is visible from the specific point on the ground.  $SVF$  ranges from 1 (fully visible sky) to 0 (invisible sky hemisphere), where  $\omega$  is the vertical angle determined by the obstacles in direction  $\pi$ . Finally, it gives information how strong might be the radiative fluxes at a particular location (Wang & Akbari, 2014).

$$\sigma_{svf}(z) = \frac{1}{360} \sum_{\pi=0}^{360} \cos\omega(\pi) \quad (\text{Equation 3.15.})$$

The impact of vegetation is taken into consideration by the usage of obstructions coefficients for direct and diffuse shortwave radiation.

$$\sigma_{sw,dir}(z) = \exp(-F \cdot LAI^*(z)) \quad (\text{Equation 3.16.})$$

$$\sigma_{sw,dif}(z) = \exp(-F \cdot LAI(z, z_p)) \quad (\text{Equation 3.17.})$$

The natural obstruction influence on atmospheric and terrestrial longwave radiation is expressed:

$$\sigma_{lw}^{\downarrow}(z) = \exp(-F \cdot LAI(z, z_p)) \quad (\text{Equation 3.18.})$$

$$\sigma_{lw}^{\uparrow}(z) = \exp(-F \cdot LAI(0, z)) \quad (\text{Equation 3.19.})$$

The term  $F$  is the extinction coefficient.  $LAI$  is defined as the one dimensional vertical leaf area index which is calculated for the natural elements from a reference level ( $z$ ) to the crown top of a tree ( $z_p$ ). The coefficient is calculated by the vertical integration of  $LAD$  over the height of the vegetation (Huttner, 2012).

$$LAI(z, z + \Delta z) = \int_{z'}^{z'+\Delta z} LAD(z') dz' \quad (\text{Equation 3.20.})$$

To anticipate the effect of the modelled urban structure on direct solar radiation  $LAI$  is replaced by  $LAI^*$ . It takes into account the angle of incidence from the incoming sun rays. Moreover, the model foresees the impact of hindrances which intersect the ray path on the

radiative environment. If the direct solar radiation is fully blocked by obstructions, the  $\sigma_{sw,dir}(z)$  is set equal to zero. If the porous elements appear, the reduction coefficient is used (Equation 3.16.).

Two equations are implemented to estimate the direct and diffused shortwave solar radiation at any point  $z$  of the mesh:

$$R_{sw,dir}(z) = \sigma_{sw,dir}(z)R_{sw,dir}^0 \quad (\text{Equation 3.21.})$$

$$R_{sw,dif}(z) = \sigma_{sw,dif}(z)\sigma_{svf}(z)R_{sw,dif}^0 + (1 - \sigma_{svf}(z))R_{sw,dir}^0 \cdot \bar{a} \quad (\text{Equation 3.22.})$$

Terms  $\sigma_{sw,dir}(z)$  and  $\sigma_{sw,dif}(z)$  are used to include the vegetation impact on the radiative fluxes.  $R_{sw,dir}^0$  and  $R_{sw,dif}^0$  describe the direct and diffused shortwave fluxes at the top boundary of the model. The former term in the Equation 3.22. corresponds to the diffused fluxes, making the assumption of isotropic scattered. Furthermore, it is weighted by the Sky View Factor which gives opportunities of including the effect of artificial hindrances. The latter incorporates the reflectivity indicator ( $\bar{a}$ ) which describes the average walls and ground surfaces albedo in the modelled area.

The longwave radiation fluxes upwards and downwards are described by the set of equations. In the model, it is assumed that the vegetation will partially absorb the longwave radiation. Then it will be altered for plants own fluxes. When it comes to the horizontal radiative environment from artificial structures, it is calculated by weighting the emitted radiation of the walls with the Sky View Factor (Toudert F. A., 2005).

$$R_{lw}^\downarrow(z) = \sigma_{lw}^\downarrow(z)R_{lw}^{\downarrow,0} + (1 - \sigma_{lw}^\downarrow(z))\varepsilon_f\sigma_B\bar{T}_{f+}^4 \quad (\text{Equation 3.23.})$$

$$R_{lw}^\uparrow(z) = \sigma_{lw}^\uparrow(z)\varepsilon_s\sigma_B T_0^4 + (1 - \sigma_{lw}^\uparrow(z))\varepsilon_f\sigma_B\bar{T}_{f-}^4 \quad (\text{Equation 3.24.})$$

$$R_{lw}^\leftrightarrow(z) = (1 - \sigma_{svf}(z))\varepsilon_w\sigma_B\bar{T}_w^4 \quad (\text{Equation 3.25.})$$

where:  $\bar{T}_{f+}^4$ ,  $\bar{T}_{f-}^4$ : average foliage temperature of the overlying (+) and the underlying (-) vegetation layer,  $T_0$ : ground surface temperature,  $\bar{T}_w$ : average surface temperature building walls,  $\varepsilon_f$ ,  $\varepsilon_s$ ,  $\varepsilon_w$ : foliage, ground surface and wall emissivity,  $\sigma_B$ : Stefan-Boltzman constant.

### Fluxes of the ground and wall surfaces

To assess the temperature of the ground surface ( $T_0$ ) the energy balance equation is used in the model:

$$R_{sw,net} + R_{lw,net} - G_0 - H_0 - LE_0 = 0 \quad (\text{Equation 3.26.})$$



The first term ( $R_{sw,net}$ ) is the net shortwave radiation and  $R_{lw,net}$  is the net longwave energy fluxes received by the surface. Further components are connected with the partition of net radiation at the soil into conduction heat ( $G_0$ ) into the ground, turbulent sensible heat ( $H_0$ ) and the latent heat ( $LE_0$ ) into the atmosphere. When the artificial surfaces (walls, roofs) are concerned, the soil heat flux is replaced by the heat transmission term ( $Q_{w,r}$ ) (Bruse & Fleer, 1998).

### Radiative fluxes of the ground and partition surfaces

Taking into account the described fluxes scheme in Chapter 3.4., the net shortwave radiation can be written as:

$$R_{sw,net} = \left( R_{sw,dir}(z=0)\cos\beta + R_{sw,dif}(z=0) \right) (1 - a_s) \quad (\text{Equation 3.27.})$$

The radiation absorbed by the modelled environment is calculated with respect to the temperature of the artificial partitions and horizontal surfaces. In the equation, there is included the height of the surface ( $z$ ), the angle of incidence of the incoming fluxes ( $\cos\beta$ ) with reference to the surface exposition and the albedo of the surface ( $a_s$ ).

To assess the longwave net radiation there is made an assumption that natural elements existing above the ground layer (upper branches of a tree), longwave fluxes connected with artificial partitions as well as reflected fluxes between buildings and surfaces have got direct influence on radiative environment. Therefore, the longwave budget is split into a fraction unshielded by buildings ( $R_{lw,net}^{us}$ ) and fraction associated with the effect of modelled hurdles ( $R_{lw,net}^s$ ) (Toudert F. A., 2005).

$$R_{lw,net}(T_0) = \sigma_{svf} R_{lw,net}^{us}(T_0) + (1 - \sigma_{svf}) R_{lw,net}^s \quad (\text{Equation 3.28.})$$

According to Deardorff (1978), the first term of the equation expresses the radiation between the ground and the vegetation can be calculated as:

$$R_{lw,net}^{us} = \sigma_{lw}^{\downarrow}(0) (R_{lw}^{\downarrow,0} - \varepsilon_s \sigma_B T_0^4) + \left( 1 - \sigma_{lw}^{\downarrow}(0) \right) \frac{\varepsilon_f \varepsilon_s}{\varepsilon_f + \varepsilon_s - \varepsilon_f \varepsilon_s} (\sigma_B \bar{T}_f^4 - \sigma_B T_0^4) \quad (\text{Equation 3.29.})$$

The effect of the obstacles which is expressed as the second term of the Equation 3.28., can be described as:

$$R_{lw,net}^s = \frac{\varepsilon_w \varepsilon_s}{\varepsilon_w + \varepsilon_s - \varepsilon_w \varepsilon_s} \{ \max(\sigma_B \bar{T}_w^4, \sigma_B T_0^4) - \sigma_B T_0^4 \} \quad (\text{Equation 3.30.})$$

The term  $\bar{T}_w$  is the average temperature of the building walls and the  $\varepsilon_w$  is their emissivity. When the fluxes of building walls are concerned, the impact of the vegetation on radiative environment is neglected. In case of the vertical partition, there is made the assumption that the shielded fraction will receive two-third of the radiation as the emitted fluxes of the facades and one-third as the radiation from the ground. For the unshielded fraction, 50% of the radiation comes from the sky and the other 50% from the ground.

### Turbulent fluxes of sensible heat and vapour

The turbulent fluxes of momentum, heat and vapour at the ground and at walls are assessed on the basis of the similarity law from Monin and Obhukov. They can be describe as:

$$H_0 = \rho c_p \left[ -K_h^0 \frac{\partial T}{\partial z} \right]_{z=0} = \rho c_p \left[ K_h^0 \frac{T_0 - \theta_{k=1}}{0.5 \Delta z_{k=1}} \right] \quad (\text{Equation 3.31.})$$

$$LE_0 = \rho L_0 \left[ -K_q^0 \frac{\partial q}{\partial z} \right] = \rho L_0 \left[ K_q^0 \frac{q_0 - q_{k=1}}{0.5 \Delta z_{k=1}} \right] \quad (\text{Equation 3.32.})$$

$$L_0 = (5.501 - 0.00237(T_0 - 273.13))10^6 \quad (\text{Equation 3.33.})$$

In the equation set, there are included the temperature ( $T$ ) as well as the humidity ( $q$ ) of ground surface ( $z = 0$ ) and the first grid point vertically ( $z = 1$ ), exchange coefficient for heat ( $K_h^0$ ) and vapour ( $K_q^0$ ) between surface and air. They are calculated with regard to thermal stratification (Asaeda & Ca, 1993). In terms of free convection the Convective Transport Theory is applied to describe vertical transport by thermals (Stull, 1994).

According to Deardorff's  $\beta$ -approach (1978), the surface humidity might be assessed based on the soil moisture content at level  $z = -1$ .

$$q_0 = \beta q_*(T_0) + (1 - \beta)q(z = 1) \quad (\text{Equation 3.34.})$$

$$\beta = \min(1, \eta(z = -1)/\eta_{fc}) \quad (\text{Equation 3.35.})$$

The term  $\eta$  defines the volumetric soil water content in the first soil layer and  $\eta_{fc}$  is its value at field capacity. Additionally, the water flux is described by soil hydraulic model where appears the supplementary sink term  $S_{\eta,0}$  connected with the surface evaporation.

$$S_{\eta,0}(k = -1) = -\frac{\rho}{\rho_w} LE_0 \frac{1}{\Delta z(k=-1)} \quad (\text{Equation 3.36.})$$

where the  $k = -1$  is the first layer of the soil model,  $\Delta z$  is the thickness of the first soil layer and  $\rho_w$  is the water density.

## Soil and artificial partitions heat fluxes

The soil heat flux is described on the basis of the surface temperature as well as the temperature of the first soil layer below the surface.

$$G_0 = \lambda_s \frac{\partial T}{\partial z} = \lambda_s (k = -1) \frac{T_0 - T_{k=-1}}{0.5 \Delta z_{k=-1}} \quad (\text{Equation 3.37.})$$

The term  $\lambda_s$  is soil heat conductivity which is dependent on the soil material and water content. When the artificial partitions are concerned, the  $G$  is replaced by  $Q_w$ .

$$Q_w = k(T_w - T_{a,i}) \quad (\text{Equation 3.38.})$$

In the equation are included the heat transmission coefficient ( $k$ ) and the inside air temperature of the building ( $T_{a,i}$ ). It is worth mentioning that the heat storage of the wall material is not taken into account (Toudert F. A., 2005).

## The soil model

The diversity of building materials that make up an urban structure is enormous. The soil sub-model allows the simulation of this heterogeneous urban environment taking into account the individual properties of both natural and totally artificial materials. Thermodynamic, hydraulical properties and albedo of material can be assign to each and every single grid cell of the surface. The soil sub-model is organised as three layers (upper layer 0-20 cm, middle layer 20-50 cm, deep layer 50-200 cm) between the ground surface and the bedrock layer (below 200 cm). For all of them, there is a possibility of defining the individual hygrothermal properties. Below the bedrock layer the daily variations of temperature and humidity are assumed negligible.

The exchange processes are simulated as a vertical transfer between layers. The horizontal parameter changes are neglected. The application estimates temperature and soil volumetric moisture content by the usage of the one dimensional predictive Equation 3.39 - 3.40.

$$\frac{\partial T}{\partial t} = K_s \frac{\partial^2 T}{\partial z^2} \quad (\text{Equation 3.39.})$$

$$\frac{\partial \eta}{\partial t} = D_\eta \frac{\partial^2 \eta}{\partial z^2} + \frac{\partial K_\eta}{\partial z} - S_\eta(z) \quad (\text{Equation 3.40.})$$

For natural materials, the  $K_s$  which is the thermal diffusivity is calculated on the basis of soil moisture ( $\eta$ ) after Tjernström (1989). The hydraulic parameters used in the Equation

3.40. such as volumetric water content ( $\eta$ ), saturation value ( $S_\eta$ ), the hydraulic conductivity ( $K_\eta$ ) and the hydraulic diffusivity ( $D_\eta$ ) are calculated after Clapp & Hornberger (1978).

### The vegetation model

Vegetation is an integral part of the urban landscape. It interacts with the surrounding environment through the heat and water vapor exchange. In the application, it is possible to schematically represent vegetation elements as one-dimensional column with height ( $z_p$ ). The amount and distribution of leaves is described by the profile of leaf area density ( $LAD$ ). The same concept was applied to the distribution of green element roots. The root area density profile ( $RAD$ ) determines underground composition of trees from the ground level to the vegetation depth ( $-z_r$ ). In the model it is possible to use 3D vegetation in the form of deciduous and coniferous trees. They are differentiated in terms of  $LAD$ . Also, the user can select a specific species of tree that has been added to the software database.

### Turbulent fluxes of heat and vapour (vegetation model)

The interaction between vegetation elements and surrounding air is described by direct heat flux ( $J_{f,h}$ ), evaporation flux ( $J_{f,evap}$ ), and transpiration flux ( $J_{f,trans}$ ). These interactions are given by:

$$J_{f,h} = 1.1r_a^{-1}(T_f - T_a) \quad \text{(Equation 3.41.)}$$

$$J_{f,evap} = r_a^{-1}\Delta q\delta_c f_w + r_a^{-1}(1 - \delta_c)\Delta q \quad \text{(Equation 3.42.)}$$

$$J_{f,trans} = \delta_c(r_a + r_s)^{-1}(1 - f_w)\Delta q \quad \text{(Equation 3.43.)}$$

where  $T_a$  is the air temperature,  $q_a$  is the specific humidity of air surrounding the vegetation leaves and  $\Delta q$  is the humidity deficit with  $\Delta q = q_*(T_f) - q_a$ .  $T_f$  is the foliage temperature and  $q_*$  is the saturation value of  $q$  at the leaf surface. The aerodynamic resistance ( $r_a$ ) is provided by the function of the leaf geometry and wind speed. According to Barden (1982), it is described as:

$$r_s = A \sqrt{\frac{D}{\max(W, 0.05)}} \quad \text{(Equation 3.44.)}$$

Parameter  $A$  depends on the selected vegetation species. For conifers and natural substrate (grass) it is  $A = 87 \text{ sec}^{0.5}\text{m}^{-1}$ . For deciduous trees it oscillates within  $A = 200 \text{ sec}^{0.5}\text{m}^{-1}$ . The  $D$  value, which is typical leaf diameter, varies from 0.02 m (conifers) to 0.5 m or more (tropical plants). The last parameter  $W$  is a wind speed at the leaf surface.  $r_s$  is dependent

on short-wave irradiance input and soil water. The photosynthetic process is estimated after Deardorff (1978) or Jacobs (1994). When evaporation and transpiration process are present, the coefficient ( $\delta_c$ ) is 1. Then, ( $f_w$ ), which describes the fraction of wet leaves, is included in Equation 3.42 - 3.43. Otherwise, only the condensation phenomenon is considered, while  $\delta_c = 0$ .

$$f_w = \left( \frac{W_{dew}}{W_{dew,max}} \right)^{2/3} \quad (\text{Equation 3.45.})$$

where  $W_{dew}$  is the amount of dew on leaf surfaces and  $W_{dew,max}$  is the maximum possible value ( $0.2 \text{ kgm}^{-2}$ ).

### Energy balance of leaves

Temperature of foliage is based on the assumption of the steady-state leaf energy budget. Then, the internal energy storage of the vegetation (a single leaf) is neglected (Toudert F. A., 2005).

$$0 = R_{sw,net}(z) + R_{lw,net}(z) - c_p \rho J_{f,h} - \rho L (J_{f,evap} + J_{f,tran}) \quad (\text{Equation 3.46.})$$

$c_p$  is the specific heat of the air,  $\rho$  is the air density and ( $L$ ) is the latent heat of vaporization. The parameter  $R_{sw,net}$ , which is the net shortwave radiation absorbed by the surface of leaves, can be obtain on the basis of the Equation 3.47.

$$R_{sw,net}(z) = (FR_{sw,dir}(z) + R_{sw,dif}(z))(1 - a_f - tr_f) \quad (\text{Equation 3.47.})$$

First non-dimensional parameter ( $F$ ) describes the orientation of leaves towards the sun. Value  $F = 0.5$  is assigned to randomly oriented leaves. The albedo of the vegetation is represented by ( $a_f$ ). Last value ( $tr_f$ ) of transmission factor is set to 0.3. Net longwave radiation flux is given by:

$$R_{lw,net}(z, T_f) = \varepsilon_f R_{lw}^\downarrow(z) + R_{lw}^{\leftrightarrow}(z) + \varepsilon_f R_{lw}^\uparrow(z) - 2\varepsilon_f \sigma_B T_f^4 - (1 - \sigma_{svf}(z)) \sigma_B T_f^4 \quad (\text{Equation 3.48.})$$

where ( $\varepsilon_f$ ) is the emissivity of leaves.

The source/sink terms, which were mentioned in Equation 3.2., are calculated after solving the Equation 3.41 - 3.43. There is taken into account the  $LAD$  on the specific heights.

$$Q_h(z) = LAD(z) J_{f,h} \quad (\text{Equation 3.49.})$$

$$Q_q(z) = LAD(z) (J_{f,evap} + J_{f,trans}) \quad (\text{Equation 3.50.})$$

Additionally, the dependency between water transpiration by the plant and water supply by the soil is included in the sub-vegetation model. If there is not enough water content in the soil, the stomatal resistance of leaves will be increased. This way, the transpiration rate will be decreased. The total transpiration of vegetation expressed by the vertical integral over the transpiration fluxes in various plant elements is given by:

$$m_{trans} = \rho \int_0^{z_p} LAD(z) J_{f,trans}(z) dz \quad (\text{Equation 3.51.})$$

Taking into consideration Pielke's (1984) suggestion, the water content comes from the underground layer. It is connected with the root density ( $RAD$ ) and the hydraulic diffusivity of the soil layer ( $D_\eta(z)$ ).

$$S_\eta(-z) = \frac{m_{trans}}{\rho_w} (RAD(-z) D_\eta(-z)) \left( \int_{-z_r}^0 RAD(-z) D_\eta(-z) dz \right)^{-1} \quad (\text{Equation 3.52.})$$

### 3.5. The human-biometeorological dimension

BioMet module allows to estimate the influence of created urban structure on human thermal comfort. The input data are the parameters calculated from the simulation of atmospheric processes. Microclimatic conditions are determined by air temperature ( $T_a$ ), mean radiant temperature ( $T_{mrt}$ ), horizontal wind speed ( $uv$ ) and specific humidity ( $q$ ). The mean radiant temperature is used to express the effect of radiation. In this case approximation is made for each grid point ( $z$ ) as:

$$T_{mrt} = \left[ \frac{1}{\sigma_B} \left( E_t(z) + \frac{\alpha_k}{\varepsilon_p} (D_t(z) + I_t(z)) \right) \right]^{0.25} \quad (\text{Equation 3.53.})$$

In the equation are considered direct irradiance  $I_t(z)$ , diffused and diffusely reflected solar radiation  $D_t(z)$  and total long-wave fluxes  $E_t(z)$ . The last one is treated as the emission from the sky, the ground and from surrounding artificial partitions of objects. There is the assumption that long-wave radiation originates from the upper hemisphere (50%) and the ground (50%). The  $T_{mrt}$  calculation is valid only at street level. It is connected with the fact that the ground influence decreases with the height (Equation 3.54.) (Huttner, 2012).

$$E_t(z) = 0.5 \left[ (1 - \sigma_{svf}(z)) R_{lw}^{\uparrow} + \sigma_{svf}(z) R_{lw}^{\downarrow,0} \right] + 0.5 \varepsilon_s \sigma_B T_0^4 \quad (\text{Equation 3.54.})$$

The long wave radiation emitted by the walls was described as the Equation 3.25. (radiative fluxes).  $R_{lw}^{\downarrow,0}$  is the downward radiation flux coming from the visible part of the sky. The second equation term - heat flux from the ground ( $0.5 \varepsilon_s \sigma_B T_0^4$ ) takes into account the actual surface temperature ( $T_0$ ).

$$D_t(z) = \sigma_{svf}(z)R_{sw,dif}^{\downarrow,0} + (1 - \sigma_{svf}(z))\bar{a}R_{sw,dif}^{\downarrow,0} \quad (\text{Equation 3.55.})$$

The total diffused radiation  $D_t(z)$  is treated as the combination of a flux coming from the sky and diffusely reflected flux from walls.  $\bar{a}$  term in the Equation 3.55. is the mean albedo of the model area.

At the end, the interconnections between human body and environmental factors are included. The absorption of the direct solar irradiance by the body is expressed by the projection factor ( $f_p$ ). It includes the position of the sun (height)(Toudert F. A., 2005).

$$I_t(z) = f_p R_{sw,dif}^{\downarrow}(z) \quad (\text{Equation 3.56.})$$

$$f_p = 0.42\cos\phi + 0.043\phi \quad (\text{Equation 3.57.})$$

Human physical conditions are determined based on body parameters (age of person, gender, weight, height and surface area - DuBois), clothing parameters (static clothing insulation), and personal metabolism (basal rate, work metabolism and walking speed).

The tool (BioMet module) allows to assess the influence of building form on thermal sensations of users living in urban spaces. This is possible on the basis of microclimatic conditions described above and certain physical parameters of humans. For this purpose are used four rational indices such as: Predicted Mean Vote (PMV), Standard Effective Temperature (SET), Physiological Equivalent Temperature (PET), Universal Thermal Climate Index (UTCI), which were found to be adjusted for conducting research in outdoor environment. A detailed description of the indices can be found in Chapter 2.3.2. The thermal comfort indices. The use of PMV has been questioned by numerous researchers. This is due to the discrepancy between the results obtained from the simulation process and the surveys with respondents (Thorsson et al., 2004). The use of SET and UTCI does not provide comparative data for different climate zones (Fischereit & Schlunzen, 2018). Moreover, the calculation of indices is conducted by assuming some simplifications of the equations. The application developers point out that some limitations due to programming assumptions should be taken into account during the research. According to them, Physiological Equivalent Temperature is the only indicator that allows correct estimation of human perceived thermal conditions. The PET is considered to be the most widely used in the field of urban microclimatology. It has been applied in studies conducted for diverse climatic zones. Therefore, it provides comparative results.

### 3.6. Model validation

The ENVI-met model is used to conduct analyzes of climatic conditions as well as thermal comfort in highly urbanized areas. Numerous authors apply the numerical-simulation-related three-step approach, i.e. modelling, validation and scenario simulation. Therefore, it can be concluded that the performance of the model constantly undergoing thorough verification. The published research results indicate that numerical simulations are characterized by the high accuracy of microclimatic predictions.

Model validation is conducted on the basis of real meteorological data. They come from a series of measurements carried out in dense, city centre areas. Then, basic microclimatic parameters are measured. According to Liu et al. (2021) the most frequently used variable to perform model validation is air temperature (over 90% of studies), followed by relative humidity (~ 28%) and mean radiant temperature (~ 13%). Tests are also carried out on the basis of surface temperature, air flow, solar radiation and longwave radiation. For thermal comfort indicators, the Physiological Equivalent Temperature (~ 10%) is taken into account.

The studies consider the difference measures of the model evaluation. The basic one is the coefficient of determination ( $R^2$ ), which is a key output of regression analysis, describing the proportion of the total variance explained by a model (used in ~65% works; Willmott, 1981). Then, the Root Mean Square Error (RMSE), the Systematic Root Mean Square Error (RMSEs), the Unsystematic Root Mean Square Error (RMSEu) are used. The last one is Willmott's index of agreement (d), which describes how error-free variables are simulated by a model. Simulations are considered to be reliable if these measures are close to the requirements:  $R^2 \rightarrow 1$ , RMSEs  $\rightarrow 0$ , RMSEu  $\rightarrow$  RMSE and  $d \rightarrow 1$ . Examples of the validation results of the ENVI-met model are presented in Table 3.3.

**Table 3.3.** Quantitative chosen measures of the performance of the ENVI-met.

Study	City, Country	Variable	Model validation
Hedquist & Brazel (2014)	Phoenix, USA	$T_A$	$R^2$ : 0.99 RMSE: 1.46 °C d: 0.94
Acero & Herranz-Pascual (2015)	Bilbao, Spain	$T_A$	$R^2$ : 0.96
		$T_{mrt}$	$R^2$ : 0.71
		RH	$R^2$ : 0.93
		PET	$R^2$ : 0.73
Duarte et al. (2015)	Sao Paulo, Brazil	$T_A$	RMSE: 1.61 °C d: 0.85



**Table 3.3.** Continuation.

Jänicke et al. (2015)	Berlin, Germany	T <sub>A</sub>	R <sup>2</sup> : 0.89 RMSE: 1.35 °C
		T <sub>mrt</sub>	R <sup>2</sup> : 0.94
Lee et al. (2016)	Freiburg, Germany	T <sub>A</sub>	R <sup>2</sup> : 0.85 RMSE: 0.66 °C d: 0.95
		T <sub>mrt</sub>	R <sup>2</sup> : 0.86 RMSE: 5.49 °C d: 0.95
		PET	R <sup>2</sup> : 0.77 RMSE: 3.98 °C d: 0.84
Salata et al. (2016)	Rome, Italy	T <sub>A</sub>	R <sup>2</sup> : 0.88 RMSE: 1.89 °C d: 0.91
		T <sub>mrt</sub>	R <sup>2</sup> : 0.96 RMSE: 2.79 °C d: 0.87
Ayyad & Sharples (2019)	Amman, Jordan	T <sub>A</sub>	R <sup>2</sup> : 0.93 RMSE: 2.45 °C d: 0.89
Bochenek & Klemm (2017-2021) <sup>1</sup>	Lodz, Poland	T <sub>A</sub>	Street canyon RMSE: 0.72 °C Forecourt RMSE: 0.61 °C

**Source:** own elaboration.

---

<sup>1</sup> Experimental studies have been conducted since 2017. The area of the study, where field measurements were performed, was the Metropolitan Area of Lodz. The results were then used to evaluate numerical models performed with the Envi-met software. The outcomes of the research project will be published in the form of a scientific publication.

## CHAPTER IV. SELECTION OF URBAN FORMS

Depending on the scale of research in the field of urban climatology, two influence zones of urban forms are distinguished. The first one is related to the impact within the street level (up to the height of the first building storey). This is when the assessment of the influence of microclimatic conditions on human comfort in the outdoor environment is carried out. Within the second zone - the level above the street (up to the roof height), the analysis of the influence of external parameters on the user of building constructions is carried out (Zielonko-Jung, 2013). According to Ratti et al. (2003), the phenomena occurring at the city microscale are particularly important for those associated with urban planning. Finding the relationship between structure indicators and microclimate parameters can contribute to the proper formation of thermal conditions in cities.

In this study, the Metropolitan Area of Lodz has been selected as the research area. The street canyon and city forecourt were considered to be characteristic urban forms.

### 4.1. Street canyon

Street canyons are the basic element of urban zone. According to Sharifi (2019), they are the backbone that determines the development of a settlement unit. Properly designed, they can contribute positively to the evolution of cities. They influence the adaptability of structures when socio-demographic and technological changes occur. They are the elements that connect the nodal points (public spaces such as squares) and are responsible for communication flows. Moreover, they influence the existence and functioning of industries (e.g. energy).

The study of street canyons is carried out at a scale covering settlement units within administrative boundaries. Then accessibility, connectivity, compatibility, diversity, density, nodality and containment of urban street canyons are considered (Abdelmonem et al., 2019). At the microscale, selected street canyon structures become the subject of study. Their form is determined by the relationship of building lines to street space. In inner city areas, the side walls of the canyon are formed by the fronts of townhouses adjacent to the street line. In case of detached houses, the side walls are formed by buildings (most often residential buildings) that are separated from the building line, which is the registered boundary of the building plot. The space between them constitutes the floor of created urban interior - the street canyon.

The literature mentions two parameters used to describe the form of a street canyon - Aspect Ratio, and Sky View Factor. The former, also called Height-to-Width ratio (Figure 4.1.), is the ratio between the height of building frontage extending on both sides of the street canyon and the distance between the buildings. It is a dimensionless index with positive values. The higher the index value, the higher the development structure appearing along the communication route. For symmetrical canyons, the AR parameter is calculated as the average value of buildings' heights occurring on both sides of the passage in relation to the distance between the buildings. For asymmetrical canyons, the ratio coefficient is expressed by Equation 4.1.

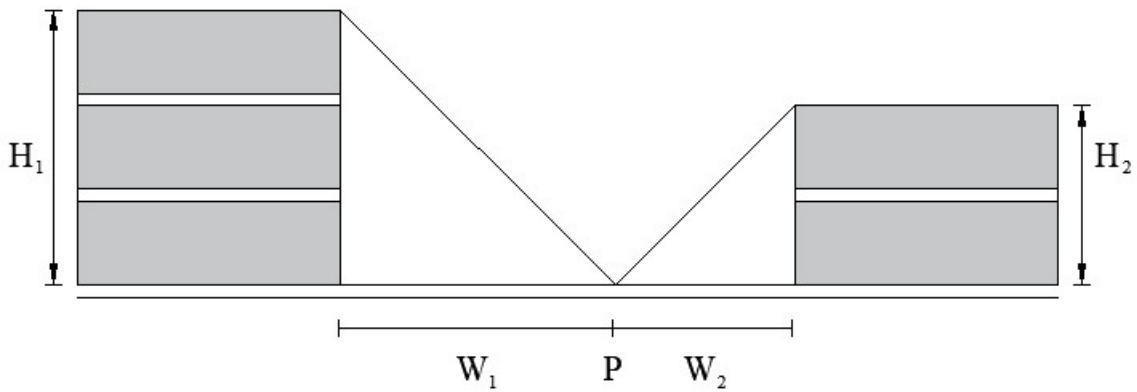


**Figure 4.1.** Parameters used to determine the Aspect Ratio for asymmetric canyons (source: own elaboration).

$$AR (H/W \text{ ratio}) = (h_1 + h_2) / 2(w_1 + w_2) \quad (\text{Equation 4.1.})$$

where:

$h_1, h_2$  - describe the height of view obscuration by building constructions at point  $P$ , while  $w_1, w_2$  - characterize the distances of vertical obscuring planes from point  $P$ .

Another parameter is the Sky View Factor ( $SVF$  or  $\psi_s$ ) characterizing the fraction of visible sky on a hemisphere centered over the analyzed location (Oke, 1981; Figure 4.2.). It is a dimensionless parameter taking values ranging from 0 to 1. The higher the index value, the lower the sky obscuration level by obstacles. It can also be argued that the lower the parameter value, the greater the degree of compactness of the urban interior. In case of characterizing the form of street canyons, this index is calculated based on Equation 4.2. (Bernard et al., 2018).

$$SVF_{can} = \cos(\text{atan}(2H/W)) \quad (\text{Equation 4.2.})$$

where:  $H/W$  is the ratio of buildings height forming the side walls of the street canyon to its width.

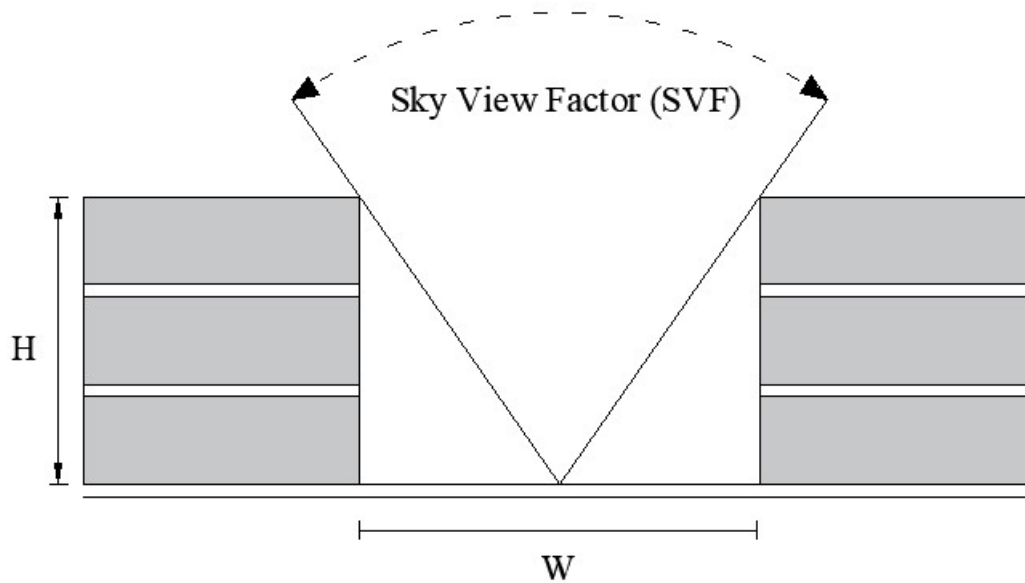


**Figure 4.2.** Sky View Factor (source: own elaboration).

### **Typicality of street canyons in Lodz**

The study area was the most urbanized part of Lodz - the Metropolitan Area. Based on the information on the urban structure of Metropolitan Area, the parameters of a typical street canyon were estimated. The development form data were collected from the state institution (Lodz Surveying Centre). They had the form of editable vector files (building geometry). Descriptive file versions (attribute tables) were obtained along with them. The information concerned 13.315 building constructions, as well as 10.050 record plots. Information such as the number of above-ground storeys, dimensions of buildings, length and width of registered parcels, and width of traffic routes was used to determine the typicality of street canyons.

At first, the dimensions of reference areas for buildings - registered plots - were determined. In this case, a method was used to calculate the parameters based on the information obtained by generation of building vertexes. The average dimensions of evidential plots were 26.77 m in width, and 42.08 m in length. Next, the parameters of buildings forming the frontage of street canyons within the Metropolitan Area of Lodz were estimated. In this case, it was also necessary to generate the points constituting the building vertexes. Based on the two-dimensional coordinates of building vertexes, the length, width, and surface area of buildings were determined. The parameters of frontal buildings (tenement houses) were on average 10.88 m wide, and 26.77 m long. In the case of building area, the parameter variation was evident. Its value averaged  $136 \text{ m}^2 (\pm 143 \text{ m}^2)$ . It means that there is a diversity of urban forms in the Metropolitan Area. This phenomenon is typical

of inner-city zones, where the functions of buildings are diversified (e.g. residential, office, retail and service, transport and communications, industrial and warehousing, other non-residential). In order to assess the parameters of side outbuildings, it was necessary to determine the degree of development of registered plots. It was 38% of the area. Taking into account the building parameters, as well as the land plots, it was assumed that there will be two symmetrical side outbuildings (8 m wide by 10 m long). The next step was to calculate the building height. This was possible on the basis of descriptive information contained in the table of attributes for the buildings. The average height of buildings fronting the side walls of street canyons of the Metropolitan Area was 4 storeys.

The street canyon floor, which is the space between the front buildings of the tenement houses, was determined based on geometric data available in vector form, as well as descriptive information contained in the attribute table for the buildings. The parameters for each of street canyons of the Metropolitan Area were calculated using the available measurement functions in QGIS software. The distance between the buildings fronting on the study area, and thus the width of canyon was 16.5 meters. Its length oscillated within 197.51 meters.

Further, the building materials of a typical street canyon interior were estimated, as well as the buildings that form the development frontage. Determination of the floor materials was possible on the basis of descriptive as well as geometric information for the Metropolitan Area obtained from the database of the Surveying Centre of Lodz. For each of the canyons, the percentage of each building material used to create the floor was calculated. The research showed that the surfaces defined as impermeable constituted approx. 98% (including the percentage of asphalt surfaces of 51%), permeable surfaces approx. 1%, and those defined as other constituted 1% of the canyons' surface. The group of impermeable pavements included asphalt, concrete, cobblestone, precast pavers, stone pavers, bituminous mass, clinker, and concrete slab. The permeable surfaces were natural soil.

Data on construction materials of the front structures were not available as descriptive files in the database of the Surveying Center of Lodz. It was necessary to obtain information from the record cards of immovable monuments held at the office of the Municipal and Regional Conservator of Monuments in Lodz. At the moment of data collection, 551 registration cards were available. The information concerned the front buildings that form the frontage of street canyons in the Metropolitan Area of Lodz. In this study, they were used to assess the dimensions of building envelope, wall construction materials, as well as

the inclination and type of roofing of the frontage buildings in street canyon. A summary of the basic information on the buildings is presented in [Table 4.1](#).

**Table 4.1.** Development parameters in the Metropolitan Area.

<b>Development parameters in the Metropolitan Area</b>	<b>Number of buildings</b>	<b>Percentage of buildings [%]</b>
building material: brick	416/551	75%
mortar: cement-lime	292/551	53%
facade: plaster	451/551	82%
roof pitch: pitched	332/551	60%
roof covering: tar paper	479/551	87%

**Source:** own elaboration.

The analyses conducted showed that ceramic brick was the primary building material. It was used in 416 structures (75.49%). Other materials mentioned were brick (70 buildings - 12.70%), clinker brick (4 buildings - 0.72%) and wood (1 building - 0.18%). In 60 cases (10.88%), the information about the building material used was not specified. However, it was indicated that it was a brick building. In most buildings, cement-lime mortar was used (292 buildings - 52.99%). Other mentioned mortars were lime (76 buildings - 13.79%), cement (5 buildings - 0.90%), lime-sand (1 building - 0.18%). For 177 cases (32.12%) no information was provided about the type of mortar used. Additionally, information was obtained on the number of buildings that were covered with plaster from the outside (451 buildings - 81.85%).

In case of roof covering analyses, the information provided in the registration cards of immovable structures was used. They were verified using the data provided by the Internet Terrain Information System for Lodz (InterSIT), as well as oblique images for the city. The dominant type of roofing was pitched roof (332 cases - 60.25%). Other mentioned types were multi-sloped (118 buildings - 21.41%), single-sloped (54 buildings - 9.80%), and flat (41 buildings - 7.44%). A significant number of buildings were covered with tar paper (479 - 86.93%). Other mentioned roofing materials were metal sheet (54 buildings - 9.80%), tile (13 buildings - 2.35%), metal tile (1 building - 0.18%). No information on the roofing material used was provided for 4 buildings.

### **Three-dimensional model of typical street canyon in Lodz**

The street canyon was the first urban form for which a 3D model was created. The geographical location chosen was the Metropolitan Area of Lodz - 19°27'59"E (longitude), 51°45'00"N (latitude). The selection was based on the available database of landmarks in the application. Geographical coordinates of one of the hotels (Grand Hotel) located at the main traffic route of the city were taken as a reference point. It was a point located in the center of the Metropolitan Area. The choice of location for the model was related to the automatic generation of model input parameter values (e.g. radiation). Therefore, providing such geographic coordinates allowed the initial conditions in the study area to be reflected.

Next, it was proceeded to create the three-dimensional structure of street canyon. Based on the analysis results conducted for the development form, the model dimensions were determined. They were 198 m long, 58 m wide, and 30 m high. Accordingly, the model resolution was 1 m x 1 m x 1 m. For the vertical structure, an equidistant grid was chosen. The result was a grid of cells with equal dimensions in all directions ( $\Delta x = \Delta y = \Delta z$ ).

The building materials of model were determined based on the analyses conducted for the Metropolitan Area. Impermeable material - concrete cube (forecourt interiors, pedestrian walkway zones) was selected as the ground surface. The interior of street canyon was covered with asphalt (roadway). When creating buildings, it was necessary to make changes in the application settings. A building wall structure characterized by the Metropolitan Area was added. It consisted of an inner layer created from ceramic brick, as well as outer layers made of plaster. The wall parameters such as thickness, absorption, transmission, reflection, emissivity, specific heat, thermal conductivity and density are shown in [Figure 4.3](#). In the database it was necessary to add the roof covering - tar paper. Its parameters are shown in [Figure 4.4](#).

Having a database of materials characterized by the Metropolitan Area, the frontage of the street canyon development (on both sides of the communication route) was created. It consisted of frontal structures measuring 27 meters in length, and 11 meters in width. Two symmetrical side outbuildings with dimensions of 8 meters in width, as well as 10 meters in length were assumed to occur on the registered plots. According to the preliminary project assumptions, the development area within the registered plots was ~ 40%. The final project consisted of seven front structures, as well as fourteen side outbuildings forming the development frontage along the canyon. The distance between the building frontages, and thus the canyon width, was 16 m ([Figure 4.5](#)).

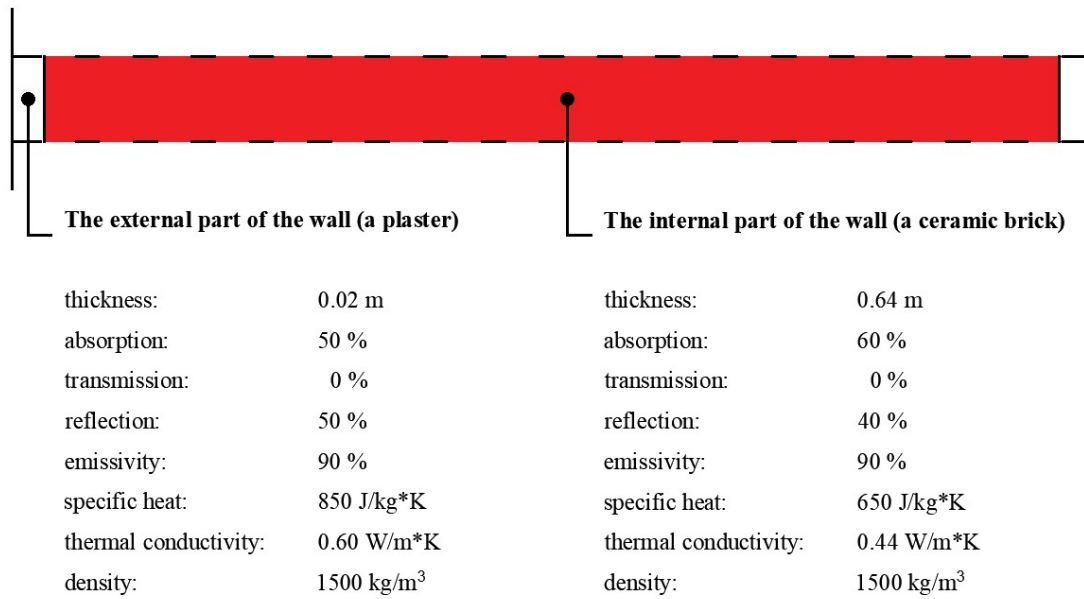


**Figure 4.3.** Wall parameters of a building characterized by the Metropolitan Area in Lodz (source: own elaboration).

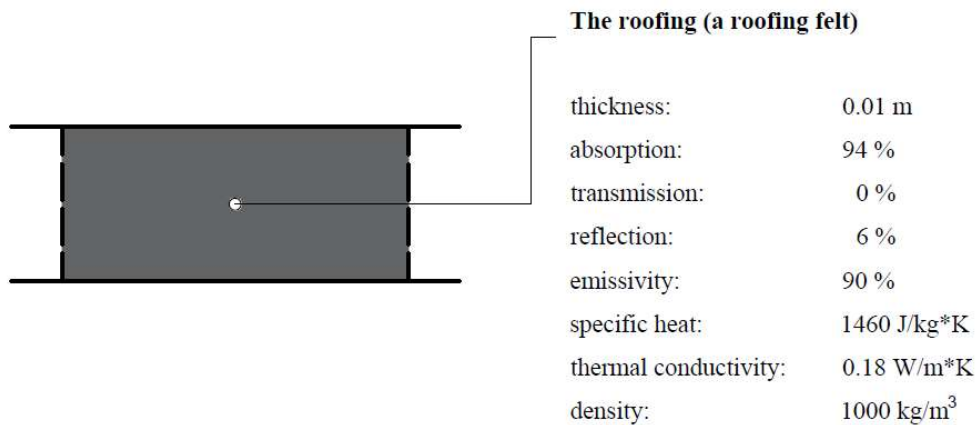


**Figure 4.4.** Roofing parameters of a building characterized by the Metropolitan Area in Lodz (source: own elaboration).

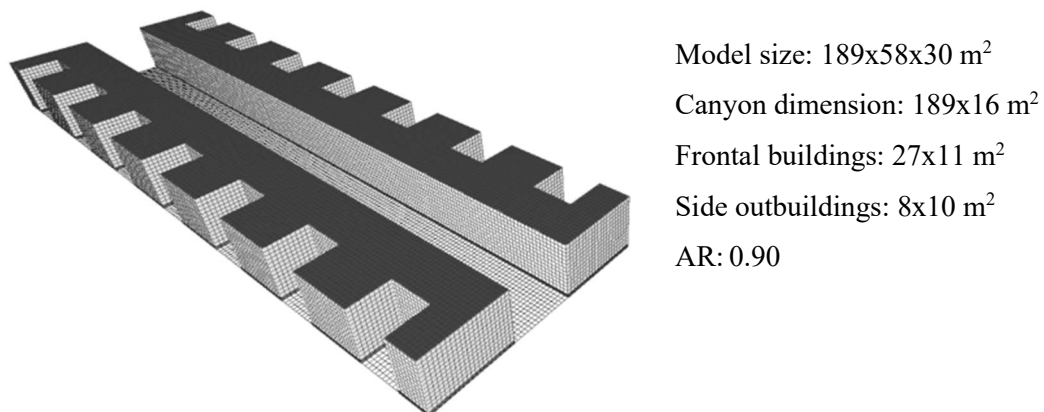


**Figure 4.5.** The model of the typical canyon in the Metropolitan Area in Lodz (source: own elaboration).



## 4.2. Forecourt

Changes in climatic conditions have the greatest impact on residents in the influence zone of building groups. This area is called the building neighborhood scale, which extends up to 1.000 meters. According to Ragheb et al. (2016), it is the land use pattern that determines the local microclimate. In particular, the influence of development form for land parcels in highly urbanized areas is emphasized (Middel et al., 2014).

The composition and interrelationships of buildings create the city's unique character. Forecourts are cited as the most desirable compact development structures. They are defined as an enclosed or semi-enclosed space by a compact arrangement of buildings within a parcel of land. They were initially associated with Asian, Middle Eastern, South American, and Mediterranean cultures. This was related to the development form aimed at improving thermal conditions in the immediate vicinity of the residence (Ghaffarianhoseini et al., 2015). Currently, a compact development structure with an internal forecourt is considered one of the most efficient forms of space management. The forecourt-type form provides the possibility to design intensive development (horizontally) with free internal space. In addition, it contributes to limiting the development of settlement units in the vertical dimension.

### Typicality of forecourts in Lodz

In order to determine the typicality of forecourts within the Metropolitan Area, vector and descriptive data were used, which were obtained from the Surveying Centre of Lodz. The information concerned the height, perimeter, and surface area of building structures and the surface area of registered plots (Figure 4.6. - 4.7.). On their basis, the morphological parameters of buildings were calculated, i.e. average building height (Equation 4.3.), site coverage ratio (Equation 4.4.), and façade to site ratio (Equation 4.5.) (Salvati et al., 2015).<sup>2</sup>

---

<sup>2</sup> Due to the fragmented structure of the city's registered plots, it was necessary to develop indicators for the urban quarters. Building constructions were assigned quarters' identification numbers. In this way, it was possible to estimate the indicators of building parameters for each of the quarters. Finally, it was assumed that the indicators could be assigned to the structure occurring in the registered plots, which were considered as reference areas.

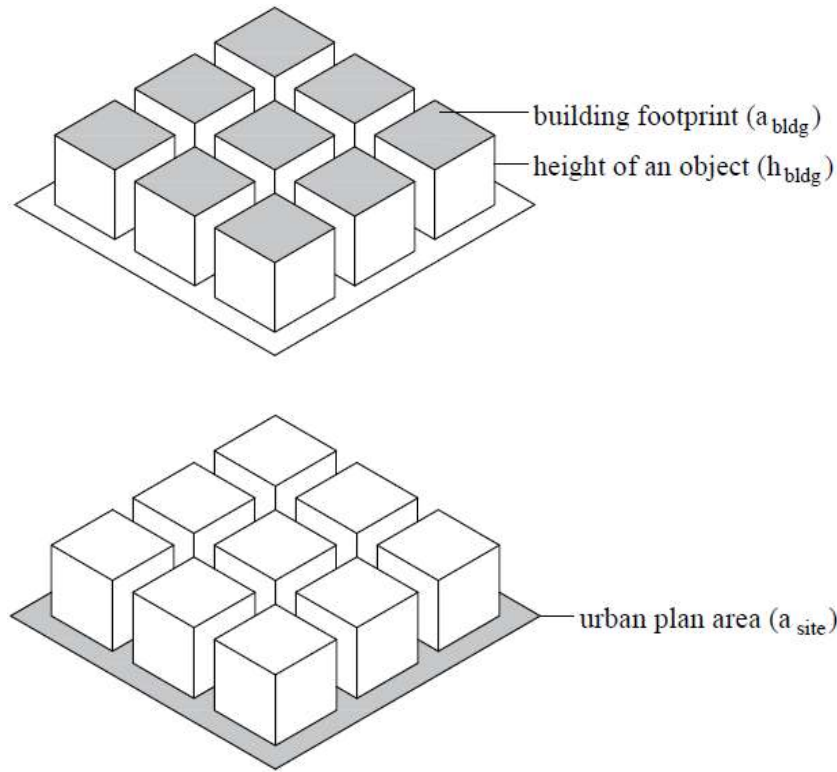


**Figure 4.6.** Morphological parameters necessary to calculate average building height and site coverage ratio (source: own elaboration based on [Salvati et al., 2015](#)).

$$h_{avg} = \frac{\sum h_{bldg} a_{bldg}}{a_{site}} \quad \text{(Equation 4.3.)}$$

Average building height ( $h_{avg}$ ) is defined as the average building height ( $h_{bldg}$ ) in a reference area ( $a_{site}$ ), normalized by building footprint ( $a_{bldg}$ ). It allows to describe the vertical development structure in the selected site. Determination of site coverage ratio ( $\rho_{urb}$ ) allows to estimate the built-up area. It is calculated as a ratio of building footprint ( $a_{bldg}$ ) to the site area ( $a_{site}$ ).

$$\rho_{urb} = \frac{\sum a_{bldg}}{a_{site}} \quad \text{(Equation 4.4.)}$$

The last one estimates the side wall area of buildings ( $VH$ ). It is calculated as the ratio of vertical surface area ( $\sum P_{bldg} h_{bldg}$ ) to the urban plan area ( $A_{site}$ ). Thus, it defines the size of urban barrier, which is the development.

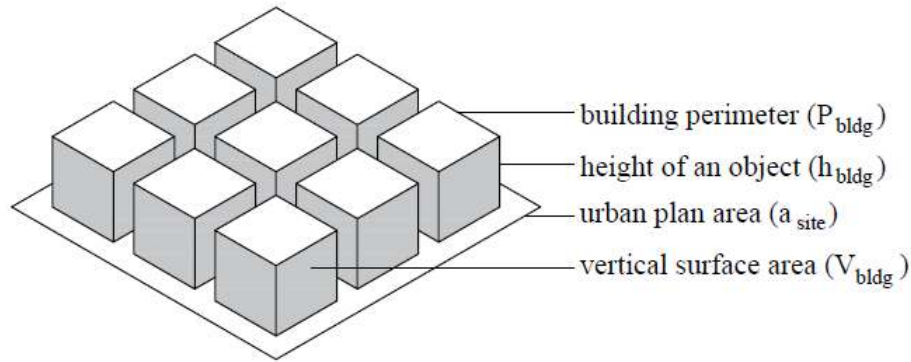


**Figure 4.7.** Morphological parameters necessary to calculate façade to site ratio (source: own elaboration based on Salvati et al., 2015).

$$VH = \frac{\sum P_{bldg} h_{bldg}}{a_{site}} \quad \text{(Equation 4.5.)}$$

Additionally, Aspect Ratio and Sky View Factor were calculated in order to describe the development structure.

Table 4.2. shows the development parameters that characterize the Metropolitan Area. It should be noted that these are values attributed to all structures (residential, office, retail and service, transportation and communications, industrial and warehouse, and other non-residential). The average building height ( $h_{avg}$ ) was  $11.31 \text{ m} \pm 1.60 \text{ m}$ . According to the Regulation of the Minister of Infrastructure of 12 April 2002 on Technical Conditions, Which Should Correspond to the Buildings and Their Location (2002), buildings with a vertical dimension of up to 12 m are considered low-rise (up to and including 4 overground storeys). Others are classified as medium-high (more than 4 to 9 storeys inclusive, which is equivalent to a height of 12 to 25 m above ground level). The degree of development ( $\rho_{urb}$ ) averaged 38% of the area of registered plots. The maximum calculated value was 62%. It should be noted that it was estimated on the basis of information for quarters of the Metropolitan Area. In reality, the degree of development of registered plots in the strict city centre zone reaches 100% (location of the building directly on the boundary). In case of quarters, the value will be lower, which is related to maintaining the distance of buildings from the plot boundary, the parameter of maximum building area on the plot, as well as the minimum percentage of biologically active area. The requirements are related to provisions of the Regulation of the Minister of Infrastructure of 12 April 2002 on Technical Conditions, Which Should Correspond to the Buildings and Their Location (2002), as well as local spatial development plans. Another parameter - facade to site ratio oscillated within the range of  $1.09 \pm 0.76$ . This means that the front wall area of development was significant

within the quarter. The buildings will be a barrier for airflow in the city. The other parameters described the degree of compactness of urban development. Aspect Ratio averaged 0.18 and Sky View Factor averaged 0.62, which means that the variation of downtown buildings is high. Although the degree of compactness of the quarters' development frontages is high, it is not possible to confirm this fact by calculating the Sky View Factor. This is due to the distribution of buildings located inside the quarters, where undeveloped areas exist. As a result, there is a large dispersion of Aspect Ratio values, as well as Sky View Factor.

**Table 4.2.** Morphological parameters of development in the Metropolitan Area.

INDICES	min value	median	max value
average building height ( $h_{avg}$ )	5.63 m	11.31 m	17.88 m
site coverage ratio ( $\rho_{urb}$ )	0.11	0.38	0.62
façade to site ratio	0.07	1.09	5.86
Aspect Ratio	0.05	0.18	0.75
Sky View Factor	0.18	0.62	0.95

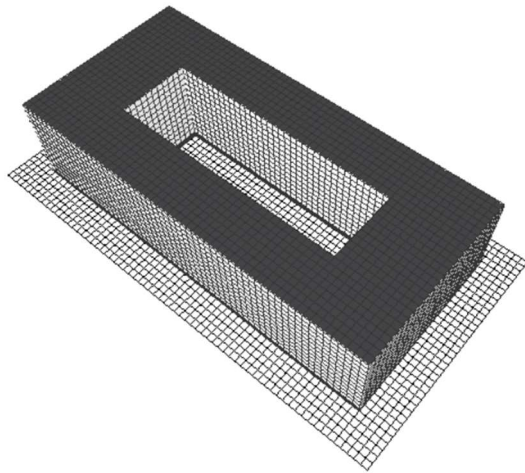
**Source:** own elaboration.

### Three-dimensional model of typical forecourt

Based on the analysis results, a typical forecourt model was developed. The Metropolitan Area was selected as the location. The choice was made on the basis of characteristic points in the city available in the ENVI-met application database. Correct definition of latitude and longitude was important due to meteorological parameters (e.g. radiation), which are generated automatically by the software.

The site dimensions were 37 m wide and 58 m long. This was consistent with the parameter assumptions for the land parcels in [Chapter IV. Selection of urban form](#). An equidistant grid was selected as the vertical grid structure. The defined model dimensions were 37 x 58 x 30 cells with a resolution of 1 m x 1 m x 1 m ([Figure 4.8.](#)). The forecourt was assumed to be a type of enclosed space through a compact layout of buildings. Accordingly, the buildings sited in the reference area were a front building (27 m x 11 m), two side outbuildings (8 m x 36 m), and a rear outbuilding (8 m x 27 m). The average building height was 7.63 m, site coverage ratio was 55%, and facade to site ratio was 2.17. Similarly to the street canyon model, the predominant building material types within the Metropolitan Area were used. Concrete pavement grey was used as the base material. The

materials characteristic of building structures within the Metropolitan Area are shown in [Table 4.1](#). Brick and plaster were selected as the primary building wall materials. The roofing material used was tar paper. Their parameters are shown in [Figure 4.3 - 4.4](#).



Model size: 37x58x30 m<sup>2</sup>  
Frontal building: 27x11 m<sup>2</sup>  
Side outbuildings: 8x36 m<sup>2</sup>  
Rear outbuilding: 8x27 m<sup>2</sup>  
AR: 0.90

**Figure 4.8.** The model of the typical forecourt in the Metropolitan Area in Lodz (source: own elaboration).

## CHAPTER V. CITY'S MICROCLIMATIC CONDITIONS

Typical meteorological years, created on the basis of 30-year data sequences (from 1971-2000), are downloadable from the website of the Institute of Meteorology and Water Management of the National Research Institute. However, in the era of progressing climatic changes, especially global warming, they do not reflect the conditions of external environment. Therefore, it is proposed to redesignate the Typical Meteorological Year for Lodz, which will allow to describe the average climatic conditions in the city.

At further stages of the research work, the information for the warmest day of a Typical Meteorological Year was used. This was due to the fact that in the summer there is an increase in people's physical activity in public spaces (Huang et al., 2016). In this study, these data were used to assess the impact of typical forms and adaptation strategies on the microclimatic conditions, as well as the thermal comfort felt by humans in the external environment. Finally, the information was used to determine the impact of adaptation strategies on the conditions inside buildings located in the Metropolitan Area of Lodz.

### **Typical Meteorological Year for the city**

Typical Meteorological Year constitutes a set of parameters characterizing the average climate of considered geographical area. It is compiled, depending on the determination method, based on hourly meteorological data over a period of at least 10 years, with a preference for 20- or 30-year sequences. The typical reference year replaces the long-term measurement and observation data with a representative period of one year, which is considered to be the most typical in the multi-year period, or is a composite of twelve months from different years of selected multi-year period. The second method is more popular due to the low probability of twelve months within a sequence that would represent the average conditions that characterize the geographic area under consideration. It is important to note that the reference year created does not describe extreme or semi-extreme conditions (Crawley, 1998).

Typical Meteorological Year for the Polish territory was prepared in relation to the introduction of [the Regulation of 6 November 2008 on the methodology for calculation of energy performance of buildings constituting an independent technical and utilitarian entity, as well as the method of preparation and examples of their energy performance certificates \(2008\)](#). This document is the result of implementation of [Directive 2002/91/EC of the](#)

European Parliament and of the Council of 16 December 2002 (2002) to improve the energy performance of buildings in the Member States of the European Union, taking into account the typical internal and external climatic conditions, as well as economic calculation. Currently in Poland the average climate conditions are determined in accordance with the provisions of Polish Standard PN-ISO 15927-4:2005 - Hygrothermal performance of buildings - Calculation and presentation of climatic data - Part 4: Hourly data for assessing the annual energy use for heating and cooling according to EN ISO 13790 (2005) which specifies how to calculate the energy demand. Although it is mostly used for energy simulations in buildings, it is possible to use it for special applications. In this case, it has been used to determine the average climate conditions in highly urbanized areas, and then to estimate the thermal comfort in public spaces.

### Microclimatic conditions in Lodz based on Typical Meteorological Year

A Typical Meteorological Year was created based on hourly measurement and observation data, i.e. dry thermometer temperature [°C], solar radiation [W/m<sup>2</sup>], relative humidity [%], and airflow at 10 m above the ground level [m/s]. Due to numerous deficiencies in the structure of measurement and observation data, hourly values of meteorological parameters from the period 2004-2015 were used. This allowed to maintain consistency and completeness of all data. The determination method of the Typical Meteorological Year is presented below.

#### PROCEDURE FOR DETERMINATION OF A TYPICAL METEOROLOGICAL YEAR (ISO 15927-4 STANDARD, 2005)

- a) Calculation of daily mean values ( $\bar{p}$ );
- b) Determination of the distribution of daily averages for each calendar month separately for each year,

$\varphi(p, m, i) = \frac{K_i}{N + 1}$	<b>(Equation 5.1.)</b>
--	------------------------

where:  $K_i$  - is the rank of i-th daily mean value for the calendar month in the entire dataset;

- c) Determination of the distribution of daily averages for each calendar month based on all years in the dataset,

$F(p, y, m, i) = \frac{J_i}{n + 1}$	<b>(Equation 5.2.)</b>
-------------------------------------	------------------------

where:  $J_i$  - is the rank of i-th daily mean values within a given month and year;

d) Calculation of Finkelstein-Schafer statistics for each month;

$$F_s(p, y, m) = \sum_{i=1}^n |F(p, y, m, i) - \varphi(p, m, i)| \quad \text{(Equation 5.3.)}$$

- e) Increasing ordering of months from multi-year measurements according to Finkelstein-Schafer statistics;
- f) Separately adding a rank to each of the six selected climatic parameters;
- g) Determination for each calendar month of three months with the lowest total rank (understood as the sum of partial ranks) and then calculating for them the absolute value of difference between the average monthly value of wind speed for the analyzed month and the multi-year average value of wind speed for a given month;
- h) Selection of the month characterized by the lowest absolute value as the reference month of a Typical Meteorological Year.

The selected months are presented in [Table 5.1](#). Based on them, the typical city conditions were determined, excluding extreme and semi-extreme situations.

**Table 5.1.** Typical Meteorological Year.

TMY CONSTRUCTION					
January	<b>2012</b>	May	<b>2009</b>	September	<b>2012</b>
February	<b>2004</b>	June	<b>2004</b>	October	<b>2011</b>
March	<b>2010</b>	July	<b>2015</b>	November	<b>2013</b>
April	<b>2010</b>	August	<b>2012</b>	December	<b>2008</b>

**Source:** own elaboration.

During the Typical Meteorological Year, air temperature ranged from -15.00 to 35.00 °C ([Figure 5.1.](#); [Appendix 1.](#)). The spring was dominated by values in the range of 5-10 °C for 40.15% of the time. In the summer the value remained in the range of 15-25 °C most of the time (64.54%). In the autumn the parameter oscillated between 10-15 °C (44.36% of the time). In the winter the largest range of air temperature was evident. However, the values were accumulated between 0 and 15 °C.

The solar radiation value oscillated between 0 and 1000 W/m<sup>2</sup> ([Figure 5.2.](#); [Appendix 2.](#)). The prevailing values ranged from 0 to 100 W/m<sup>2</sup>. In the spring they occurred 59.22% of the time; summer 52.59% of the time; autumn 77.17% of the time; winter 85.54% of the time. The radiation value reaching the surface was relatively low in the city area.



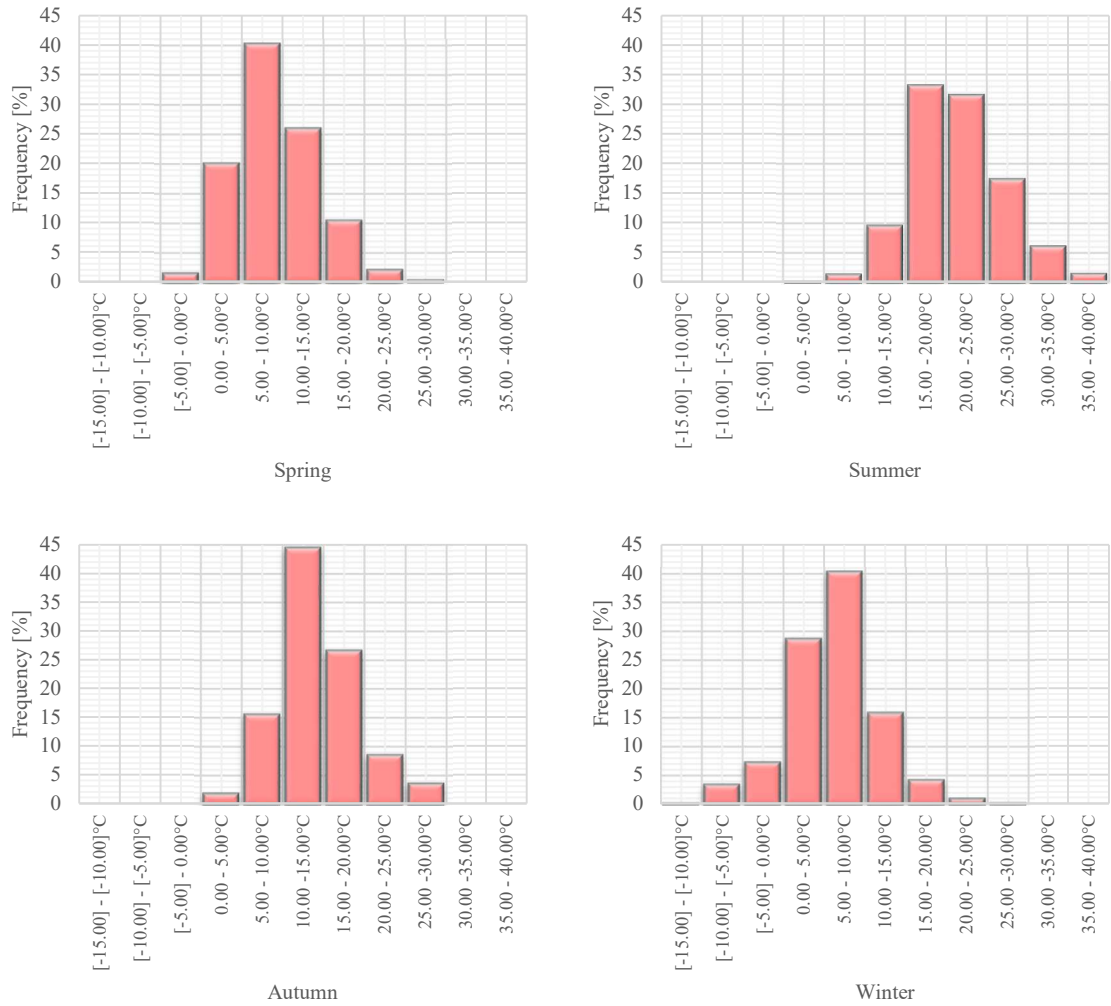


**Figure 5.1.** Frequency of air temperatures for each weather period (Typical Meteorological Year)(source: own elaboration).

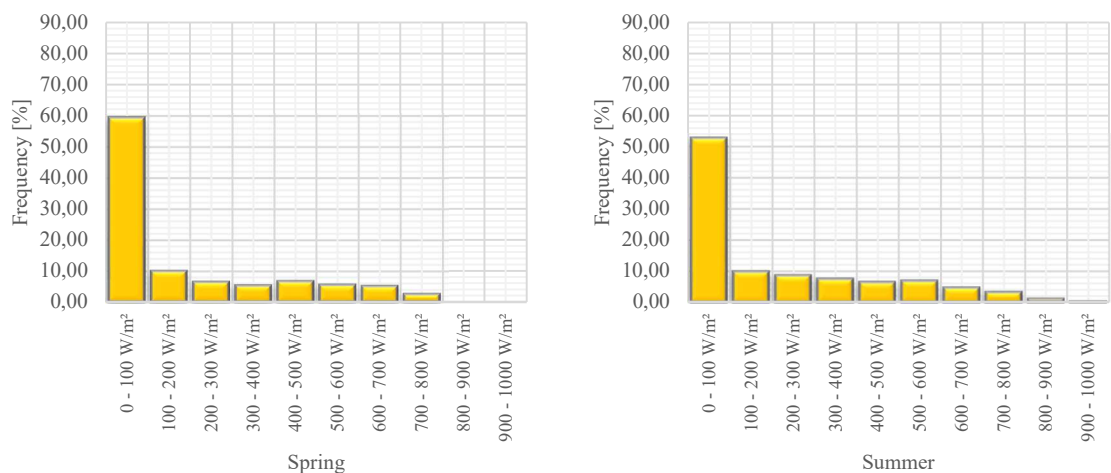


**Figure 5.2.** Frequency of solar radiation for each weather period (Typical Meteorological Year)(source: own elaboration).

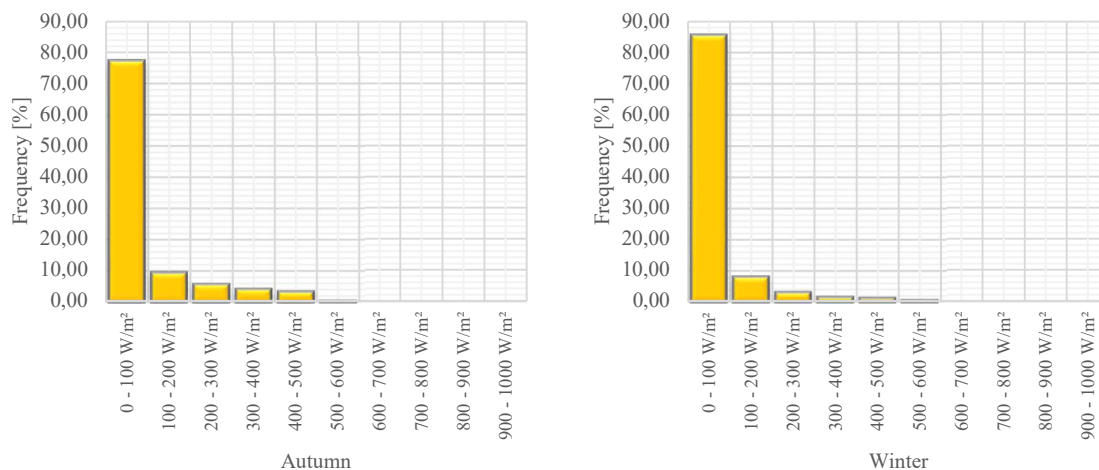


**Figure 5.2.** Continuation.

Relative humidity ranged from 20% to 100% (Figure 5.3.; Appendix 3.). The greatest range of this parameter was observed in the spring and the summer. Then, values from 40% to 100% prevailed (spring for 84.22% of time; summer season for 97.08% of time). In the autumn, as well as in the winter, values of this parameter were cumulated in ranges from 80% to 100% (autumn for 73.98% of time; in winter for 76.71% of time).

The analysis results showed that wind speed reached up to 5 m/s (spring - 85.61% of the time; summer 87.76% of the time; autumn 84.38% of the time; winter - 77.32% of the time)(Figure 5.4.; Appendix 4.). In extreme cases the airflow above 10 m/s was observed. However, these were incidental situations.

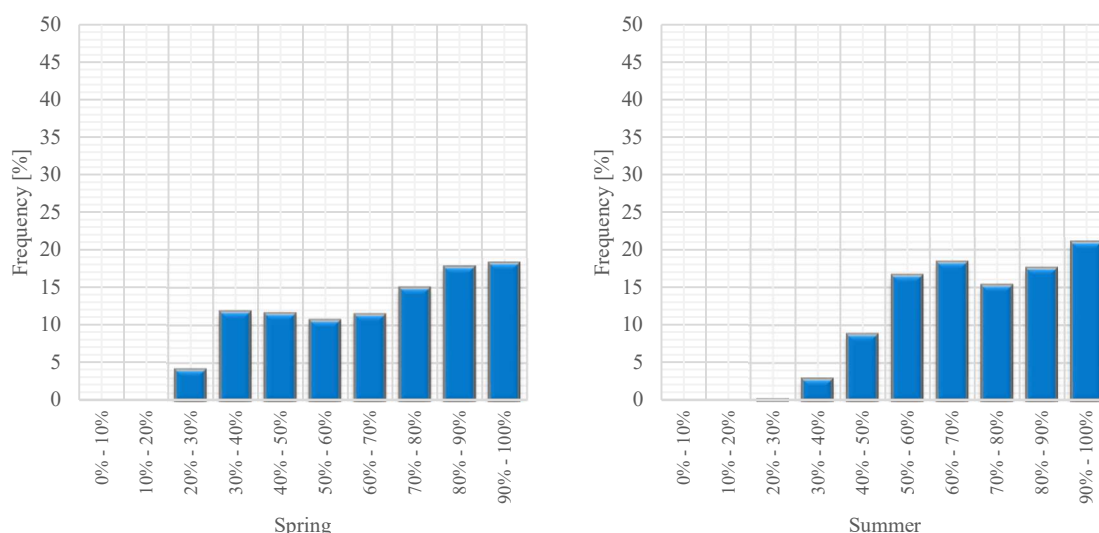


**Figure 5.3.** Frequency of relative humidity for each weather period (Typical Meteorological Year)(source: own elaboration).

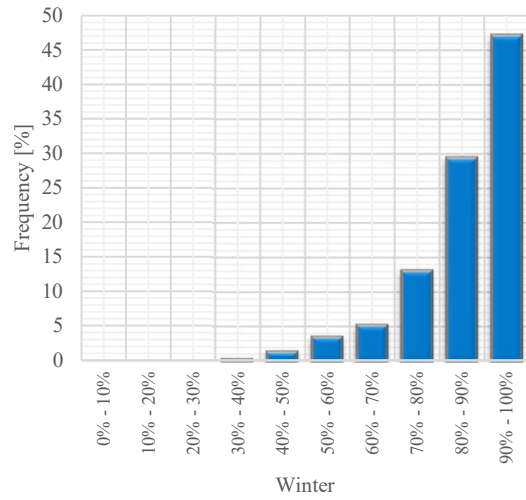
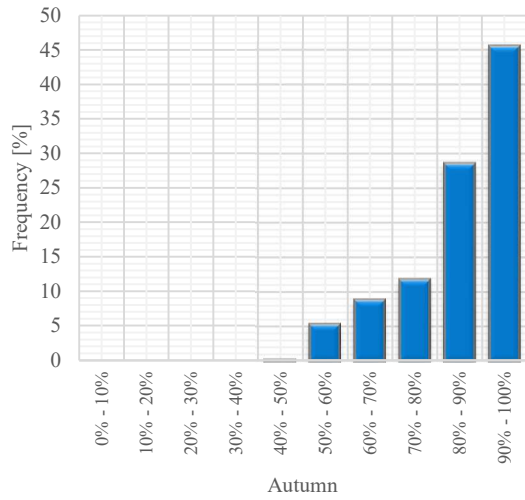


**Figure 5.3.** Continuation.

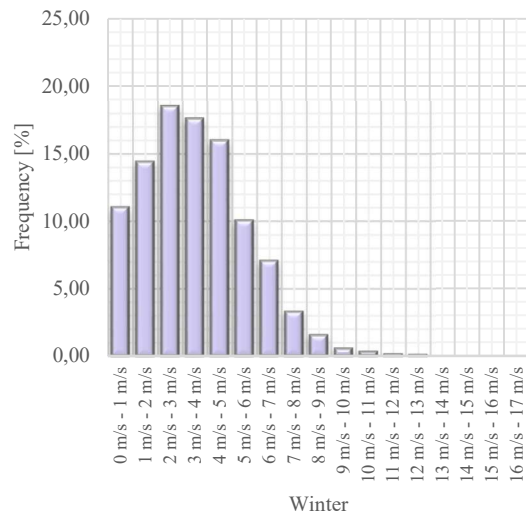
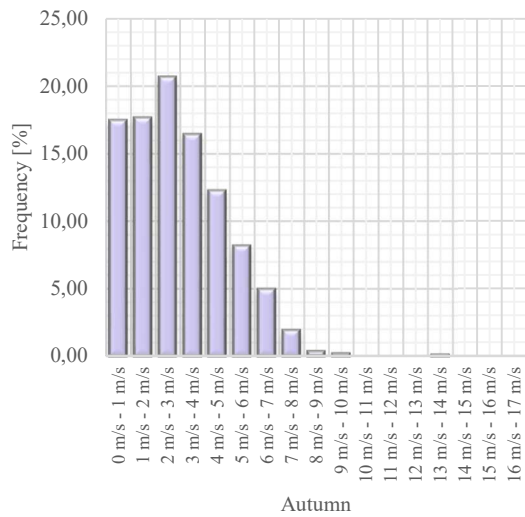
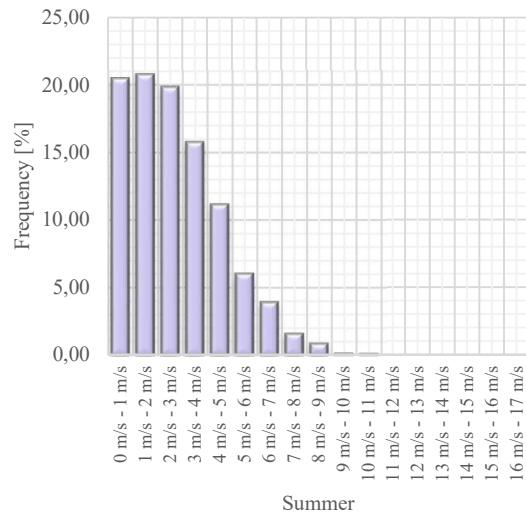
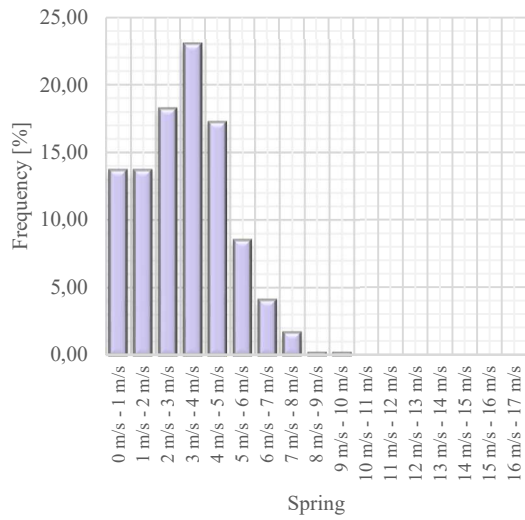


**Figure 5.4.** Frequency of individual wind speed values at 10 m height for each weather period (Typical Meteorological Year)(source: own elaboration).

These conditions characterized the suburban zone, where the meteorological station was located. In relation to conducting research in the central part of the city - the Metropolitan Area, it was necessary to take into account the change in the wind speed profile due to different ground roughness conditions. For this purpose, **an authorial approach was implemented, which consisted in linking the conditions of suburban - inner city zone.** Initially, the value of frictional velocity in the suburban area was determined using a modified version of the logarithmic equation (Equation 5.4. - 5.5.; Żurański, 2005).

$\bar{U}_{(z)} = \frac{u_*}{K} * \ln \frac{(z - z_d)}{z_0}$	<b>(Equation 5.4.)</b>
$u_* = \frac{\bar{U}_{(z)}}{\ln \frac{(z - z_d)}{z_0}} * K$	<b>(Equation 5.5.)</b>

where:  $\bar{U}_{(z)}$  - average wind speed at 10 m height [m/s],  $u_*$  - frictional velocity [m/s],  $K$  - von Kármán constant (0.4),  $z$  - height above the ground level [m],  $(z - z_d)$  - effective height [m],  $z_d$  - displacement length [m],  $z_0$  - aerodynamic roughness length (also called roughness parameter or roughness height) [m].

The above equation is valid from the level  $z \cong (z_d + 10)$ , below this level the value of wind speed should be considered constant and equal to  $\bar{U}(z_d + 10)$ (Flaga, 2008). Therefore, the frictional velocity at the Lublinek site was calculated using a simplified form of Equation 5.6.

$u_* = \frac{\bar{U}_{(z)}}{\ln \frac{10}{z_0}} * K$	<b>(Equation 5.6.)</b>
--	------------------------

Next, the frictional velocity for the inner city area was determined using the relationship proposed by Simiu (Equation 5.7.; Simiu, 1975), which enabled the wind speed profiles of the suburban area and the Metropolitan Area to be related. According to the modified Davenport classification (Wieringa, 1992), the roughness of suburban area was assumed to be  $z_o \approx 0.03$  m, while the inner city area was  $z_o \approx 1.00$  m.

$$\frac{u_*}{u_{*1}} = \left( \frac{z_0}{z_{01}} \right)^{0,0706} \quad \text{(Equation 5.7.)}$$

where:  $u_*$  - frictional velocity in the Lublinek area [m/s],  $u_{*1}$  - frictional velocity in the inner city area of Lodz [m/s],  $z_0$  - roughness coefficient for the Lublinek area [m],  $z_{01}$  - roughness coefficient for the inner city area of Lodz [m].

Finally, the wind speed was calculated for the Metropolitan Area. [Table 5.2.](#) presents the wind speeds in the suburban zone and the corresponding parameter values in the inner city area. The analyses conducted showed that the dominant group are the values ranging from 0 m/s to 5 m/s in the suburban area during the year. Therefore, in the most intensively urbanized zone, the parameter values will oscillate within the range of 0.31 m/s - 1.86 m/s.

**Table 5.2.** Wind speeds in the suburban area and their values in the Metropolitan Area.

Wind speed at 10 m height [m/s]									
Suburban zone	0	1	2	3	4	5	6	7	8
<b>City centre</b>	0.31	0.62	0.93	1.24	1.55	1.86	2.17	2.48	2.79
Suburban zone	9	10	11	12	13	14	15	16	17
<b>City centre</b>	3.09	3.40	3.71	4.02	4.33	4.64	4.95	5.26	5.57

**Source:** own elaboration.

During the Typical Meteorological Year, the air inflow was mainly from the western sector and the eastern sector as well ([Figure 5.5.](#); [Appendix 5.](#)). In the first case it was 21.46% of the time (spring); 26.64% of the time (summer); 21.09% of the time (autumn); 26.25% of the time (winter). In the second, 15.91% of the time (spring); 14.74% of the time (summer); 19.36% of the time (autumn); 18.07% of the time (winter). It is worth noting that a significant percentage was the air inflow from the southwest sector (11.74% of the time - spring; 12.93% of the time - summer; 22.74% of the time - autumn; 19.23% of the time - winter).

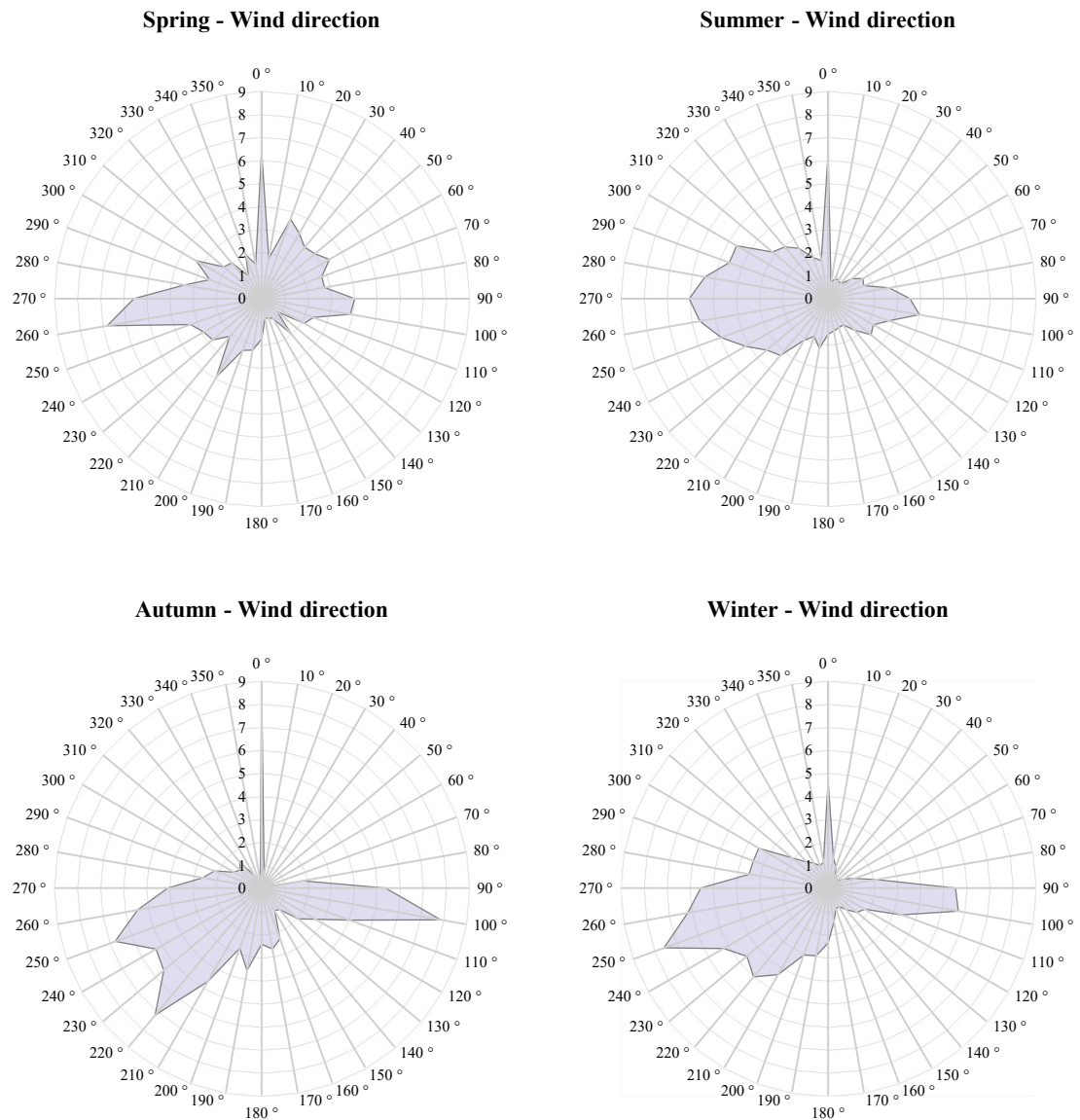


**Figure 5.5.** Frequency of individual wind directions for each weather period (Typical Meteorological Year)(source: own elaboration).

A Typical Meteorological Year describes the average conditions that prevail in the city of Lodz. Extreme as well as semi-extreme situations are excluded. In this study, at further stages of the research, the information was used as input parameters for the simulation of atmospheric processes. The assessment of the impact of adaptation strategies on the microclimate as well as human thermal comfort in the external environment was made for the warmest day of a Typical Meteorological Year (05/07/2015). The input data used are presented in [Table 5.3](#).

**Table 5.3.** The warmest day of a Typical Meteorological Year.

Hour	<b>0:00</b>	<b>1:00</b>	<b>2:00</b>	<b>3:00</b>	<b>4:00</b>	<b>5:00</b>	<b>6:00</b>	<b>7:00</b>	<b>8:00</b>
Temperature [°C]	17.50	15.50	14.80	14.60	16.70	21.10	23.40	26.80	29.60
Humidity [%]	70.00	81.00	85.00	85.00	82.00	63.00	57.00	50.00	40.00
Hour	<b>9:00</b>	<b>10:00</b>	<b>11:00</b>	<b>12:00</b>	<b>13:00</b>	<b>14:00</b>	<b>15:00</b>	<b>16:00</b>	<b>17:00</b>
Temperature [°C]	31.00	31.70	32.70	33.30	33.70	34.20	34.00	34.00	33.50
Humidity [%]	30.00	28.00	26.00	24.00	21.00	20.00	20.00	21.00	22.00
Hour	<b>18:00</b>	<b>19:00</b>	<b>20:00</b>	<b>21:00</b>	<b>22:00</b>	<b>23:00</b>			
Temperature [°C]	31.60	28.10	23.90	22.40	20.60	19.70			
Humidity [%]	27.00	36.00	52.00	55.00	64.00	69.00			
Wind direction - east									
Wind speed - 0.80 [m/s]									

Source: own elaboration

## CHAPTER VI. NUMERICAL SIMULATION OF MICROCLIMATIC AND THERMAL CONDITIONS

According to Darbani et al. (2021), urban form development becomes increasingly important in highly urbanized areas. It is emphasized that a properly designed building structure can improve climatic conditions as well as thermal comfort. Therefore, more and more attention is focused on the appropriate planning provisions that allow to mitigate the discomforting thermal conditions experienced by people in urban spaces, especially during the summer season. Numerous authors indicate that the provisions should take into account the varying orientation as well as dimensions of different forms (Rodríguez-Algeciras et al., 2018). In this way, it will be possible to modify thermal conditions (by limiting sunlight), or wind conditions (by ensuring free airflow).

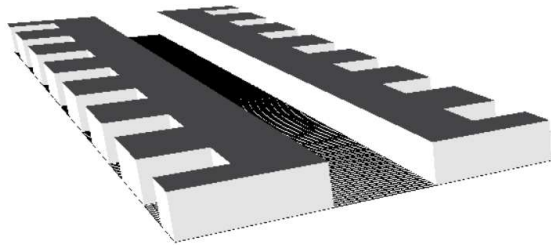
The following chapter describes the analysis results of the influence of building geometry on microclimatic conditions. Different heights of buildings were taken into account. The average dimensions of street canyon (MR - Mean Ratio) occurring in the Metropolitan Area of Lodz have been taken as the reference point. In the HR (High Ratio) scenario, twice as high building heights were assumed. The development structure forming the street canyon frontage was intensified. In the LR (Low Ratio) scenario, twice lower height of buildings was assumed. It should be noted that the study considered structures with different orientations, i.e. (1) east-west, (2) and north-south. The scenarios are shown in Figure 6.1. (the left column).

Next, the analyses were conducted for the second of characteristic building forms, the urban forecourt. Similarly, the mean forecourt (MF) dimensions of building structures found in the Metropolitan Area were assumed for the base structure. In the High Forecourt (HF) scenario, twice as high buildings were taken into account, while in the Low Forecourt (LF), twice as low. The models created are presented in Figure 6.1. (the right column).

For both the street canyons and forecourt development, the weather conditions prevailing during the warmest day of a Typical Meteorological Year (05.07.2015, determined according to the standards described in Chapter V. City's microclimatic conditions) were adopted as input data for the simulations. Hourly values of temperature and relative humidity at 2m height were included. For radiation it was necessary to calculate an adjustment factor. This resulted from overestimation of the parameter value by the software (automatic settings). In this case, the radiation adjustment factor was - 0.82. Also,

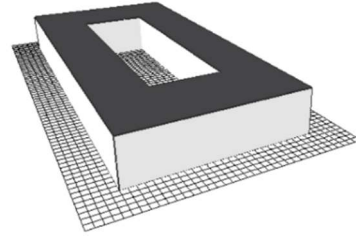


the wind speed was corrected. The study was conducted for the Metropolitan Area of the city, while the obtained value of airflow was related to the conditions in the suburban area (Lodz-Lublinek). In order to correct the airflow values, the author's method described in [Chapter V. City's microclimatic conditions](#) was used. The wind speed in the Metropolitan Area was 0.80 m/s. The last parameter - air inflow to the city was set as eastern.



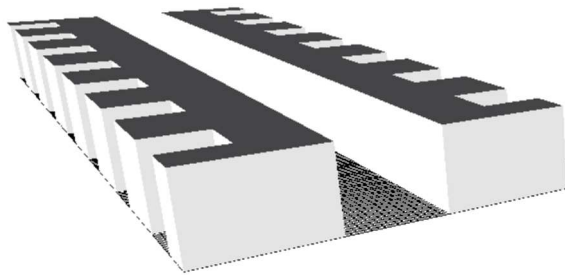
Low Ratio Scenario - Canyon (**LR**)

Building height = 7m  
Street width = 16m  
Height-to-Width ratio = 7/16



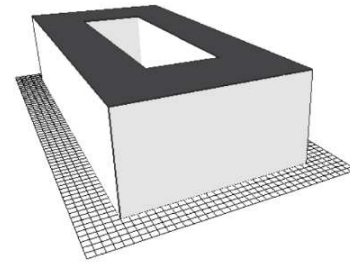
Low Ratio Scenario - Forecourt (**LF**)

Building height = 7m  
Forecourt width = 11m  
Height-to-Width ratio = 7/11



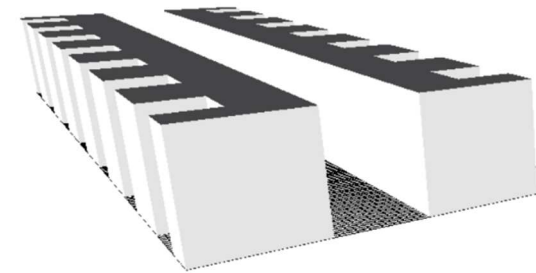
Mean Ratio Scenario - Canyon (**MR**)

Building height = 14m  
Street width = 16m  
Height-to-Width ratio = 14/16



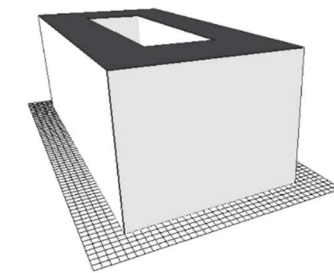
Mean Ratio Scenario - Forecourt (**MF**)

Building height = 14m  
Street width = 11m  
Height-to-Width ratio = 14/11



High Ratio Scenario - Canyon (**HR**)

Building height = 21m  
Street width = 16m  
Height-to-Width ratio = 21/16



High Ratio Scenario - Forecourt (**HF**)

Building height = 21m  
Street width = 11m  
Height-to-Width ratio = 21/11

**Figure 6.1.** Geometry of considered urban forms (left column - canyons; right column - forecourts)(source: own elaboration).

## 6.1. Canyons

### *Microclimatic conditions in the east-west oriented canyons*

Microclimatic conditions during the warmest day of a Typical Meteorological Year in street canyons with east-west orientation were evaluated. The subject of analysis was the influence of building height on microclimate. For comparison, meteorological parameters measured at two characteristic measurement points located in the middle of canyons, in the distance of 2.5 m from building walls, at the northern facade (E-WN) and at the southern facade (E-WS) are presented. The measurements were conducted during the day (3 pm) to assess the maximum influence of buildings on thermal conditions. Also the analysis of parameters was carried out at night (3.00 am). The results are presented in [Figure 6.2](#).

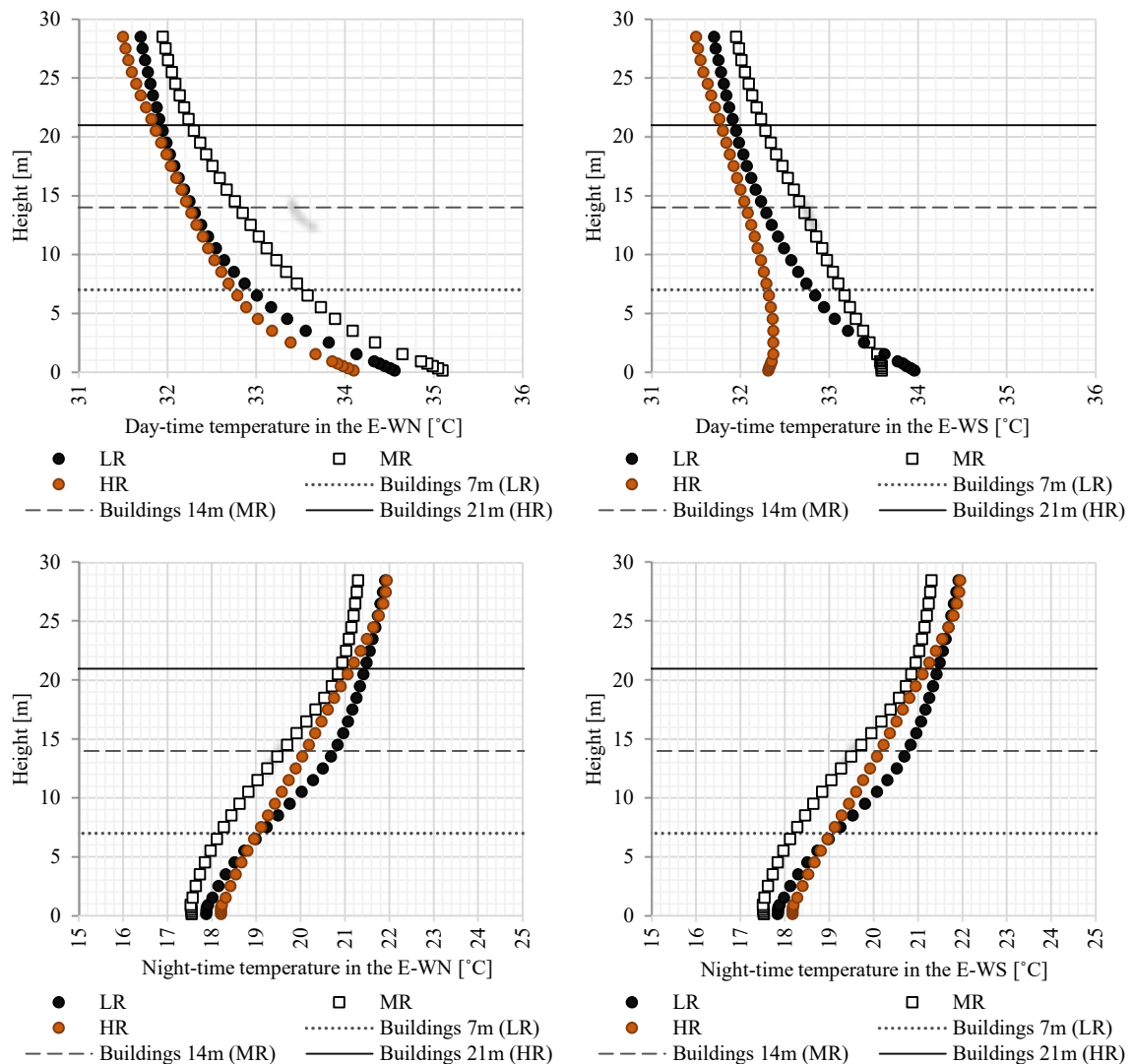


**Figure 6.2.** Air temperature in canyons with east-west orientation (top left - at north facade (E-WN); top right - at south facade (E-WS), 3 pm; bottom left - at north facade (E-WN), bottom right - at south facade (E-WS), 3 am)(source: own elaboration).

The greatest reduction in air temperature was achieved in the HR scenario (building height = 21m). The buildings reduced the solar radiation reaching both horizontal surfaces (floor) and vertical surfaces (walls) during the day. It should be noted that sun hours were 10h at the north facade. The sun hours at the south facade were much shorter, i.e. 3h. The effect was a reduction in temperature, especially at the pedestrian level at the more heavily shaded south facade. The temperature reduction was 1.28°C (up to a height of 3.5 meters). At the residential level it was at - 0.89°C.

The highest temperature values were recorded in the MR scenario. A much lower development (14m) caused the canyon to have a stronger insolation than in the HR case (sun hours = 10h in E-WN, 5h in E-WS). Radiation reached the north elevation of the canyon. Concrete surfaces with low albedo absorbed a significant amount of solar energy. The remaining part was shortwave diffuse radiation absorbed by the other pavements. This effect was less intense for the LR scenario. The lower building structure (7m) with much less surface area did not intercept radiation as much as in the MR scenario.

The situation was different at night time. High buildings (HR) prevented heat exchange on the artificial surfaces-environment path. This resulted in a slow dissipation of energy into the environment. Thus, the least favorable conditions were observed within the canyon with east-west orientation. The most favorable scenario appeared to be MR (building height = 14m).

Also, the effect of changing the geometry of buildings was to modify the pavement temperature (Figure 6.3.). The higher the buildings, the lower the canyon floor temperature was. The 24-hour average reduction in the parameter was 1.32°C (LR), 3.11°C (MR), 3.32°C (HR)(differentiation = E-WN – E-WS).

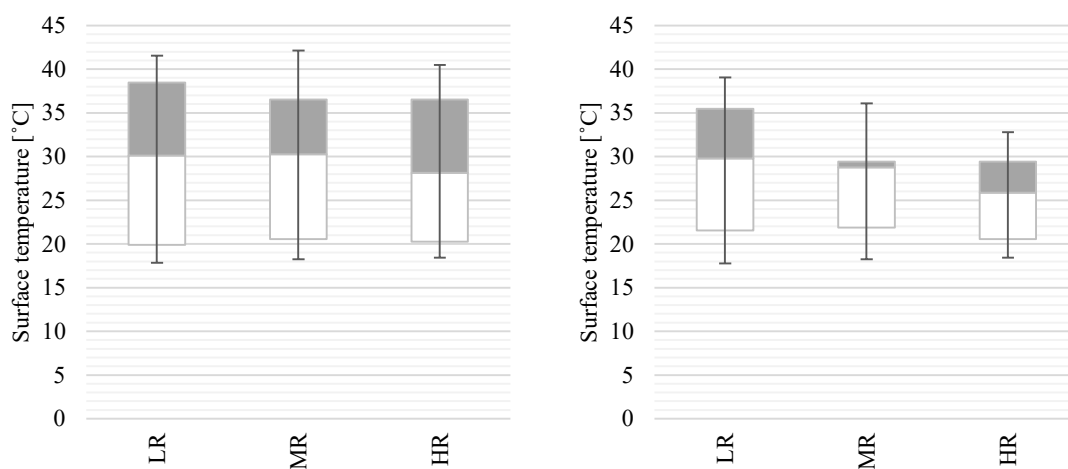


**Figure 6.3.** Surface temperature in canyons with east-west orientation (left - at north facade (E-WN); right - at south facade (E-WS))(source: own elaboration).

It should be noted that the eastern direction of air inflow was assumed in the models (Figure 6.4.). Negligible exchange of air masses (LR and MR) was observed at the pedestrian movement level. Increasing the building height to 21m (HR) resulted in an increase in wind speed of 0.74 m/s in the canyon with an east-west orientation. The development frontages formed a corridor that enhanced air exchange.

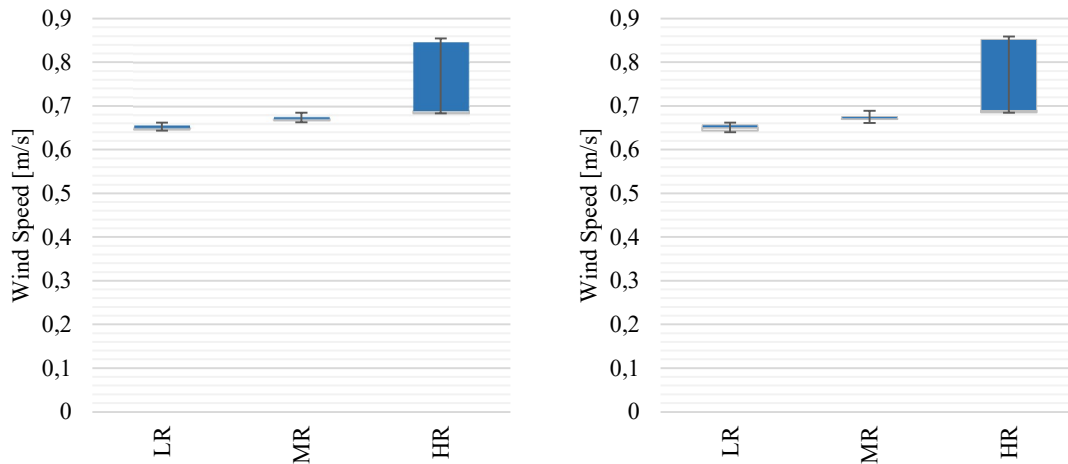


**Figure 6.4.** Airflow in canyons with east-west orientation (left - at north facade (E-WN); right - at south facade (E-WS))(source: own elaboration).

#### *Microclimatic conditions in the north-south oriented canyons*

The second case was related to changes occurring in canyons with north-south orientation. Microclimatic conditions in the spaces were presented based on readings taken at two characteristic measurement points, i.e. at the eastern (N-SE) and western (N-SW) facades, in the middle of canyons, 2.5 m from building walls. Readings were taken for daytime (3 pm) as well as nighttime (3 am)(Figure 6.5.).

Conditions appeared to be more favorable than in the canyon with east-west orientation. The area was less sunny. Sun hours were 6h (LR), 4h (MR), and 2.5h (HR). The most favorable scenario appeared to be - HR. The buildings provided a physical barrier to the influx of solar radiation in the canyon. As a result, a reduction in air temperature of 1.98°C at the pedestrian movement level, and 1.85°C at the residential height (N-SW) was achieved. In the MR scenario, the worst thermal situation was observed. It was a more strongly insolated area than in HR. Building materials absorbed a significant amount of solar energy during the day. Also of great importance was the change in radiation fluxes - reflection from the building walls - resulting in an increase in air temperature in the canyon.

It should be noted that the height of buildings at 21m (HR) caused an adverse effect on thermal conditions at night. The buildings constituted an anthropogenic obstacle. It impeded

the heat exchange on the way artificial surfaces (floor, walls of buildings) - environment. This resulted in higher air temperature. In other scenarios, where lower buildings were assumed, the exchange took place in a more efficient way. As a result, the prevailing thermal conditions were more favorable, both at the pedestrian movement and residential levels. It should be noted that the dynamics of parameter change with height was small up to the height of the roof layer at night. A relatively constant air temperature was maintained.

The change of building height resulted in a modification of the canyon-floor surface temperature (Figure 6.6.). The highest values were recorded in sunny areas. The mean diurnal difference was 0.54°C (LR), 0.76°C (MR), 0.20°C (HR) within the canyon (differentiation = N-SW – N-SE). In the first case (LR), the floor heated relatively uniformly throughout the day. The absorbed heat was dissipated into the environment at night. In the MR scenario, there was a noticeable difference in the floor heating. The site received strong sunlight at the east facade during the day. The buildings cast a shadow at the west facade causing a reduction in air temperature. However, during the nighttime, the compact layout of buildings hindered the transfer of energy to the environment. In the latter (HR), the 24-hour average surface temperature was the lowest. The buildings cast shadows protecting the floor from heating during the day.

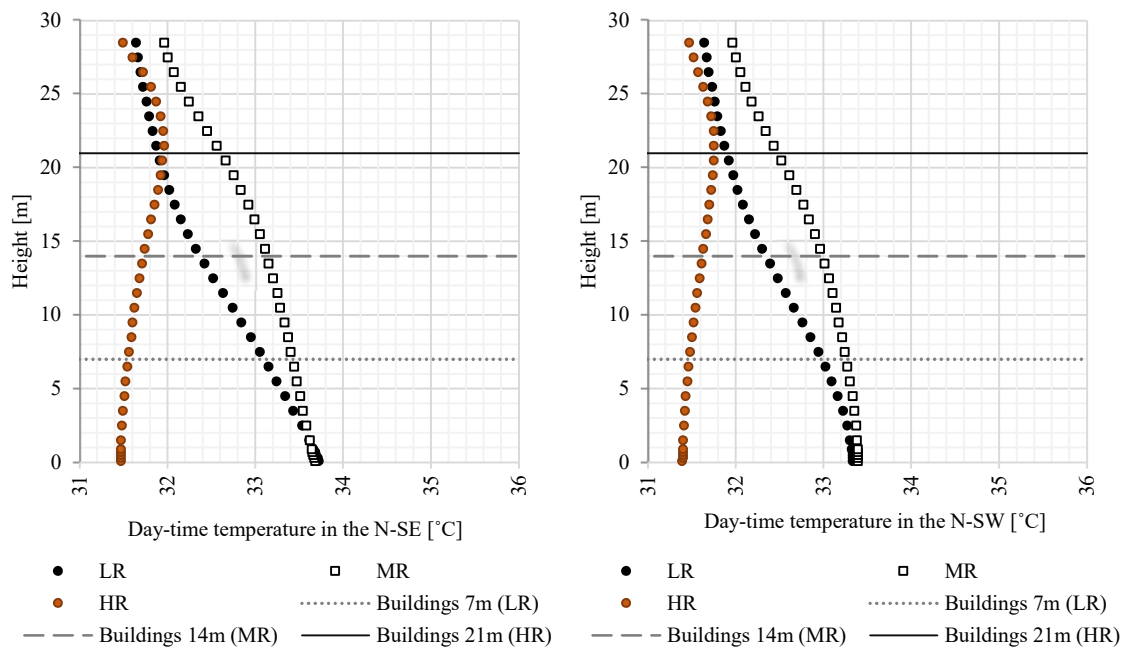


**Figure 6.5.** Air temperature in canyons with north-south orientation (upper left - at east facade (N-SE); upper right - at west facade (N-SW), 3 pm; lower left - at east facade (N-SE), lower right - at west facade (N-SW), 3 am)(source: own elaboration).

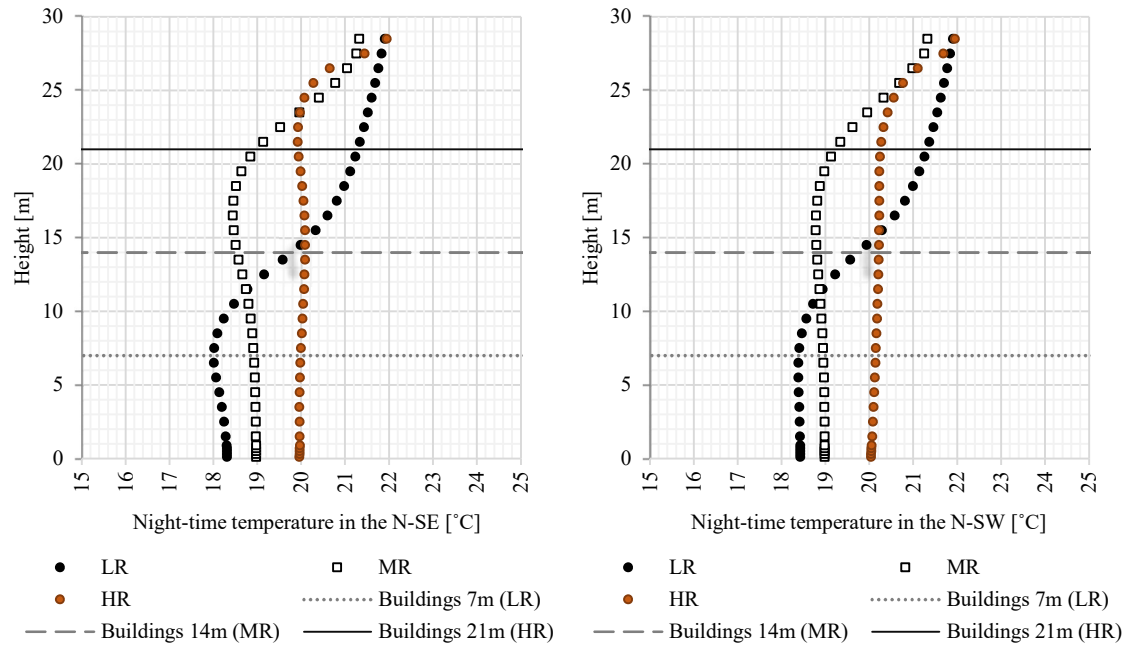


Figure 6.5. Continuation.

It should be mentioned that in the canyon with north-south orientation the airflow would be impeded (assumed eastern direction). The structure of buildings was a kind of obstacle for air exchange. In fact, there was a stagnation (Figure 6.7).

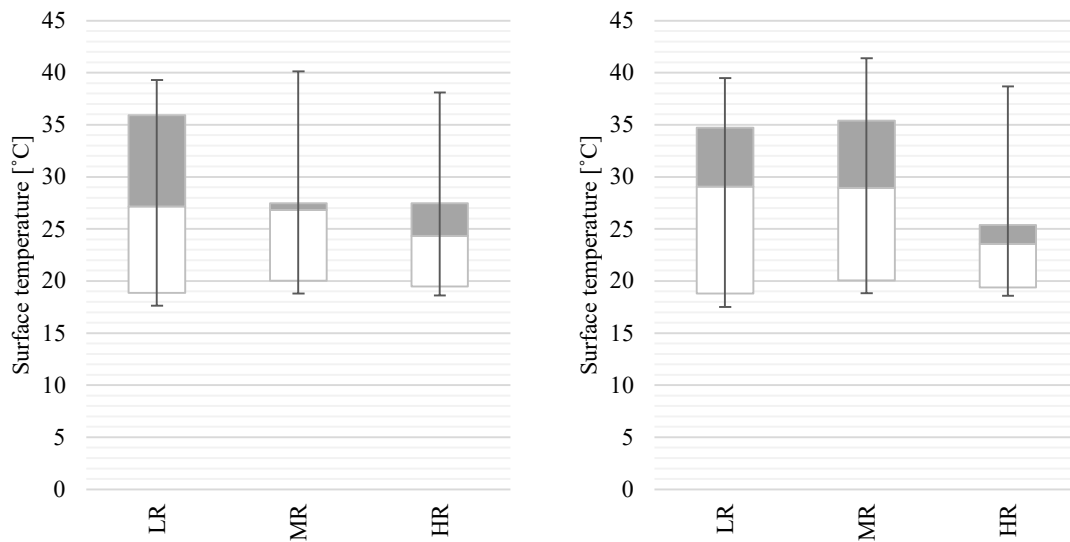
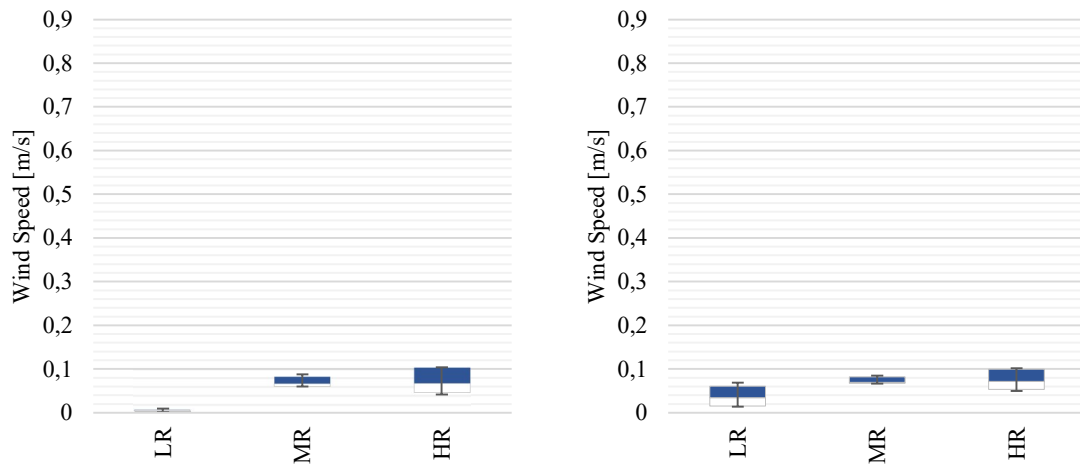


Figure 6.6. Surface temperature in canyons with north-south orientation (left - at east facade (N-SE); right - at west facade (N-SW))(source: own elaboration).



**Figure 6.7.** Airflow in canyons with north-south orientation (left - at east facade (N-SE); right - at west facade (N-SW))(source: own elaboration).

### *Thermal comfort in the east-west oriented canyons*

Thermal comfort of a person in an outdoor environment was estimated using PET index (description of the index is presented in [Chapter 2.3.2. The thermal comfort indices](#)). The study was conducted for a 35-year-old person, with a height of 1.75 m, weight of 75 kg, who moved at a speed of 1.21 m/s in a public space. Thermal insulation of clothing for the summer period, i.e. 0.50 clo, was taken into account. The results of the effect of building structure on human thermal comfort are shown in [Figure 6.8](#). Readings were taken at the north facade (E-WN) as well as the south facade (E-WS) to show the effect of building geometry on thermal comfort within the canyon with east-west orientation. Measurements were conducted at pedestrian movement height (h=1.5 m), at residential level (h=5.5 m), and directly above the building roofs (h= 1.5 m above the roof, depending on the height of buildings). The situation that takes place during the day (3 pm), as well as at night (3 am) is shown.

At the outset, it should be emphasized that the geometry of buildings contributed significantly to the modification of index. It reduced the solar radiation and thus the surface temperature. As a result, it affected the mean radiant temperature - a key parameter in PET calculations.

The development caused a significant reduction in the index, especially at the south facade during the day. The conditions defined as ‘very hot’ (E-WN) managed to be reduced to ‘hot’ (E-WS, MR scenario) and even ‘warm’ (E-WS, HR scenario) at the pedestrian movement level. Only in HR was a beneficial modification noted at the residential level (h=5.5 m, ‘warm’ conditions). Insolation was effectively reduced by 21 m high objects

(HR). This resulted in much more favorable thermal conditions and thus the sensation of people residing in the canyon area. In other cases, thermal sensations were at the ‘very hot’ level. The PET was over 42°C, which was associated with the possibility of ‘heat stroke’ in humans.

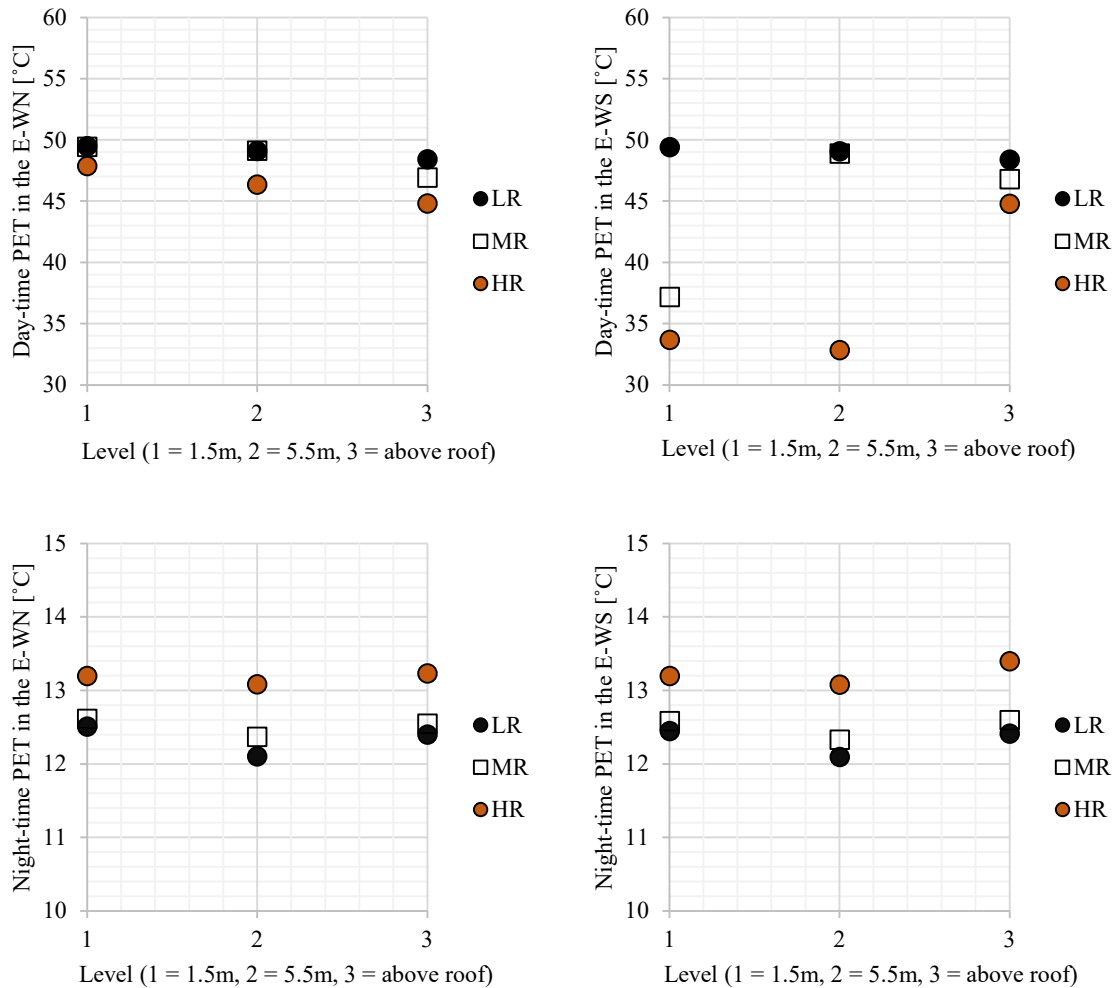


**Figure 6.8.** PET in canyons with east-west orientation (top left - at north facade (E-WN); top right - at south facade (E-WS), 3 pm; bottom left - at north facade (E-WN), bottom right - at south facade (E-WS), 3 am) (source: own elaboration).

An acceptable situation was observed during the night time (all scenarios). The PET values were slightly higher for the scenario related to the facade of buildings up to 21 m (HR). Buildings constituting a physical barrier slowed down the heat exchange between artificial surfaces (floor, walls) and the environment. This resulted in more favorable conditions at the ‘slightly cool’ level. In other cases, conditions at the ‘cool’ level (less favorable) were recorded.



### *Thermal comfort in the north-south oriented canyons*

The human-perceived thermal comfort in the canyon with north-south orientation was evaluated. Readings were taken at the east facade (N-SE) as well as the west facade (N-SW). Daytime (3 pm) and nighttime (3 am) conditions were considered. The results are shown in [Figure 6.9](#).

The situation was more favorable in areas shaded by buildings during the day. Then the conditions were described as ‘hot’ (LR, MR) and ‘warm’ (HR) at the pedestrian movement level. It should be mentioned that a significant reduction in PET occurred at the residential height in the HR scenario (building height = 21 m, ‘warm’ conditions). A similar situation was observed with a building height of 14 m (MR), but only with a shaded western facade. The buildings were too low to guarantee residential level shade at the east facade. This resulted in thermal discomfort already appearing at the residential level with a strongly sunny - eastern facade (N-SE, MR). In other cases, thermal sensations reached levels above 42°C, indicating the possibility of ‘heat stroke’ among people.

In the canyon with north-south orientation, lowering the building height to 7m resulted in a longer period of prevailing ‘very hot’ conditions - up to 10h (LR), an hour longer compared to the canyon with east-west orientation. For MR a more favorable situation was noted, this time was reduced to 6h (2 h shorter). In HR the appearance of ‘very hot’ conditions was noted between 11 am and 1 pm. The most unfavorable conditions was ‘hot’ in the east-west oriented canyon (HR).

The thermal situation can be considered favorable during the nighttime. Comfortable conditions were achieved in the scenario where the building height was 21 m (HR). Sensations were comfortable both within the canyon and above the building roofs. The buildings created a physical barrier to canyon-environment heat exchange. Therefore, a higher air temperature was maintained within the canyon. This resulted in a more favorable thermal situation. ‘Slightly cool’ conditions were recorded up to the height of roof layer in other cases (LR, MR). ‘Cool’ conditions occurred above the building roofs. Here, the lower height of buildings enabled the absorbed heat to be dissipated by building materials (floors, walls). As a result, cooler conditions persisted in the area at night.

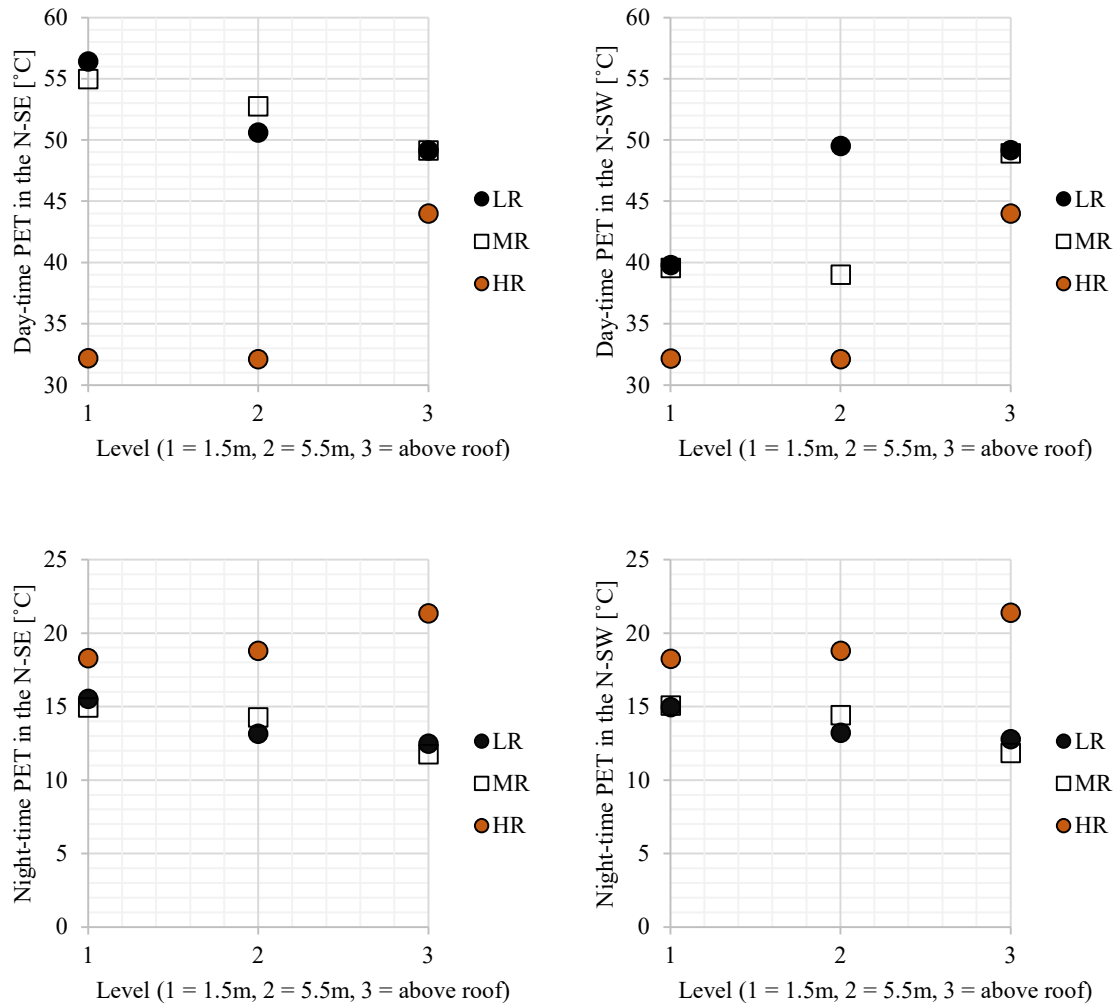


**Figure 6.9.** PET in canyons with north-south orientation (top left - at east facade (N-SE); top right - at west facade (N-SW), 3 pm; bottom left - at east facade (N-SE), bottom right - at west facade (N-SW), 3 am)(source: own elaboration).

## 6.2. Forecourts

### *Microclimatic conditions in the east-west oriented forecourt*

Thermal conditions in the urban forecourt area were evaluated. Information was obtained from two measurement points. The readings taken at the north facade (E-WN) are shown in [Figure 6.10](#). Similar results were obtained at the south facade, and therefore their graphical presentation was omitted. The study included both daytime (3 pm) and nighttime (3 am) conditions. Thanks to this approach, it was possible to assess the maximum effect of the building structure on the microclimate. It was also possible to check what the effect would be when the temperature conditions were extreme, when it was warmest (3 pm), and when it was coldest (3 am).

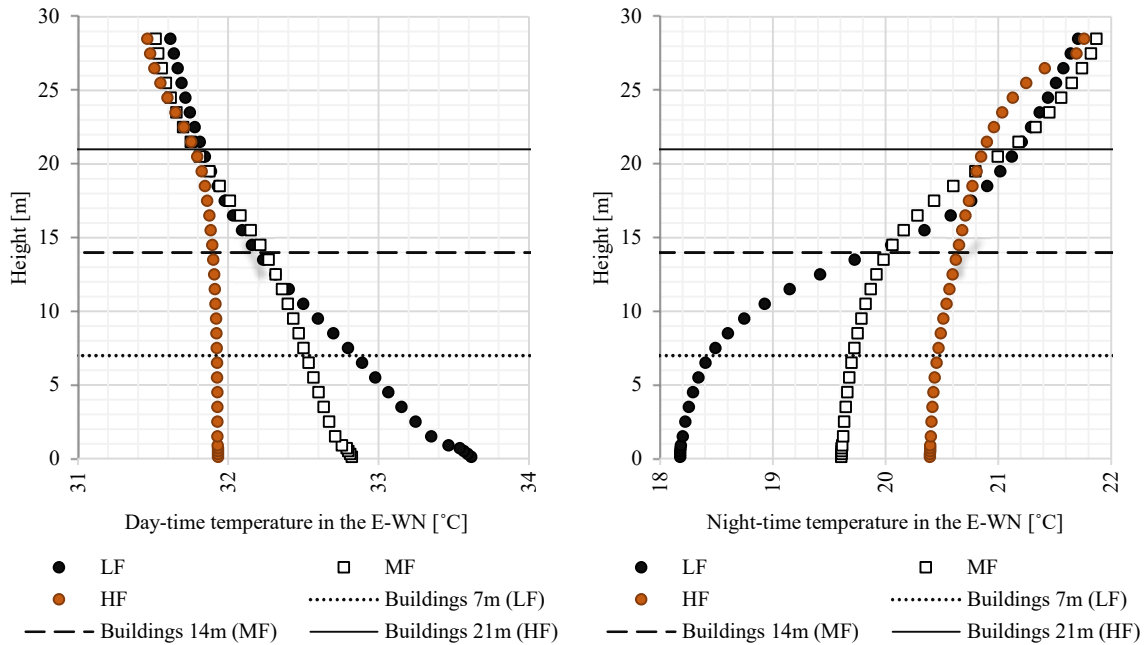


**Figure 6.10.** Air temperature in forecourts with east-west orientation (left - at the north facade (E-WN), 3 pm; right - at the north facade (E-WN), 3 am)(source: own elaboration).

The building structure affected the microclimate in the urban forecourt. During the daytime, the most effective scenario appeared to be the HR related to the facade of buildings to a height of 21 m. The buildings allowed the reduction of solar inflow to the forecourt area. Sun hours were less than 1h. This was an extremely favorable situation that led to a temperature reduction of  $0.78^{\circ}\text{C}$  at pedestrian movement level ( $h=1.5\text{ m}$ ),  $0.64^{\circ}\text{C}$  at residential height ( $h=5.5\text{ m}$ ) compared to MF. The forecourt was more strongly insulated when the buildings height was at 14 m. Then, the north facade was insolated (sun hours = 8h). Lowering the buildings to 7m had a negative effect on the thermal conditions. Even the area near the south facade was subjected to insolation (sun hours = 5h). The temperature exceeded  $33^{\circ}\text{C}$  at the pedestrian movement level.

However, other phenomena occurring in the forecourt must be taken into account. The layout of buildings influenced the floor heating. The sunny surfaces absorbed much of the daytime radiation (Figure 6.11.). The difference could be  $9.43^{\circ}\text{C}$  (LF),  $9.00^{\circ}\text{C}$  (MF),  $1.51^{\circ}\text{C}$  (HF)(value difference = E-WN – E-WS). Unfortunately, the result was an increase in air temperature, especially in the afternoon. At that time, energy was being dissipated into the environment.

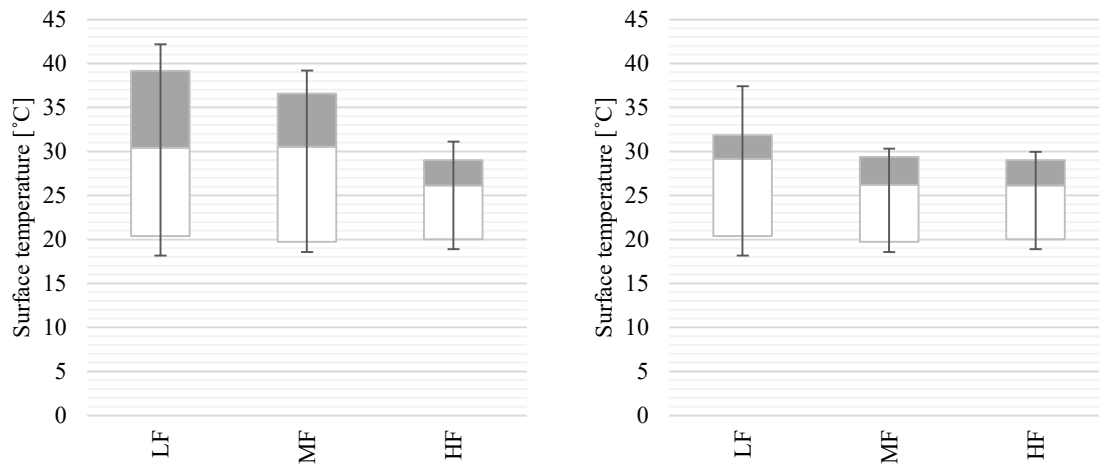


**Figure 6.11.** Surface temperature in forecourts with east-west orientation (left - by north facade (E-WN); right - by south facade (E-WS))(source: own elaboration).

After sunset, the buildings were a key factor in modifying the thermal conditions. The higher the buildings, the slower the forecourt cooled down. The structure with a height of 21 m (HF) resulted in significantly higher air temperatures at night. It was compact enough to prevent cooler air masses from entering the forecourt. In this case, convective motions were observed that modified the thermal conditions. Advective movement only took place from the roof layer level.

#### *Microclimatic conditions in the north-south oriented forecourt*

The influence of height of the north-south oriented urban forecourt layout on the thermal conditions was presented on the basis of readings taken at the eastern facade (N-SE)([Figure 6.12.](#)). The situation was similar at the western facade. Therefore it was decided to present graphically the measurements taken at the eastern, more insolated facade. Daytime (3 pm) and nighttime (3 am) conditions were taken into account.

The dependence of air temperature on layout geometry was evident for this structure as well. For buildings with a height of at least 14 m there was a reduction in temperature in the forecourt. Then there was a relatively constant value of the parameter in the area (MF, HF), both at the pedestrian movement and residential level. The unfavorable situation occurred in the forecourt, which was formed by buildings with a height of 7m (LF). There was an increase in air temperature, especially at the pedestrian movement level. This was due to the stronger insolation of forecourt during the day (sun hours > 5h).

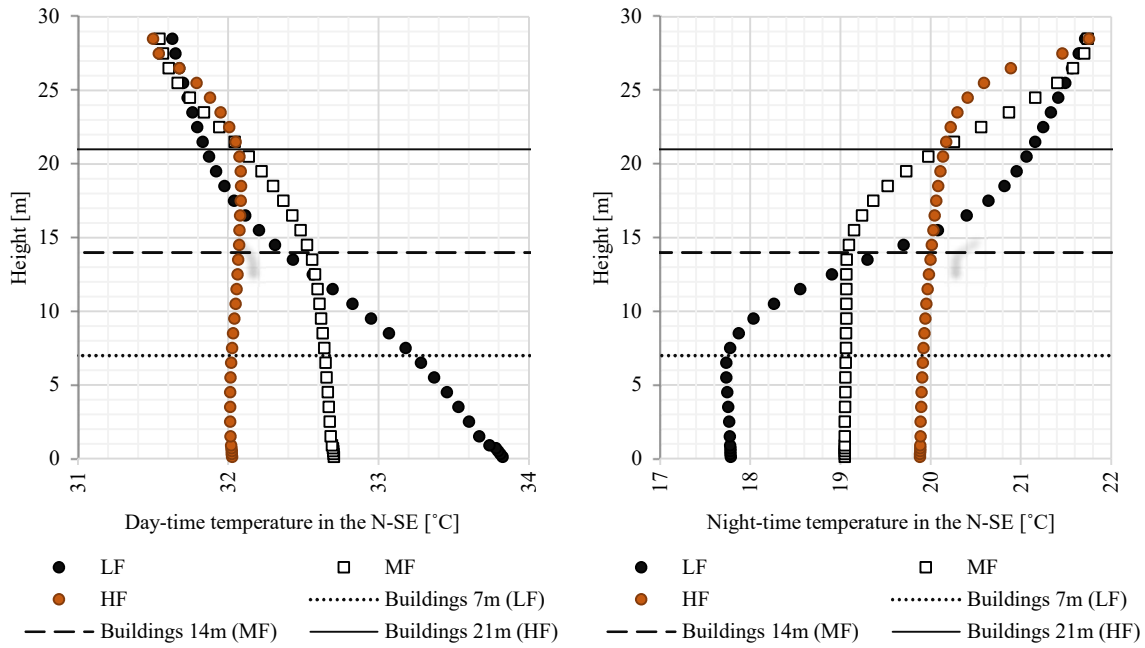


**Figure 6.12.** Air temperature in forecourts with north-south orientation (left - at the eastern facade (N-SE), 3 pm; right - at the eastern facade (N-SE), 3 am)(source: own elaboration).

The pavement temperature was also modified (Figure 6.13.). It was increased to 42.40°C (LR), 35.97°C (MF), and 33.24°C. Unfortunately, the building materials used, in this case concrete, largely absorbed solar radiation during the day. Energy dissipation occurred at night when the ambient temperature was significantly lower than the vertical surfaces (plastered walls) and horizontal surfaces (concrete floor). Additionally, the buildings impeded the dissipation of energy. As in the forecourt with east-west orientation, the buildings were a physical barrier for air exchange. This occurred largely through convective air movements.

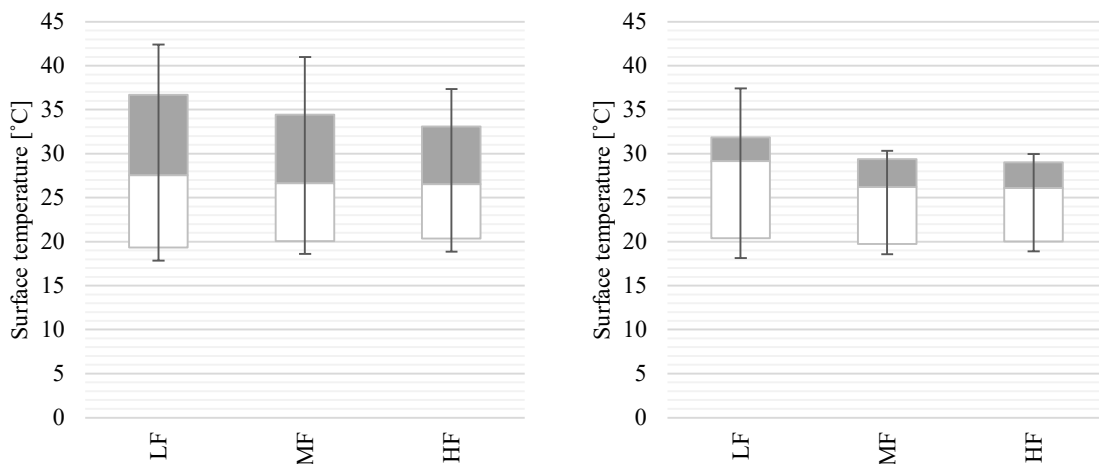


**Figure 6.13.** Pavement temperature in forecourts with north-south orientation (left - at east facade (N-SE); right - at west facade (N-SW))(source: own elaboration).

### Thermal comfort in the east-west oriented forecourts

The analyses conducted showed that the geometry of buildings contributed significantly to thermal sensation in forecourts with east-west orientation (Figure 6.14.). Buildings with a height of 21 m (HR) resulted in reduced solar radiation reaching the ground surface. The result was a reduction in thermal discomfort from ‘very hot’ to ‘hot’, especially at the pedestrian movement and residential levels near the south facade. It was also possible to shape thermal sensations at the ‘hot’ level at pedestrian height by the north facade with such buildings’ geometry. The buildings effectively shaded the canyon area. Thus, more favorable thermal conditions were observed.

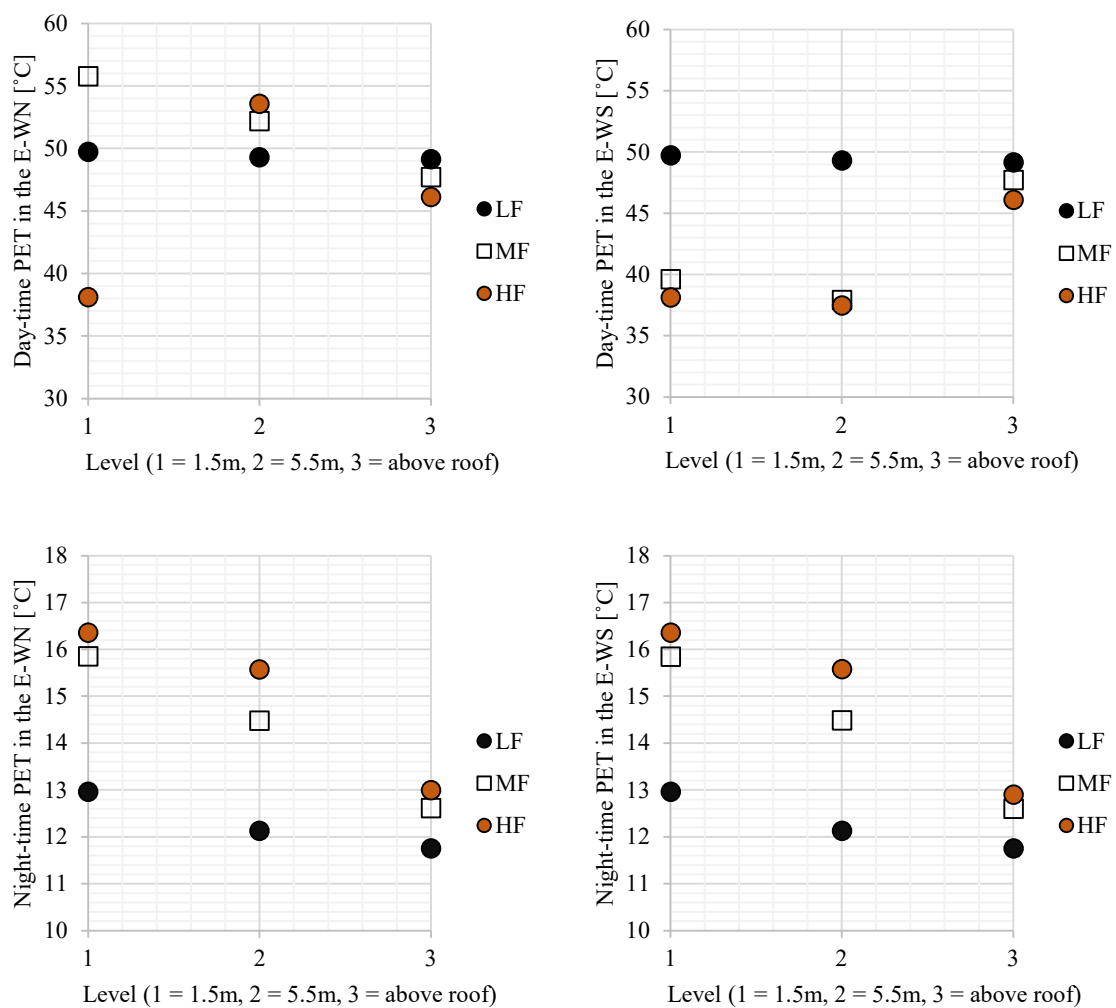


**Figure 6.14.** Effect of building structure on thermal comfort in the east-west oriented forecourt (upper left - E-WN, upper right - E-WS, **3 pm**; bottom left - E-WN, bottom right - E-WS, **3 am**)(source: own elaboration).

The situation was different at the residential level by the north facade. Here, shortwave diffuse radiation was the primary influence. Sunlight reaching the walls was reflected. The higher the building, the higher the amount of shortwave diffuse radiation. This resulted in

the highest PET values recorded at the residential level in the HF scenario (buildings height =21 m). Also, unfavorable conditions described as ‘very hot’ prevailed at a building height of 14 m.

Favorable thermal conditions were observable during the nighttime. Thermal sensations described as ‘slightly cool’ prevailed at the pedestrian movement and residential levels (MF, HF). They were more conducive than in the LF scenario, where slightly lower values of the PET index (sensations of ‘cool’ type) were recorded. This was due to the fact that higher air temperatures were maintained with a building height of at least 14 m in the forecourts. This is when heat transfer was slower. In addition, the compact, closed structure of buildings prevented free airflow. Convective movements were observed within the forecourt. Horizontal (advective) flow took place above the roof levels.

*Thermal comfort in the north-south oriented forecourts*

The prevailing thermal conditions were more favorable in the forecourt with north-south orientation (Figure 6.15.). Significant reductions in thermal discomfort were achieved with a building height of 14 m. The building structures cast a shadow on the east facade up to the residential level. Then the thermal sensations of a person staying in the outdoor environment were at the ‘hot’ level, both at the eastern and western facades (MF, HF scenarios). It should be noted that with 7m high buildings, conditions became more uncomfortable (LF) at the east facade. This was undoubtedly influenced by the heating of canyon floor, as well as the structure walls. The result was an increase in air temperature and thus thermal discomfort.

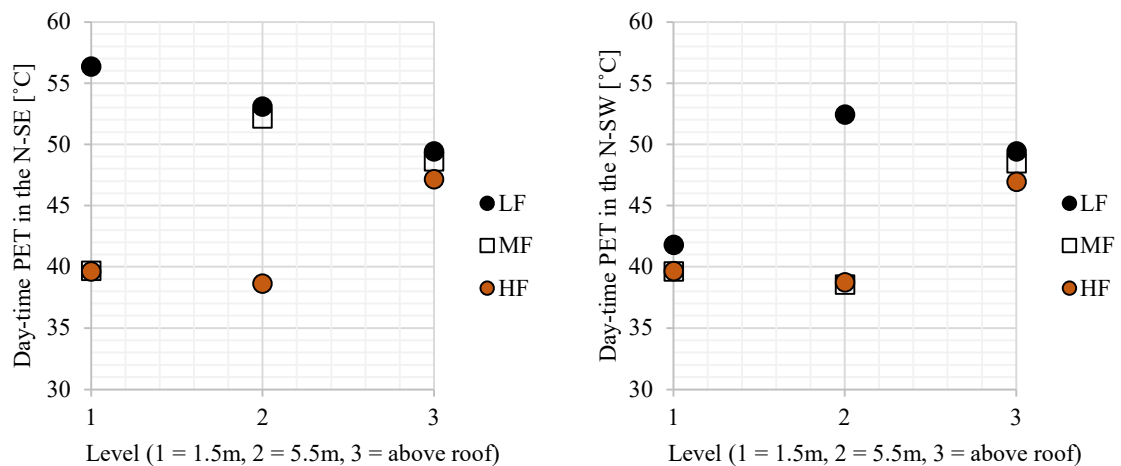


**Figure 6.15.** Effect of building structure on thermal comfort in the north-south oriented forecourt (upper left - N-SE, upper right - N-SW, 3 pm; bottom left - N-SE, bottom right - N-SW, 3 am)(source: own elaboration).

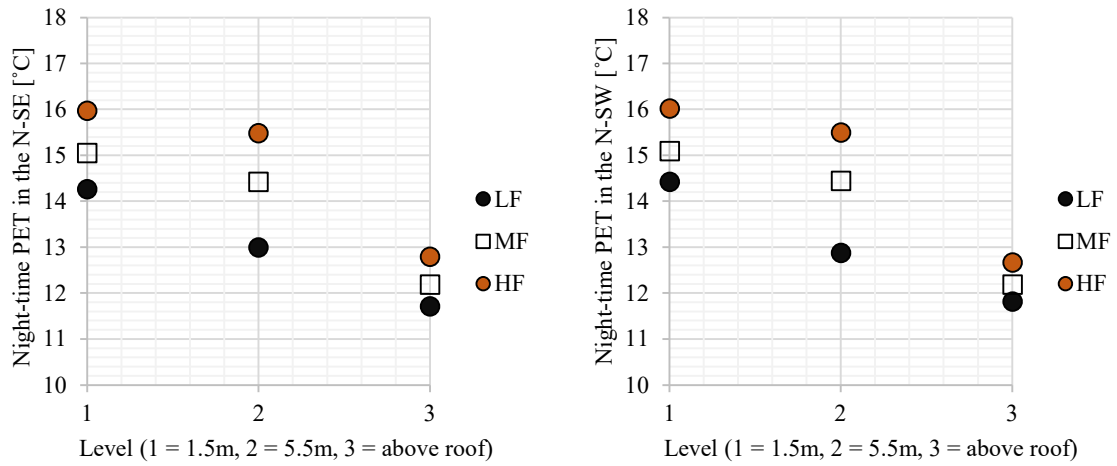


**Fig. 6.15.** Continuation.

Conditions appeared to be more favorable at night than in the forecourt with east-west orientation. Higher PET values were recorded at the pedestrian movement level and also at the residential level (all scenarios). The forecourt structure decreased the energy exchange processes up to the height of roof layer, inhibited heat exchange with the environment. The wind direction - east was also a key element. The forecourt shape elongated on the north-south axis caused the movement of air masses directly above the roof layer. Only convection movements were recorded within the forecourt.



# CHAPTER VII. INFLUENCE OF ADAPTATION STRATEGIES ON EXTERNAL ENVIRONMENT

## 7.1. The role of greenery

### The nature-based scenarios for the street canyons

The scenarios considered were related to the introduction of passive technologies in the form of green roofs, walls, and tall greenery (deciduous trees) into a highly urbanized environment. The research concerned thermal conditions in the area of a typical street canyon. The impact of implemented passive solutions was estimated in the zone of influence of microclimatic conditions on the pedestrian (1.5 m height, the level of human movement in public spaces), the occurrence of dwellings (5.5 m height; to estimate the impact of microclimate on residents in buildings), as well as over the building roofs (15.5 m height). The analyzed solutions are shown in [Figure 7.1](#).

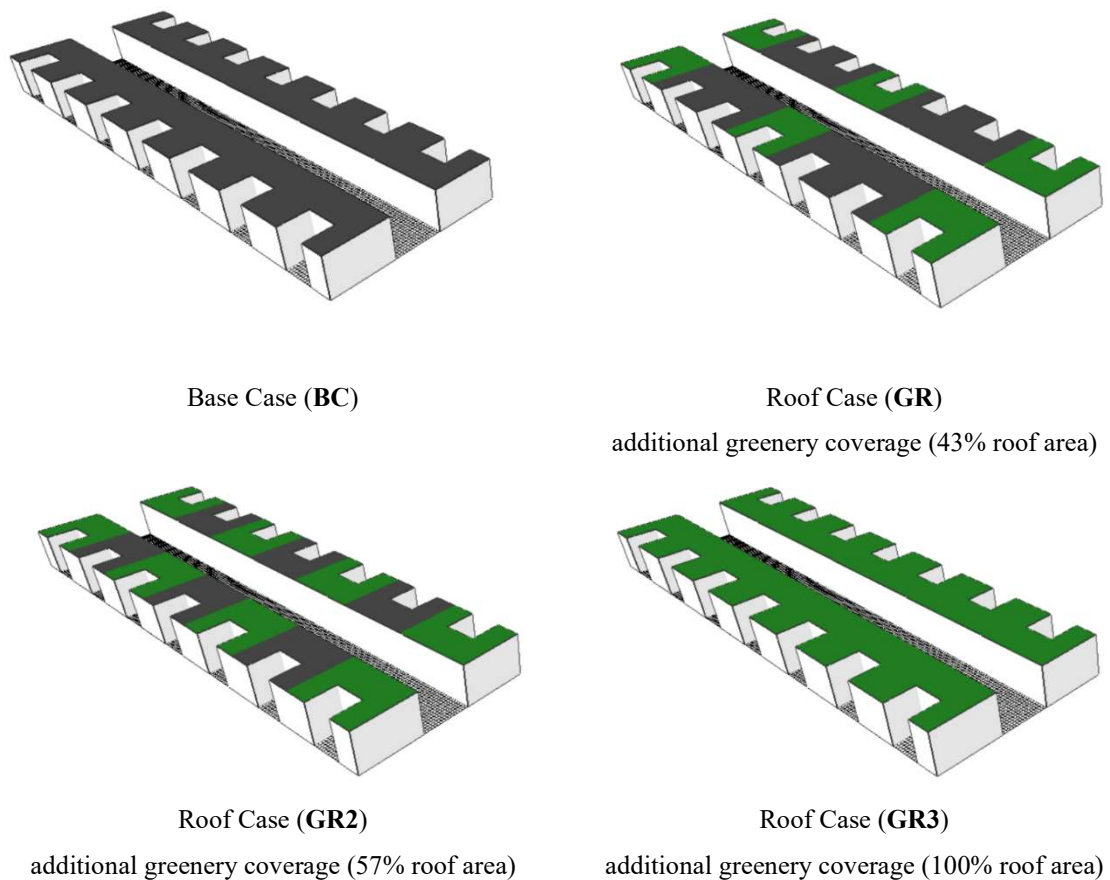


**Figure 7.1.** Green scenarios in the canyons (source: own elaboration).

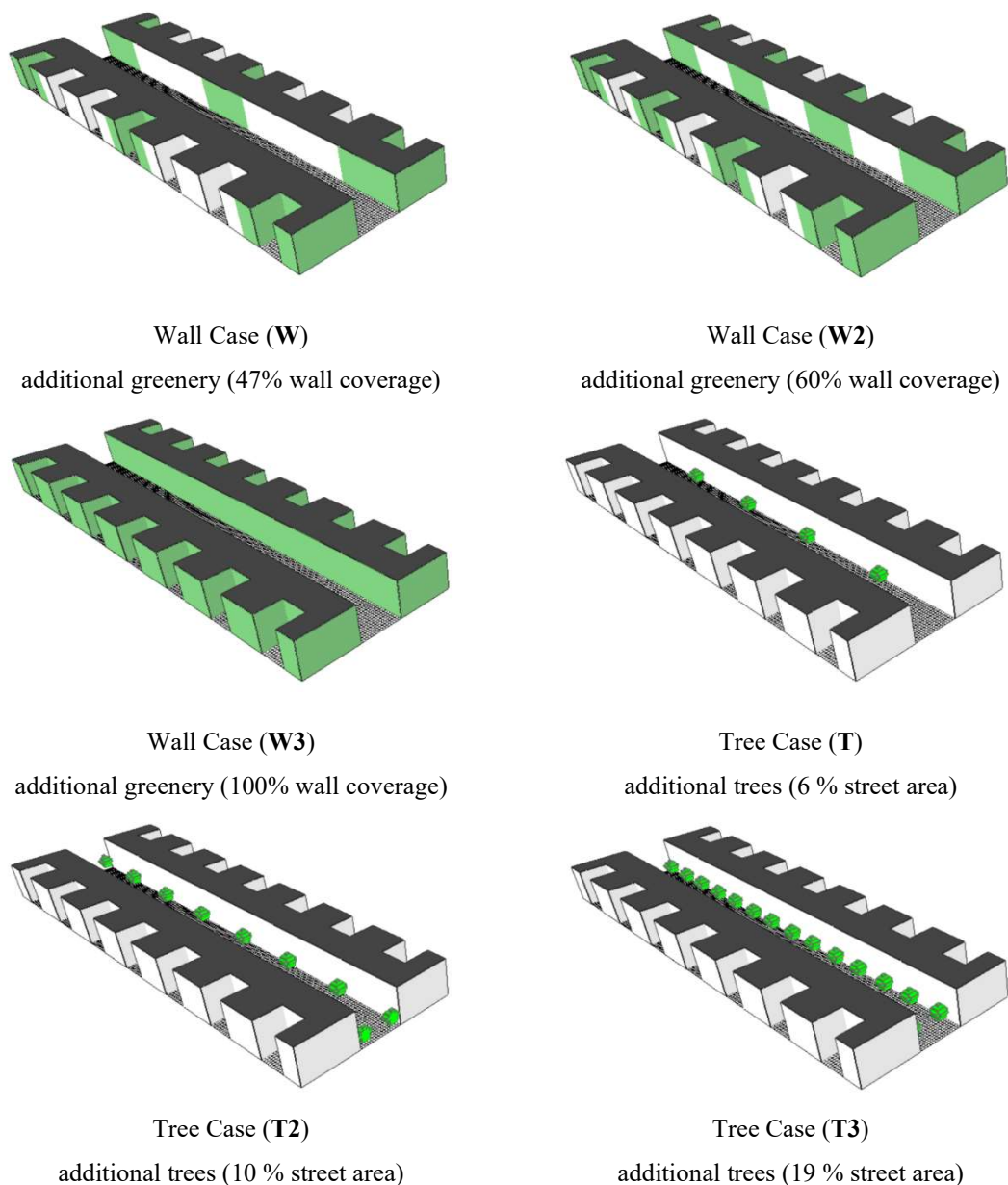


**Figure 7.1.** Continuation.

### **Green Roof Cases (GR, GR2 and GR3)**

The scenarios were related to the introduction of green roofs on buildings forming the structure of a typical street canyon (Figure 7.2.). An extensive construction was assumed. It consisted of a substrate layer (15 cm, sandy loam) with planted grass (30 cm). In the first scenario - Roof Case (GR), 43% of the surface of existing buildings was covered with greenery. Passive solutions were introduced on every third building. In the next scenario, Roof Case (GR2), 57% of the building surface was covered with greenery. Plantings were

introduced on every second roof. The last scenario - Roof Case (GR3) assumed that roofs were completely covered with greenery.

It should be emphasized that from the application point of view the last of the scenarios is not possible to implement. However, it was taken into account in order to illustrate the maximum impact of a given solution on thermal conditions.

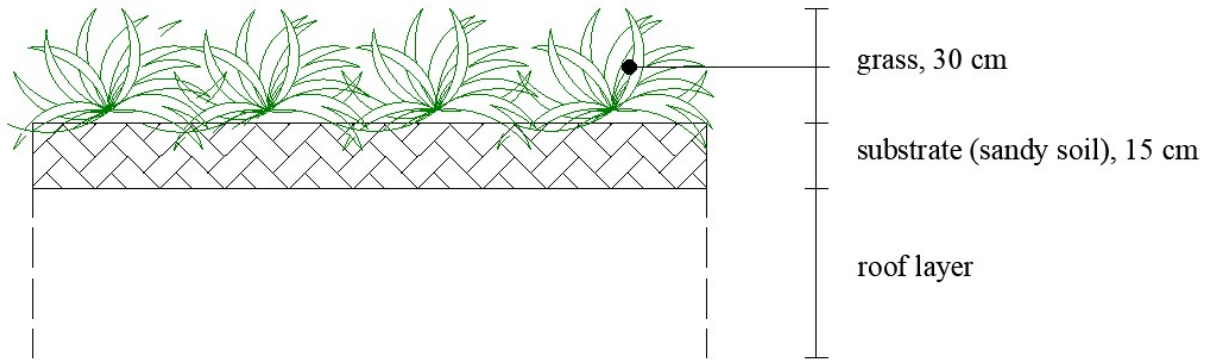


**Figure 7.2.** The construction of the green roof (source: own elaboration).

### **Green Wall Cases (W, W2 and W3)**

The presented scenarios assumed the introduction of passive solutions in the form of green walls (Figure 7.3.). It was considered to cover the building facades with climbing plants - ivy. Wall Case (W) involved covering 47% of vertical surfaces with greenery. In the second case - Wall Case (W2) it was assumed to introduce 60% of surfaces planted with vegetation. The last of the considered - Wall Case (W3) took into account the total greenery coverage of the model walls.

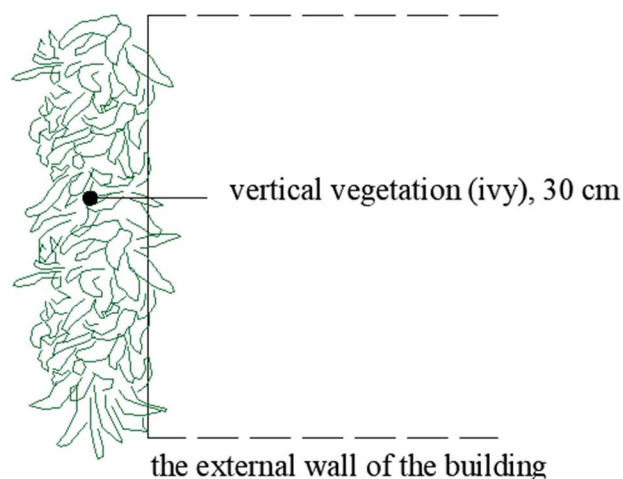


**Figure 7.3.** The construction of the green wall (source: own elaboration).

As it was mentioned above - W3 - is a scenario treated as a hypothetical solution. Its practical application is not possible due to complex geometry of building constructions, i.e.

occurrence of window and door openings. However, the general idea was presented in order to show the potential impact of solutions on thermal conditions, as well as on human comfort.

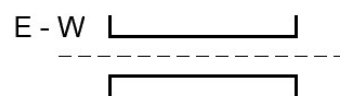
### **Tree Cases (Tree Case - T, T2 and T3)**

The simulations included the use of tall greenery in the form of deciduous trees measuring 5 m x 5 m x 7 m, with the widest crown part extending at a height of 4 meters. Tree Case - T assumed the presence of 8 deciduous trees that occupied 6% of the canyon area. They were introduced at distances of 42 meters. Another of the Tree Case scenarios (T2) assumed the introduction of 12 trees, which represented 10% of the communication route. The plantings were implemented at distances of 27 meters. The last one - Tree Case (T3) involved the introduction of 28 trees covering 19% of the canyon area. The distance between the greenery was 15 meters. The location was selected in terms of the real possibility of planting trees in the inner-city area. In this way, the collision issue of introduced green solutions with areas serving as access roads to buildings was eliminated (usually the gateways are located in the middle of frontal buildings)([Appendix A](#)).

The last scenario (T3) may be identified with the measures implemented in the inner-city of Lodz. Revitalization measures consist in the introduction of evenly distributed vegetation (trees) in public spaces. In accordance with legal requirements, greenery coverage is to constitute at least 15% of the area of street canyons ([Resolution No. VI/211/19, 2019](#)).

### **Impact of nature-based solutions on microclimatic conditions in the east-west oriented canyon**

#### **Green roofs**



Simulations were carried out for scenarios related to the introduction of green roofs in the east-west oriented canyon. Preliminary analysis showed that the dynamics of changes in thermal conditions were similar at selected characteristic points, i.e., at the north facade (E-WN) and at the south facade (E-WS)(Their locations are shown in [Figure 7.4](#).<sup>3</sup>). Therefore, the impact of green solutions is presented based on the data acquired at the

---

<sup>3</sup> Information was taken at specific points located at a considerable distance from the domain border, 2.5 m from the building facades. The choice was dictated by limiting the boundary effects on microclimatic conditions in the canyons.

measurement point at the north facade (E-WN). The effect of vegetation on the microclimate during the daytime (3 pm) as well as during the nighttime (3 am) was shown. The change in air temperature with altitude is shown in [Figure 7.5](#).<sup>4</sup>

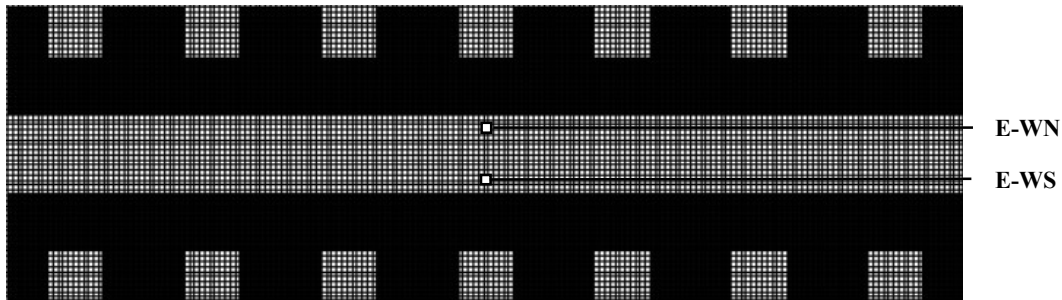


**Figure 7.4.** Location of E-WN and E-WS measurement points in the street canyon (source: own elaboration).

The study showed that covering the roof slopes with vegetation contributed to a slight modification of the ambient temperature. The most beneficial impact was recorded for scenario GR3 (100%). The average diurnal reduction in air temperature was  $0.46^{\circ}\text{C}$  directly above the building roofs. As height decreased, the impact of vegetation decreased  $-0.11^{\circ}\text{C}$  (at residential level = 5.5 m),  $0.13^{\circ}\text{C}$  (at pedestrian movement height = 1.5 m). The solution had a soothing effect during the day (max change of air temperature =  $0.50^{\circ}\text{C}$ , GR3). Despite the insignificant effect on air temperature, the introduction of green roofs contributed to a reduction in the temperature of roof slopes. They warmed up to  $20\text{-}25^{\circ}\text{C}$ . In other cases, the temperature was over  $60^{\circ}\text{C}$  (roofing tar paper).

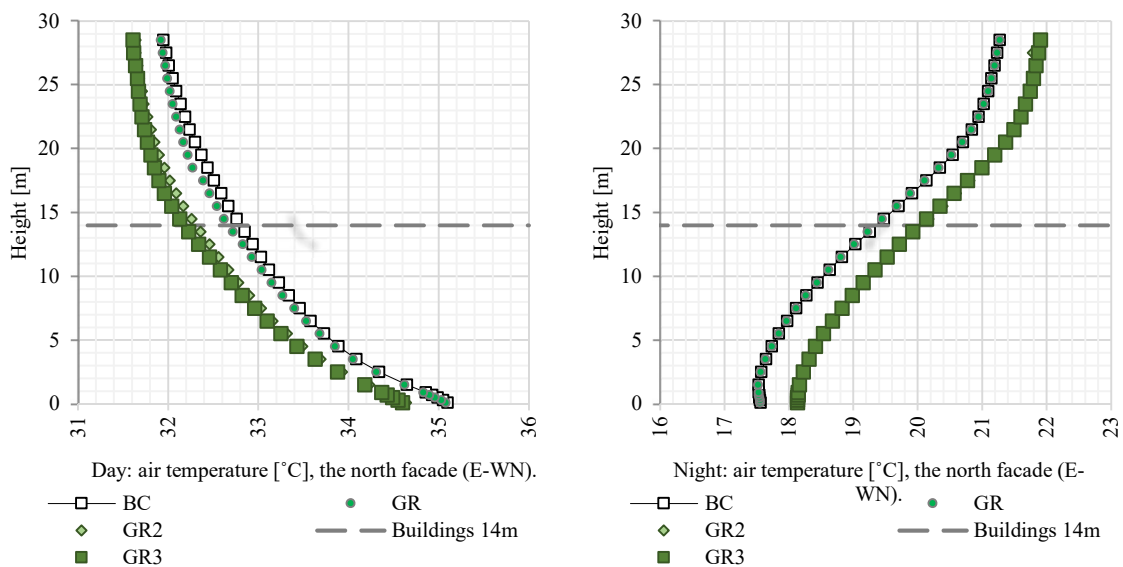
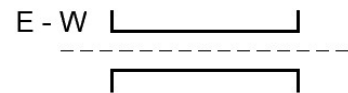


**Figure 7.5.** Impact of green roofs on thermal conditions of the east-west oriented canyon (source: own elaboration).

<sup>4</sup> Tabular summary attached as [Appendix 6](#).

Unfortunately, the unfavorable influence of greenery during the night time was noted. Then, the air temperature over the roofs was higher (0.65°C; GR3). A similar effect was observed in the GR2 scenario (57%). The reason for this effect can be found in the heat exchange on the vegetation-environment path. Green roofs released the absorbed energy at night. As a result, the air temperature in the canyon increased. Moreover, the effect was more intense directly above the roof layer. This was caused by heat dissipation through the highly heated roof surfaces. Covering the roof slopes with vegetation in 43% (GR), did not significantly affect the thermal conditions.

### Living facades



Analyses included the impact of green walls on thermal conditions within the east-west oriented canyon (Figure 7.6.<sup>5</sup>). The applied solutions contributed similarly to the change in air temperature. The mean diurnal difference was 0.38°C (W), 0.36°C (W2), 0.49°C (W3) in the E-WN during the day. Vegetation had a soothing effect on thermal conditions in the area. The greenery reduced the amount of solar radiation reaching the facade surfaces. It constituted a kind of physical barrier. Thus, it protected the walls from strong heating during the day. The buildings, which were covered with vegetation, heated up to 35-39°C. In other cases, a value of 39-42°C was recorded (plastered buildings). Adverse impact was observed during night time. The air temperature increased by 0.63°C (W), 0.62°C (W2), 0.70°C (W3) in the E-WN; 0.64°C (W), 0.63°C (W2) and 0.72°C (W3) in the E-WS.

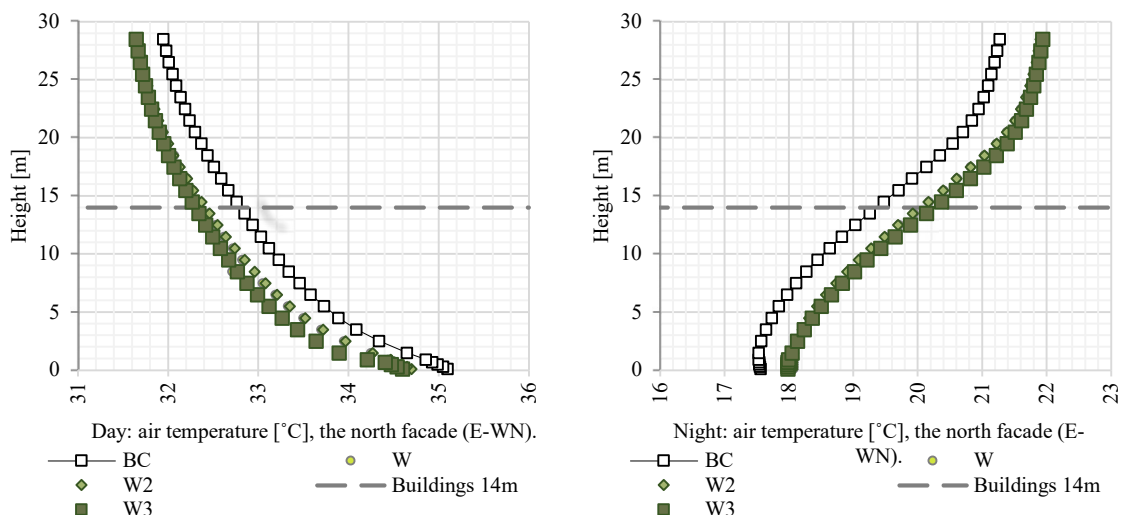
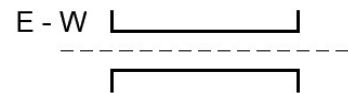


**Figure 7.6.** Impact of green walls on thermal conditions of the east-west oriented canyon (source: own elaboration).

<sup>5</sup> Tabular summary attached as [Appendix 7](#).

This effect was related to the fact that the evapotranspiration process took place in the outdoor environment. It included the transpiration, which was being done by the leaves' stomata. Moreover, it took into account the evaporation (water was released from the plant surface to the atmosphere). As the effect, the ambient temperature was reduced in the day-time. Unfortunately, the heat exchange on the vegetation-ambient path contributed to an increase in the air temperature at night-time.

### High greenery



In order to show the influence of introduced solutions - high greenery on thermal conditions, the selected points were located in the vicinity of trees, at the height of 1.5 m, at a distance of 2.5 m from the northern frontage (E-WN-T), as well as from the southern development (E-WS-T)(Their location is presented in [Figure 7.7](#)). A comparison of the scenarios is shown in [Figure 7.8](#).<sup>6</sup>

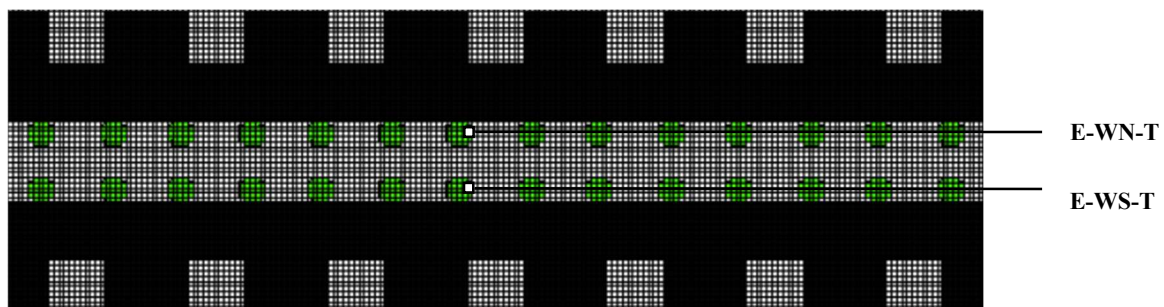


**Figure 7.7.** Location of E-WN-T and E-WS-T measurement points in the street canyon (source: own elaboration).

Trees created a kind of ‘cool enclave’ during the day. Already the introduction of 6% greening (T - scenario) contributed to a reduction in air temperature, i.e. 0.63°C (E-WN-T), 0.66°C (E-WS-T) at pedestrian movement level. The effect decreased with the distance from greenery. Adverse modification of thermal parameters was observable at night time. The increase in air temperature was 0.81°C (T), 0.70°C (T2), 0.66° (T3) at the E-WN-T point (north facade). Similar conditions were observed at the south facade (E-WS-T).

Trees limited the heating of facades during the day. The temperature of building walls was 34-39°C in the immediate vicinity of high greenery. In other cases it reached 39-42°C (plastered buildings). In addition, the author conducted a study of the temperature of canyon pavement. It turned out that trees effectively influenced the modification of thermal

<sup>6</sup> Tabular summary attached as [Appendix 8](#).

conditions of the floor. There was observed a reduction of 1.55°C (T), 1.57°C (T2), 1.61°C (T3) in the E-WN-T; 1.49°C (T), 1.56°C (T2), 1.81°C (T3) in the E-WS-T during the day under the tree crowns.

Considering the analyses results, it should be concluded that the introduction of 10% greening of the canyons seems to be the most favorable solution. It is as effective as the other scenarios in reducing daytime thermal parameters. In addition, it contributes to a lesser extent to increasing the values of air temperature and pavement temperature at night.

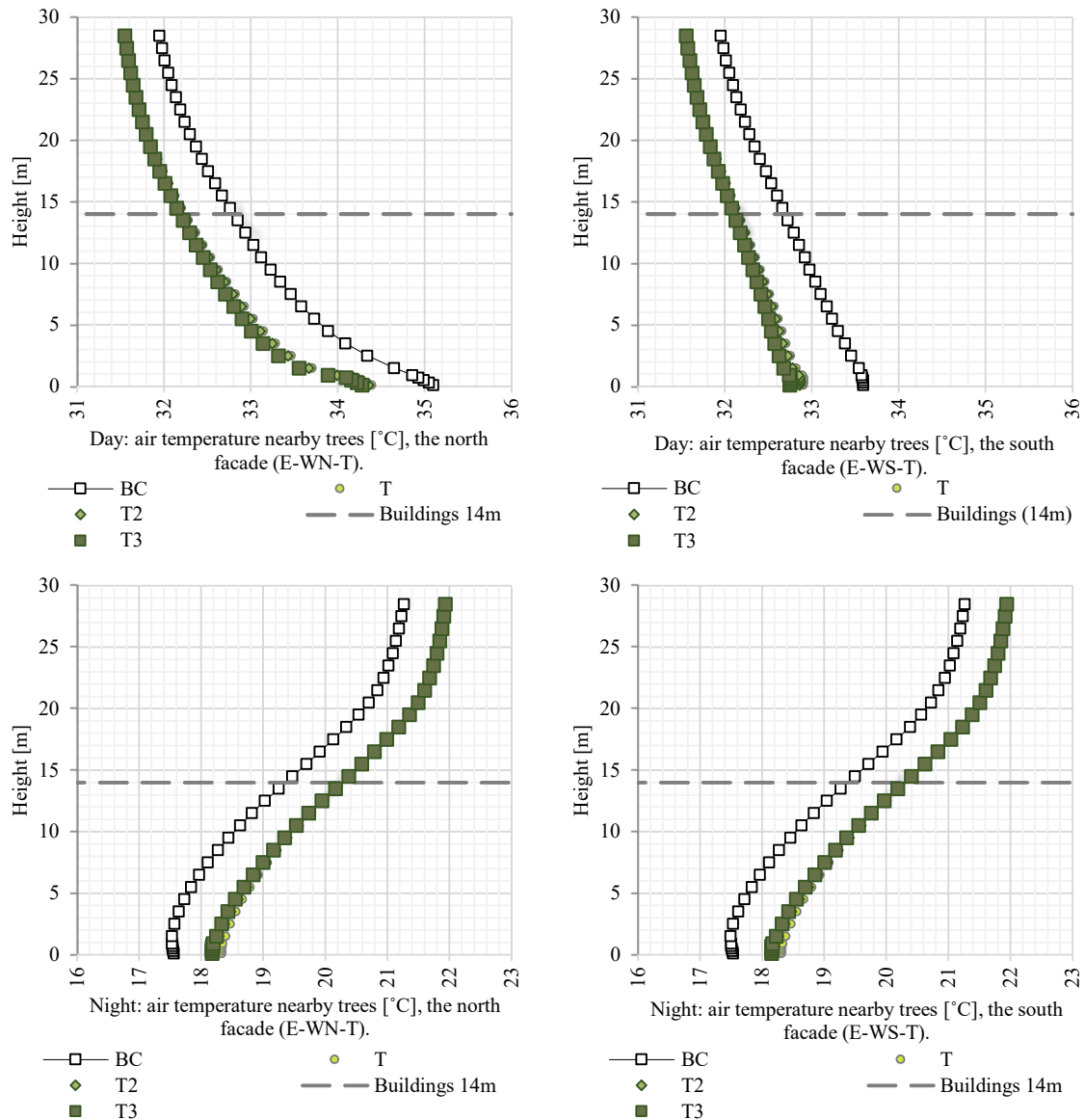


**Figure 7.8.** Impact of tall greenery on thermal conditions in the east-west oriented canyon (left column - E-WN-T; right column - E-WS-T)(source: own elaboration).



## Impact of nature-based solutions on microclimatic conditions in the north-south oriented canyon

### Green roofs

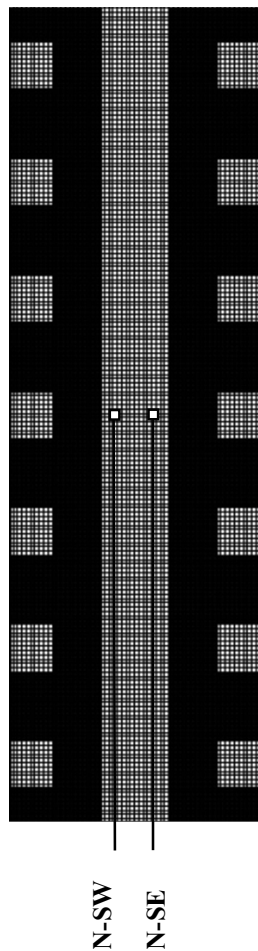


**Figure 7.9.** Location of N-SW and N-SE measurement points in the street canyon (source: own elaboration).

The situation was different in the north-south oriented canyon (The location of measurement points is shown in [Figure 7.9](#)). The GR scenario (every third building covered with low vegetation - 57%) resulted in a similar outcome as GR3 (100% coverage of roof slopes)([Figure 7.10](#)).<sup>7</sup> The strongest impact of greenery was observed in the immediate vicinity of applied solution. The average reduction of the parameter was 0.85°C (GR), 0.62°C (GR2), 0.90°C (GR3) in the N-SE during the day. Greenery contributed to increase the air temperature during night time. The modification was small within the canyon (up to 0.37°C in the N-SE). Above the building roofs, the difference was noticeable (1.64°C in the N-SE).

In this case, the influence of building layout on thermal conditions should be emphasized. Distribution of air temperature was dependent on the geometry of building structures. They directly influenced the amount of solar radiation reaching the ground surface. The effect was to modify the air temperature as well as the pavement. The buildings shaped the aerodynamic conditions of this area. It was a physical barrier for free movement of air masses (east wind direction was assumed). The inflowing warm masses encountering the buildings were carried above the roof layer. After flowing over the green roof they were cooled down. Then, they penetrated into the canyon interior modifying the thermal conditions. It was possible to observe the impact at the western facade. In this area, the cooler air masses had a soothing effect on pedestrian movement.

<sup>7</sup> Tabular summary attached as [Appendix 9](#).

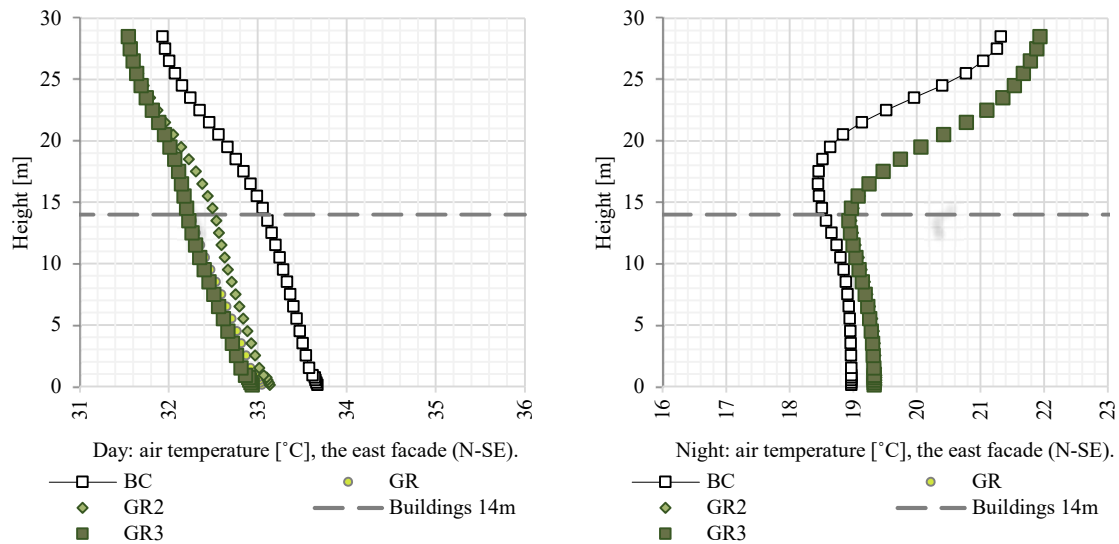
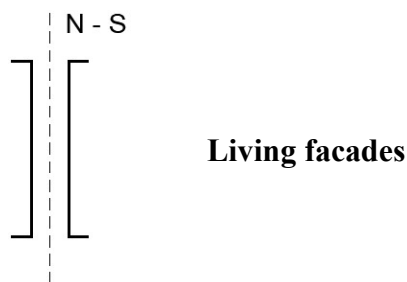


**Figure 7.10.** Impact of green roofs on thermal conditions in the north-south oriented canyon area (source: own elaboration).



The analyses showed that the application of greenery on the building facades had a relatively low efficiency (Figure 7.11.<sup>8</sup>). The solution of 47% coverage of vertical surfaces with vegetation (W) had a similar effect as 100% greening of building facades (W3). The average reduction in air temperature oscillated between 0.43°C (W,

W2), 0.37°C (W3) in the N-SE during the day. Vegetation caused the parameter to increase at night. This is when a rise in temperature of up to 1.64°C (in the N-SE) was observed. The maximum change was recorded immediately above the Urban Conopy Layer (>14 m). Here, the reason can be found in the heat exchange on the roof-environment path. The low albedo of the roof covering caused strong heating of the surface during the day (above 60°C). As a result, there was an increase in air temperature at night. Then, the energy was released to the environment.

Modification of thermal conditions of building constructions was also significant. The temperature of green walls was reduced to 35-39°C. Other buildings heated up more strongly (external facades covered with plaster - over 39°C) during the day. The opposite effect could be observed at night. Where vegetation was introduced, a higher temperature (by 1°C) was observed. The reason was the evapotranspiration process, i.e. heat exchange

<sup>8</sup> Tabular summary attached as [Appendix 10](#).

on the vegetation-environment path. Greened facades more slowly released energy during the night time.

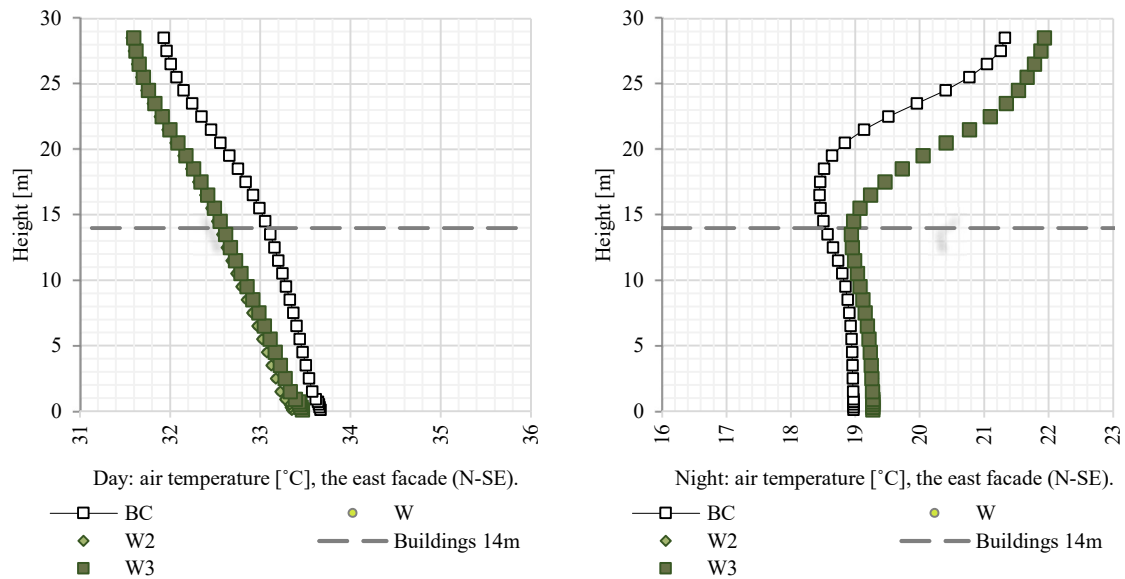


**Figure 7.11.** Impact of green walls on thermal conditions in the north-south oriented canyon area (source: own elaboration).

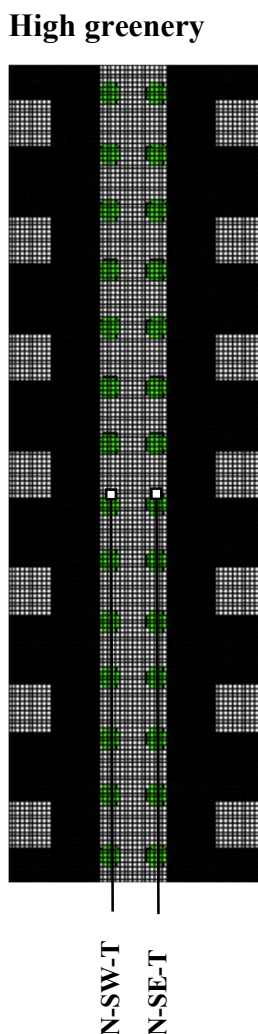


**Figure 7.12.** Location of N-SW-T and N-SE-T measurement points in street canyon (source: own elaboration).

The effect of tall greenery on thermal conditions was assessed in the north-south oriented canyon. Preliminary analyses showed that similar dynamics of changes in thermal parameters in the immediate vicinity of trees were recorded at both the east (N-SE-T) and west (N-SW-T) facades (Figure 7.12.). Therefore, the change in outside air temperature was illustrated using information obtained from a selected measurement point located in the central zone of the canyons, at the east facade (N-SE-T), at a distance of 2.5 m from the walls, in the immediate vicinity of the trees (Figure 7.13.; Appendix 11.). The aim was to show the effect of tall greenery on the canyons' thermals.

Trees constituted 'islands of coolness' during the day. Temperature reduction was 0.66°C (T), 0.67°C (T2), 0.72°C (T3) in the N-SE-T in the immediate vicinity of trees at the pedestrian movement level. The soothing effect of vegetation decreased with distance. However, it should be noted that above the Urban Canopy Layer

(>14m) there was a noticeable effect of tall greenery on air temperature. It was reduced by 0.63°C (T), 0.70°C (T2), 0.63°C (T3) in the N-SE-T during the day.

Trees had an effect on the thermal conditions of building facades. They prevented solar radiation from reaching the vertical surfaces. This resulted in the temperature of building walls oscillating between 35-39°C. They shaded the canyon floor. Then, the temperature reduction was 1.34°C (T), 1.35°C (T2), 1.45°C (T3) in the N-SE-T.

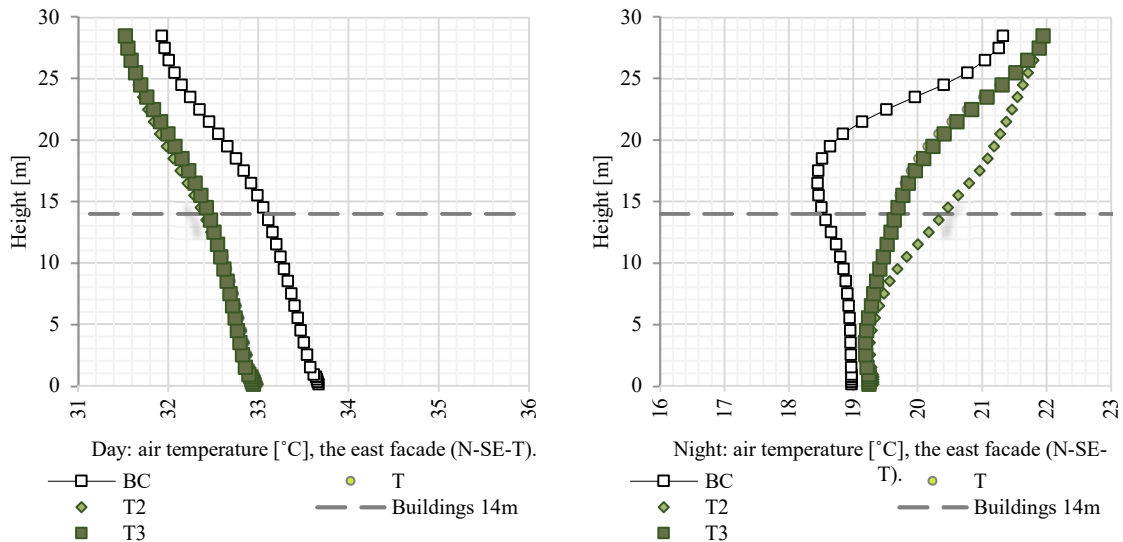


**Figure 7.13.** Impact of tall greenery on thermal conditions of the north-south oriented canyon (source: own elaboration).

Thermal conditions deteriorated during the night time. A particularly unfavorable situation was recorded for the T2 scenario (10% green coverage). There was a significant increase in temperature above the tree crowns (1.55°C in the N-SE-T). The maximum change was 2.56°C (at 18.5 m height; in the N-SE-T). In this case, the influence of phenomena occurring above buildings must be taken into account. Here, the heat exchange between the roof slope and the surroundings becomes important.

### Thermal comfort

In the further part of the work, in order to determine the influence of passive solutions on human thermal comfort, the value of the PET coefficient was analyzed. Readings were taken at the north facade (E-WN) as well as the south facade (E-WS) to show the impact of building geometry on thermal comfort within the east-west oriented canyon. Measurements were conducted at pedestrian movement height ( $h=1.5$  m) as well as at residential level ( $h=5.5$  m). The situation that occurs during the daytime (3 pm) and nighttime (3 am) was shown. The impact of passive solutions on human thermal comfort is shown in [Figure 7.14](#).

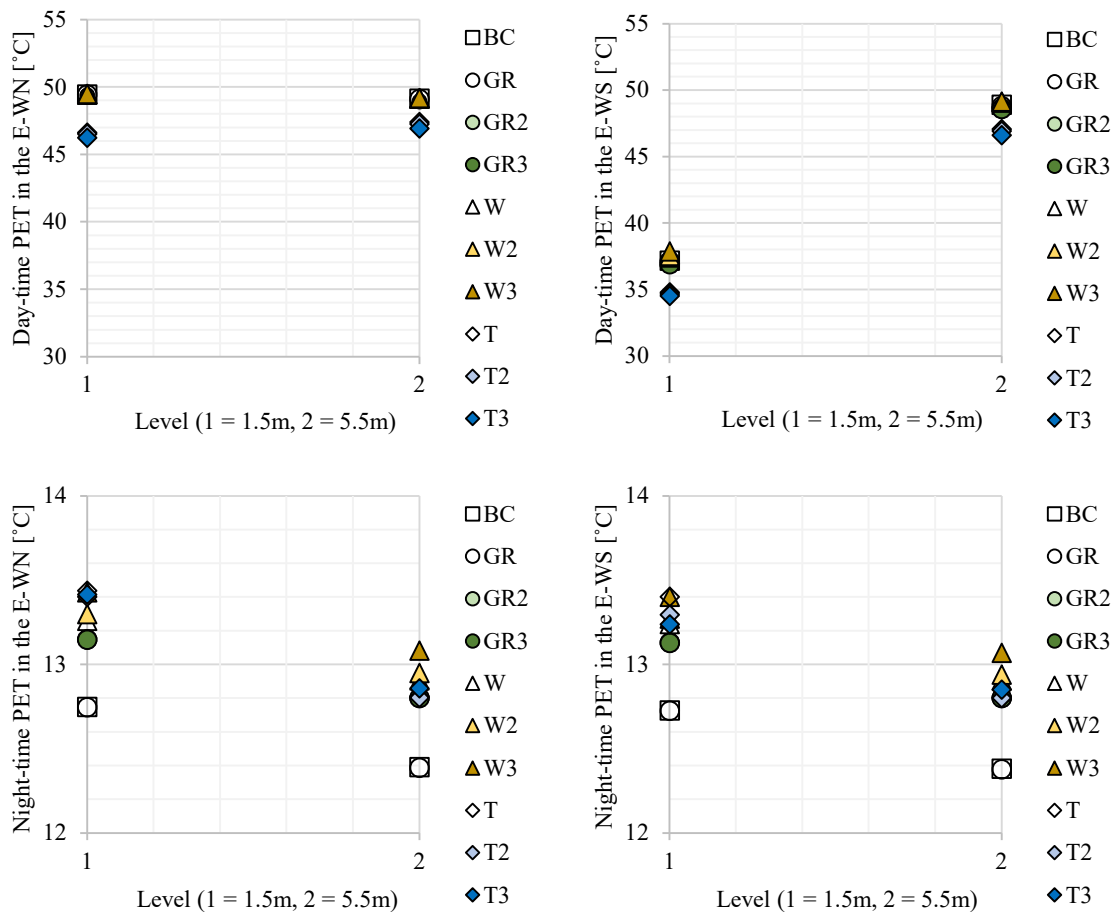


**Figure 7.14.** Impact of green solutions on thermal comfort in the east-west oriented canyon (upper left - E-WN, upper right - E-WS, **3 pm**; bottom left - E-WN, bottom right - E-WS, **3 am**)(source: own elaboration).

The PET variation was evident within the street canyon during the day (up to a height of 14 m). In places where the buildings provided a physical barrier to the inflow of solar radiation, lower index values were recorded, particularly at the south facade at pedestrian movement level. Thermal comfort was reduced from ‘very hot’ (E-WN) to ‘warm’ (E-WS). There was visible blurring of the boundary of influence of building geometry on thermal sensation at residential height. Solar radiation contributed in a significant way to increase thermal discomfort. This is when thermal conditions were described as ‘very hot’.

The PET index oscillated between 12-14°C during the night time. More favorable conditions prevailed at the pedestrian level (‘slightly cool’). The heated horizontal surfaces (canyon floor) and vertical surfaces (building walls) released the heat accumulated during the day to the environment. This resulted in slightly higher PET values at the pedestrian movement level. From the residential level, thermal - ‘cool’ conditions were recorded. This is when the influence of energy exchange processes on the pavement-environment path decreased.

The passive technologies implemented translated into thermal sensations. The introduction of tall greenery had the greatest impact on thermal conditions. The strategy of 6% greening (T) proved to be as effective as the introduction of 19% canyon green cover (T3). Conditions that were initially described as ‘very hot’ (BC) were reduced to ‘warm’ (Tree Scenarios). This effect was observed with the south facade at the pedestrian movement level. The synergistic effect of building form as well as tall greenery enabled a significant reduction in thermal discomfort.

The effect of green roofs on thermal sensation was virtually unnoticeable during the day. The prevailing conditions were described as ‘very hot’ (E-WN), and ‘warm’ (E-WS). It was only from 57% of the greening level (GR2) onwards that an effect on thermal comfort at night was observed. The scenario proved to be as effective as 100% vegetation coverage of roofs (GR3).

The implementation of green walls adversely affected the perceived daytime thermal conditions. The PET value was slightly increased. This fact was probably due to the property of vegetation to reflect solar radiation. Albedo of greenery was higher than that of artificial surfaces (plastered walls of buildings). As a result, a large part of the radiation was reflected by the plants and then absorbed by the other canyon surfaces. The increase in PET values should be considered as a beneficial phenomenon during the night time. This is when conditions close to ‘neutral’ are maintained. This effect was achieved after the introduction of living facades in the canyons. They caused modification of air temperature. This was due to the fact of evapotranspiration process, which involved the vegetation releasing energy to the environment. In this case, the most effective solution was to completely cover the walls with vegetation (W3). Then there was observed increase of PET by 0.68°C (h=1.5 m), 0.23°C (h=5.5 m), 0.40°C (h=15.5 m). It should be noted that the index value was influenced by the energy exchange along the artificial surfaces (floor) - pedestrian level environment.

Next, analyses were conducted within the north-south oriented canyon. Readings were taken at measurement points located at the east facade (N-SE), as well as the west facade (N-SW). The results are shown in [Figure 7.15](#).

Undoubtedly, the development structure contributed to the modification of daytime conditions in the canyon. It was effective in reducing sunlight levels, especially at the western facade. Lower PET values were recorded in the shaded areas - up to residence height (5.5 m). Perceived thermal conditions were at the ‘hot’ level. Although the north-south oriented canyon area received twice as much sunlight as the east-west oriented canyon, less favorable conditions were observed. It can be surmised that this was due to

impeded airflow. The model assumed wind inflow from the east during the warmest day of a Typical Meteorological Year. As a result, objects forming the building frontage constituted a barrier impeding free air exchange.

The PET index oscillated between 14-16°C at night. More favorable conditions were observed up to the height of roof layer ('slightly cool'). The energy exchange between the artificial surfaces and the surroundings caused an increase in the canyon air temperature.

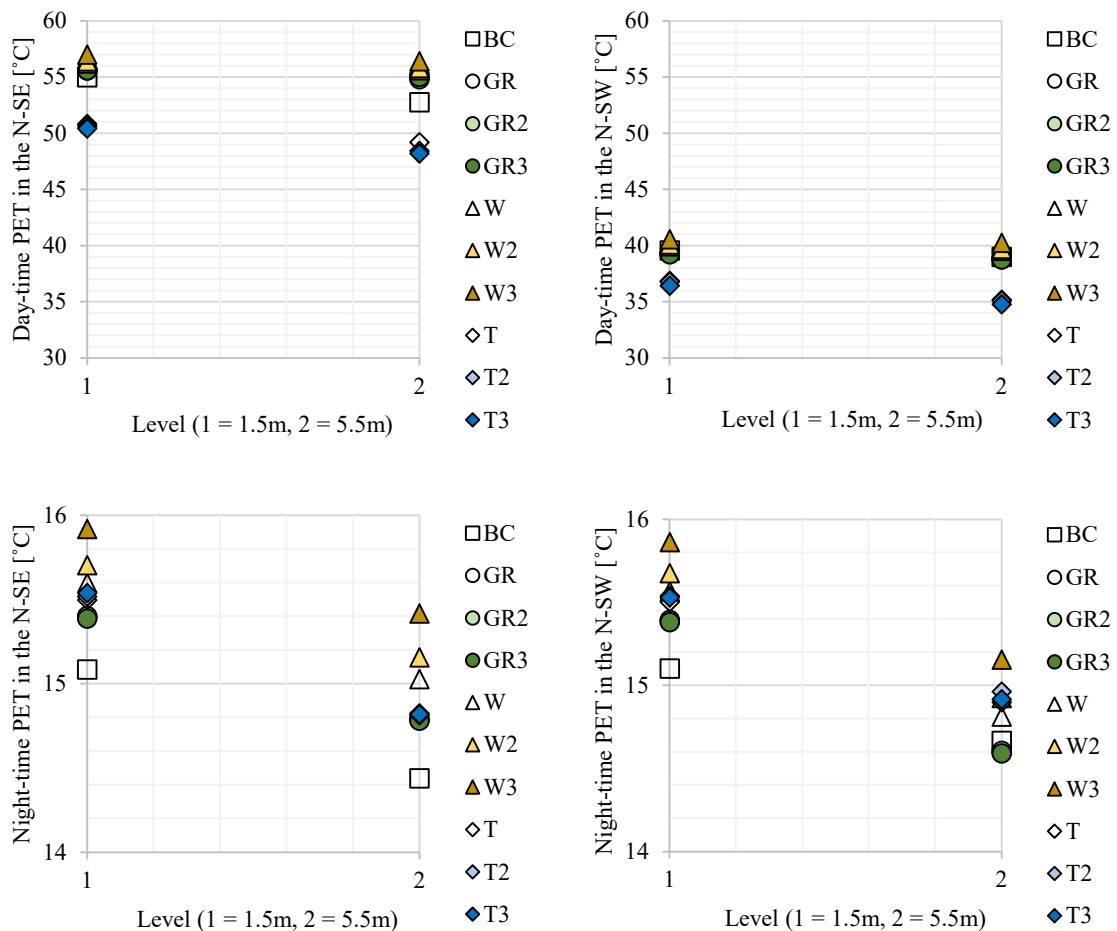


**Figure 7.15.** Impact of green solutions on thermal comfort in the north-south oriented canyon (upper left - N-SE, upper right - N-SW, **3 pm**; bottom left - N-SE, bottom right - N-SW, **3 am**)(source: own elaboration).

The passive solutions implemented had an impact on thermal comfort. The most favorable scenarios were associated with planting trees in the canyon. Implementation of 6% area greening (T) was as effective as 19% green coverage ratio (T3). Thermal discomfort was experienced in the heavily sunlit areas (eastern part of the canyon), despite the significant reduction in PET, conditions remained at the 'very hot' level. In shaded areas (at the west elevation), the effect was a reduction to 'hot' conditions.

The living facades caused an increase in PET values. This could be due to the fact that vegetation reflects a significant amount of solar radiation. As a result, the thermal conditions

during the day deteriorated, especially at the pedestrian ( $h=1.5$  m) and residential ( $h = 5.5$  m) levels. However, they had a soothing effect at night. They minimally increased the air temperature in the canyon. Then, thermal conditions were described as ‘slightly cool’.

### The nature-based scenarios for the forecourts

The second urban form considered was a compact residential structure, which is regarded as characteristic of the Metropolitan Area. The forecourt layout is described in [Chapter IV. Selection of the urban forms](#). The influence of building form on the basic microclimatic parameters is presented in [Chapter VI. Numerical simulation of microclimatic and thermal conditions](#). This part considers the impact of passive technologies on the thermal conditions within the forecourt development. The applied solutions are shown in [Figure 7.16](#).

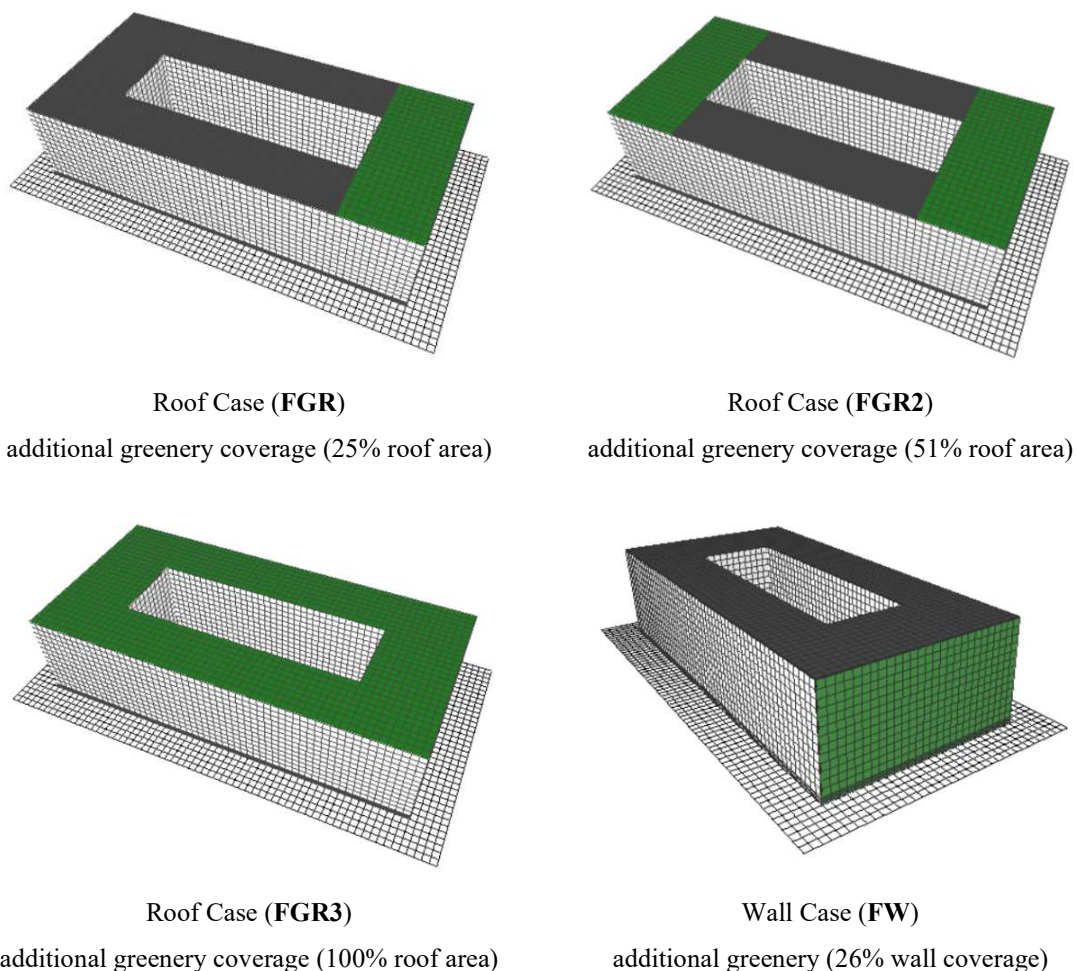
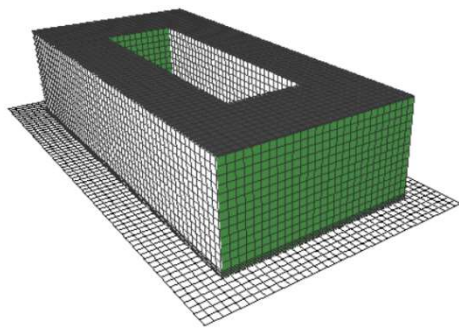


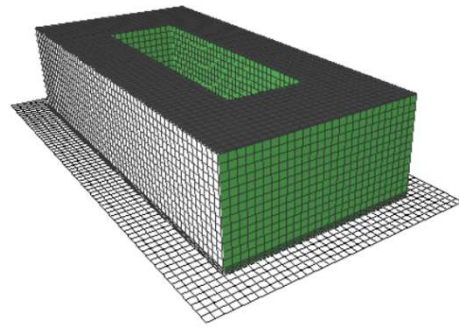
**Figure 7.16.** Green scenarios in the forecourts (source: own elaboration).





Wall Case (FW2)

additional greenery (51% wall coverage)



Wall Case (FW3)

additional greenery (100% wall coverage)

**Figure 7.16.** Continuation.

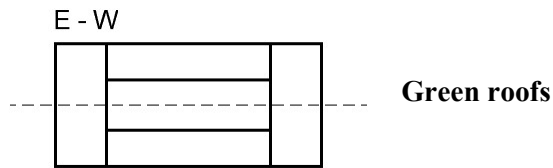
### **Green Roof Cases (FGR, FGR2, FGR3)**

The scenarios were related to the implementation of green roofs on building structures. The Forecourt Green Roof (FGR) scenario involved covering the roof of 27 x 11 m front building with greenery, resulting in an area of 297 m<sup>2</sup> (25%). The Forecourt Green Roof (FGR2) included the use of passive technology on the front building as well as the rear outbuilding. The area used for the green roof was 594 m<sup>2</sup>, or 51% of the total building area. The last scenario considered - Forecourt Green Roof (FGR3) was treated as a theoretical scenario. It was assumed that all roof surfaces would be covered with greenery. In practice, this solution would be impossible to implement.

### **Green Wall Cases (FW, FW2, FW3)**

Other scenarios involved passive solutions - living facades to mitigate climate change. The Forecourt Green Wall (FW) involved the introduction of green walls within a typical forecourt development. Vegetation was planted on the front building facades. The area covered by the transformation was 532 m<sup>2</sup>. In the Forecourt Green Wall (FW2) scenario, the front building facades and the rear outbuilding were planted. This represented 1 064 m<sup>2</sup>. The last case considered involved the total greening of building facades (2 072 m<sup>2</sup>). The scenario of Forecourt Green Wall (FW3) should be considered theoretical. In practice, it would be impossible to implement a complete green facade coverage. Window and door openings would have to be included in the design. The area which would be subject to transformation would be significantly reduced. The percentage of greenery would be smaller.

## Impact of nature-based solutions on microclimatic conditions in the east-west oriented forecourt



The influence of green roofs on microclimatic conditions was tested within the forecourt development.

The presented measurements were conducted at the north facade (E-WN). A similar effect was recorded at the south facade (E-WS)(The location of points is shown in [Figure 7.17](#)). The impact of solution during both daytime (3 pm) and nighttime (3 am) was assessed. The results are shown in [Figure 7.18](#).<sup>9</sup>

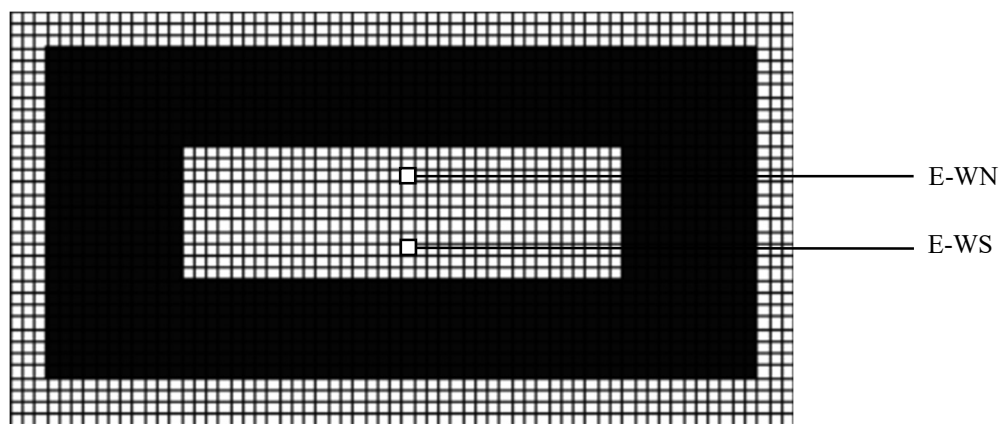


**Figure 7.17.** Location of E-WN and E-WS measurement points in the urban forecourt (source: own elaboration).

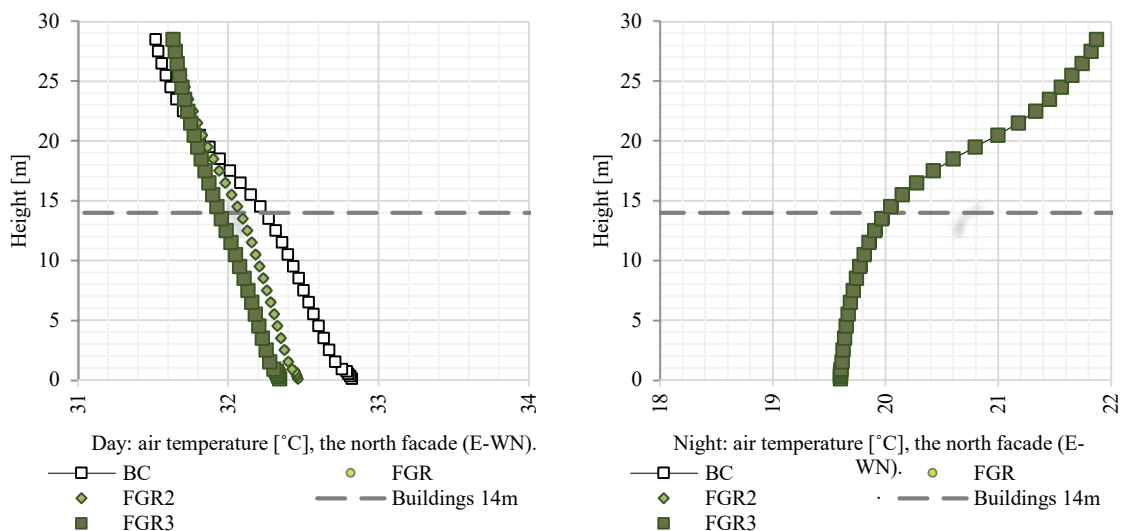
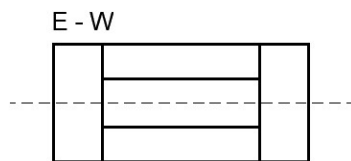


**Figure 7.18.** Impact of green roofs on thermal conditions of the east-west (E-WN) oriented urban forecourt (source: own elaboration).

<sup>9</sup> Tabular summary attached as [Appendix 12](#).

Green roofs slightly lowered the temperature of the outside air during the day in the city forecourt with an east-west orientation. The reduction was 0.31°C (FGR), 0.32°C (FGR2), 0.44°C (FGR3) in the pedestrian zone. It should be noted that the applied solution did not affect the thermal conditions at night.

When assessing the effectiveness of green roofs, it was necessary to take into account their thermal properties. They had a higher albedo than artificial surfaces. They reflected more radiation, thus becoming ‘urban islands of coolness’ during the day. Covering with vegetation reduced the roof temperature to 24°C. In other cases it was over 60°C.



**Green walls**

The next step was to assess the impact of green walls on the thermal conditions in the urban forecourt area (Figure 7.19.<sup>10</sup>).

The study showed that the impact of solution was virtually imperceptible with respect to air temperature. A minimal soothing effect occurred at the pedestrian movement level. Unfortunately, the vegetation covering the buildings contributed negatively to the modification of wall temperature.

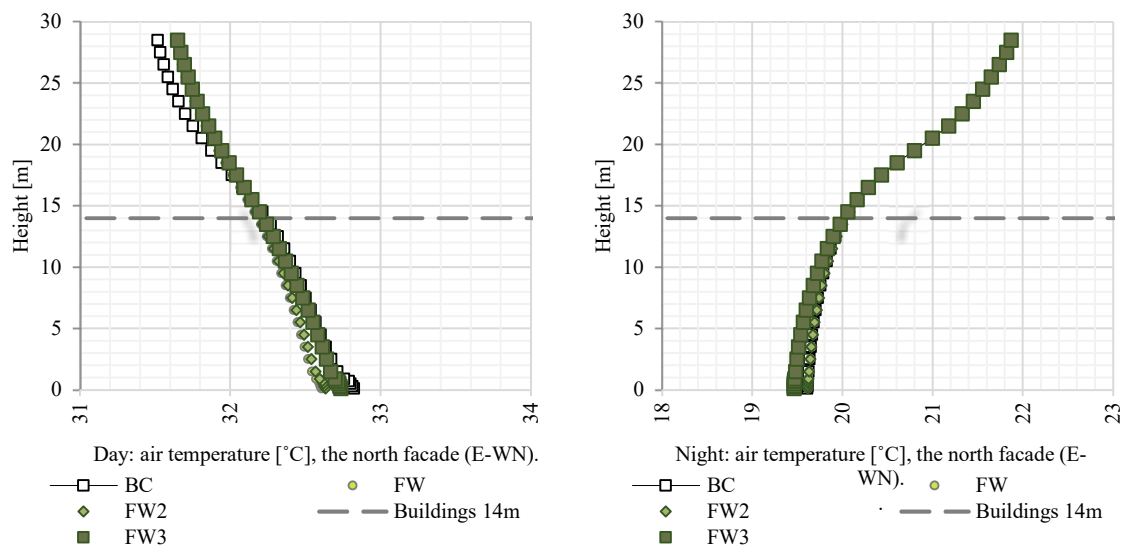


**Figure 7.19.** Impact of green walls on thermal conditions of the east-west (E-WN) oriented urban forecourt (source: own elaboration).

There was an increase in the parameter to 32°C for the south facade (from 29°C), and to 44°C for the north facade (from 36°C). This was a major change in the forecourt development area. The reason is to be found in the multiple reflections of solar radiation from the buildings. In this case, the geometry of buildings adversely affected the thermal

<sup>10</sup> Tabular summary attached as [Appendix 13](#).

conditions of the area. The structure of narrow, long forecourts caused vegetation to intercept more energy. During the nighttime, the opposite trend was noticeable. Significant facade areas covered with vegetation had lower temperatures than plastered buildings (by up to 2°C).

### Impact of nature-based solutions on microclimatic conditions in the north-south oriented forecourt

#### Green roofs

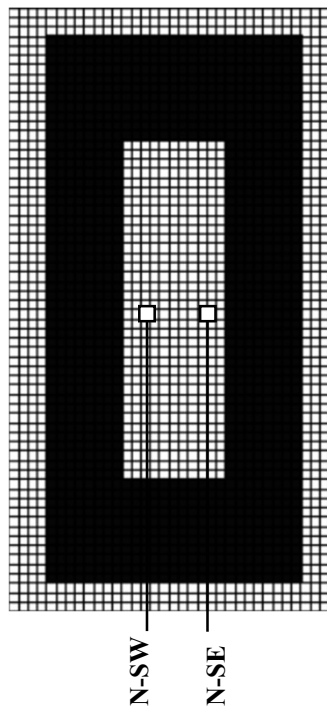


**Figure 7.20.** Location of N-SW and N-SE measurement points in the urban forecourt (source: own elaboration).

A similar impact was observed in the north-south oriented forecourt.<sup>11</sup> The research results confirmed that green roofs were not an efficient solution that would translate into a reduction in air temperature (Figure 7.21.<sup>12</sup>). The effect of vegetation was practically imperceptible when the area occupied by it was less than 57% of the roof coverage. It was only when the slope was completely greened (FGR3) that a minimal soothing effect was evident. The change was 0.12°C (FGR), 0.14°C (FGR2), 0.31°C (FGR3) at the pedestrian movement level. However, there was an observable effect of vegetation on the temperature of roofs, which only heated up

to 24°C. Roofs covered with tar paper heated up to 60°C.

An unusual situation was evident at night. The introduction of green roofs on the buildings of urban forecourt with north-south orientation resulted in lower air temperature (FGR: 0.18°C, FGR2: 0.19°C, FGR3: 0.23°C). The reason could be found in the soothing effect of wind. The air flowing over the roof layer was cooled. It then flowed into the forecourt. The effect was a reduction in temperature. In addition, warm masses resulting from the evapotranspiration process flowed over the building roofs. They were blown outside the forecourt.

<sup>11</sup> Location of measurement points is presented in Figure 7.20.

<sup>12</sup> Tabular summary attached as Appendix 14.

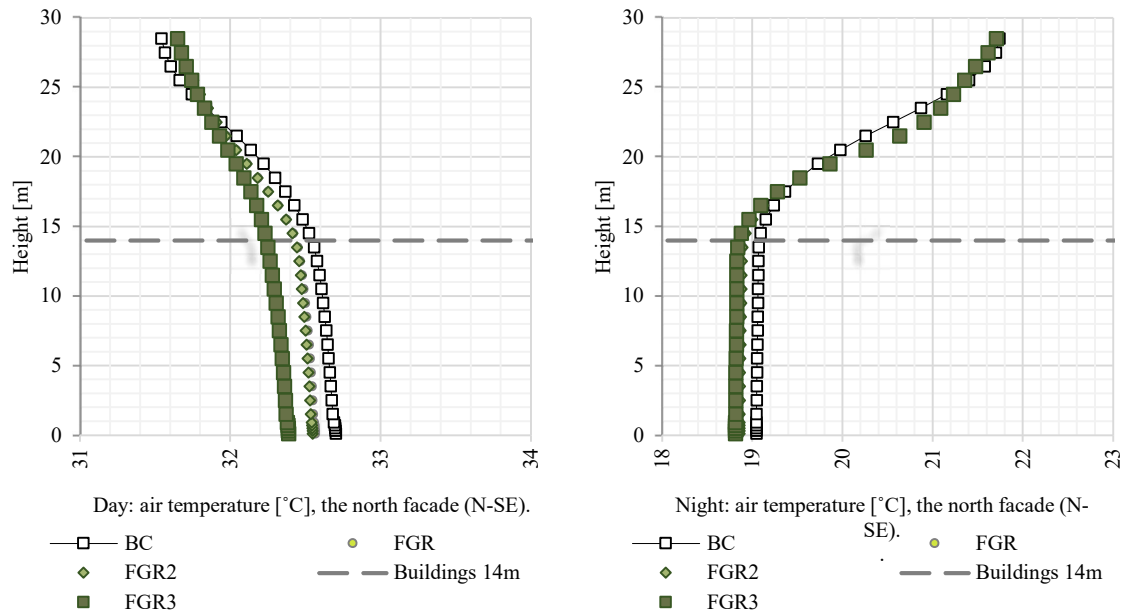
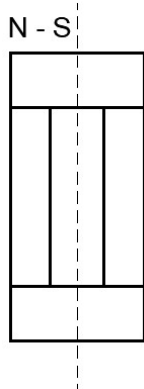


**Figure 7.21.** Impact of green roofs on thermal conditions of the north-south (N-SE) oriented urban forecourt (source: own elaboration).



Living facades did not significantly modify thermal conditions in the north-south oriented forecourt (Figure 7.22.<sup>13</sup>). Their effect on air temperature was virtually imperceptible during the day. Even the significant amount of greenery (FW3), i.e. covering all the building facades with vegetation, did not allow to reduce the parameter. On the other hand, it translated into the temperature of building walls. It increased to 34°C (from 32°C - west facade), 40°C (from 38°C - east facade). This effect was related to the radiation conditions in the forecourt. Some of radiation was absorbed by vegetation. A significant amount was reflected, especially by the one planted at the eastern (sunny) facade, and then intercepted by the other facades of the forecourt. As a result, unfavorable thermal conditions were noted.

At night the green walls had a slight cooling effect. The total vegetation coverage of the facade translated to an average air temperature reduction of 0.24°C (FW3) within the forecourt. A similar effect was observed for the other scenarios (FW, FW2). Moreover, vegetation caused a modification of the wall temperature. Those covered with greenery were heated up to 17°C. The temperature of plastered facades was lower by 2-3°C. This was

<sup>13</sup> Tabular summary attached as [Appendix 15](#).

caused by the slower energy release to the environment by the green walls, compared to the plastered facades.

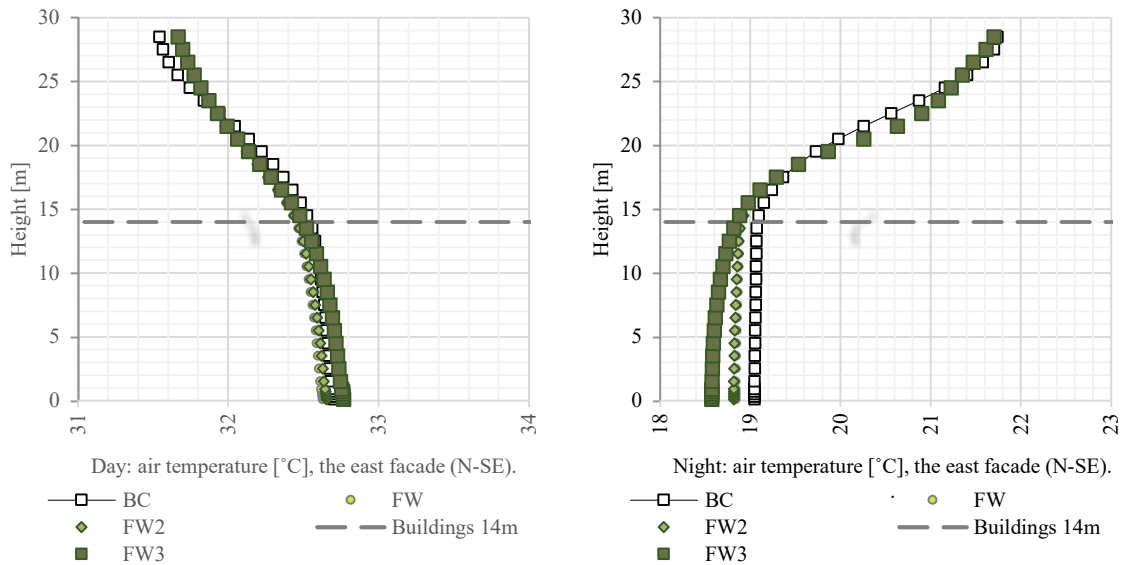


**Figure 7.22.** Impact of green walls on thermal conditions of the north-south (N-SE) oriented urban forecourt (source: own elaboration).

### Thermal comfort in the forecourts

Thermal comfort was assessed at the east-west oriented forecourt. Thermal sensations were assessed using readings taken at the north facade (E-WN), as well as the south facade (E-WS). Characteristic points located in the middle of forecourt at a distance of 2.5 m from the building walls were selected. The aim was to show the variation of conditions in the forecourt. In addition, it was possible to determine the influence of building geometry on the thermics of the area. The results are presented in [Figure 7.23](#).

In the east-west oriented forecourt area, the thermal conditions varied. The highest PET values were recorded at the strongly insulated north façade (PET > 49°C). Thus, thermal discomfort prevailed there. A more favorable situation was observed at the shaded - south façade (PET > 39°C, which meant the conditions of 'hot'). This was a significant change that was noted at both the pedestrian and residential levels. It appeared that depending on the geometry of development it would be possible to shape the thermal comfort index - PET. If the buildings on the south side were high enough to guarantee the shadow cast on the north facade, the thermal sensations would remain at the 'hot' level.

The implementation of vegetation in a highly urbanized environment resulted in a slight modification of thermal conditions. In sunny areas there was a minimal change in PET depending on the solution used (green roof, green wall). The most effective was the

introduction of green roofs in the forecourt. This may have been caused by the effect of low vegetation (grass) on lowering the ambient temperature. Air masses cooled as they flowed over the buildings. Heavier air with higher density entered the forecourt. As a result, more favorable thermal conditions were shaped. The remaining scenarios should be considered ineffective in shaping thermal comfort in the forecourt area.

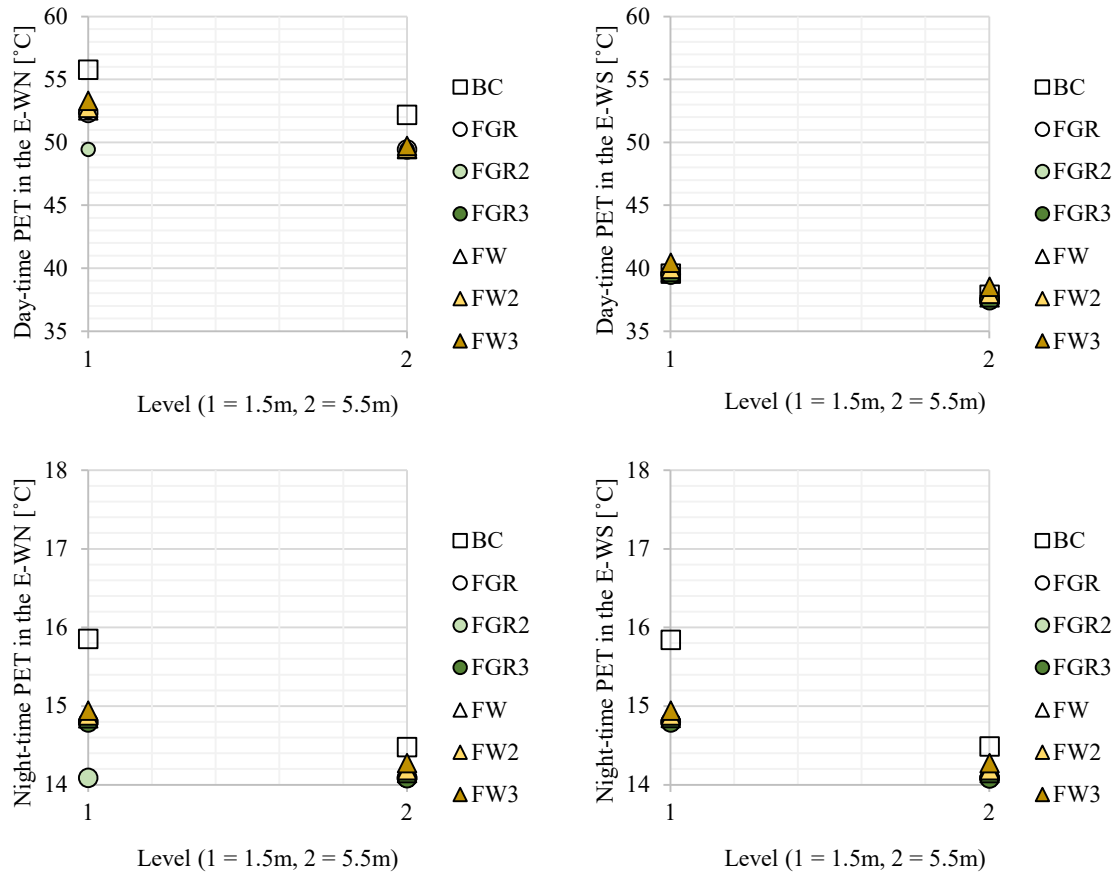


**Figure 7.23.** Impact of green solutions on thermal comfort in the east-west oriented forecourt (upper left - E-WN, upper right - E-WS, 3 pm; bottom left - E-WN, bottom right - E-WS, 3 am)(source: own elaboration).

A similar situation occurred in the north-south oriented forecourt (Figure 7.24.). In places where buildings cast shadows, i.e. at the eastern facade (at pedestrian movement height), as well as at the western facade (up to habitation height), more favorable thermal conditions were visible. They remained at ‘hot’ levels during the day. In other cases, PET values exceeded 42°C (‘extreme heat stress’).

The implementation of vegetation caused discomfort conditions to persist. It even contributed to a minimal increase of PET index during the daytime. It should be noted that meteorological parameters such as mean radiant temperature, air temperature, humidity as well as wind velocity were taken into account when estimating heat sensations. In this case, the building structure contributed to a partial reduction of solar radiation in the forecourt.

The structures were subject to insolation from the residential level at the east facade. They absorbed a significant amount of energy during the day (low albedo of the plastered walls). Also, the effect of reflected shortwave radiation on the thermology of area was observed. Solar radiation was reflected from the building facades, then intercepted by other surfaces both horizontal (floor) and vertical (walls). The air flow in the forecourt was not without significance. The exchange of energy primarily took place through convective movements. This was due to the buildings, which prevented the inflow of cooler air from the assumed eastern direction. The introduction of greenery intensified this effect. The cause was the processes of transpiration, i.e. evaporation of water from the above-ground parts of plants, which caused an increase in humidity on the site. The compilation of the influence of all parameters translated into higher PET values in the north-south oriented forecourt.

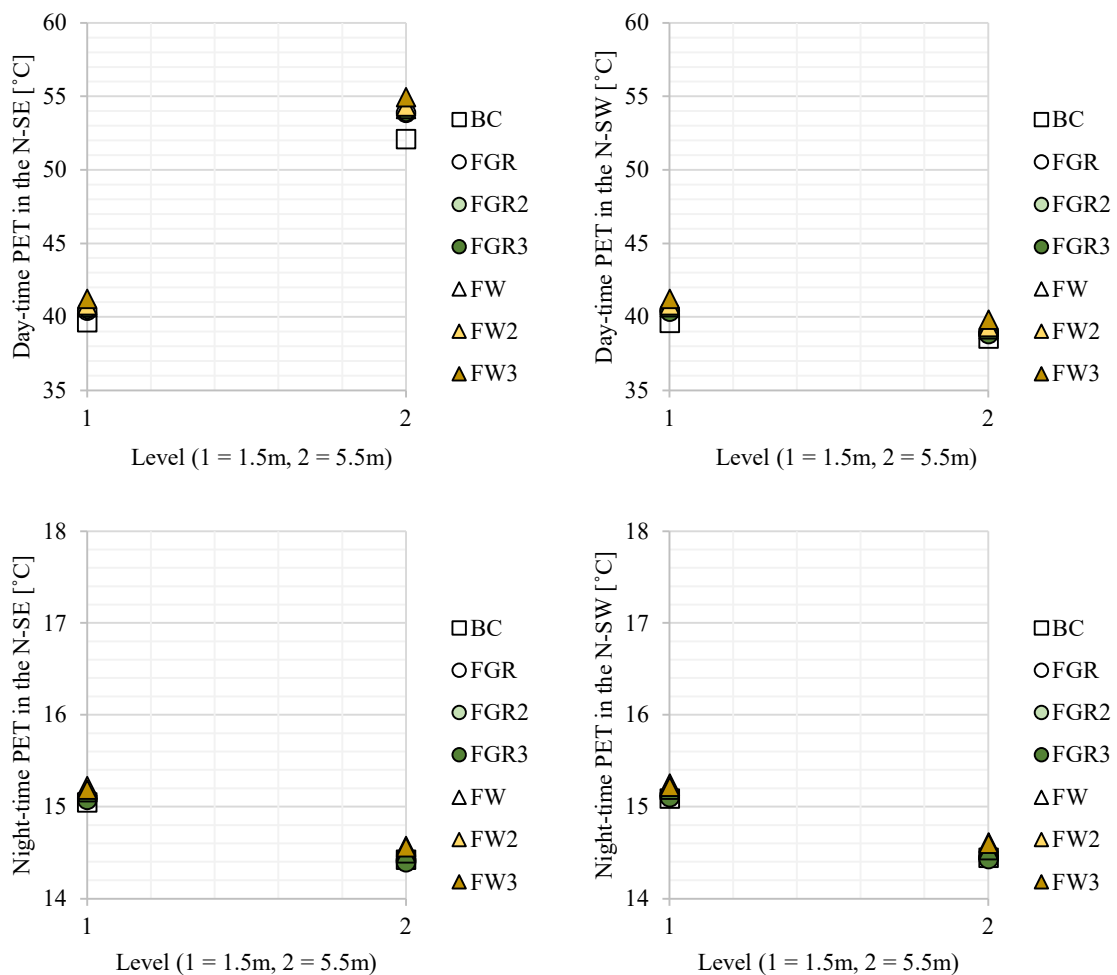


**Figure 7.24.** Impact of green solutions on thermal comfort in the north-south oriented forecourt (upper left - N-SE, upper right - N-SW, **3 pm**; bottom left - N-SE, bottom right - N-SW, **3 am**)(source: own elaboration).



## 7.2. The impact of blue infrastructure

The use of blue infrastructure in cities is listed among the primary adaptation strategies. Its invaluable impact is discussed in [Chapter 2.2. Climate change adaptation strategies in urban environment](#). With the implementation of natural solutions in highly urbanized areas, more and more scientific studies are being carried out that indicate to what extent blue infrastructure can contribute to climate change mitigation. However, the studies conducted tend to be specific (single) case studies.

This chapter estimates the impact of blue infrastructure that could be implemented in the form of bioretention planters in the space of a typical street canyon of the Metropolitan Area of Lodz ([Figure 7.25. - 7.26.](#))<sup>14</sup>. Two cases were considered, i.e.:

- **Bioretention Planters Scenario (BP)** - implementation of four bioretention planters, the area of which would be 128 m<sup>2</sup>, symmetrically distributed in the space of street canyon, in such a way as to maintain the possibility of pedestrian communication as well as vehicular traffic;
- **Bioretention Planters Scenario (BP2)** - implementation of 12 bioretention planters with a total area of 384 m<sup>2</sup>. They were distributed symmetrically, between the pedestrian zone and the street. The only restriction was to keep pedestrian and vehicular traffic within the canyon area.

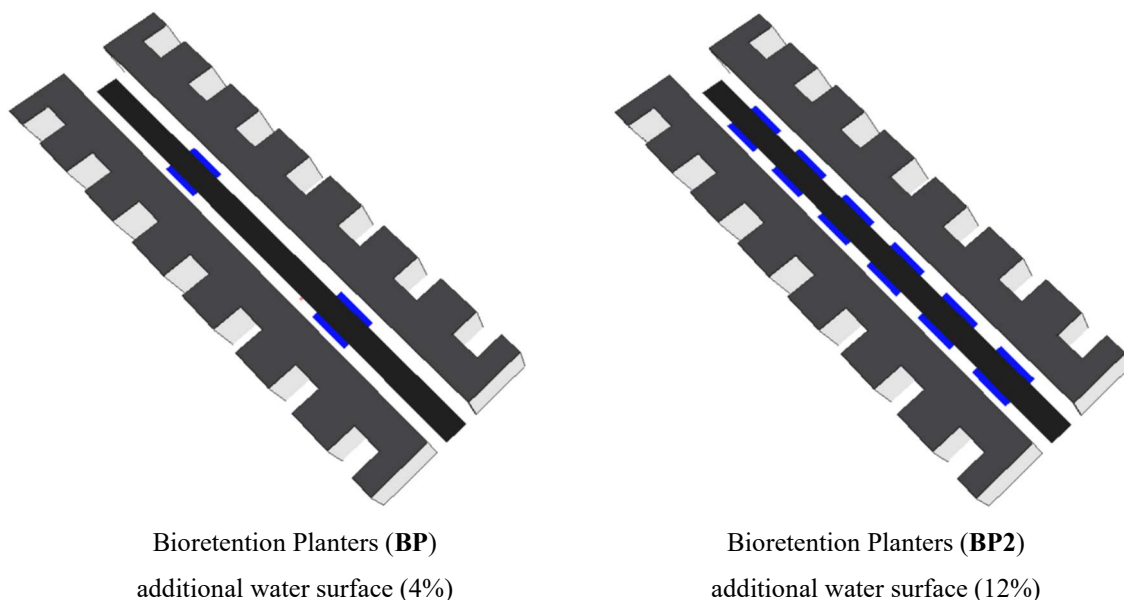


**Figure 7.25.** Blue solutions introduced in the canyons (source: own elaboration).

<sup>14</sup> The constructions of bioretention planters, which can be potentially implemented in the city, were presented in [Figure 7.26](#).

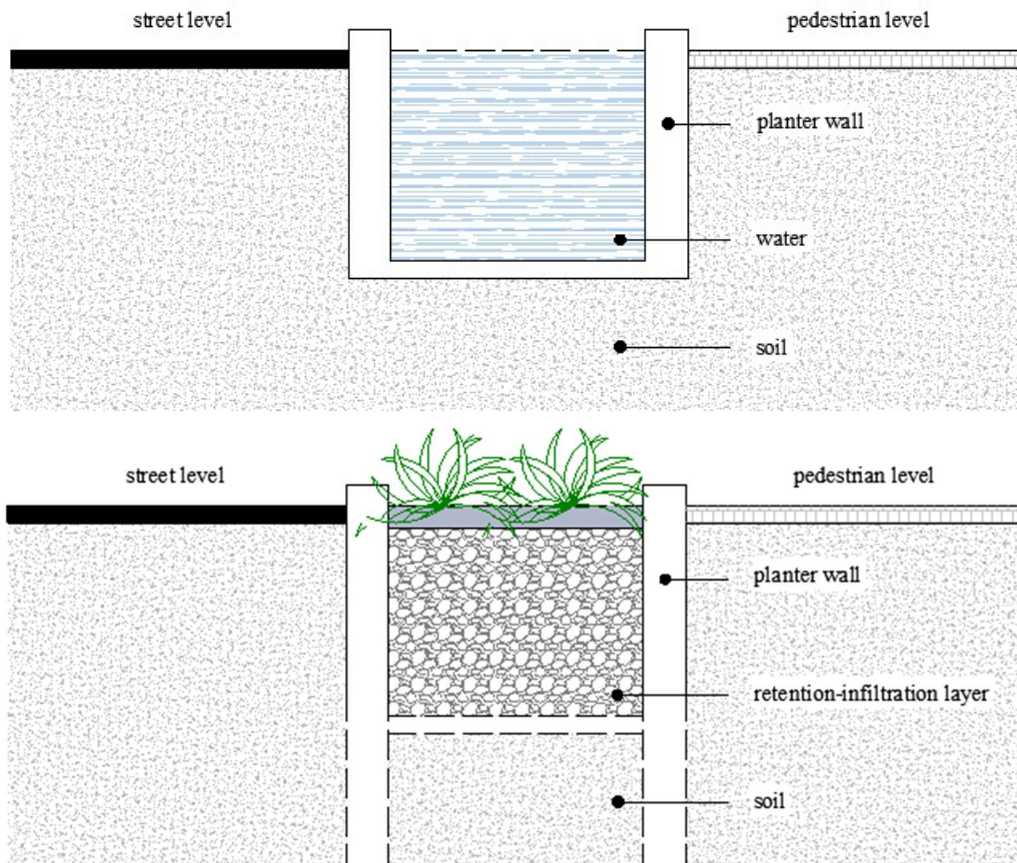
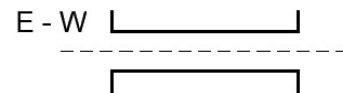


Figure 7.26. The potential constructions of bioretention planters (source: own elaboration).

### Microclimatic conditions in the east-west oriented street canyons

#### Bioretention planters



Simulations of the impact of blue infrastructure were conducted for the warmest day of a Typical Meteorological Year. Readings of changes in meteorological parameters were taken in the immediate vicinity of bioretention planters, at a distance of 2.5 m from the building frontage, at the north facade (E-WN), to illustrate the direct impact of the solution on the microclimatic conditions in the east-west oriented canyon. The changes that occur in the street zone (E-WA), i.e. the further surroundings, were also taken into account (Figure 7.27.). In this case, an attempt was made to assess the impact of solutions in places where land use (asphalt pavement) negatively affects the microclimate of canyon space. Analyses were conducted during the daytime (3 pm) as well as during the nighttime (3 am)(Figure 7.28.<sup>15</sup>).

<sup>15</sup> Tabular summary attached as [Appendix 16](#).

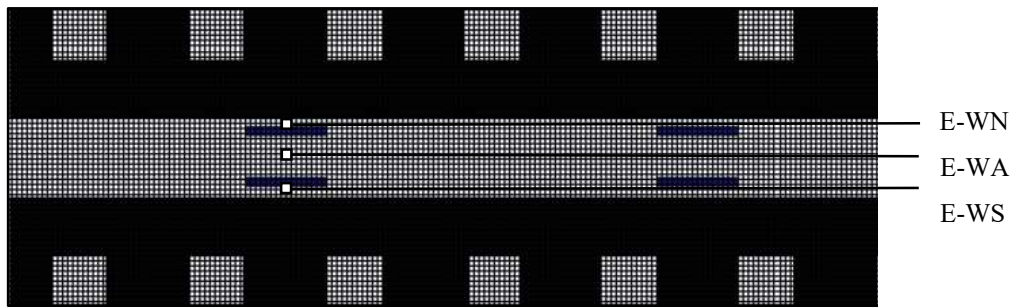


**Figure 7.27.** Location of E-WN, E-WA, and E-WS measurement points in the street canyon (source: own elaboration).

The implementation of blue infrastructure made a significant contribution to the improvement of thermal conditions in the east-west oriented canyon area. The solution of introducing only four bioretention planters (BP) was as effective as the scenario involving much more water surface (BP2). Directly above the surface of the bioretention planters, there was a temperature decrease of as much as  $2.52^{\circ}\text{C}$  ( $h = 0.30\text{ m}$ ). This was  $1.98^{\circ}\text{C}$  in the pedestrian movement zone. With height, the soothing effect of implemented solutions decreased. At the residential level, it was  $1.14^{\circ}\text{C}$  ( $h=5.5\text{ m}$ ), while above the building roofs it was  $0.61^{\circ}\text{C}$  ( $h=15.5^{\circ}\text{C}$ ). The impact of blue infrastructure was noticeable in the canyon space. However, the opposite trend was noted at nighttime. The water surfaces caused an increase in air temperature. The most adverse change was observed at 1.5-5.5 m (BP and BP2). It was  $0.97^{\circ}\text{C}$ . The phenomenon was due to the fact that water has a large heat capacity. Absorption of a significant amount of solar radiation occurred during the day.

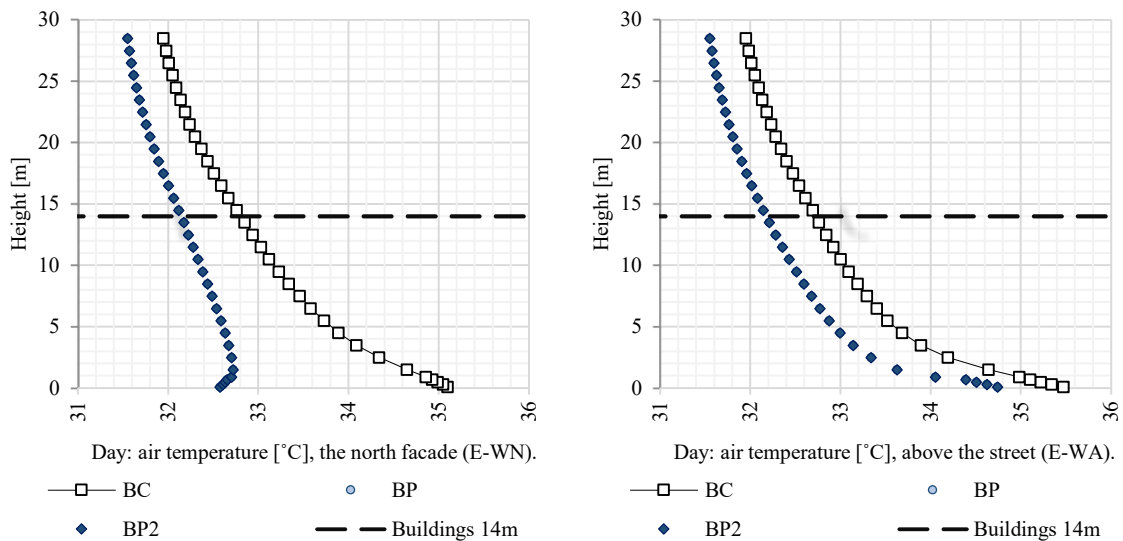


**Figure 7.28.** Impact of blue solutions on thermal conditions in the east-west oriented canyon (left column - E-WN; right column - E-WA)(source: own elaboration).

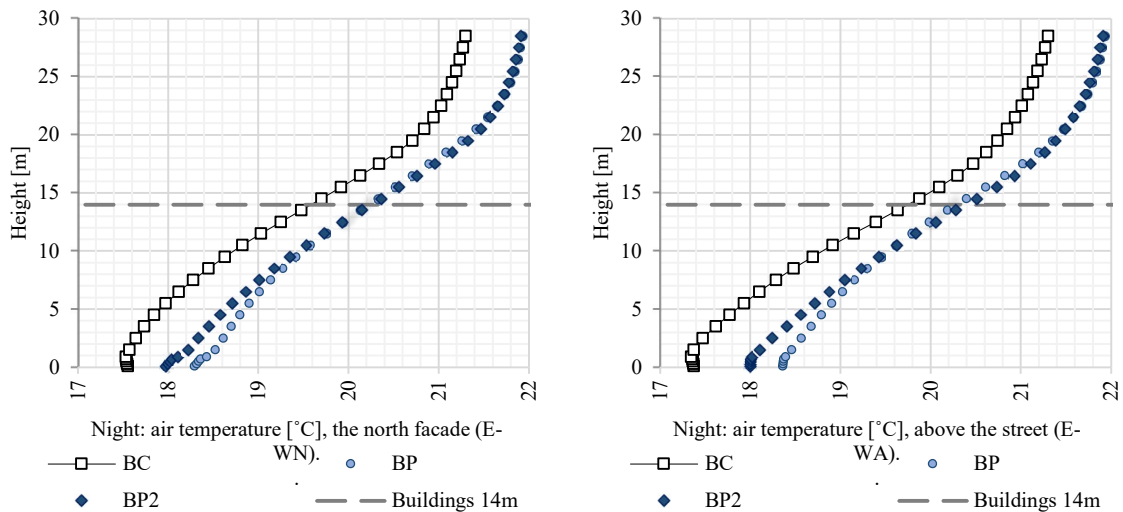


Figure 7.28. Continuation.

### Microclimatic conditions in the north-south oriented street canyons

#### Water reservoirs

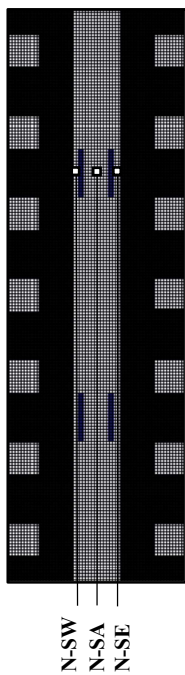


Figure 7.29. Location of N-SW, N-SA, and N-SE points in a street canyon (source: own elaboration).

Next, simulations were conducted for the north-south oriented canyon. The readings took place in the immediate vicinity of bioretention planters (1) at the east facade (N-SE), 2.5 m away from the building walls, (2) in the street zone (N-SA)(Figure 7.29.). Due to the fact that the impact of blue infrastructure was similar in both measurement points, the author presented only the results obtained at the eastern facade. The impact of water surfaces on thermal conditions was estimated during the daytime (3 pm) and also during the nighttime (3 am)(Figure 7.30.<sup>16</sup>).

The north-south oriented canyon was a less sunny area (sunhours = 4h, N-SE). It had significantly lower air temperatures than the east-west oriented canyon. However, the implementation of blue infrastructure features resulted in a similar modification of thermal conditions. Air temperatures were below 33°C not only in the immediate vicinity of bioretention planters, but also in the street zone. An increasing soothing effect of the blue infrastructure could be observed with altitude.

The implementation of water surfaces contributed less to the reduction of air temperature in the north-south oriented canyon. This effect was due to airflow. The assumed

<sup>16</sup> Tabular summary attached as [Appendix 17](#).

east wind direction contributed to enhancing the effect of water resources in the east-west oriented canyon space. In the second case - the north-south oriented canyon, the geometry of system constituting a physical barrier prevented the free movement of air masses. Therefore, the reduction in air temperature was slightly smaller.

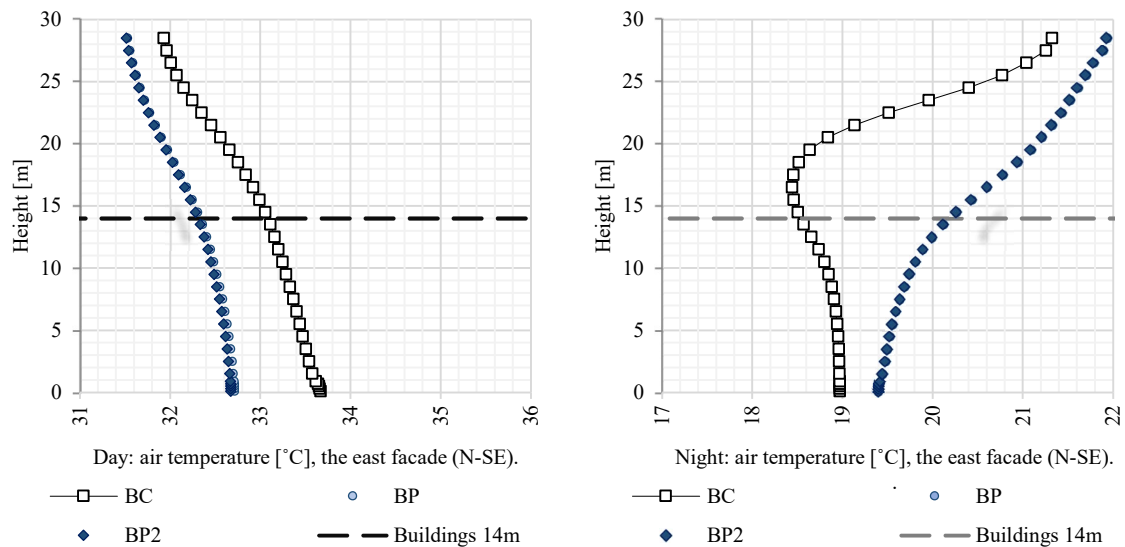


**Figure 7.30.** Impact of blue solutions on thermal conditions in the north-south oriented canyon (left column - N-SE, 3 pm; right column - N-SE, 3 am)(source: own elaboration).

### Thermal comfort in the street canyons

The impact of blue infrastructure on human-perceived thermal comfort was assessed in the east-west oriented canyon area. Analyses were conducted at the measurement point located at the north facade (E-WN), as well as the south facade (E-WS). The study included the zone directly at the building frontage to show the influence of both the building structure and water elements on the thermal sensations of humans residing in the outdoor environment. The assessment was carried out at the pedestrian movement level (h=1.5 m), as well as the residential level (h=5.5 m)(Figure 7.31.). The analysis was conducted using the Physiological Equivalent Temperature (PET) index.

The building structure influenced the thermal sensations that were experienced by humans in the east-west oriented canyon area (this theme is described in detail in Chapter VI. Numerical simulation of microclimatic and thermal conditions). It contributed to the beneficial modification of microclimatic conditions. In shaded areas there was a visible decrease in thermal sensations from the level described as ‘very hot’ to ‘warm’. The impact of buildings was much stronger than that of the implemented blue infrastructure.

In the sunny areas, despite the implementation of water surfaces, thermal discomfort was felt, especially at the northern facade (E-WN). Unfortunately, conditions were at the ‘extreme heat stress’ level. In the second case of the south facade, up to the residential level, the thermal sensation was successfully reduced from ‘hot’ to ‘warm’ by means of bioretention planters. The solution proved to be beneficial in the canyon area.

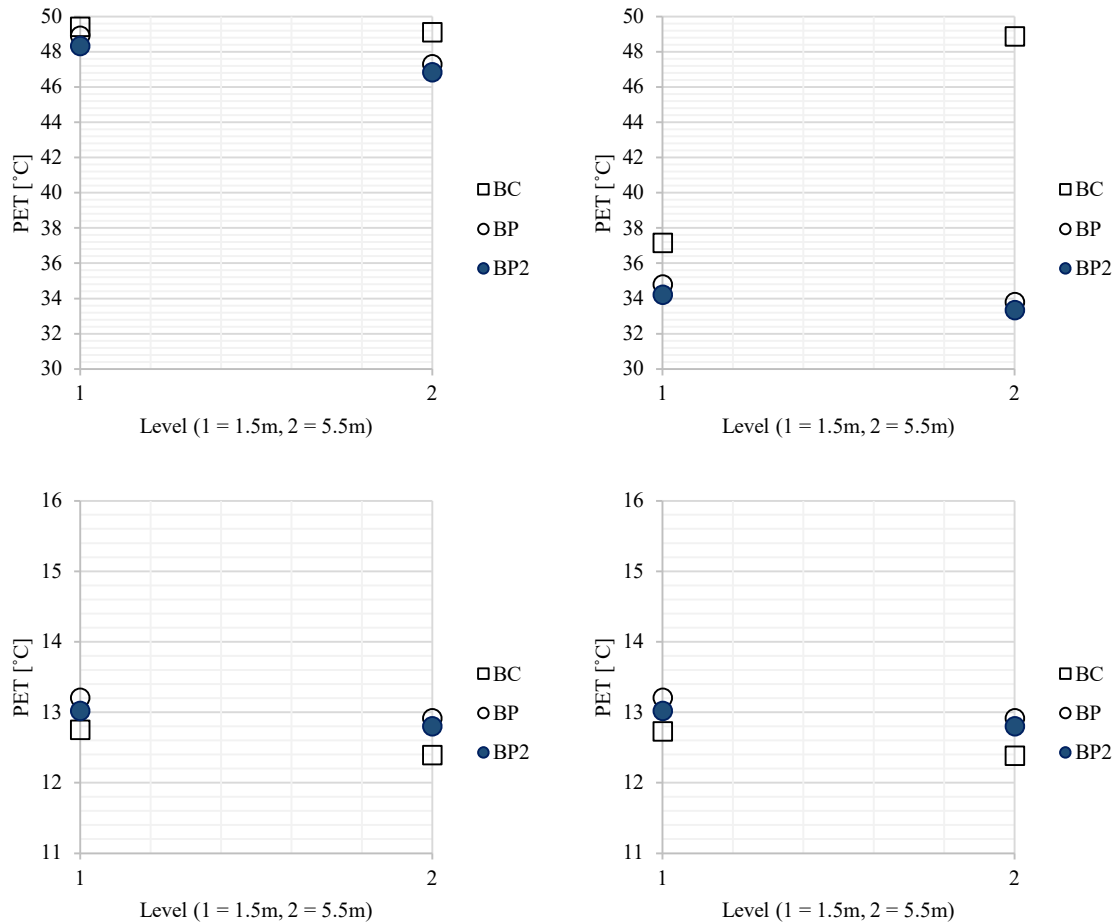


**Figure 7.31.** Impact of blue infrastructure on thermal comfort in the east-west oriented canyon (upper left - E-WN, upper right - E-WS, **3 pm**; bottom left - E-WN, bottom right - E-WS, **3 am**)(source: own elaboration).

At night, the water surfaces caused an increase in PET values. However, it was a positive phenomenon that allowed conditions described as ‘slightly cool’ to be maintained. This was due to the release of heat absorbed by the bioretention planters. When the air temperature started to decrease, the energy was released to the environment. As a result, the PET index increased, and thus more favorable thermal conditions perceived by humans in space were formed.

Next, thermal sensations were assessed in the north-south oriented canyon area (Figure 7.32.). Values were read at a point located at the east facade (N-SE, sunlit) and also at the west facade (N-SW, shaded to habitation level). In this case, significantly higher PET values

were observed. This was due to the parameters that were taken into account when calculating PET, in particular airflow. It was insignificant in the north-south oriented canyon area. The building structure effectively inhibited the inflow of cool air masses. Extreme thermal discomfort was felt in the sunny areas. This was an extremely unfavorable situation. In fact, such conditions could cause heat stroke. In the shaded areas, the use of blue infrastructure elements was able to reduce the thermal sensation level from ‘very hot’ to ‘hot’.

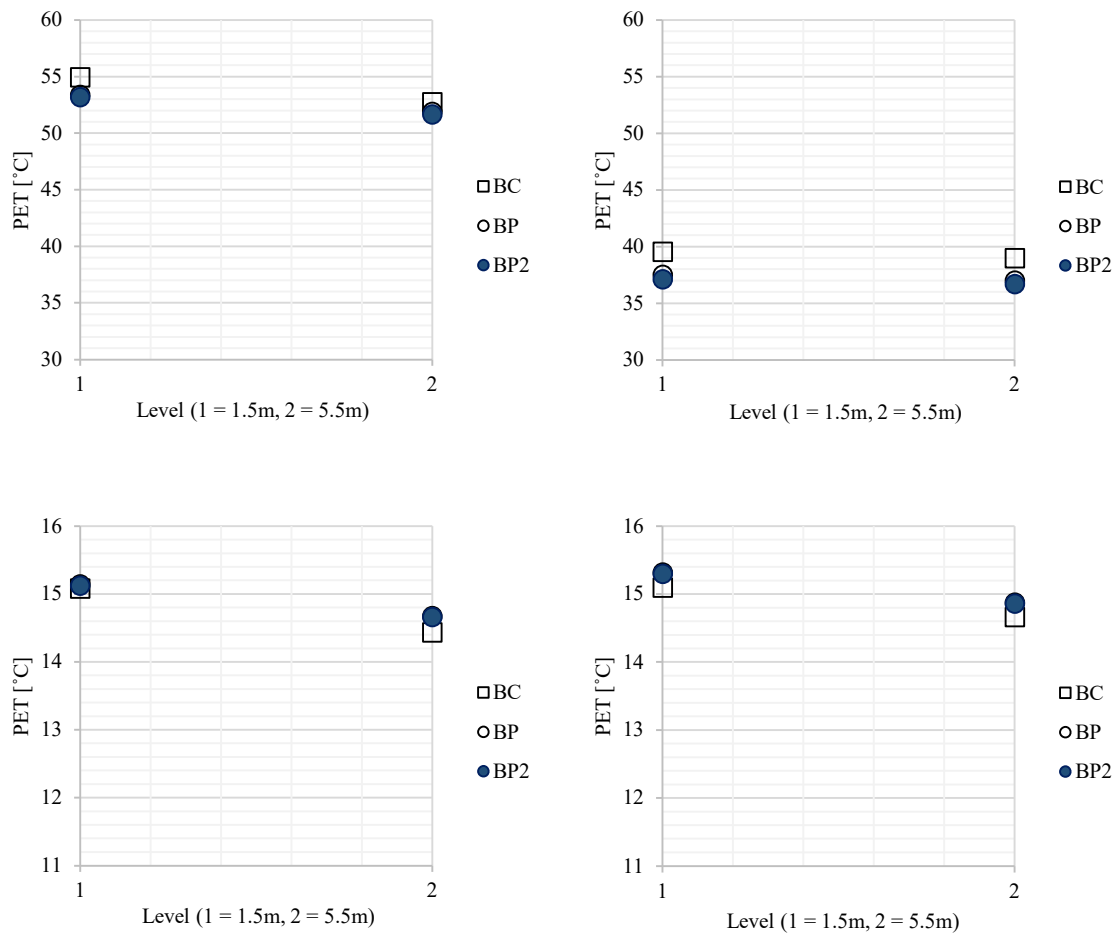


**Figure 7.32.** Impact of blue infrastructure on thermal comfort in the north-south oriented canyon (upper left - N-SE, upper right - N-SW, **3 pm**; bottom left - N-SE, bottom right - N-SW, **3 am**)(source: own elaboration).

During the nighttime, thermal conditions were at the ‘slightly cool’ level. The PET value was slightly higher than in the east-west oriented canyon. This was undoubtedly influenced by the obstructed airflow. Also, slower heat dissipation of heated artificial surfaces (asphalt, concrete) translated into higher PET values. However, the situation should be considered favorable.

## Implementation of the blue infrastructure in forecourts

The compact structures of inner-city development seem to be isolated systems. Enclosing small spaces on all sides with buildings results in a peculiar microclimate formed in the interiors of urban forecourts. Unfortunately, this results in the need for case-specific research. In this study, urban forecourts occurring in the Metropolitan Area of Lodz are considered. The impact of blue infrastructure in the form of water reservoirs introduced in the middle of forecourts on the thermal conditions was assessed (Figure 7.33.)<sup>17</sup>. Two cases were considered:

- **Water Reservoir (WR)** - involving the implementation of a 3 x 13 m (42 m<sup>2</sup>) water reservoir,
- **Water Reservoir (WR2)** - involving the implementation of a water surface with dimensions of 3 x 28 m in the middle of forecourt (84 m<sup>2</sup>). They were created in such a way as to enable communication within the forecourts. The free space between the building walls and the water reservoirs was maintained (4 m).

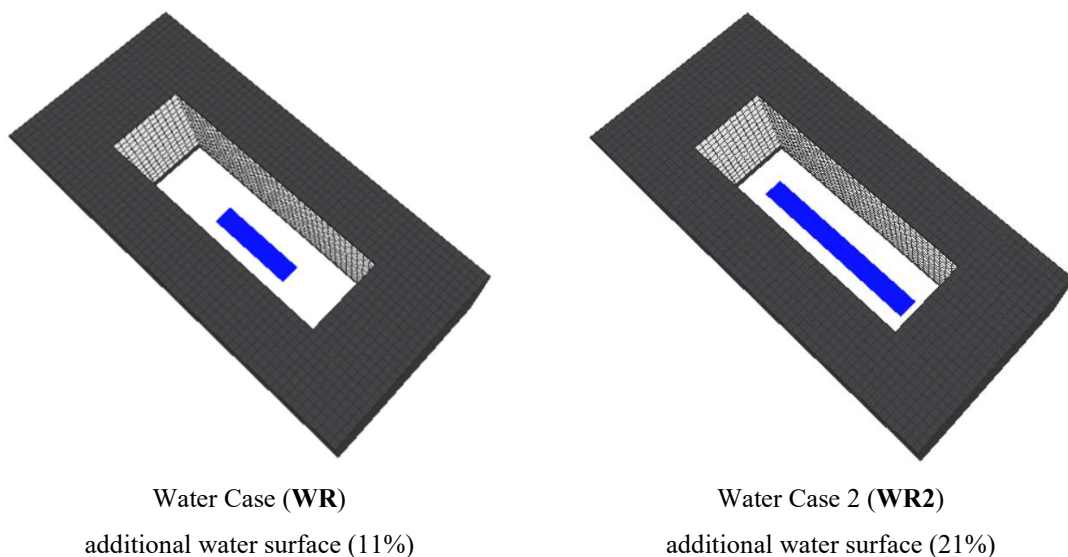


**Figure 7.33.** Blue solutions introduced in urban forecourts (source: own elaboration).

<sup>17</sup> The construction scheme of water reservoir was presented in Figure 7.34.



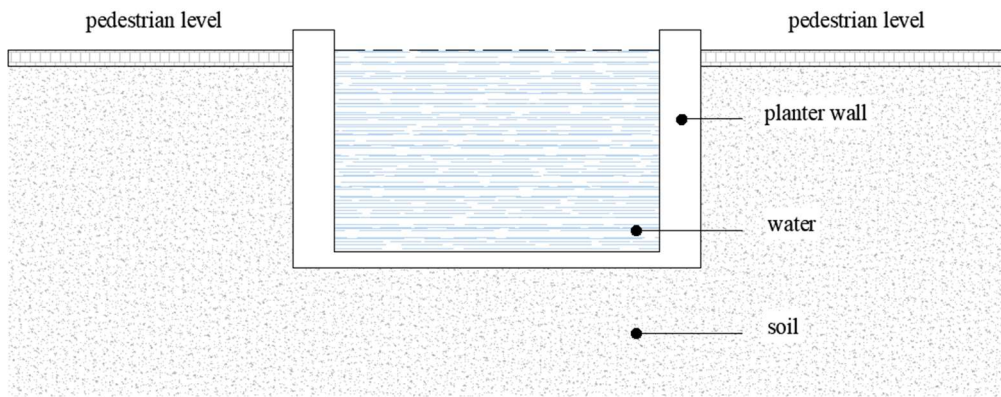
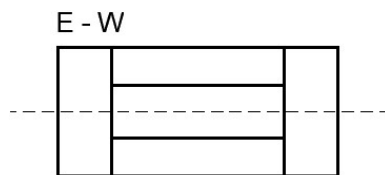


**Figure 7.34.** The construction scheme of water reservoir (source: own elaboration).



**Water  
reservoirs**

Initial analyses were conducted at the characteristic points, i.e. at the north facade (E-WN), as well as the south facade (E-WS) in the east-west oriented forecourt

(Figure 7.35.). The implementation of blue infrastructure had a similar effect in reducing air temperature at both the north and south facades. Therefore, results are only presented for the selected point (E-WN).

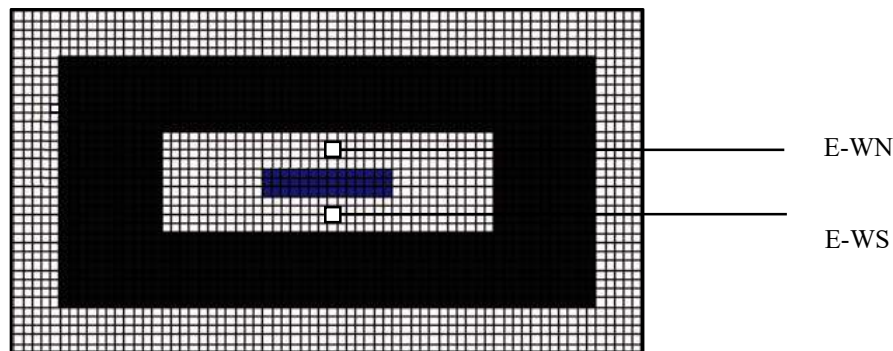


**Figure 7.35.** Location of E-WN and E-WS measurement points in the forecourt (source: own elaboration).

The implementation of water reservoirs in the middle of urban forecourt resulted in a slight modification of thermal conditions. The soothing effect of the solution was practically unnoticeable (Figure 7.36.<sup>18</sup>). It appears that the geometry of buildings was a key factor in the compact structures of the inner-city. It determined the prevailing microclimatic conditions (this issue is described in detail in Chapter VI. Numerical simulation of microclimatic and thermal conditions).

<sup>18</sup> Tabular summary attached as Appendix 18.

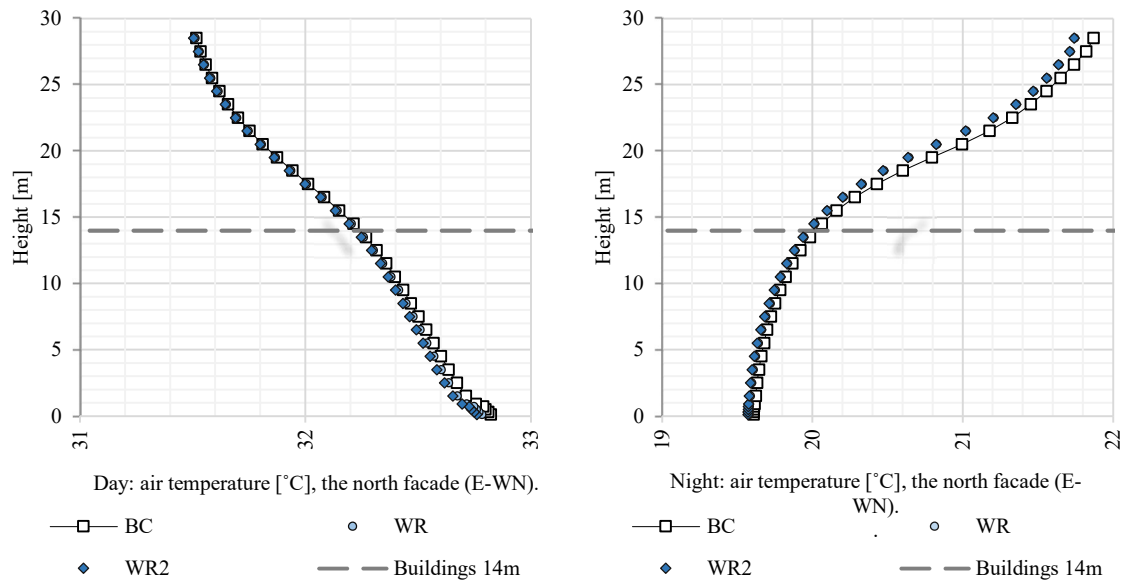


**Figure 7.36.** Impact of blue solutions on thermal conditions in the east-west oriented forecourt (source: own elaboration).

### Water reservoirs

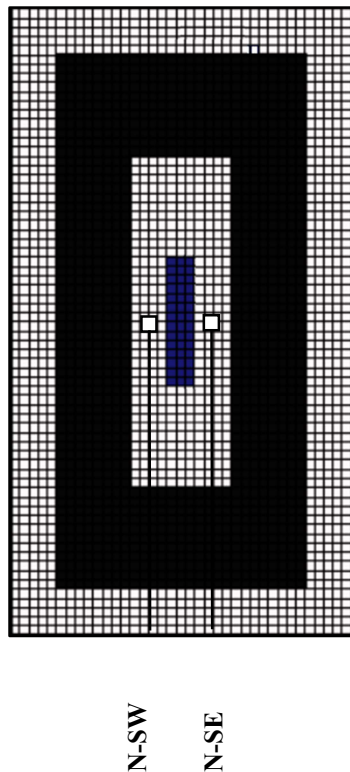


**Figure 7.37.** Location of N-SW and N-SE measurement points in the urban forecourt (source: own elaboration).

The author conducted analyses of the conditions in the north-south oriented forecourt. The results are presented for the point located at the eastern facade (N-SE)(Figure 7.37.). The impact of the introduced water reservoir solution was insignificant (Figure 7.38.<sup>19</sup>). Air temperature was kept relatively constant in the forecourt area. During the day it was higher than over the building roofs. It was due to the strong heating of the paved forecourt floor, as well as the walls of building structures. The air exchange was important, which was hindered due to the fact that the system was closed on all sides with medium-high buildings. This resulted in air exchange based on convective movements in the forecourt. Advective movement was observed above the roof level.

At night time, the temperature was maintained at 19°C in the north-south oriented forecourt. It was much lower than above the building roofs. Here, the reason is to be found in the energy exchange process between the building system

<sup>19</sup> Tabular summary attached as [Appendix 19](#).

and the surroundings. Heat was transferred from strongly heated surfaces (floors, walls) to the surroundings. Increase of air temperature over the roofs was additionally caused by giving up the heat from roofing (tar paper).

The implementation of blue infrastructure elements did not contribute significantly to the modification of air temperature. However, it should be noted that there are non-climatic advantages of this type of solutions (aesthetic, social). Therefore, the implementation of water reservoirs in urban spaces should be considered.

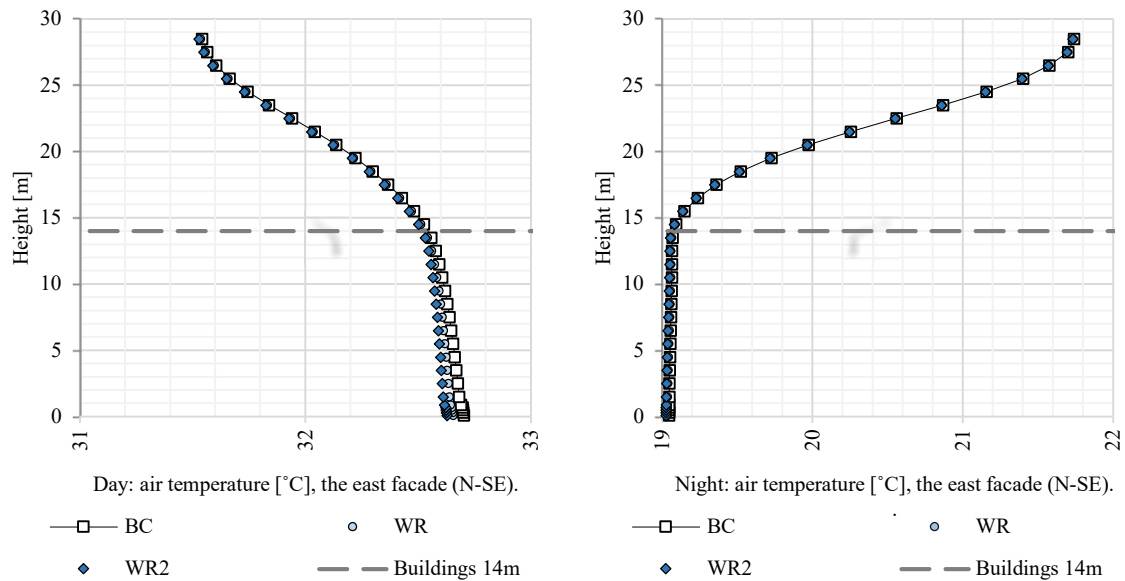


**Figure 7.38.** Impact of blue solutions on thermal conditions in the north-south oriented forecourt (left column - N-SE, 3 pm; right column - N-SE, 3 am)(source: own elaboration).

### Thermal comfort in the forecourts

Thermal sensations experienced by the human in the external environment were considered. As an example, the measurement results conducted at the north facade (E-WN) were used (Figure 7.39.). This was the location with the least favorable conditions as a result of strong insolation of the area. Blue infrastructure in the form of a water reservoir introduced in the middle of canyon did not help improve thermal conditions. Thermal discomfort was experienced in the heavily sunlit areas. Conditions were described as ‘very hot’ during the day (PET index above 42°C indicating the possibility of heat stroke among people). At night, ‘slightly cool’ conditions were recorded and should be considered favorable.

Also in the north-south oriented forecourt, the impact of blue infrastructure was virtually imperceptible (N-SE, Figure 7.40.). The reduction in thermal conditions was due to the

layout of buildings. Buildings with a height of 14 m shaded the east facade causing thermal sensations to remain ‘warm’ in the pedestrian movement zone. Where the area was exposed to sunlight, thermal discomfort was experienced. At night conditions were described as ‘slightly cool’. The PET values were slightly lower than in the east-west oriented forecourt area. In this case, the reason was the shorter daytime insolation of the area. Thus, the building materials used in the forecourt absorbed less solar energy. As a result, there was less intense heat exchange during the night time.

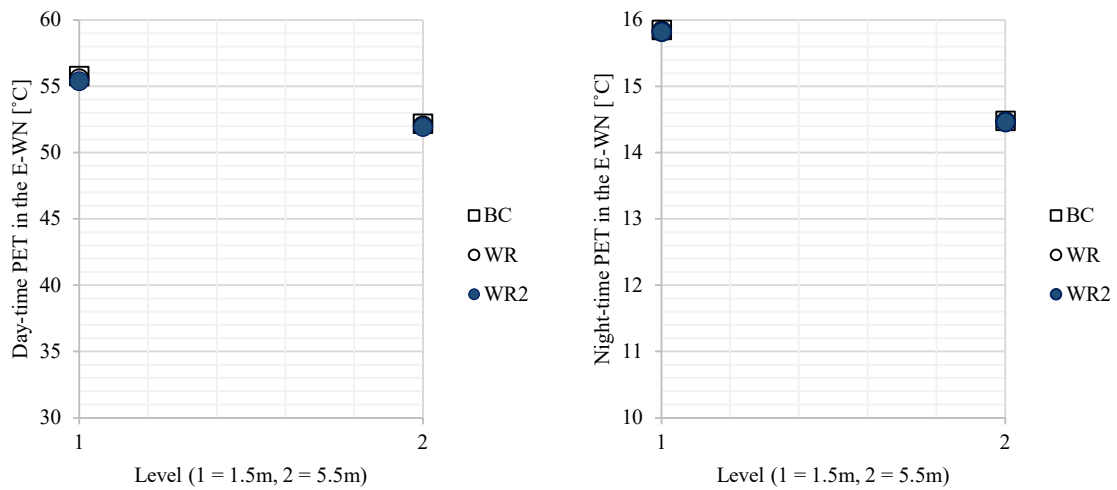


**Figure 7.39.** Impact of blue infrastructure on thermal comfort in the east-west oriented forecourt (left - E-WN, 3 pm; right - E-WN, 3 am)(source: own elaboration).

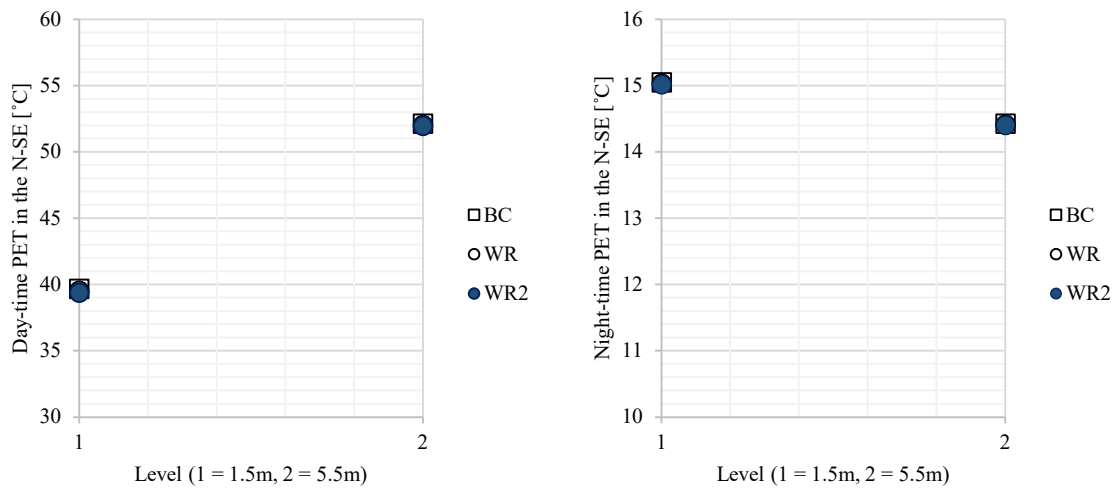


**Figure 7.40.** Impact of blue infrastructure on thermal comfort in the north-south oriented forecourt (left - N-SE, 3 pm; right - N-SE, 3 am)(source: own elaboration).

### **7.3. The effectiveness of climate change adaptation strategies within the context of analyzed urban form**

For years it has been emphasized that Lodz, being one of the largest cities in Poland, is particularly vulnerable to the effects of climate change. The dense, compact structure of the urban layout, historical processes and the development dynamics will exacerbate the negative environmental impact. To counteract the threats, the city has been included in the adaptation program to climate change. The assumptions include creation of local spatial development plans taking into account the Municipal Adaptation Plans. Among the strategies implemented, the use of natural solutions can be distinguished. These consist of introducing plantings, leaving old trees to the extent possible, and ensuring an adequate proportion of biologically active areas ([Resolution No. XL/1074/17, 2017](#), [Resolution No. XLVIII/1227/17, 2017](#), [Resolution No. XLVIII/1228/17, 2017](#)). The blue infrastructure is intended to be a complementary element to the green network. Undoubtedly, the above-mentioned measures will positively influence the climate of urban spaces, especially during the period of prevailing high temperatures in the city. However, their potential impact has not yet been documented. The effectiveness of solutions depends on many parameters (the geometry of buildings, their mutual arrangement, proportion of impermeable surfaces, and environmental components). Therefore, it is necessary to adapt measures to the specific context. Unfortunately, to date, it has not been observed that planning activities are supported by scientific studies that consider the impact of development transformations on climatic conditions.

This paper is the first study to address the impact of blue-green solutions on microclimate conditions and thermal comfort within selected urban forms in Lodz. Solutions that are suggested as potential planning measures to improve the quality of human life in the city (green roofs, living facades, high-greenery, bioretention planters, and water reservoirs) were taken into account. Their impact was assessed both for street canyons, which are the primary space in which pedestrians move, and urban forecourts, which are enclaves where everyday life of residents takes place and where social ties between neighbors are formed. Two orientations of the above mentioned structures were taken into account, i.e. east-west and north-south, which resulted from the city's communication network, and thus its urban layout.

## **The urban street canyons contex - Lodz**

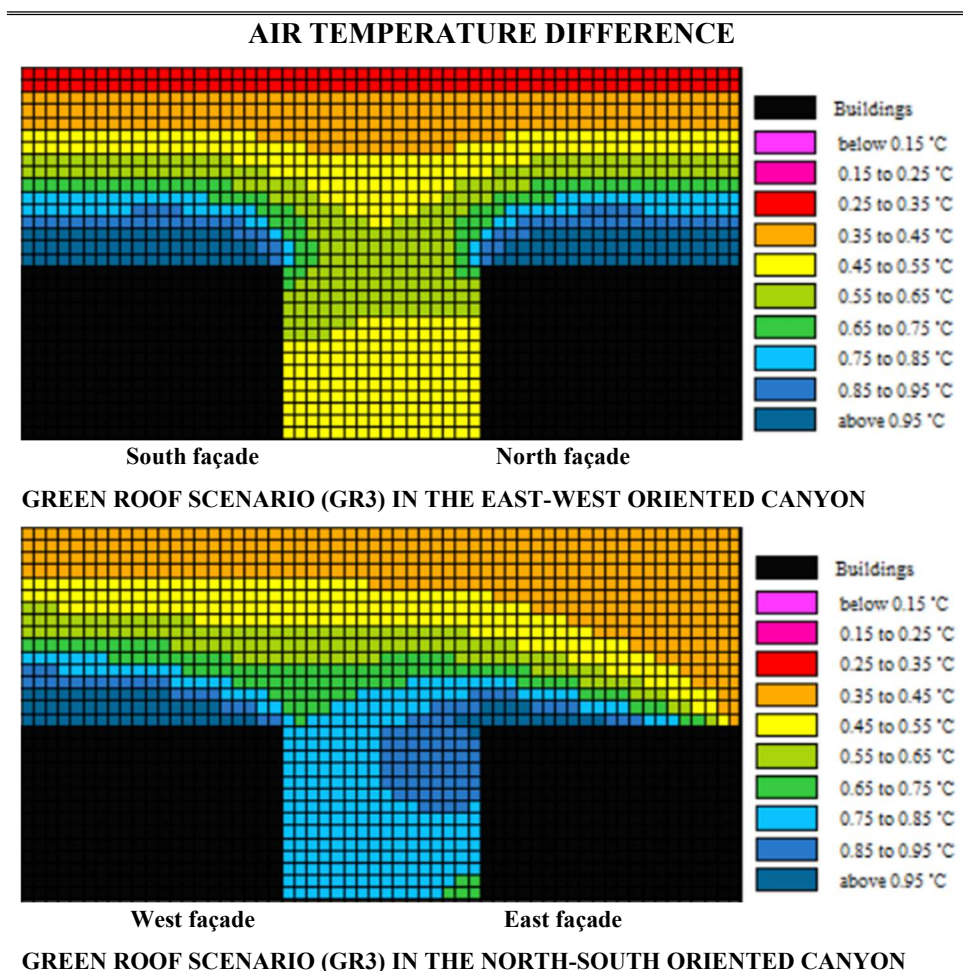
The blue-green adaptation strategies contribute to the improvement of climatic conditions. This is achieved by (1) reduced direct solar radiation reaching horizontal surfaces, (2) captured diffuse short-wave radiation that is reflected by building walls and later used in the process of plant photosynthesis, (3) reduced temperature not only of the environment but also of pavements, especially those made of materials characterized by low albedo, (3) increased humidity, and (4) modification of urban airflow.

The effectiveness of the adaptation strategies introduced depends on the urban layout form. According to Ng et al. (2012), building height is a key parameter when implementing adaptation measures in the form of natural solutions in cities. A study conducted in Hong Kong showed that planting high-rise buildings ( $h = 60$  m) with vegetation had no cooling effect on the pedestrian movement zone. Even if the roof slopes were 100% covered with greenery, no significant improvement in climatic conditions would be obtained.

The research conducted in the street canyons of the Lodz Metropolitan Area showed that the selected strategies positively influenced the changes in microclimatic conditions. In the cases analysed, i.e. medium-high buildings (14 m), the green roofs were the most effective solution in the north-south oriented canyons (Table 7.1.). This was related to the assumed air inflow from the east. The air as it moved over the green canopy cooled down. Then a denser mass entered the canyon. It displaced the heated, lighter air. The effect was to reduce the temperature of the air inside the canyon. The solution was almost as effective at the pedestrian movement level as it was above the roof layer. In the east-west oriented canyon, the effect on meteorological parameters was most intense directly above the building roofs. In this case, the key parameter turned out to be the airflow, which projected the effectiveness of implemented solution.

The literature review confirms the fact that green roofs have a beneficial effect on the microclimatic conditions of urban spaces. Herath et al. (2018) conducted a study in tropical Sri Lankan urban context (tropical rainforest climate). They attempted to apply vegetation as elements of mitigation efforts in the context of climate change. Green roofs (50% coverage, 100% coverage) were considered by them as potential solutions. It was shown that changing the roof cover functioned as a constant heat sink. Vegetation, the albedo of which was much higher than that of building materials, absorbed less solar radiation. Some of the absorbed light was used in photosynthesis and also during evaporative heat transfer.

**Table 7.1.** Impact of green roofs on air temperature in canyons.



Air temperature difference in the canyon with east-west orientation [°C] - the north point (E-WN)						
Height (m)	GR		GR2		GR3	
	day	night	day	night	day	night
1.5m	- 0.03	- 0.01	- 0.42	0.63	- 0.47	0.63
5.5m	- 0.05	0.00	- 0.41	0.70	- 0.48	0.69
15.5m	- 0.13	- 0.03	- 0.50	0.68	- 0.63	0.64
Air temperature difference in the canyon with north-south orientation [°C] - the east point (N-SE)						
1.5m	- 0.65	0.37	- 0.56	0.39	- 0.76	0.35
5.5m	- 0.73	0.33	- 0.60	0.36	- 0.82	0.32
15.5m	- 0.80	0.62	- 0.56	0.64	- 0.82	0.62

**Source:** own elaboration.

Thus, they respectively obtained air temperature reduction of 1.79°C, 1.76°C in pedestrian movement zone. Intensification of vegetation cover on building roofs (up to 100%) did not translate into significant temperature reductions. The scenario associated with 50% low vegetation cover of the roof area was more effective. This is confirmed by the conclusions obtained from the research carried out in the areas of street canyons in the Metropolitan Zone of Lodz (moderately warm climate zone).

Numerous authors emphasize that the implementation of green solutions influences the parameters related to thermal conditions of urban areas. Green roofs modify the temperature of roof slopes, which affects the microclimatic conditions inside buildings. In summer, they reduce the heating of roofs. The difference may be even 30°C (Eumorfopoulou & Aravantinos, 1998, Wong et al., 2003, Saiz et al., 2006). In Lodz, the maximum temperature of green roofs was 25°C, which meant a 35°C reduction in the parameter compared to buildings covered with tar paper roofs. As a result, energy consumption in buildings could be reduced. According to Saiz et al. (2006), summer cooling load could be lowered by 6%. During peak hours, cooling load in the upper floor may reach 25%.

Another adaptation strategy was the use of green walls, considered as one of the more practical solutions due to their low interference with the land use (they occupy a small space). Three cases were considered, i.e. 47%, 60%, 100% ivy coverage of building facades forming street canyon frontages. The greening of all building walls in the east-west canyon area was found to be the most effective (Table 7.2.). The reduction in air temperature was 0.76°C at the level of people movement. The more intense impact of the solution was associated with the eastern air inflow, which although small during the warmest day of the Typical Meteorological Year, influenced the appearance of soothing effect in the canyon. Even above the building roofs, there was a noticeable decrease in air temperature. In the second case - the north-south oriented canyon, the effect of ivy cover on building facades was smaller (0.24 - 0.54°C). The maximum temperature decrease took place above the roof slopes. Here, the reason is to be found in the effect of assumed airflow in shaping the conditions within the canyons.

**Table 7.2.** Impact of green walls on air temperature in canyons.

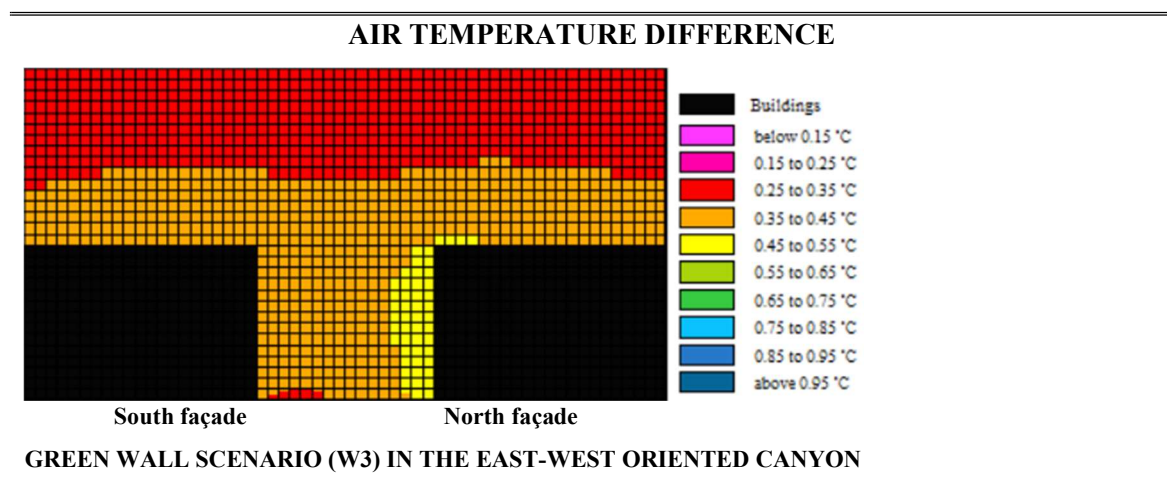
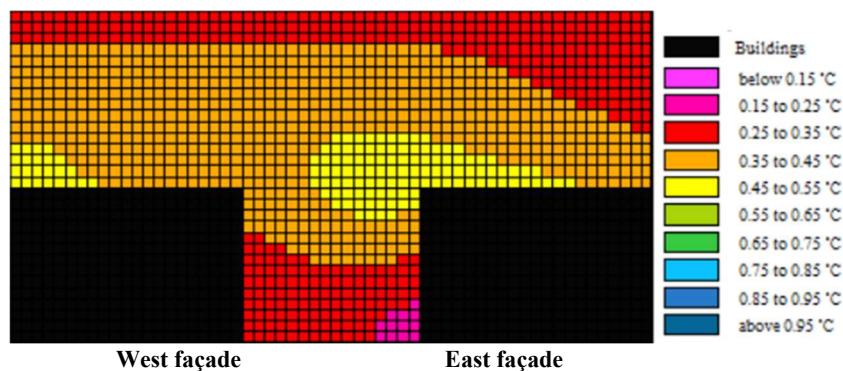




Table 7.2. Continuation.



GREEN WALL SCENARIO (W3) IN THE NORTH-SOUTH ORIENTED CANYON

Air temperature difference in the canyon with east-west orientation [°C] – the north point (E-WN)						
Height (m)	W		W2		W3	
	day	night	day	night	day	night
1.5m	- 0.40	0.55	- 0.38	0.53	- 0.76	0.51
5.5m	- 0.40	0.62	- 0.38	0.59	- 0.61	0.65
15.5m	- 0.39	0.70	- 0.39	0.69	- 0.48	0.89
Air temperature difference in the canyon with north-south orientation [°C] – the east point (N-SE)						
1.5m	- 0.35	0.32	- 0.35	0.32	- 0.24	0.30
5.5m	- 0.41	0.29	- 0.41	0.29	- 0.33	0.27
15.5m	- 0.54	0.61	- 0.54	0.61	- 0.50	0.62

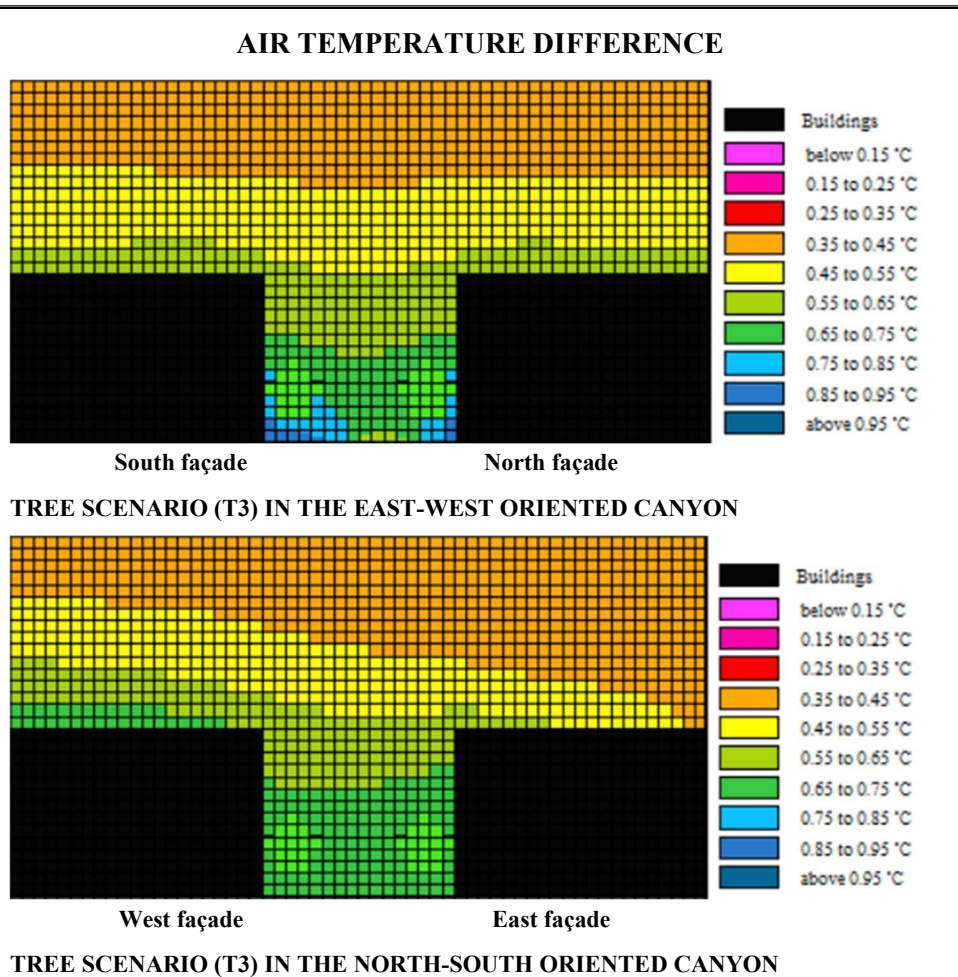
Source: own elaboration.

Studies on the application of vertical greenery confirm that the implementation of this type of solution causes a beneficial modification of the thermal conditions in the outdoor environment. Living facades effectively intercept solar radiation. The absorbed part is used for biological functions, metabolism, and transpiration. Another part is reflected by vegetation to the environment. Therefore, the ambient temperature is modified (Hoelscher et al., 2016).

Tall greenery is considered to be one of the more effective solutions leading to a beneficial modification of climatic conditions in areas of dense, compact inner-city development (Table 7.3.). The introduced forestation causes shading of the area. The effect is reduction of air temperature in the canyons. The analyses carried out showed that the effects of strategy implementation based on tree planting were greatest in their direct vicinity in street canyons located in the Metropolitan Area of Lodz. The assumption was to introduce tall greenery symmetrically distributed along the building frontages. The maximum reduction of air temperature, which reached over 0.95°C, was observed under the tree crowns. The greater the proportion of vegetation, the greater the temperature reduction in canyons. Airflow proved to be the key parameter. The synergistic effect of tall greenery

appeared when the wind direction was parallel to the canyon axis. It allowed lowering the ambient temperature at a considerable distance. In addition, the trees contributed to changes in the floor temperature (up to 1.81 °C). The dense tree crowns protected the pavement from excessive sunlight during the day. They also contributed to decreasing the temperature of building walls (3-5 °C).

**Table 7.3.** Impact of trees on air temperature in canyons.



Air temperature difference in the canyon with east-west orientation [°C] - the north point (E-WN)						
Height (m)	T		T2		T3	
	day	night	day	night	day	night
1.5m	- 0.63	0.81	- 0.66	0.70	- 0.76	0.66
5.5m	- 0.59	0.82	- 0.62	0.75	- 0.73	0.71
15.5m	- 0.47	0.82	- 0.62	0.75	- 0.73	0.71
Surface temperature	- 1.55	0.26	- 1.57	0.19	- 1.61	0.20
Air temperature difference in the canyon with north-south orientation [°C] - the east point (N-SE)						
1.5m	- 0.66	0.26	- 0.67	0.31	- 0.72	0.35
5.5m	- 0.64	0.32	- 0.66	0.40	- 0.69	0.30
15.5m	- 0.62	1.26	- 0.70	2.17	- 0.63	1.31
Surface temperature	- 1.34	- 0.23	- 1.35	- 0.21	- 1.45	- 0.18

Source: own elaboration.

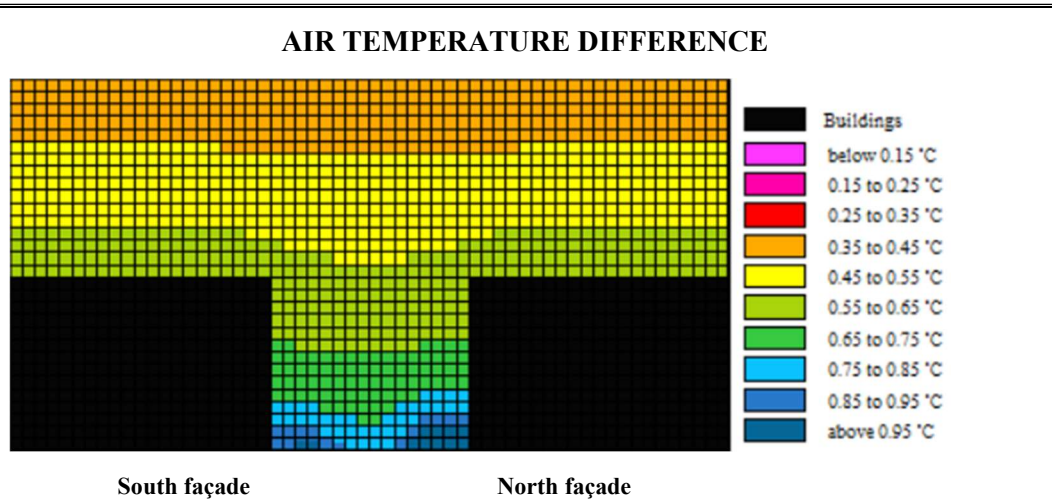
Numerous authors confirm the possibility of using tall greenery as one of the adaptation strategies in highly urbanized areas. Morakinyo & Lam (2016) conducted a study on the effect of tall greenery on climatic conditions in geometrically diverse canyon forms. They assumed at the outset that the least comfortable situation would be observed in the east-west oriented canyons. This was due to the strong insolation of the area, especially at the north facade. The authors showed that the higher the buildings forming the frontage, the greater the reduction in daytime temperature inside the canyon. The opposite trend was observed at nighttime. The buildings acted as a barrier to thermal exchange. As a result, trapped longwave radiation caused an increase in temperature. The introduction of tall greenery was proposed as a solution to reduce the sunlight in the area. The vegetation resulted in a slight temperature reduction of 0.20°C inside the canyon. A much better effect was obtained by Tsoka et al. (2021), who confirmed a moderate impact of tall greenery within a compact urban area. A study conducted in Thessaloniki, Greece, showed that trees cause a maximum temperature reduction of 1°C in the pedestrian movement zone. Their influence decreases with distance. They also contribute to modify conditions inside buildings. The use of trees influences the shading, thus reducing the heating of buildings. This allows to reduce the energy consumption for cooling in summer. Cooling loads can be reduced by 54.34%.

The implementation of blue infrastructure in the form of bioretention planters in the street canyon areas of the Metropolitan Area of Lodz was found to be the most effective solution to affect the ambient temperature (Table 7.4.). Water elements proved to be twice as effective a strategy that can be used to mitigate the effects of climate change in the inner-city areas. The reduction in air temperature was as much as 1.93°C in the pedestrian movement zone, 1.15°C at residential heights, and 0.61°C directly above the building roofs in the east-west oriented canyons. This effect was caused by air inflow from the east direction. The combination of the effect of water as a cooling surface and the free flow of air had a positive impact on thermal conditions. In the north-south oriented canyon, the strategy was less efficient. However, the effect, which was temperature reduction, was greater compared to the implementation of tall greenery.

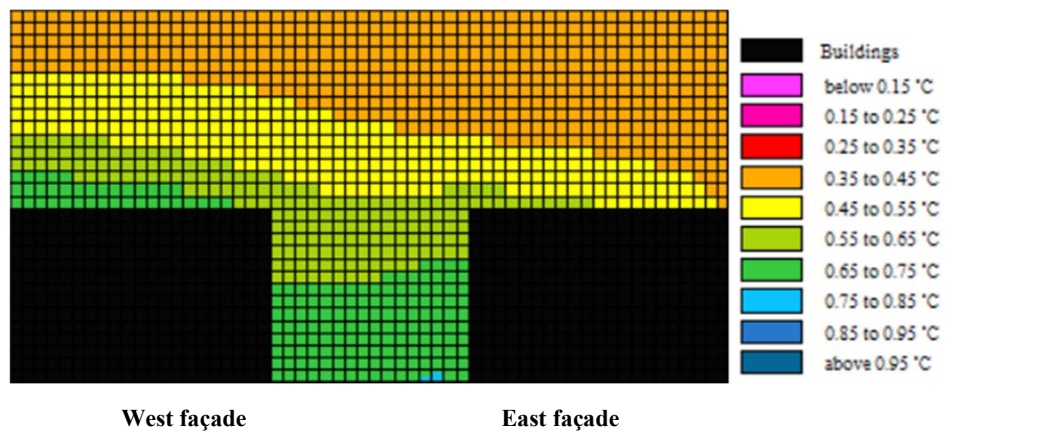
The form of blue strategy used will translate into the effectiveness of solution. In built-up inner-city areas it is not possible to introduce water reservoirs with significant areas. However, it is possible to apply bioretention planters, the depth of which will be greater than 1 m. Then the water bodies will have a lower temperature than the surroundings during the day. This effect is due to a combination of the physical properties of water - the large heat capacity and the ability to transport heat away from its surface by turbulent mixing.

During the nighttime, the natural surface will have a much higher temperature due to the slow transfer of heat to the surroundings.

**Table 7.4.** Impact of blue infrastructure on air temperature in canyons.



**BIORETENTION PLANTER SCENARIO (BP2) IN THE EAST-WEST ORIENTED CANYON**



**BIORETENTION PLANTER SCENARIO (BP2) IN THE NORTH-SOUTH ORIENTED CANYON**

Air temperature difference in the canyon with east-west orientation [°C] - the north point (E-WN)				
Height (m)	BP		BP2	
	day	night	day	night
1.5m	- 1.93	0.99	- 1.93	0.69
5.5m	- 1.15	1.05	- 1.15	0.87
15.5m	- 0.61	0.82	- 0.61	0.86
Air temperature difference in the canyon with north-south orientation [°C] - the east point (N-SE)				
1.5m	- 0.87	0.48	- 0.91	0.48
5.5m	- 0.80	0.62	- 0.84	0.62
15.5m	- 0.75	1.97	- 0.77	1.97

Source: own elaboration.

Völker et al. (2013) conducted a review of 27 studies on the impact of blue infrastructure on climatic conditions in urbanized areas. They showed that the impact of solutions varies.

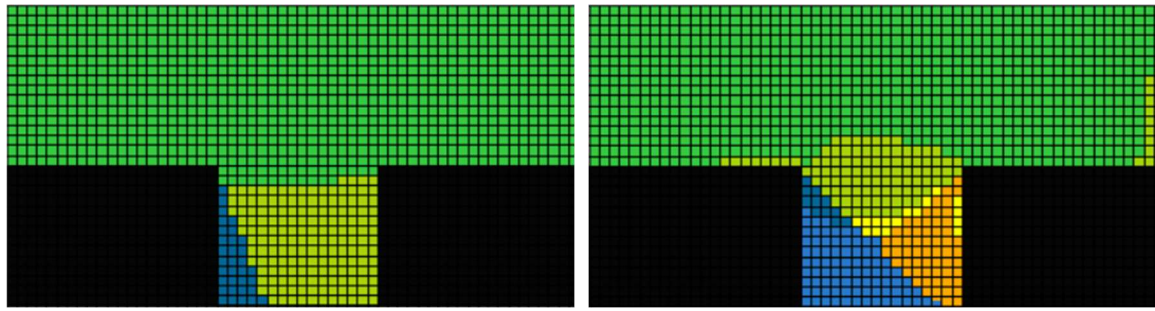
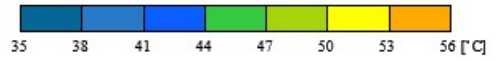
It can range from 0.40°C (pond in park) to 5.63°C (urban wetlands). The soothing effect is dependent on geographic location and thus meteorological conditions. According to Hathway & Sharp (2012), blue strategies are efficient when the air temperature is above 20°C. Their effectiveness is influenced by urban layout, proportion of impervious surfaces, or natural components. The study by Jacobs et al. (2020) in a warm temperate climate zone showed a maximum effect of aquatic surfaces at 0.60°C. The authors emphasized that there are two dominant factors determining the effectiveness of blue infrastructure, i.e. (1) the surface-air temperature gradient, and (2) the location of measurement point.

Adaptive strategies influence the thermal conditions that prevail in street canyon spaces (Figure 7.41.). However, their implementation does not translate into a significant improvement in human sensation in the outdoor environment. Research conducted in the Metropolitan Area of Lodz showed that thermal sensations were highly dependent on the geometry as well as orientation of buildings that form the canyon frontage. In places where shadow was cast by buildings, it was possible to reduce the conditions from 'extreme heat stress' even to 'warm'. This was a significant change resulting solely from the urban layout considered. Taking into account the impact of blue-green adaptation strategies, it is important to admit that it was small. The maximum change was 0.44°C (GR3), 0.07°C (W3), 3.21°C (T3) at the north facade in the east-west oriented canyon; 1.60°C (GR3), 0.91°C (W), 4.57°C (T3) at the east facade in the north-south oriented canyon.

This fact is confirmed in a study conducted by Peng & Jim (2013). They assessed the effectiveness of applying extensive green roofs in a residential area in Hong Kong (China). The implemented solutions were able to reduce air temperature by 0.40-0.70°C. Next, they evaluated the impact of intensive green roofs where 6 m trees were planted. The temperature reduction was at the level of 0.50-1.70°C. Introduced greenery did not significantly improve the thermal sensation in the pedestrian movement zone. The change in PET values was only 0.10-0.20°C.

Also the study of Scharf & Kraus (2019) supports these conclusions. It is important to mention that green walls have an equally insignificant effect on the thermal sensations of humans in the outdoor environment. According to Resler et al. (2020), the soothing effects of greenery are limited in highly urbanized areas. There are many factors that determine the effectiveness of implemented solutions (root distribution, Leaf Area Index, and water content).

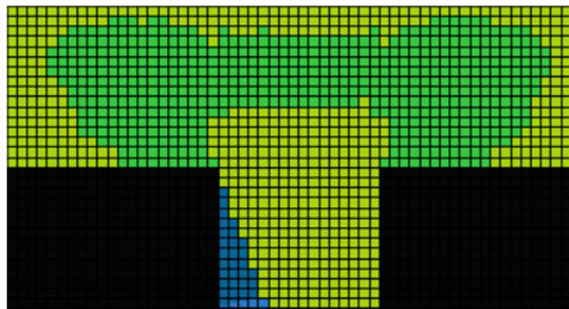
**PET IN CANYONS**



South façade

North façade

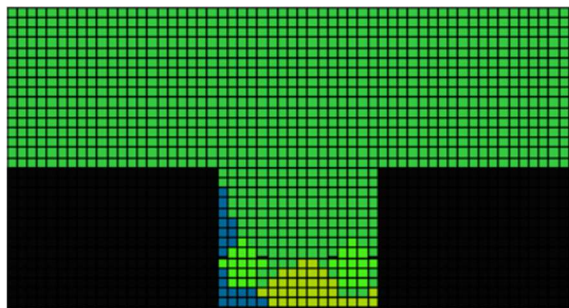
**GREEN ROOF SCENARIO (GR3) IN THE EAST-WEST ORIENTED CANYON**



South façade

North façade

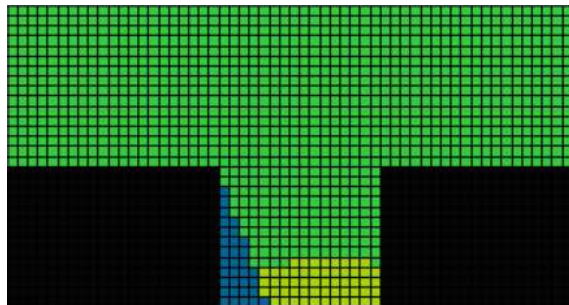
**GREEN WALL SCENARIO (W3) IN THE EAST-WEST ORIENTED CANYON**



South façade

North façade

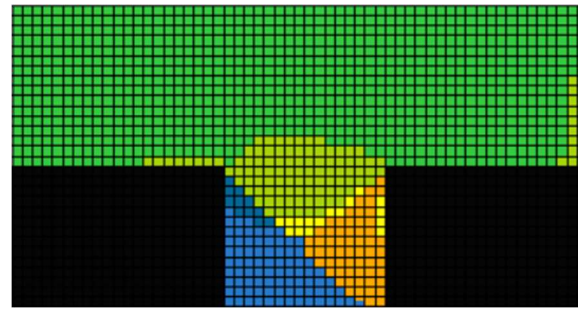
**TREE SCENARIO (T3) IN THE EAST-WEST ORIENTED CANYON**



South façade

North façade

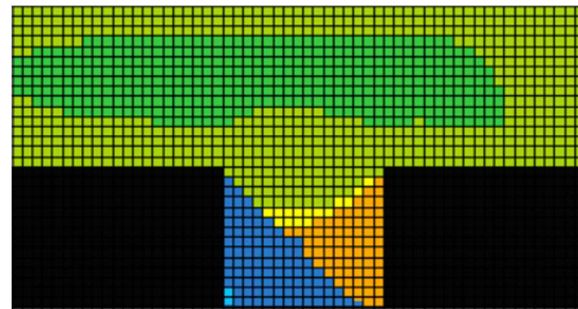
**BIORETENTION PLANTER SCENARIO (BP2) IN THE EAST-WEST ORIENTED CANYON**



West façade

East façade

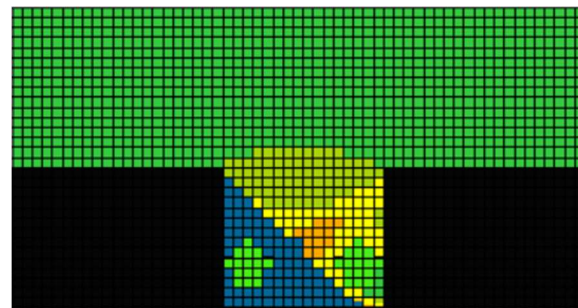
**GREEN ROOF SCENARIO (GR3) IN THE NORTH-SOUTH ORIENTED CANYON**



West façade

East façade

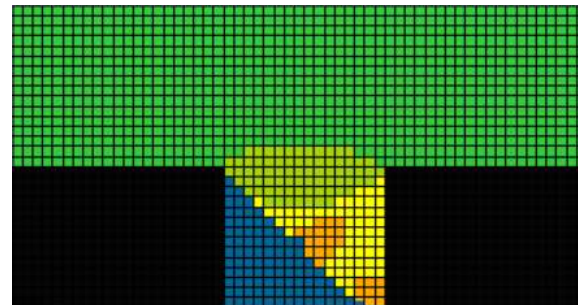
**GREEN WALL SCENARIO (W3) IN THE NORTH-SOUTH ORIENTED CANYON**



West façade

East façade

**TREE SCENARIO (T3) IN THE NORTH-SOUTH ORIENTED CANYON**



West façade

East façade

**BIORETENTION PLANTER SCENARIO (BP2) IN THE NORTH-SOUTH ORIENTED CANYON**

**Figure 7.41.** Impact of selected adaptation strategies on human thermal sensations in outdoor environments - street canyons (source: own elaboration).

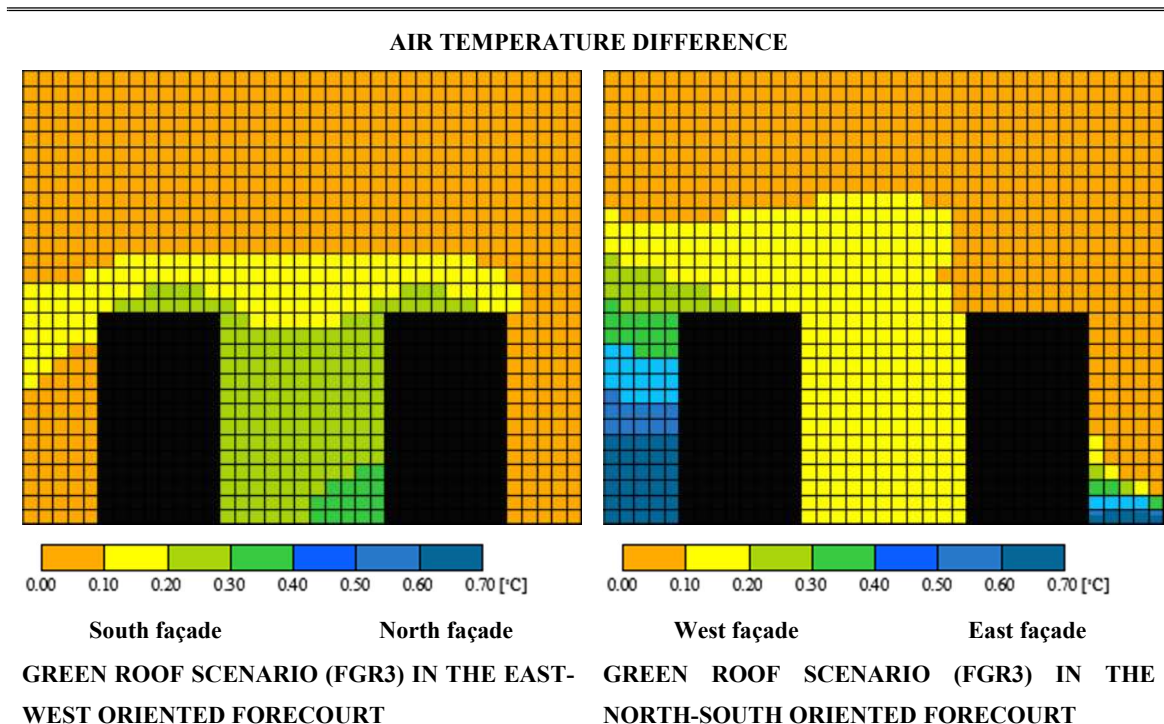
In reality, the implementation of green roofs and walls might be connected with high maintenance costs, if these techniques are efficient. The implementation of trees in cities is considered to be the most effective of the green adaptation strategies. Aboelata & Sodoudi (2020) conducted a study in a warm desert climate zone (Cairo, Egypt). They considered two scenarios involving the implementation of tall greenery at 30%, and 50% in an area of dense, compact residential development. Reduction in thermal comfort index - PET was 1-2°C. This showed that the development structure had a greater effect on the modification of human thermal sensations than adaptation strategies. Also, blue infrastructure does not significantly reduce thermal discomfort. The study of Jacobs et al. (2020) confirmed the fact that the modification of PET values was small. The authors considered natural solutions in the form of canals, ditches, as well as urban ponds in the Netherlands. The maximum change that was observed was less than 1°C (70% of the analyzed cases).

### **The Nature Based Solution benefits in the forecourts of Lodz**

The impact of blue-green infrastructure in urban forecourt areas was limited. In the isolated inner forecourts, microclimatic conditions were not significantly improved. In terms of air temperature reduction, a change was observed for the solution involving the implementation of green roofs (Table 7.5.). The maximum reduction of this parameter was 0.44°C in the east-west oriented forecourt. However, this effect should be associated with the exchange of air masses, which after flowing over the vegetation fell into the forecourt (cooling effect). In the second case - north-south orientation - the solution efficiency was much lower. Reduction occurred only outside the building area, in the place where cooled, denser, and thus heavier air fell down.

However, it is found that green roofs can contribute to the modification of thermal conditions of an area, despite having little impact on external weather conditions. Li et al. (2019) assessed the effectiveness of greenery implementation in the form of both horizontal (extensive system - grass covering of roof slopes) and vertical (leafy vegetation supported on an external structure) on service buildings with an internal forecourt in the city of Ningbo, China. They estimated that the use of green infrastructure contributed to improved indoor conditions. Cooling load reduction was 8.8% and heating load reduction was 1.85%. As a result, the energy efficiency of buildings was increased.

**Table 7.5.** Impact of green roofs on air temperature in urban forecourts.



Air temperature difference in the forecourt with east-west orientation [°C] - the north point (E-WN)						
Height (m)	FGR		FGR2		FGR3	
	day	night	day	night	day	night
1.5m	- 0.31	0	- 0.32	0	- 0.44	0
5.5m	- 0.26	0	- 0.26	0	- 0.38	0
15.5m	- 0.13	0	- 0.13	0	- 0.26	0
Air temperature difference in the forecourt with north-south orientation [°C] - the east point (N-SE)						
1.5m	- 0.13	- 0.18	- 0.15	- 0.19	- 0.31	- 0.23
5.5m	- 0.12	- 0.19	- 0.14	- 0.19	- 0.31	- 0.24
15.5m	- 0.11	- 0.14	- 0.11	- 0.14	- 0.28	- 0.18

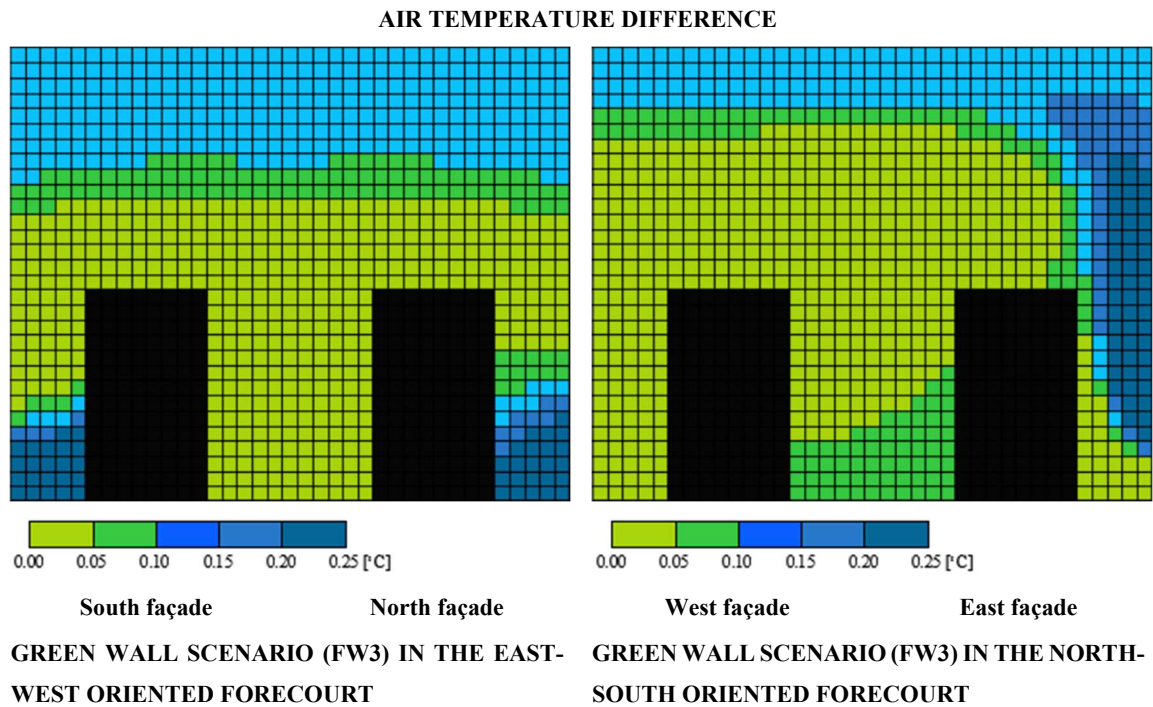
**Source:** own elaboration.

The introduction of living facades also has a limited effect on meteorological conditions in the outdoor environment (Figure 7.6.). It causes a slight reduction in air temperature in the squares inside the forecourt development. However, according to Zhang et al. (2019), it is considered as one of the more desirable adaptation solutions that contributes simultaneously to the energy efficiency of building structures, environmental, economic, social and aesthetic benefits. The authors assessed the impact of green walls on the ambient conditions of the Building Energy Efficiency Research Centre at the South China University of Technology in Guangzhou, China. They estimated that the temperature of concrete exterior walls was 51.4°C. Screening the partitions with vegetation resulted in a reduction of 14.2°C. This resulted in more favorable thermal conditions inside the building, i.e.



reduced air temperature by 3.5°C. This improved the thermal sensation experienced by people inside the Research Centre.

**Table 7.6.** Impact of green walls on air temperature in urban forecourts.



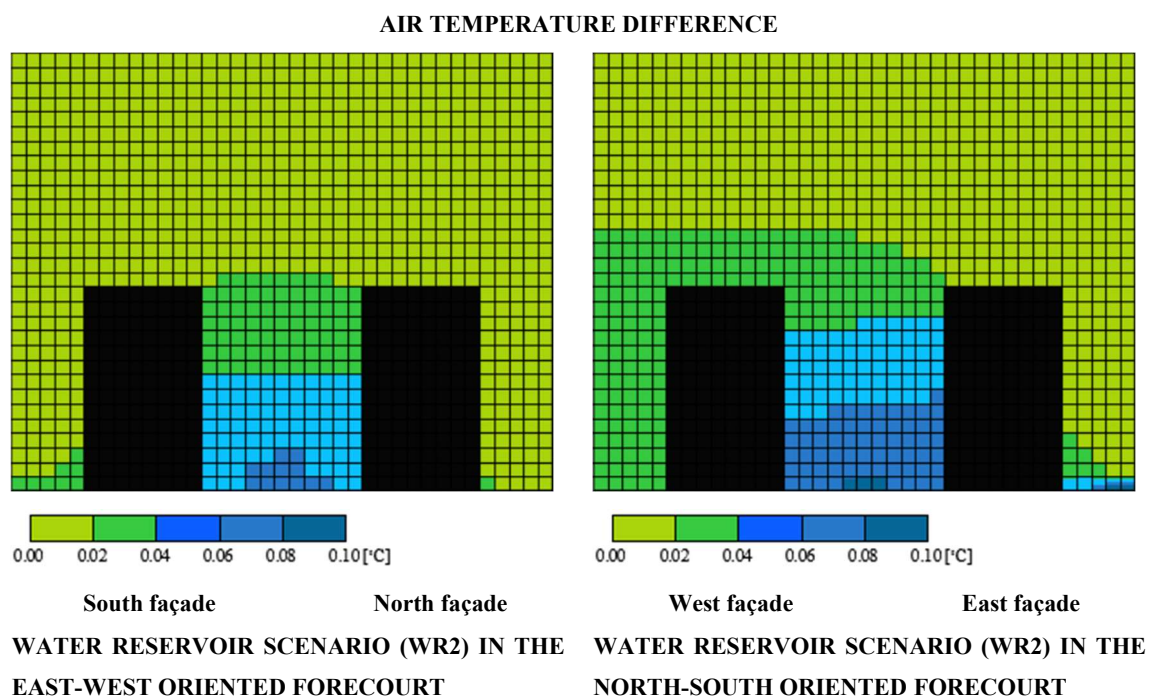
Air temperature difference in the forecourt with east-west orientation [°C] - the north point (E-WN)						
Height (m)	FW		FW2		FW3	
	day	night	day	night	day	night
1.5m	- 0.17	0.01	- 0.15	0.00	- 0.05	- 0.15
5.5m	- 0.12	0.02	- 0.10	0.01	- 0.01	- 0.11
15.5m	- 0.04	0.02	- 0.03	0.02	- 0.01	0.01
Air temperature difference in the forecourt with north-south orientation [°C] - the east point (N-SE)						
1.5m	- 0.07	- 0.21	- 0.05	- 0.23	0.06	- 0.47
5.5m	- 0.07	- 0.21	- 0.05	- 0.23	0.05	- 0.46
15.5m	- 0.01	- 0.15	- 0.09	- 0.15	- 0.06	- 0.17

**Source:** own elaboration.

Modification of meteorological parameters in the external environment proves to be extremely difficult. The implementation of water reservoirs is of limited use in highly urbanized areas, especially within compact housing developments (Table 7.7.). Analyses conducted for the Metropolitan Area of Lodz showed a marginal effect of water reservoir on the ambient temperature (<0.10°C). Such an effect was probably related to airflow, which was prevented in the forecourts. According to Jin et al. (2017), for the cooling effect of blue infrastructure to occur, proper ventilation of the area is essential. The authors conducted a study for a residential development in Harbin (China). They tested the effectiveness of

selected adaptation strategies. The implementation of water reservoirs with a large surface area resulted in a maximum temperature reduction of 4.4°C. However, for the soothing effect to occur, the airflow had to be ensured (1.98 m/s). Then, the cooling effect of the solution could be felt even at a distance of 10m.

**Table 7.7.** Impact of blue infrastructure on air temperature in urban forecourts.



Air temperature difference in the forecourt with east-west orientation [°C] - the north point (E-WN)				
Height (m)	WR		WR2	
	day	night	day	night
1.5m	- 0.04	- 0.04	- 0.06	- 0.05
5.5m	- 0.02	- 0.04	- 0.04	- 0.04
15.5m	- 0.01	- 0.05	- 0.02	- 0.06
Air temperature difference in the forecourt with north-south orientation [°C] - the east point (N-SE)				
1.5m	- 0.05	- 0.01	- 0.07	- 0.02
5.5m	- 0.04	- 0.01	- 0.06	- 0.02
15.5m	- 0.01	0	- 0.02	- 0.01

**Source:** own elaboration.

The use of blue-green strategies does not allow a significant improvement in the thermal comfort of the outdoor environment. Drapella-Hermansdorfer & Gierko (2020) point out that within urban forecourts, the development geometry is crucial. It is the geometry that limits insolation and thus guarantees a much more favorable thermal sensation during hot summer days. Adaptation strategies can only support planning measures that are implemented in highly urbanized areas. This fact is confirmed by the research conducted in the Metropolitan Area of Lodz (Figure 7.42.). The application of selected blue-green

strategies did not guarantee the comfort conditions in urban forecourts. The change was minimal. This was influenced by meteorological parameters, including mean radiant temperature, air temperature, relative humidity, and wind velocity, which are taken into account when estimating the thermal comfort index. In this case - the isolated urban form of Lodz forecourts prevented the free airflow.

Literature studies confirm that urban building parameters become a key issue. The introduction of natural adaptation strategies translates, to a small extent, into an improvement of meteorological parameters and, therefore, of thermal comfort perceived by humans. Acero et al. (2019) assessed the effectiveness of vertical greenery implementation in a forecourt surrounded by high-rise buildings in Singapore. This was an area of considerable size (399 m x 414 m). Free airflow was guaranteed between the buildings located around the forecourt. As a result, the spatial-mean PET reduction was 4°C at the east facade, which receives a lot of daytime sunlight. A much smaller effect was observed when blue infrastructure elements were applied. According to Sözen & Oral (2019), who conducted a study in Mardin, Turkey, the maximum PET reduction was 1.4°C. They confirmed that the impact of blue-green strategies was dependent on the development dimensions, height-to-width ratio, and the number of layout openings.

#### PET IN FORECOURTS

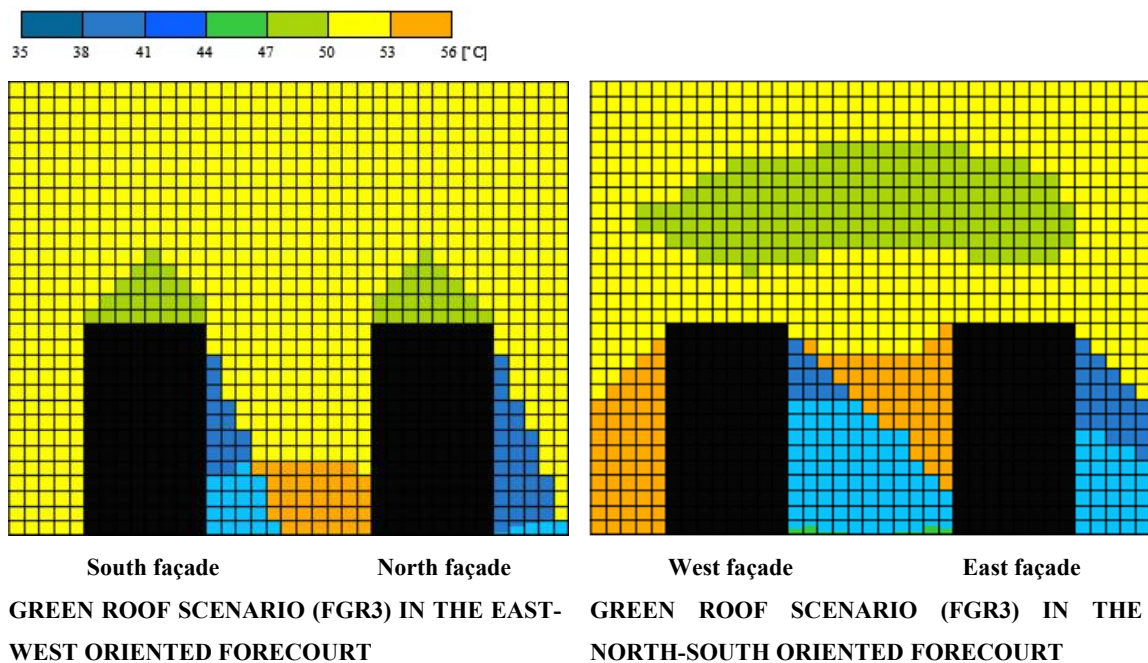


**Figure 7.42.** Impact of selected adaptation strategies on human thermal sensation in outdoor environments - urban forecourts (source: own elaboration).

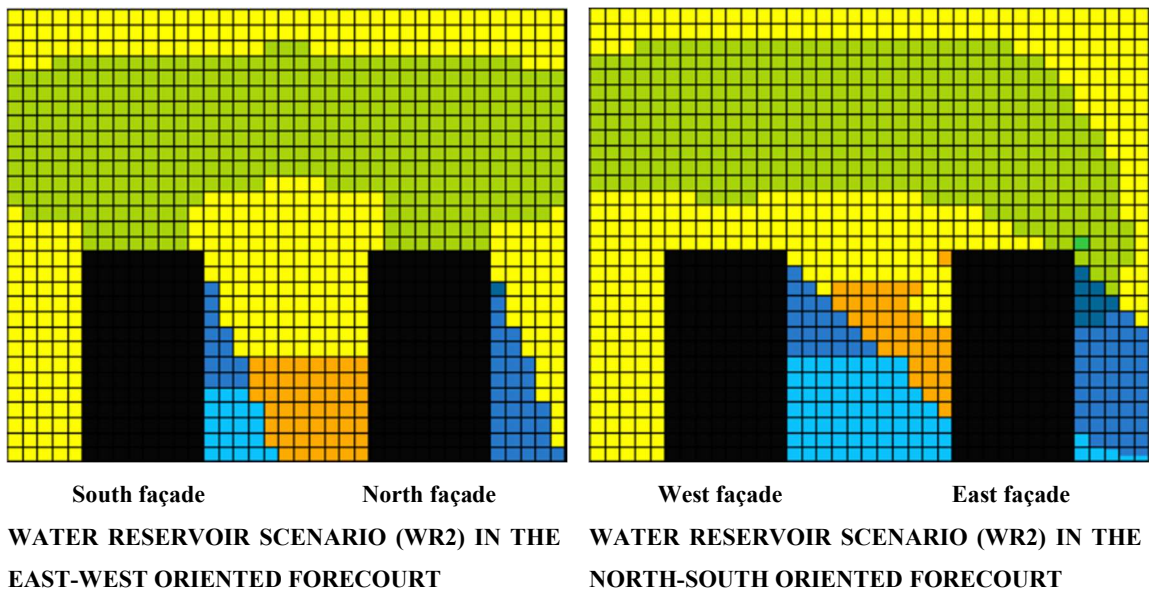
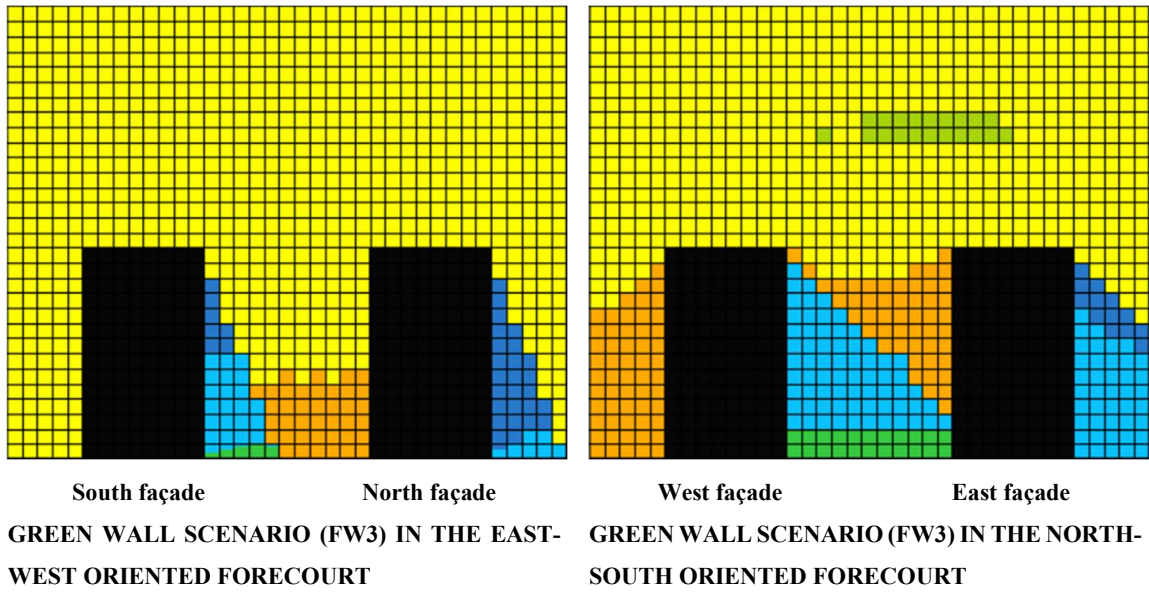


Figure 7.42. Continuation.

## CHAPTER VIII. INDOOR THERMAL CONDITIONS

European Union countries are involved in leading efforts to develop a sustainable, secure and low-carbon energy system. A set of policy initiatives, called the European Green Deal, was announced in September 2020 ([European Commission, European Green Deal, 2020](#)). It aims to reduce greenhouse gas emissions by at least 40% by 2030 (compared to 1990). The key issue is to improve the energy efficiency of buildings, especially with regard to historic buildings located in the inner cities. They are considered to be the most sensitive to changes in external weather conditions ([European Commission, Climate and Energy Policy Framework to 2030, 2020](#)).

For more than a decade, there has been a proposal to improve the energy efficiency of existing buildings, including cultural heritage sites in Poland. The provisions are included in [the Directive \(EU\) 2018/844 of the European Parliament and of the Council of 30 May 2018 amending Directive 2010/31/EU on the energy performance of buildings and Directive 2012/27/EU on energy efficiency \(Text with EEA relevance\)\(2018\)](#). Activities will cover both the transformation of building structures and the implementation of passive and active technical systems. It is assumed that natural adaptation strategies, including elements of blue-green infrastructure, will contribute to reduction of energy demand. Green roofs and living facades are mentioned as basic solutions. In addition, the above-mentioned directives draw attention to the shaping of microclimatic parameters in the rooms. Increasing the quality of indoor environment is supposed to translate into improvement of, among others, thermal comfort of users ([the Directive \(EU\) 2018/844 of the European Parliament and of the Council, 2018](#)).

This chapter presents an attempt to integrate the existing knowledge of urban climatology with building physics. The conducted series of analyses (described in [Chapter VI. Numerical simulation of microclimatic and thermal conditions](#), [Chapter VII. Influence of adaptation strategies on external environment](#)) allowed for the evaluation of microclimatic conditions prevailing in the areas of typical for the Metropolitan Area development forms (street canyons, as well as city forecourts). At a further stage of the study, the information was used to determine internal thermal comfort. The impact of adaptation strategies, such as green roofs and living facades, on indoor thermal comfort parameters of buildings was considered.

## The impact of adaptation strategies on thermal comfort

Passive strategies are among the solutions that can be used to modify the energy performance of buildings. If done correctly, the conversion project will contribute to a reduction in energy demand (reduced need for heating and cooling). The change of characteristics will translate into a higher comfort level, as well as the well-being of users.

In this study, the impact of adaptation strategies, which were (1) green roofs (**GR** scenario), and (2) green walls (**GW** scenario) on selected indoor thermal comfort parameters was analyzed. The information on the residential building located at the crossroad of Jaracza/Piotrkowska Streets (address: Jaracza 1), in the inner city, in the Metropolitan Area of Lodz, was used for the assessment. The data were obtained from archival databases of public institutions, including the City Conservator of Monuments and the City Surveying Centre. On their basis, a prototype of a room intended for human habitation was made. The horizontal projection of a residential building with services on the ground floor, made at the height of the second storey (the level of residential premises in the strict city center) was used. For building partitions, the parameters described in [Chapter IV. Selection of urban forms](#) have been adopted. The analyses included thermal conditions in the living room ([Appendix B, Figure 8.1.](#))<sup>20</sup> It was assumed that the room is located on the south building side. Consequently, the maximum influence of external weather conditions on the thermal comfort was taken into account (the southern facade was subjected to the strongest insolation)([Figure 8.2.](#)). Fully adiabatic conditions were assumed for the external partitions of the analyzed room, except the external southern elevation.

The structures included in the model are shown in [Figure 8.3. - 8.4.](#) Their influence on the thermal conditions inside the living rooms was estimated using DesignBuilder software.

The computational model of green roof used in DesignBuilder is discussed below. Next, the effect of selected passive strategies on the thermal sensation of living room occupants located in a multi-storey residential building has been described.

---

<sup>20</sup> To conduct analyses of thermal conditions, including internal thermal comfort, the DesignBuilder program was used. It was required to create model of a room intended for permanent human habitation. It resulted from the fact that thermal sensations are determined separately for each room in the building.

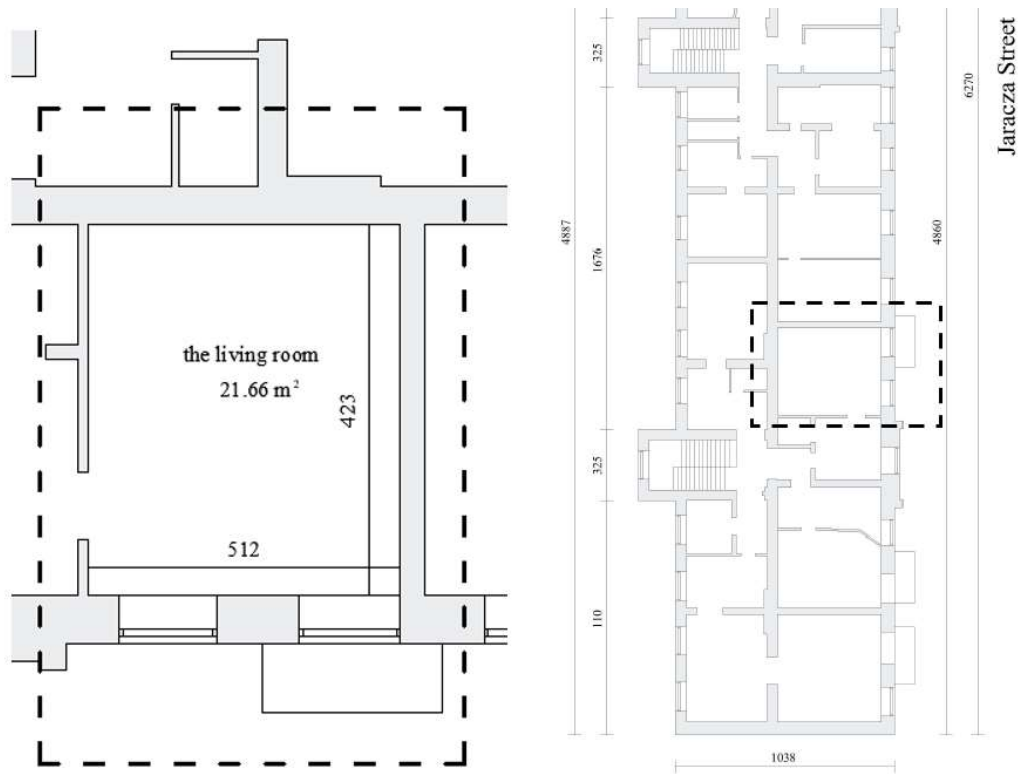


**Figure 8.1.** The living room parameters used to create the prototype (source: own elaboration).

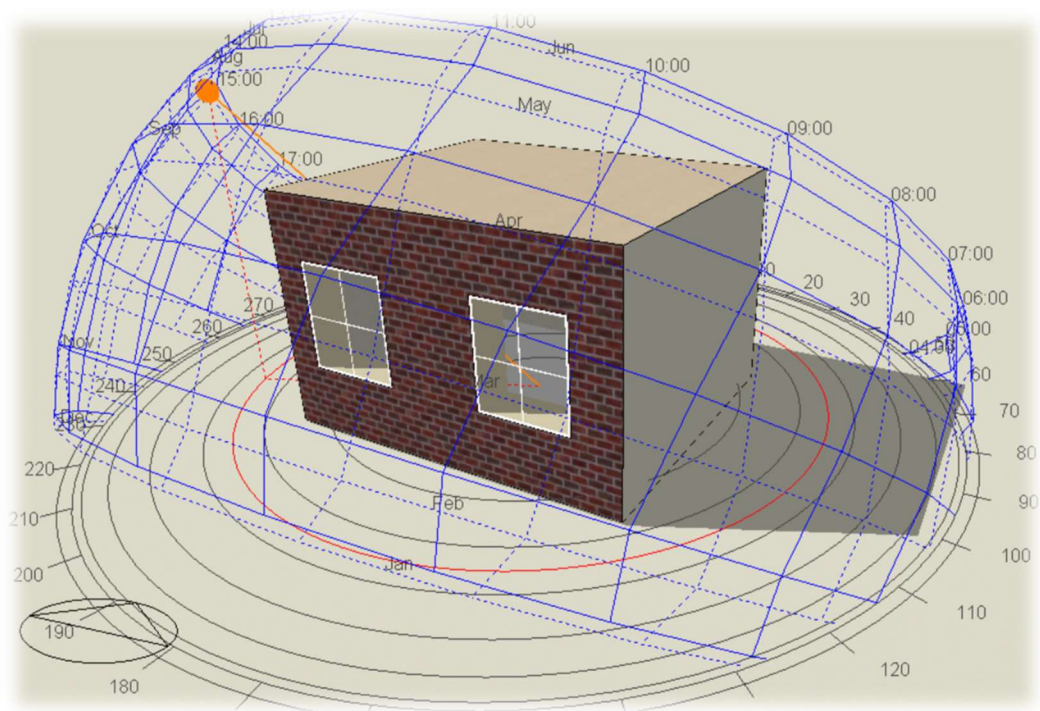


**Figure 8.2.** The living room model of a residential building in the Metropolitan Area of Lodz (source: own elaboration).

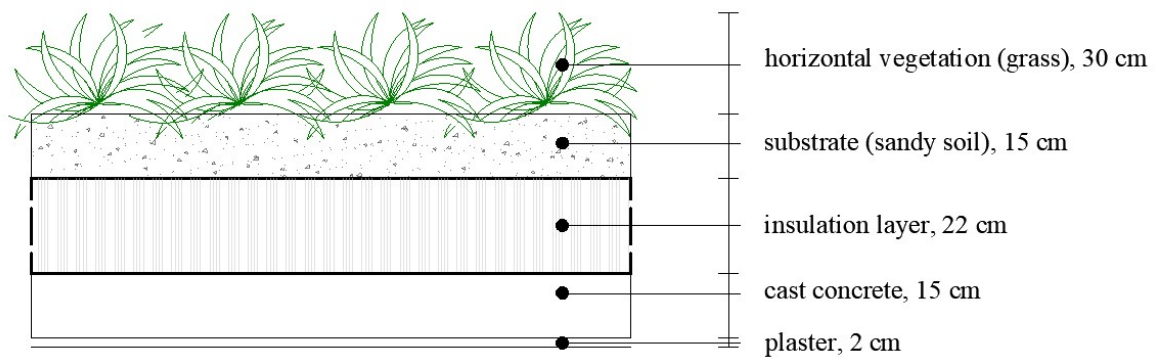


**Figure 8.3.** The construction of green roof - RTR2021/GR scenario (source: own elaboration).

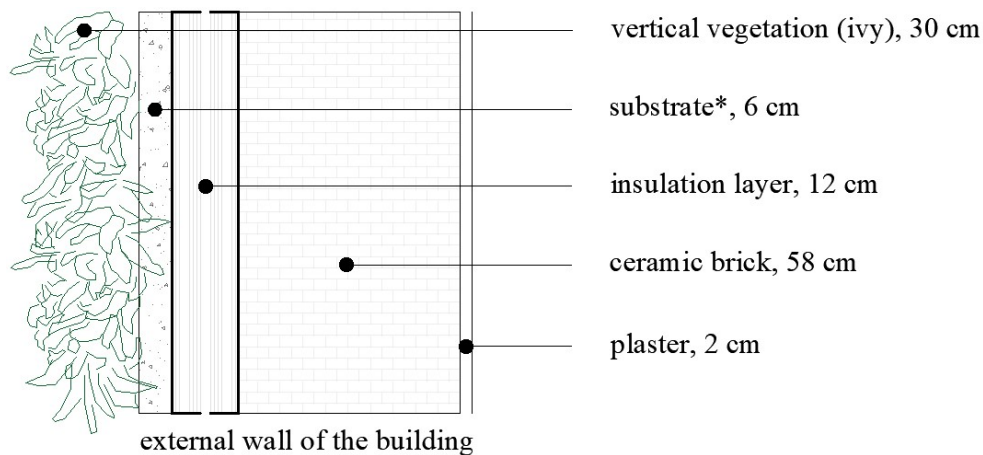


**Figure 8.4.** The construction of green wall - WTR2021/GR scenario (source: own elaboration).

### The model of green adaptation strategies

Analyses of the effects of selected adaptation strategies on indoor thermal comfort were conducted in EnergyPlus software with DesignBuilder interface. The modular structure of the application allowed the implementation of Sailor’s model (2008), which was based on the fast all season soil strength model (FASST) developed by Frankenstein and Koenig for the US Army Corps of Engineers (2004). It considered the long, short wavelengths exchanges by the soil and vegetation, effects of greenery on convective (sensible heat) thermal flow, evapotranspiration (latent heat) through soil and vegetation, heat storage and transfer through the substrate (Figure 8.5.).

---

\* DesignBuilder requires plantings of greenery directly on the substrate layer. In order to investigate the influence of climbing vegetation on the thermal conditions prevailing in buildings, it is necessary to modify the software settings. A structure made of brick can be adopted as an 'imitation' of the substrate layer by modifying the parameters of the material.





**Figure 8.5.** Simplified representation of the energy balance in the passive construction (source: on the basis of Sailor, 2008, Kumar, 2017).

The impact of selected passive strategies on the thermal conditions in the interior of buildings is estimated based on the one-dimensional Sailor's model. The main heat fluxes that describe the foliage energy balance are given by (Equation 8.1.) the short and longwave radiation absorption and longwave radiation emitted by the foliage, (Equation 8.2.) the longwave radiation exchange between the foliage and the soil surface, (Equation 8.3.) the convection heat exchange between the foliage and the air in the canopy, (Equation 8.4.) the latent heat flux by evapotranspiration in the foliage.

$$(\sigma_f [I_s(1 - \alpha_f) + \epsilon_f I_{ir} - \epsilon_f \sigma T_f^4]) \quad \text{Equation 8.1.}$$

where:  $\sigma_f$  is the foliage fraction coverage,  $I_s$  is the total solar irradiance ( $\text{W/m}^2$ ),  $\alpha_f$  is the shortwave albedo of the foliage layer,  $\epsilon_f$  is the foliage emissivity,  $I_{ir}$  is the total infrared irradiance ( $\text{W/m}^2$ ),  $\sigma$  is the Stefan-Boltzman constant ( $5.67 \times 10^{-8} \text{ W/m}^2 \text{K}^4$ ),  $T_f$  is the foliage surface temperature ( $^\circ\text{C}$ ).

$$\left( \frac{\sigma_f \epsilon_f \epsilon_s \sigma}{\epsilon_f + \epsilon_s - \epsilon_f \epsilon_s} (T_o^4 - T_f^4) \right) \quad \text{Equation 8.2.}$$

where:  $\epsilon_s$  is the ground emissivity,  $T_o$  is the soil surface temperature ( $^\circ\text{C}$ ).

$$(H_f = (1.1 \times LAI \rho_{af} c_p C_f W_{af}) \times (T_{af} - T_f)) \quad \text{Equation 8.3.}$$

where:  $H_f$  is the heat sensible flux ( $\text{W/m}^2$ ), LAI is leaf area index ( $\text{m}^2/\text{m}^2$ ),  $\rho_{af}$  is density of air at foliage temperature ( $\text{kg/m}^3$ ),  $c_p$  is specific heat of air at constant pressure (1005.6

J/kg°C),  $C_f$  is the bulk heat transfer coefficient,  $W_{af}$  is the wind speed within the canopy (m/s),  $T_{af}$  is the air temperature within the canopy (°C).

$$\left( L_f = l_f \times LAI \rho_{af} C_f W_{af} r'' \times (q_{af} - q_{f,sat}) \right) \quad \text{Equation 8.4.}$$

where:  $L_f$  is foliage latent heat flux (W/m<sup>2</sup>),  $l_f$  is latent heat of vaporization at ground temperature (J/kg),  $r''$  is the surface wetness factor,  $q_{af}$  is mixing ratio for air within foliage canopy,  $q_{f,sat}$  is saturation mixing ratio at foliage temperature.

On the basis of the [Equations 8.1. - 8.4.](#) the foliage energy balance is assessed ([Equation 8.5.](#)).

$$F_f = \sigma_f [I_s(1 - \alpha_f) + \varepsilon_f I_{ir} - \varepsilon_f \sigma T_f^4] + \frac{\sigma_f \varepsilon_f \varepsilon_s \sigma}{\varepsilon_f + \varepsilon_s - \varepsilon_f \varepsilon_s} (T_o^4 - T_f^4) + H_f + L_f \quad \text{Equation 8.5.}$$

The heat balance of the soil surface is the resultant of the ([Equation 8.6.](#)) the short and longwave radiation absorption and longwave radiation emission of the soil, ([Equation 8.2.](#)) the longwave radiation exchange between the foliage and the soil surface, ([Equation 8.7.](#)) the convection heat exchange between the soil and the air in the canopy, ([Equation 8.8.](#)) the latent heat flux by evapotranspiration in the soil, ([Equation 8.9.](#)) the heat flux conducted through the soil.

$$\left( (1 - \sigma_f) [I_s(1 - a_g) + \varepsilon_s I_{ir} - \varepsilon_s T_o^4] \right) \quad \text{Equation 8.6.}$$

where:  $a_g$  is the shortwave albedo of the ground.

$$\left( H_g = \rho_{ag} c_p C_h^s W_{af} \times (T_{ag} - T_o) \right) \quad \text{Equation 8.7.}$$

where:  $H_g$  is the ground sensible heat flux (W/m<sup>2</sup>),  $T_{ag}$  is the air temperature within the canopy (Kelvin),  $C_h^s$  is the bulk coefficient,  $\rho_{ag}$  is the density of air near the soil surface (kg/m<sup>3</sup>).

$$\left( \left( L_g = C_h^g l_f W_{af} \rho_{ag} \times (q_{af} - q_g) \right) \right) \quad \text{Equation 8.8.}$$

where:  $L_g$  is ground latent heat flux (W/m<sup>2</sup>),  $C_h^g$  is sensible heat flux bulk transfer coefficient at ground layer,  $q_g$  is mixing ratio at ground temperature.

$$\left( K \times \frac{\partial T_o}{\partial z} \right) \quad \text{Equation 8.9.}$$

where:  $K$  is the ground thermal conductivity,  $z$  is the depth of the soil.

The abbreviated soil energy balance is given by the [Equation 8.10](#).

$$F_g = (1 - \sigma_f)[I_s(1 - a_g) + \varepsilon_s I_{ir} - \varepsilon_s T_0^4] - \frac{\sigma_f \varepsilon_f \varepsilon_s \sigma}{\varepsilon_f + \varepsilon_s - \varepsilon_f \varepsilon_s} (T_0^4 - T_f^4) + H_g + L_g + K \times \frac{\partial T_0}{\partial z}$$

**Equation 8.10.**

Heat fluxes are highly dependent on the foliage fraction coverage, which represents the degree of shading of the surface by greenery. The parameter is dependent on the Leaf Area Index, i.e. the projected area of leaves divided by the soil surface area ([Equation 8.11](#)).

$$\sigma_f = 1 - \exp(-0.75 \times LAI) \quad \text{Equation 8.11.}$$

The presented computational model, implemented in DesignBuilder software, has been used to assess the impact of passive adaptive strategies on the thermal conditions in the rooms of a residential building located in the Metropolitan Area of Lodz. The research covered building structure as well as building materials characteristic for the historic city center (see [Chapter IV. Selection of urban forms](#)). Selected passive solutions, i.e. green roofs and living facades, were taken into account (more in [Chapter VII. Influence of adaptation strategies on external environment](#)).

The parameters of computational models of the passive adaptation strategies that were used in this study are presented in [Table 8.1 - 8.2](#). The automatic settings of the application were modified in order to take into account the specificity of selected natural solutions. Changes were made for: height of plants, Leaf Area Index, leaf reflectivity, leaf emissivity, minimum stomatal resistance, max volumetric moisture content at saturation, min residual volumetric moisture content, and initial volumetric moisture content.

**Table 8.1.** Parameters of computational models of the applied adaptation strategies (roof).

<b>The scenario connected with the modification of the roof construction</b>		
<b>Scenarios</b>	<b>Thickness</b>	<b>Heat transfer coefficient (U - value)</b>
Last Floor (LF)	32 cm	2.54 W/(m <sup>2</sup> ·K)
Green Roof (GR)	62 cm	2.54 W/(m <sup>2</sup> ·K)
Roof Technical Requirements 2021 (RTR2021)	54 cm	0.15 W/(m <sup>2</sup> ·K)
Roof Technical Requirements 2021/Green Roof (RTR2021/GR)	84 cm	0.15 W/(m <sup>2</sup> ·K)

**Table 8.1.** Continuation.

<b>Parameters of the vegetation layer</b>	
Height of plants	0.30 m
Leaf area index ( <i>LAI</i> )	1.5 m <sup>2</sup> /m <sup>2</sup>
Leaf reflectivity ( $\alpha_f$ )	0.22
Leaf emissivity ( $\varepsilon_f$ )	0.95
Minimum stomatal resistance	180 s/m
Max volumetric moisture content at saturation	0.44
Min residual volumetric moisture content	0.01
Initial volumetric moisture content	0.15

**Source:** own elaboration.

**Table 8.2.** Parameters of computational models of the applied adaptation strategies (outer wall).

<b>The scenario connected with the modification of the wall construction</b>		
<b>Scenarios</b>	<b>Thickness</b>	<b>Heat transfer coefficient (U - value)</b>
Living Zone ( <b>LZ</b> )	66 cm	0.60 W/(m <sup>2</sup> ·K)
Green Wall ( <b>GW</b> )	96 cm	0.60 W/(m <sup>2</sup> ·K)
Wall Technical Requirements 2021 ( <b>WTR2021</b> )	78 cm	0.20 W/(m <sup>2</sup> ·K)
Wall Technical Requirements 2021/Green Wall ( <b>WTR2021/GW</b> )	108 cm	0.20 W/(m <sup>2</sup> ·K)
<b>Parameters of the vegetation layer</b>		
Height of plants	0.30 m	
Leaf area index ( <i>LAI</i> )	1.5 m <sup>2</sup> /m <sup>2</sup>	
Leaf reflectivity ( $\alpha_f$ )	0.22	
Leaf emissivity ( $\varepsilon_f$ )	0.95	
Minimum stomatal resistance	180 s/m	
Max volumetric moisture content at saturation	0.11	
Min residual volumetric moisture content	0.01	
Initial volumetric moisture content	0.11	

**Source:** own elaboration.

## **Thermal conditions in the rooms of residential building located in the Metropolitan Area of Lodz**

### *Passive solutions - roofs*

The study investigated the effectiveness of implementing adaptation strategies on residential buildings in the Metropolitan Area of Lodz. The following scenarios were considered:

- Last Floor (**LF**): thermal conditions in rooms located at the height of the last floor. Considered as a baseline scenario.
- Green Roof (**GR**): implementation of a green roof. The structure is shown in [Figure 8.3](#). (without the insulation layer).
- Roof Technical Requirements 2021 (**RTR2021**): the design included the use of an additional insulation layer for the building envelope (22 cm). This was implemented to meet current regulatory requirements for renovated buildings ([Figure 8.3](#). - without the vegetation layer).
- Roof Technical Requirements 2021/Green Roof (**RTR2021/GR**): the scenario assumed implementation of roof insulation. The outer layer was an extensive green roof ([Figure 8.3](#)).

The impact of passive natural solutions on indoor thermal comfort was considered. It was estimated in living rooms located in the residential zone (at the level of occurrence of dwelling units). For this purpose, the created living room prototype with southern exposure was used. Simulations were carried out for the hottest day of the Typical Meteorological Year.

The assessment also included an alternative scenario (RTR2021). Adaptation of the residential building to the requirements of [the Regulation Of The Minister Of Infrastructure Of 12 April 2002 On Technical Conditions, Which Should Correspond To The Buildings And Their Location \(2002\)](#) was considered. The building structure was modified. Insulation material was implemented on the roof (thickness: 22 cm). Finally, according to the legal requirements of [the Regulation \(2002\)](#), an appropriate value of the heat transfer coefficient was obtained ( $U_c < 0.15$  [W/(m<sup>2</sup> ·K)]).

The last scenario (RTR2021/GR) involved a combination of existing building solutions along with passive adaptation strategies. The building was insulated. An extensive green roof was used as a natural solution. The simulation results are shown in [Figure 8.6](#).

The analyses showed that implementation of an extensive green roof on the residential building improved the internal thermal comfort of the occupants. The operative temperature was reduced by 0.28°C (24-hour average value). Although this is a relatively small change, the impact of the passive solution on the external microclimate conditions should be kept in mind (Chapter VII. Influence of adaptation strategies on external environment). Moreover, green roofs provide numerous non-climatic benefits.

Modification of roof covering (introduction of additional insulation) turned out to be a more effective solution. Meeting the minimum legal requirements of the Regulation (2002) for buildings undergoing reconstruction allowed for an improvement in the quality of indoor environment. The thermal comfort index was reduced by 1.79°C. However, this was a strategy related to significant reduction in the heat transfer coefficient for the envelope. In this case, there was no additional impact on the microclimatic conditions in the external environment.

The last one was related to the combination of material solutions with natural design (RTR2021/GR). This was the most effective of the scenarios considered. The users' thermal sensations were reduced by 1.84°C.

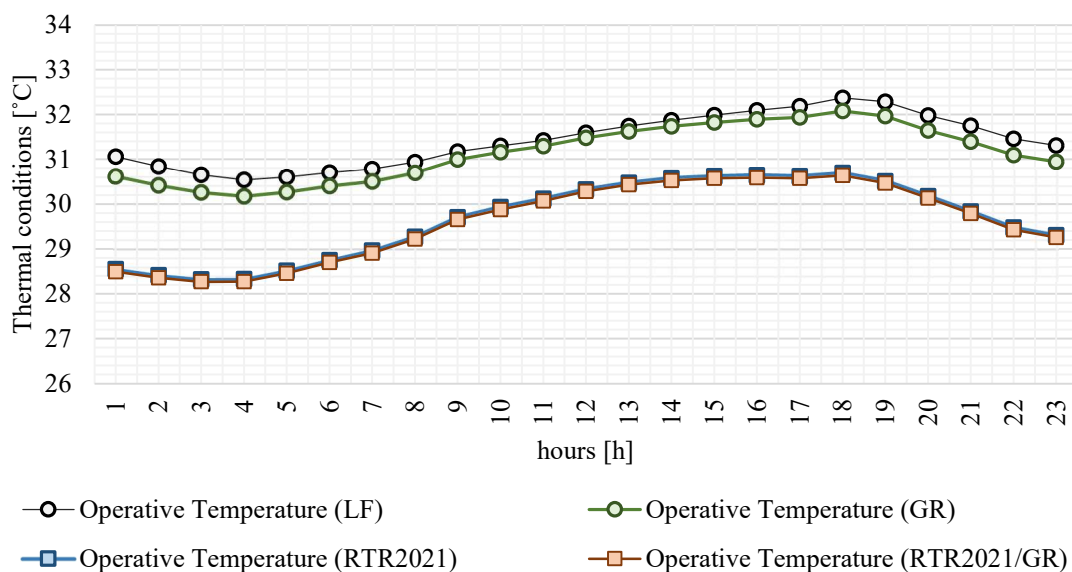


Figure 8.6. Operative temperature (scenarios related to roof structure modification)(source: own elaboration).

Passive solutions - walls

Passive solutions that are related to the use of green walls are considered as an effective method to improve both the microclimatic conditions of external environment and internal thermal comfort. Therefore, scenarios involving structural modification of the external building envelope of rooms located in the living zone were analyzed, i.e.:

- Living Zone (**LZ**): thermal conditions prevailing in rooms located at the residential level in the Metropolitan Area of Lodz. Treated as a baseline scenario.
- Green Wall (**GW**): implementation of a green wall. The design is shown in [Figure 8.4](#). (without insulation layer).
- Wall Technical Requirements 2021 (**WTR2021**): implementation of additional insulation of the building envelope (thickness: 22 cm)([Figure 8.4](#). - without the vegetation layer). As a result, the minimum requirements of the Regulation (2002) on thermal insulation for renovated buildings have been met.
- Wall Technical Requirements 2021/Green Wall (**WTR2021/GW**): the living room envelope was insulated. In addition, extensive green wall construction was implemented ([Figure 8.4](#)).

If the building was modernized, it would be necessary to adapt it to the current legal requirements. [The Regulation Of The Minister Of Infrastructure Of 12 April 2002 On Technical Conditions, Which Should Correspond To The Buildings And Their Location \(2002\)](#) includes provisions concerning thermal insulation of external partitions (walls). From January 2021, in accordance with [§134\(2\) of the Regulation \(2002\)](#), the heat transfer coefficient is  $U_c < 0.20$  [ $W/(m^2 \cdot K)$ ]. Therefore, the alternative scenario that involves implementation of an additional insulation layer of the building was considered. The results are presented in [Figure 8.7](#).

As the analysis showed, the most effective solution to significantly improve the internal thermal conditions was the implementation of vegetation in the external building envelope. Thermal comfort index decreased by 2.41°C. In practice, planting the building walls with vegetation would translate into improved internal conditions. The modification would also include external environmental parameters (see [Chapter VII. Influence of adaptation strategies on external environment](#)). In the very center of cities, the strategy could be implemented, as an external structure, even on historic buildings.

In case of object modernization, it would be necessary to adapt the structure to legal requirements (scenario WTR2021/GW). The analysis of study results indicates that the combination of material solutions (insulation of the building) along with the application of natural solutions (green walls) would allow to reduce the thermal comfort index by 1.69°C. This is a significant change that would contribute to the improvement of energy performance of the building. The effect would be to reduce the use of internal technical installations (heating/cooling system).

The last case - scenario WTR2021 - was the least effective strategy. The reduction in operating temperature was 0.99°C.

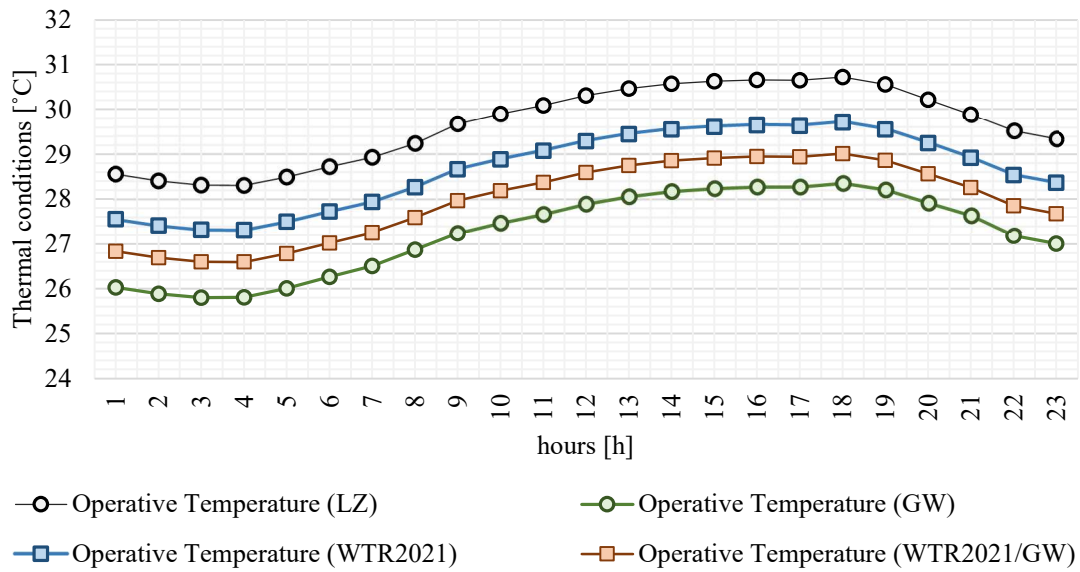


**Figure 8.7.** Operative temperature (scenarios related to modification of living space wall structures)(source: own elaboration).



## CHAPTER IX. DISCUSSION

### 9.1. The influence of urban form on microclimatic conditions and outdoor thermal comfort

The building layout geometry is considered a key factor in shaping the meteorological conditions in highly urbanized areas. According to Deng & Wong (2020), the Aspect Ratio, which expresses the layout proportions, i.e. the building height ratio in relation to the space width between buildings, affects the environmental parameters of public spaces. Complementing adaptation strategies, it will translate into reduction of insolation of the area, as well as modification of airflow, especially in the pedestrian movement zone (De & Mukherjee, 2018). Thus, it will have the effect of improving thermal sensations experienced in the outdoor environment. Therefore, it should be taken into account during the transformation of urban layouts, including at the initial stages of agreement - creation of provisions of local spatial development plans.

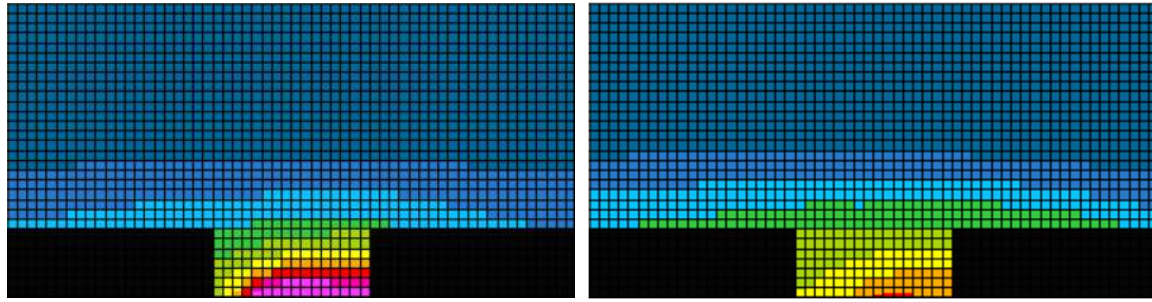
This study analyzed the influence of building geometry on thermal conditions of an area. Scenarios for street canyons (Low Ratio (LR,  $AR \approx 0.4$ ), Mean Ratio (MR,  $AR \approx 0.9$ ) and High Ratio (HR,  $AR \approx 1.1$ )), as well as for urban forecourts (Low Forecourt (LF,  $AR \approx 0.6$ ), Mean Forecourt (MF,  $AR \approx 1.2$ ) and High Forecourt (HF,  $AR \approx 1.9$ )) were considered. Two orientations were included: east-west and north-south, which resulted from the checkerboard layout of the city structure. The scenarios are discussed in detail in [Chapter VI. Numerical simulation of microclimatic and thermal conditions](#).

The results confirm the influence of building parameters on thermal conditions in the street canyon areas ([Figure 9.1.](#)). The most favorable situation was observed for the scenario where the height of building structures was 21 m. They contributed to effective reduction of solar radiation and thus lowering the temperature inside the street canyon. The building structures' walls were protected from daytime heating. The floor temperature was much lower. With the direction of air inflow parallel to the axis of street canyons, improved anemometric conditions were observed (canyon with east-west orientation). In other cases, less favorable thermal conditions were observed.

## AIR TEMPERATURE IN CANYONS

### EAST-WEST ORIENTATION

### NORTH-SOUTH ORIENTATION



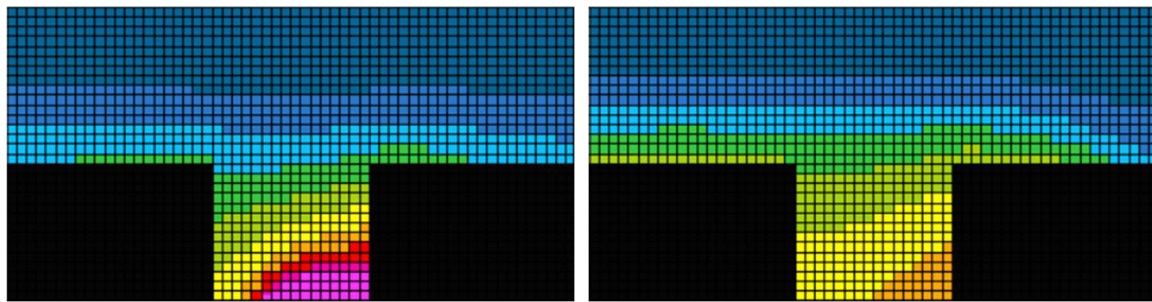
South façade

North façade

West façade

East façade

### LOW RATIO SCENARIOS



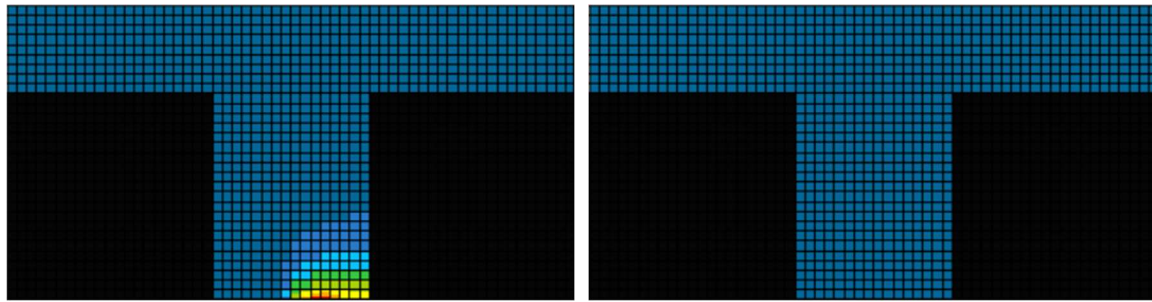
South façade

North façade

West façade

East façade

### MEAN RATIO SCENARIOS



South façade

North façade

West façade

East façade

### HIGH RATIO SCENARIOS



**Figure 9.1.** Air temperature in east-west oriented canyons (the left column), in north-south oriented canyons (the right column), during the warmest day of the Typical Meteorological Year (05.07.2015)(source: own elaboration).

The influence of layout proportions on climatic conditions is emphasized in numerous scientific studies. Deng & Wong (2020) conducted a study on the effect of geometry of street canyon layouts on thermal parameters in Nanjing, China. Layouts with varying Aspect Ratios (from AR = 1 to AR = 8) were considered. It was shown that less comfortable thermal

conditions were observed for shallow canyons ( $AR \leq 1$ ). The building heights were too low to effectively reduce the insolation of an area, thus affecting the ambient temperature. Only for deeper canyons the thermal conditions were observed to improve. The north-south orientation of the structures was considered favorable. Then, the canyons were subject to less daytime heating. Solar hours were much shorter than in canyons with east-west orientation. Such a relationship was also evident for Lodz.

In addition to the direct relation to meteorological conditions, the influence of building geometry on thermal sensations experienced by humans in street canyon spaces is also observed. Sözen & Oral (2019) conducted a study in Mardin, Turkey. The authors showed that the improvement of conditions took place for deep canyons ( $AR > 1$ ). The higher the building structure that formed the canyons' frontage, the greater the reduction of comfort index, PET. It was reduced to 39-42°C, conditions described as 'hot'-'very hot'. In the present study, i.e., elevating the development to a height of 21 meters (Aspect Ratio  $\approx 1.1$ ), thermal sensations were reduced to the 'hot' level in the pedestrian movement zone (Figure 9.2.). In other cases, sensations as high as 'extreme heat stress' ( $PET > 53^\circ\text{C}$ ) were recorded.

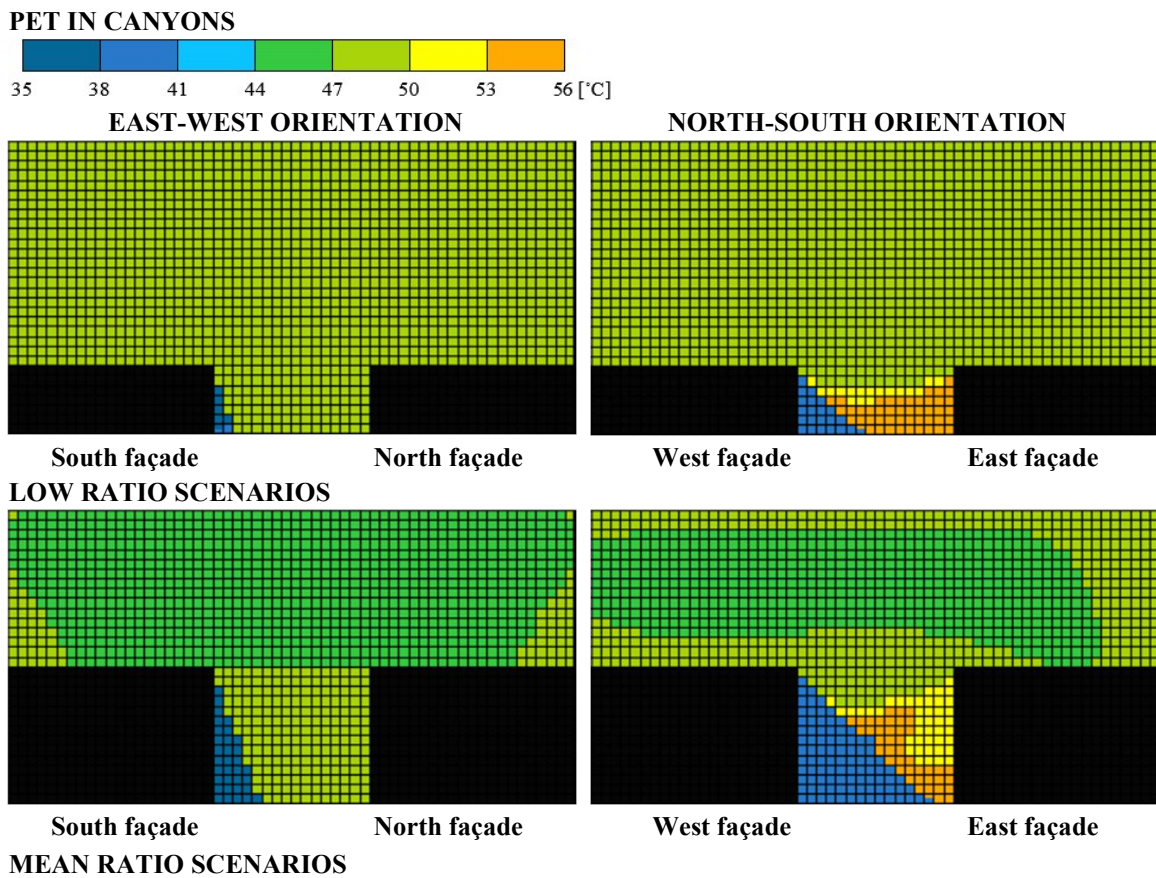


**Figure 9.2.** PET in east-west oriented canyons (the left column), in north-south oriented canyons (the right column), during the warmest day of the Typical Meteorological Year (05.07.2015)(source: own elaboration).

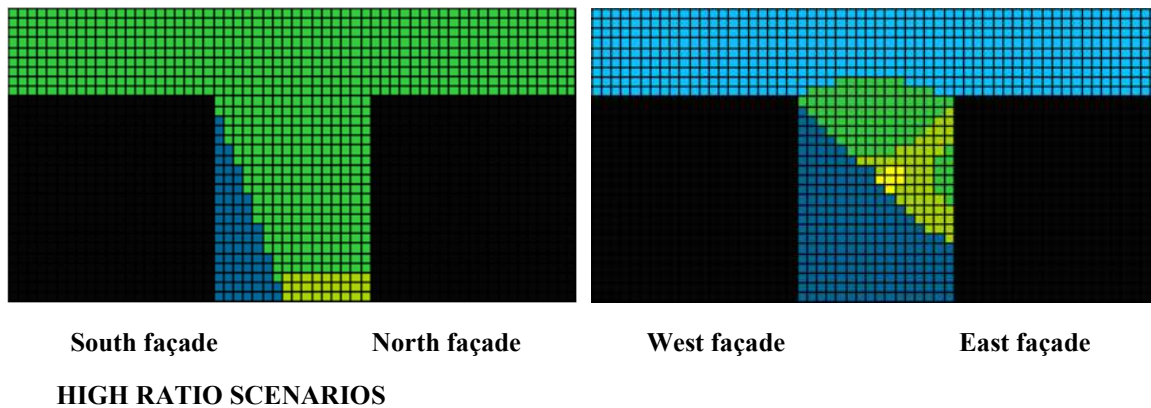


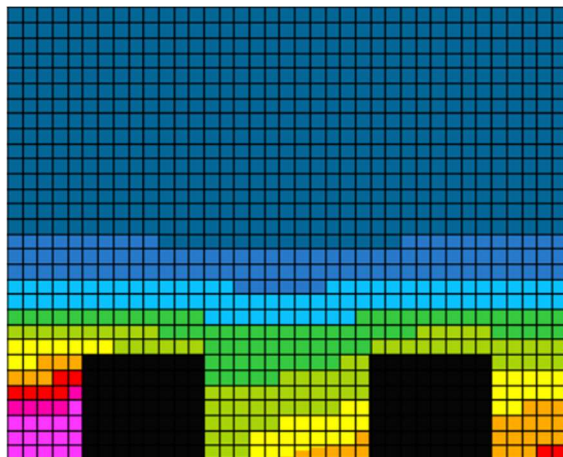
**Figure 9.2.** Continuation.

Studies carried out for urban forecourts in the Metropolitan Area of Lodz show different relationships (temperate climate zone). Much more favorable thermal conditions were recorded when the building height was at least 4 storeys (Figure 9.3.). When the buildings were 6 storeys high, the thermal conditions within the forecourts were relatively stable (air temperature around 32°C). Rodríguez-Algeciras et al. (2018) point out that the north-south orientation is more favorable. Studies conducted in the Metropolitan Area of Lodz confirm this assumption. Forecourt areas with a north-south orientation showed (1) shorter sunhours, (2) lower ambient temperature, (3) and also lower pavement temperature compared to forms with an east-west orientation. However, it became a problematic issue with these types of structures to ensure free airflow. The facilities effectively prevented the exchange of air masses within the forecourts.

Modification of building heights in highly urbanized areas remains a controversial issue. On the one hand, studies show that raising the height of buildings contributes to improving thermal conditions. The solar radiation is limited, thanks to which building materials absorb less heat. This reduces the ambient temperature and improves thermal comfort, especially at the pedestrian level (Figure 9.4.). However, higher buildings result in poorer airflow in urban areas, aerodynamic phenomena causing local air turbulence and deterioration of aerosanitary conditions (accumulation of pollutants).

It is not always possible to raise the building heights to the assumed level. This is due to technical and constructional aspects, as well as legislative restrictions related to the provisions of local spatial development plans, especially for historic buildings. In the areas of historic urban layouts we deal with complexes of buildings and single structures under legal protection. The respect for cultural heritage becomes an important issue.

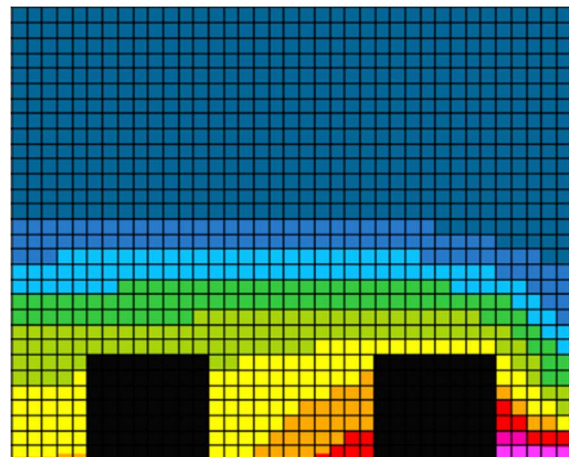
**AIR TEMPERATURE IN CANYONS  
EAST-WEST ORIENTATION**



South façade

North façade

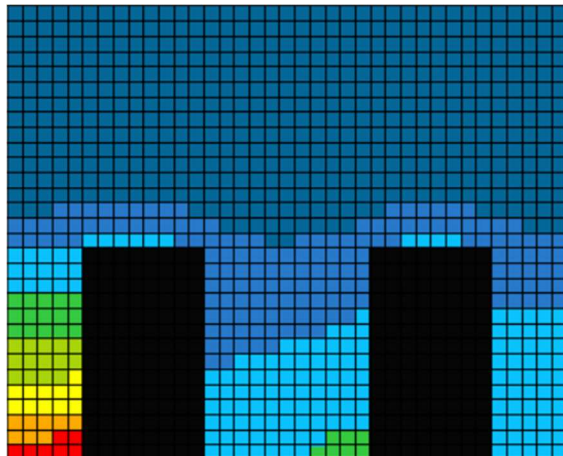
**NORTH-SOUTH ORIENTATION**



West façade

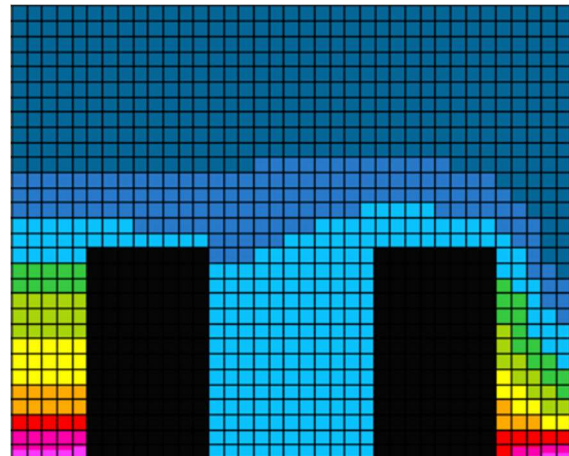
East façade

**LOW FORECOURT**



South façade

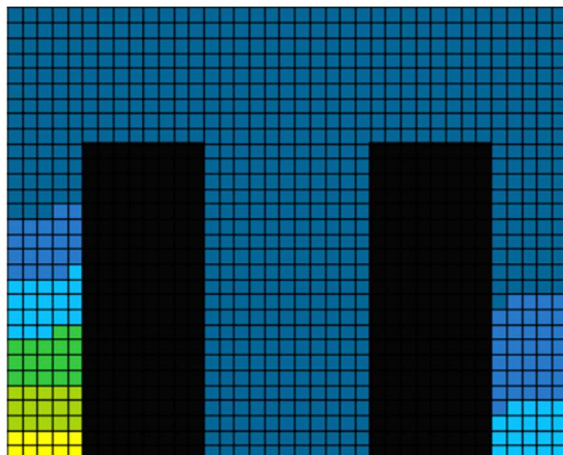
North façade



West façade

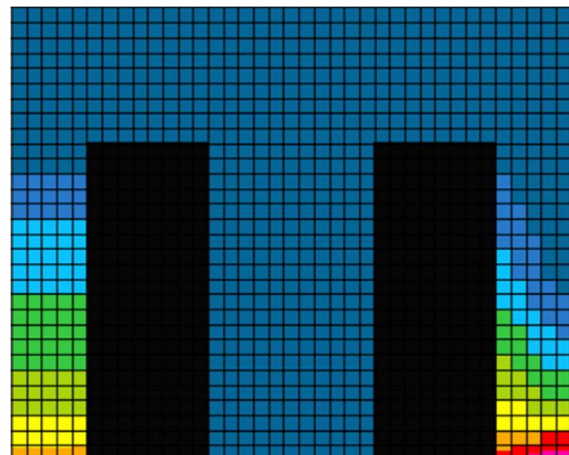
East façade

**MEAN FORECOURT**



South façade

North façade



West façade

East façade

**HIGH FORECOURT**

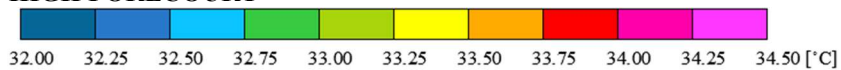


**Figure 9.3.** Air temperature in east-west oriented urban forecourts (the left column), in north-south oriented urban forecourts (the right column), during the warmest day of the Typical Meteorological Year (05.07.2015)(source: own elaboration).

**PET IN CANYONS**

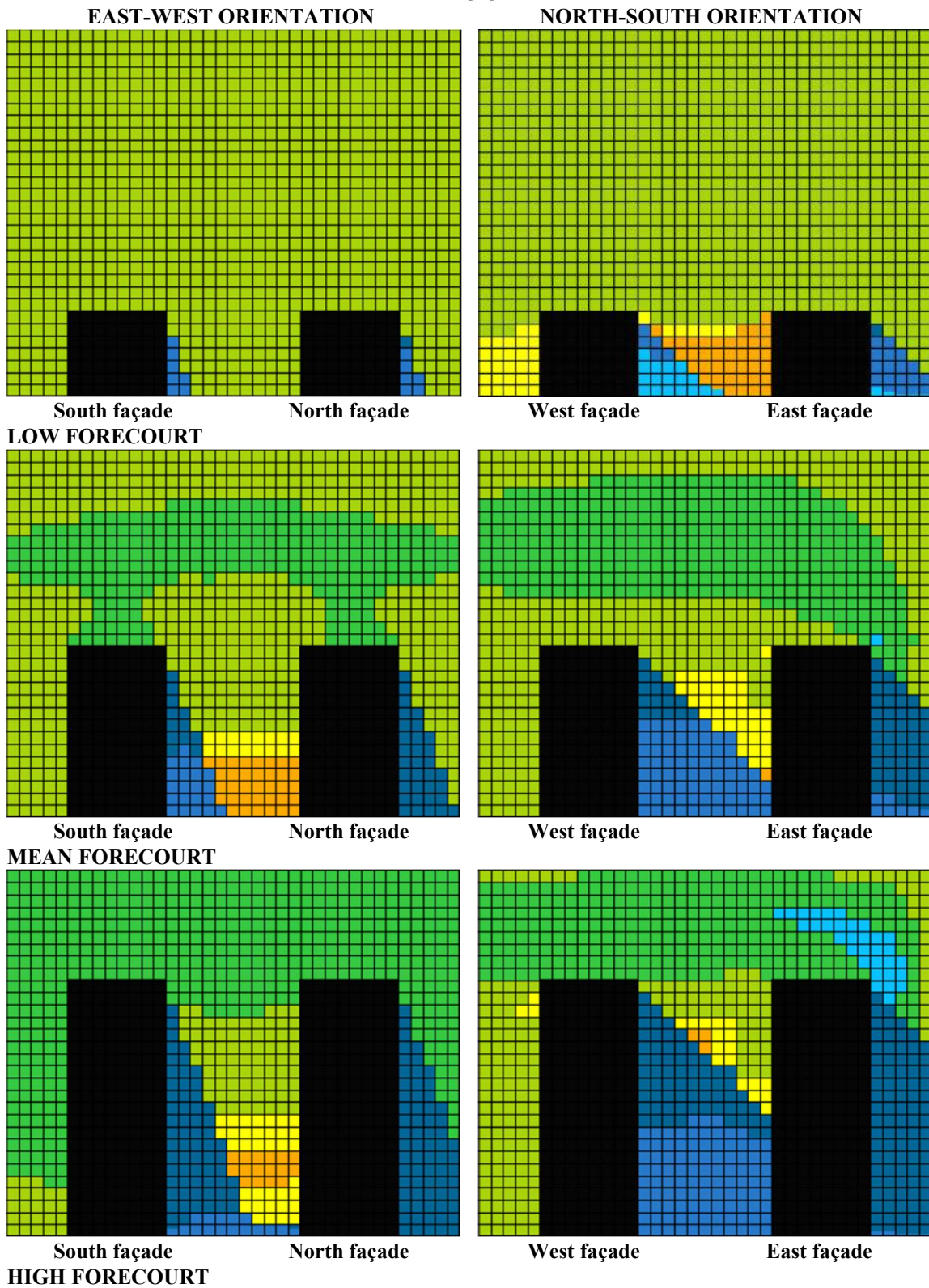
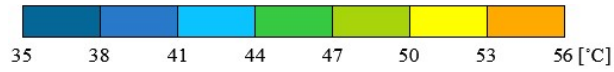


**Figure 9.4.** PET in east-west oriented urban forecourts (the left column), in north-south oriented urban forecourts (the right column), during the warmest day of the Typical Meteorological Year (05.07.2015)(source: own elaboration).

A sustainable approach to urban transformation becomes a challenge for designers. It is very often a compromise between preserving historical structures and improving the residents' living conditions.

## **9.2. The influence of external environment on indoor thermal comfort**

Immediate action to mitigate the effects of climate change has been advocated for a decade. Developments in the building sector become a key issue. Integration of material solutions along with passive natural adaptation strategies is mentioned as one of the concepts. Implementation of vegetation in the form of horizontal (green roofs) and vertical (green walls) aims at modification of the climatic conditions with simultaneous minor changes in the spatial development of the area. The effect is to improve outdoor environmental performance, provide water retention, enrich biodiversity, or increase energy efficiency of buildings (Khotbehsara, 2019).

The present study included an evaluation of the effectiveness of passive adaptation strategies on residential buildings located in the Metropolitan Area of Lodz (Chapter 8.1. [The impact of adaptation strategies on thermal comfort](#)). The actions considered were related to changing the roof covering of existing buildings and those undergoing modernization. In the first case, an extensive green roof (GR scenario) was implemented on a multi-storey building that had not been insulated. The analyses showed that it influenced both the modification of meteorological conditions in the external environment ([Rozdz. VII. Influence of adaptation strategies on external environment](#)) and internal thermal conditions ([8.1. The impact of adaptation strategies on thermal comfort](#)). The operative temperature, which is an indicator of thermal comfort of users, was reduced. In the second case the modernized buildings, fulfilling the requirements included in [the Regulation Of The Minister Of Infrastructure Of 12 April 2002 On Technical Conditions, Which Should Correspond To The Buildings And Their Location \(2002\)](#), were taken into consideration. In modernized buildings, which meet the requirements of thermal protection, no significant influence of the adaptation strategy on thermal comfort inside the rooms was noticed (RTR2021/GR). This was due to the use of an additional thermal insulation layer, located directly under the substrate layer, which effectively reduced the influence of external conditions on building performance.

The impact of passive solutions depends on local conditions (climate zone, terrain, or building structure)([Table 9.1. - 9.2.](#)). Li et al. (2019) conducted a study in Ningbo, China (warm temperate climate zone). The study investigated the use of horizontal (extensive

green roof) and vertical systems (climbing vegetation on an external structure) on a service facility. They showed that the implementation of green adaptation strategies resulted in a reduction of air temperature in the building (up to 1°C). The result was a reduction in energy demand for cooling (8.83%) and heating (1.85%).

Studies on the effectiveness of green roof application on a residential building were conducted by Gargari et al. (2016). The building constituted part of a complex that was built to meet the housing needs of the residents of Pisa, Italy (in a warm temperate climate zone). The municipal authorities decided to carry out adaptation measures due to the requirements of EU regulations, which require the improvement of building energy efficiency. Extensive and intensive design scenarios were considered. They were differentiated in terms of plant height, foliage index (LAI), and insulation material used (with/without EPS).

**Table 9.1.** Study of the influence of green roof construction on the thermal comfort of building occupants.

<b>Development</b>	<b>Climate zone</b>	<b>Reduction of the comfort index</b>
Li et al. (2019)	Ningbo, China Moderately warm climate	1°C
Gargari et al. (2016)	Pisa, Italy Moderately warm climate	2°C
Niachou et al. (2001)	Loutraki, Greece Moderately warm climate	2°C
Ragab & Abdelrady (2020)	Cairo, Alexandria, Aswan, Egypt Warm desert climate	3-4°C

**Source:** own elaboration.

Analysis of the study results by Gargari et al. (2016) showed that implementation of an extensive green roof reduces the temperature of roof envelope by 25°C. This translates into thermal sensations of the room occupants. The comfort index, which is the operative temperature, can be reduced by ~1°C. The effect is even greater when considering intensive construction. Reduction of indoor air temperature occurs with intensification of vegetation density, as well as the use of a thicker layer of substrate as an additional layer of building insulation.

It turns out that the effectiveness of passive strategy is dependent on the geographical location. The higher the outside air temperature, the greater the impact of green roofs on thermal conditions inside buildings. The key parameters are the type of construction



(insulation layer occurring directly under the substrate), the thickness of substrate, and the vegetation implemented.

The analyses were also carried out for the construction involving implementation of climbing vegetation on the external partitions of a residential building located in the Metropolitan Area of Lodz. Adaptation strategy contributed to significant improvement of microclimate conditions. It reduced outdoor air temperature, limited the heating of building walls, and thus allowed modification of indoor environmental parameters (see [Chapter VII. Influence of adaptation strategies on external environment](#) and [Chapter VIII. Indoor thermal conditions](#)). Thermal comfort index, which was the operative temperature, was reduced by as much as 2.41°C (average daily value). This was more effective solution, in terms of indoor thermal conditions, compared to the implementation of extensive green roof.

According to Shaheen et al. (2020), the implementation of climbing vegetation on the facades of buildings can translate into a significant improvement in thermal conditions. The authors conducted a study for public building located in Cairo, Egypt. A double skin green facade was used, which is a design that involves leaving free space between the external building envelope and the natural layer. The most efficient scenario involved 1.5m of free space (wall - climbing vegetation). The result was a reduction in the thermal comfort index of 2-3°C.

**Table 9.2.** Study of the influence of green wall construction on the thermal comfort of building occupants.

<b>Development</b>	<b>Climate zone</b>	<b>Reduction of the comfort index</b>
Shaheen et al. (2020)	Cairo, Egypt Warm desert climate	2-3°C
Assimakopoulos et al. (2020)	Athens, Greece Continental Mediterranean climate	0.5°C
Mabdeh et al. (2020)	Jordan Mediterranean/continental subtropical climate	1-2°C
Djedjig et al. (2013)	Athens, Greece Continental Mediterranean climate	1.5°C

**Source:** own elaboration.

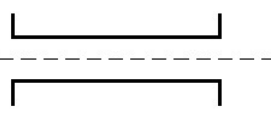
Assimakopoulos et al. (2020) point out that green walls form a shading installation. They provide a mechanism to mitigate adverse outdoor conditions. However, their effect is

dependent on the designed structure. The effect depends on the thermal insulation materials of building walls, the type of substrate, and the amount of greenery implemented. The authors conducted a series of analyses on the implementation of passive adaptation strategies on a residential building located in Athens, Greece. They showed that (1) the type of thermal insulation material affects the energy efficiency of buildings, (2) the effect of green walls on climatic parameters is most intense during the summer, (3) the type of vegetation used results in thermal comfort for the occupants of rooms located in residential structures. However, in this case, the achieved result, i.e. reduction of operative temperature, was at the level of 0.5°C. This represented a slight improvement in thermal sensation.

### 9.3. Recommendation for planners

The adaptation of urban structures to climate change has become a challenge for building, architecture and urban planning professionals. Adaptation activities cover various spatial scales, starting from the scale of the whole city, through activities carried out within quarters and ending with individual buildings. They all lead to the improvement of climate conditions and human thermal comfort in urban spaces.

Based on a thorough analysis of the selected cases, planning guidelines were developed in the form of recommendation sheets for typical urban forms found in the Metropolitan Area of Lodz. Sheets for street canyons and urban forecourts are presented below, taking into account their orientation with respect to the world's directions.

<b>RECOMMENDATION SHEET</b>	
<b>EAST-WEST ORIENTED STREET CANYON</b>	E - W 
<b>Guidelines for the implementation of blue-green infrastructure elements</b>	
<p>(1) Implementation of green roofs with a minimum of 50% roof slope coverage, particularly on structures forming the south frontage of the canyon.</p> <p>Objective: reduction of ambient temperature, with the provision that more favorable conditions in the pedestrian movement zone will occur with air inflow perpendicular to the canyon axis; reduction of roof slope temperature.</p>	

(2) Creation of green walls with a minimum of 40% of facade, with a recommendation for use on the north canyon frontage.

Objective: reduction of ambient temperature; reduction of solar radiation absorption by building walls.

(3) Implementation of tall greenery, subject to the planting of deciduous species resistant to urban conditions, at distances of 27 meters, with a maximum height of 7 meters in the pedestrian movement zone.

Objective: reduction of ambient temperature in the immediate vicinity of trees; reduction of canyon floor insolation, thereby reduction of pavement heating; reduction of development walls insolation reducing the temperature of building facades.

(4) Implementation of bioretention planters, 16 x 2 meters, at distances of 60 meters in the canyons.

Objective: reduction of ambient temperature; modification of surface temperature; intensification of air exchange based on convective movements.

### Diagrams of the proposed adaptation solutions

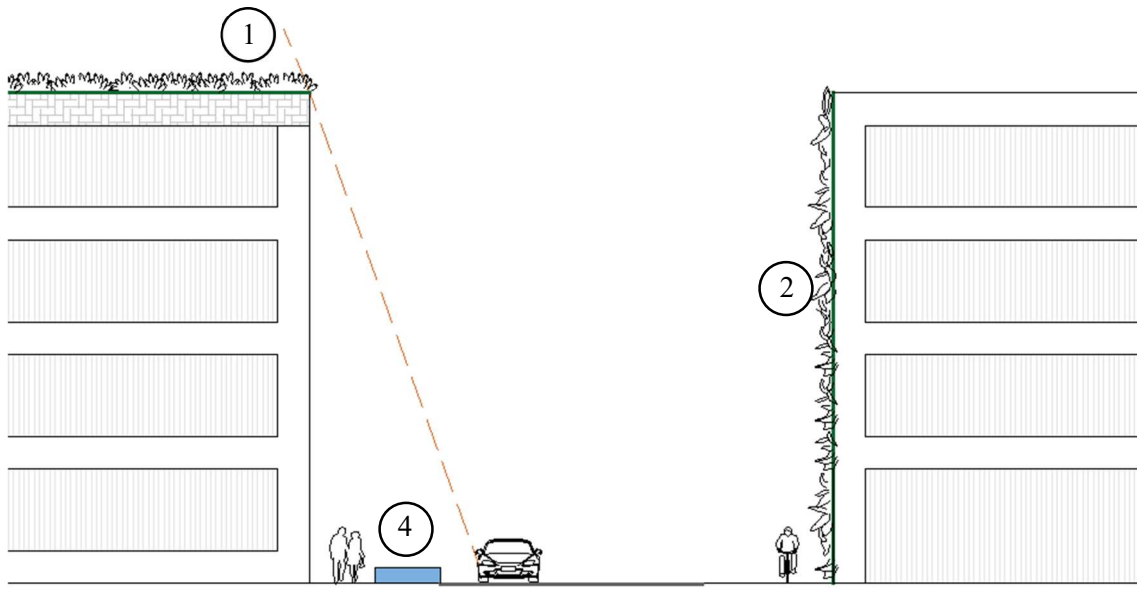


**Figure 9.5.** Adaptation measures in the east-west oriented canyon (1. green roof, 2. green wall, 3. tall greenery, 4. bioretention planter)(source: own elaboration).



**Figure 9.5.** Continuation.

<b>RECOMMENDATION SHEET</b>	
<b>NORTH-SOUTH ORIENTED STREET CANYON</b>	
<b>Guidelines for the implementation of blue-green infrastructure elements</b>	
<p>(1) Implementation of green roofs with a minimum area of at least 40% of roof slope coverage.</p> <p>Objective: reduction of ambient temperature, with the provision that more favorable conditions in the pedestrian movement zone will occur with air inflow perpendicular to the canyon axis; reduction of roof slope temperature.</p>	

(2) Creation of green walls with at least 40% of facade.

Objective: reduction of ambient temperature; reduction of solar radiation absorption by building walls.

(3) Implementation of tall greenery, subject to planting deciduous species resistant to urban conditions, at distances of 42 meters, with a maximum height of 7 meters in the pedestrian movement zone.

Objective: reduction of ambient temperature in the immediate vicinity of trees; reduction of canyon floor insolation, thereby reduction of pavement heating; reduction of development walls insolation reducing the temperature of building facades.

(4) Implementation of bioretention planters, 16 x 2 meters, at distances of 60 meters in the canyons.

Objective: reduction of ambient temperature; modification of pavement temperature; intensification of air exchange based on convective movements.

### Diagrams of the proposed adaptation solutions

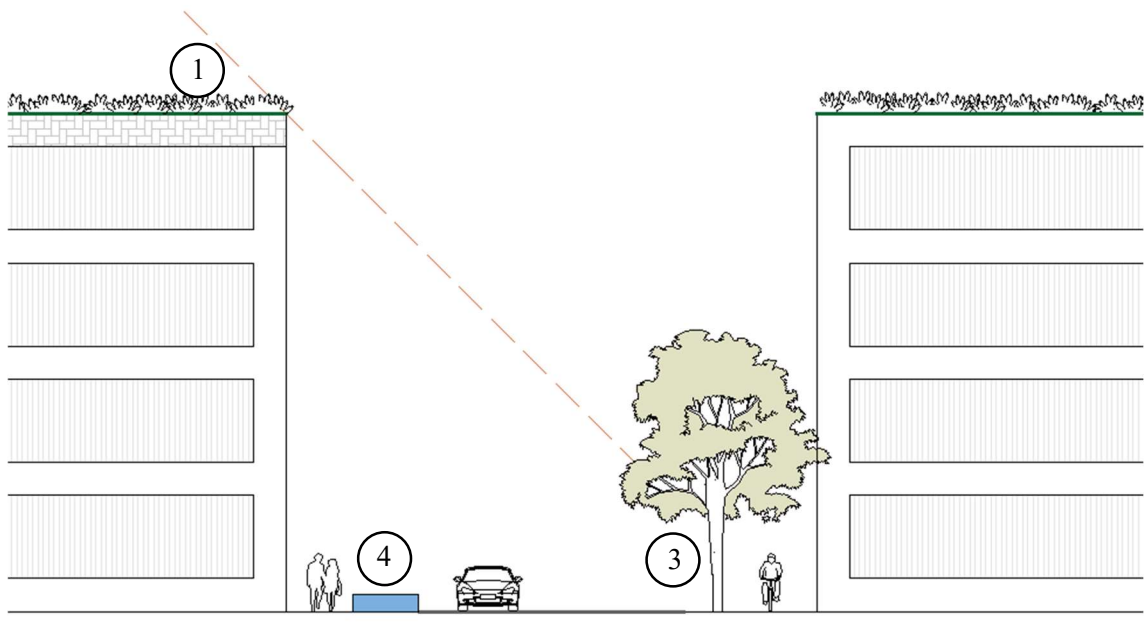


**Figure 9.6.** Adaptation measures in the north-south oriented canyon (1. green roof, 2. green wall, 3. tall greenery, 4. bioretention planter)(source: own elaboration).

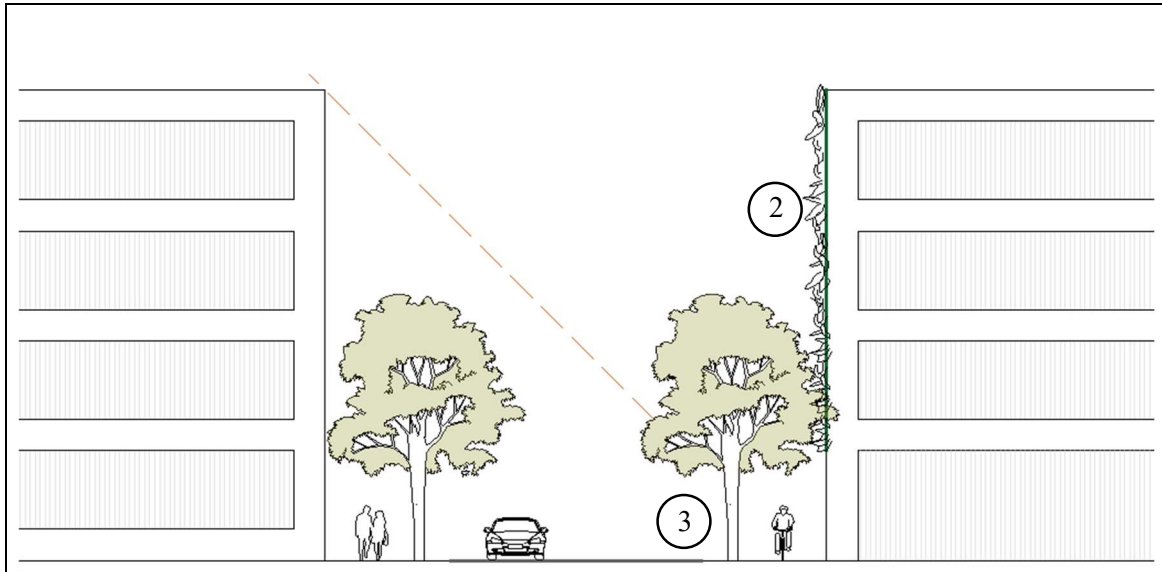
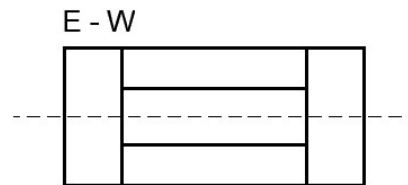


**Figure 9.6.** Continuation.

## RECOMMENDATION SHEET

**EAST-WEST ORIENTED  
URBAN FORECOURT**



### **Guidelines for the implementation of blue-green infrastructure elements**

(1) Implementation of green roofs on urban forecourt front structures.

Objective: reduction of ambient temperature, with the provision that more favorable conditions in the pedestrian movement zone will occur when the air inflow is parallel to the forecourt axis; reduction of roof slope temperature.

(2) Creation of green walls on the northern outbuildings of the urban forecourts.

Objective: reduction of ambient temperature; reduction of solar radiation absorption by building walls.

(3) Implementation of blue infrastructure elements in urban forecourts.

Objective: reduction of ambient temperature; modification of surface temperature; intensification of air exchange based on convective movements.

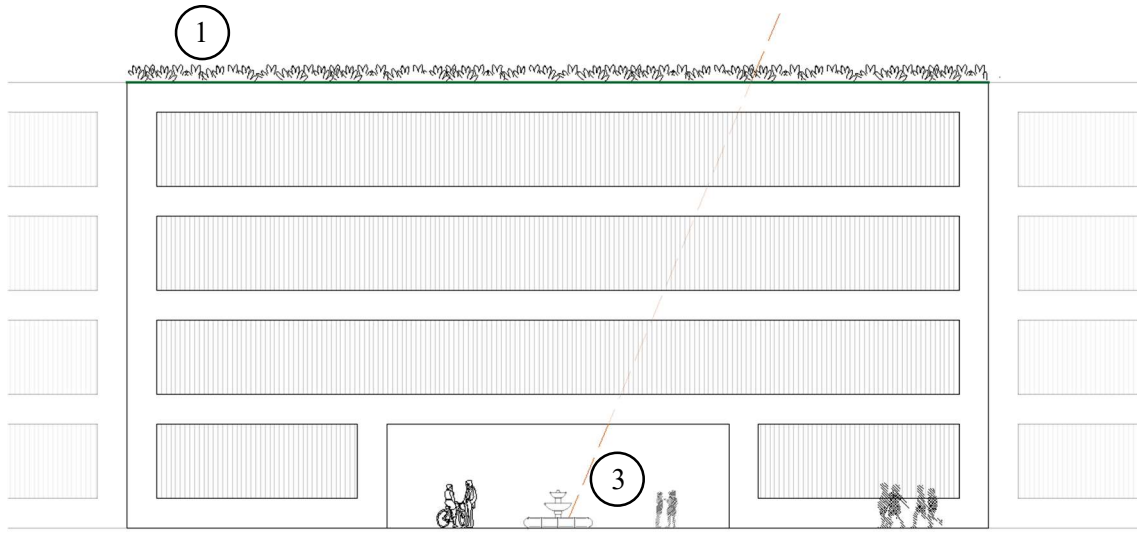


**Figure 9.7.** Adaptation measures - east-west oriented urban forecourt (1. green roof, 3. blue-green infrastructure)(source: own elaboration).

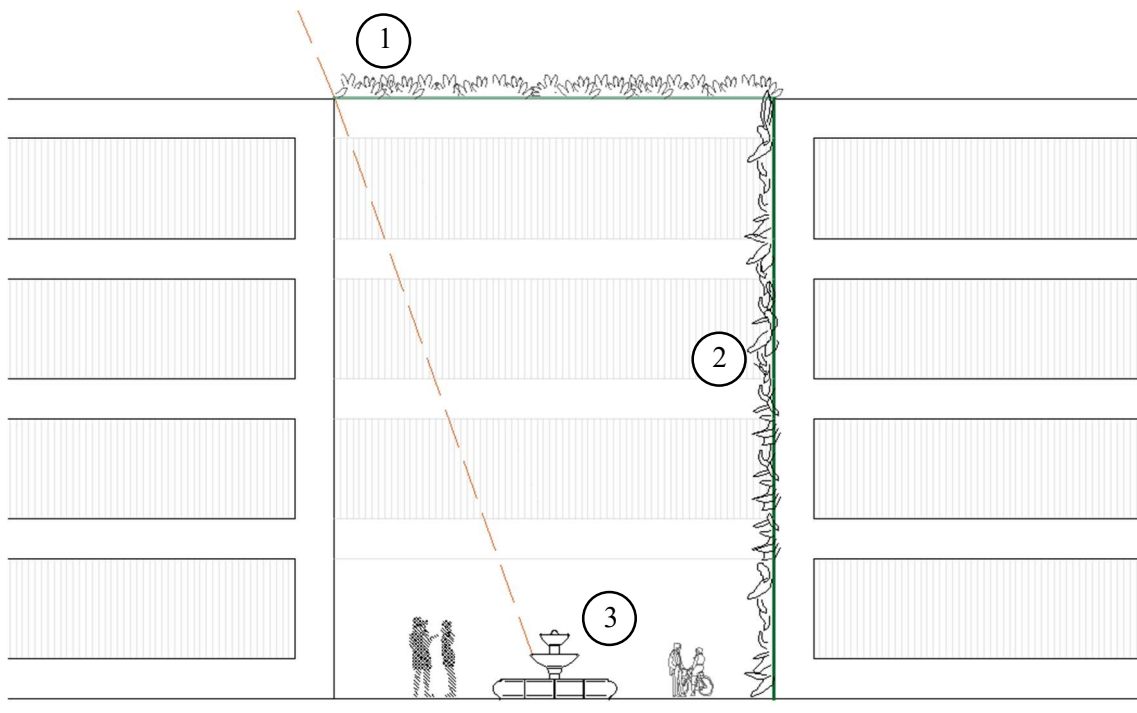
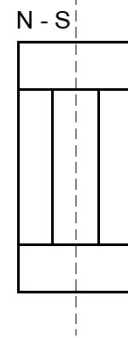


**Figure 9.8.** Adaptation measures - east-west oriented urban forecourt (1. green roof, 2. green wall, 3. blue-green infrastructure)(source: own elaboration).

## RECOMMENDATION SHEET

### NORTH-SOUTH ORIENTED URBAN FORECOURT



#### Guidelines for the implementation of blue-green infrastructure elements

(1) Implementation of green roofs on the urban forecourt front structures.

Objective: reduction of ambient temperature, with the provision that more favorable conditions in the pedestrian movement zone will occur when the air inflow is parallel to the forecourt axis; reduction of roof slope temperature.

(2) Creation of green walls on the eastern outbuildings of the city forecourts.

Objective: reduction of ambient temperature; reduction of solar radiation absorption by building walls.

(3) Implementation of blue infrastructure elements in urban forecourts.

Objective: reduction of ambient temperature; modification of surface temperature; intensification of air exchange based on convective movements.

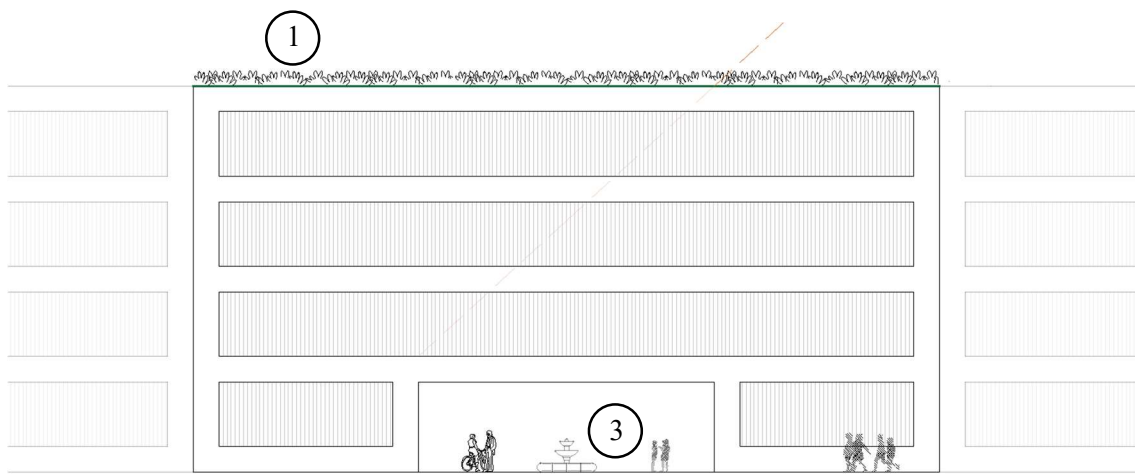
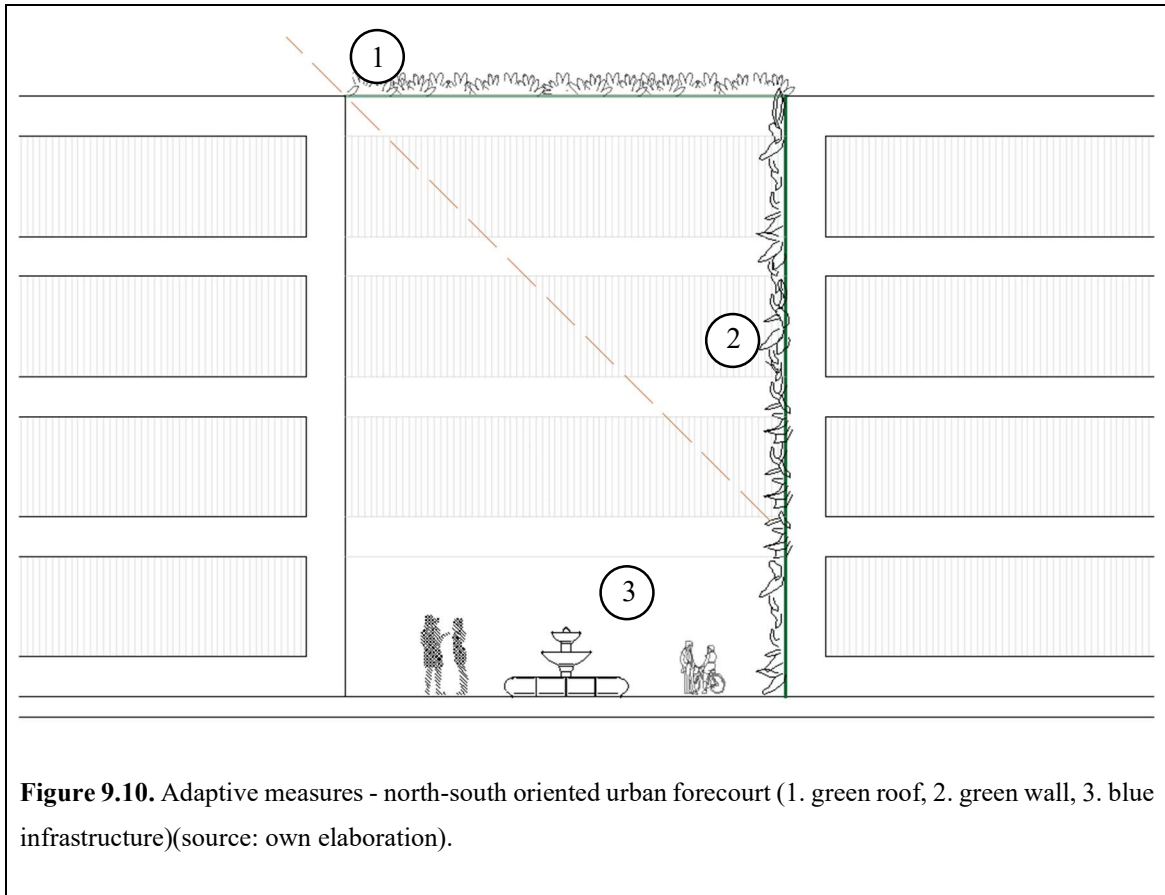


**Figure 9.9.** Adaptive measures - north-south oriented urban forecourt (1. green roof, 3. blue infrastructure)(source: own elaboration).





## ROZDZIAŁ X. CONCLUSIONS AND RECOMMENDATIONS

### 10.1. Conclusions

One of the challenges facing modern cities is the need to adapt to changing climatic conditions. Measures taken in this regard are complex and interdisciplinary. They require a combination of knowledge from the fields of architecture and urban planning, construction, environmental engineering and climatology.

The present paper is part of the current research stream in the field of urban physics and constitutes a kind of “bridge” between scientific research on the influence of urban structures on microclimate and human comfort and practical implementation of adaptation strategies. There are many publications on the possibilities and methods of combating climate change in urban areas. However, it should be noted that the effectiveness of implemented adaptation methods varies greatly and depends on many parameters. The nature of the city, its location, environmental conditions, the layout and type of buildings are just a few of the many elements that determine their effectiveness. Therefore, an in-depth knowledge of the city’s specificity has a key role here.

To address the current problems of cities in adjustment to climate change, an attempt was made to evaluate the effectiveness of selected adaptation strategies such as green walls, green roofs, tree rows, and water elements. The focus was on the Metropolitan Area of Lodz, which is crucial for the city’s identity, constituting its historical core, and at the same time one of the most degraded and in need of revitalization parts of the city. So far, the research carried out in this area has focused mainly on the phenomenon of Urban Heat Island, turbulent air flow and the spread of pollutants. This study may be considered the first to address the issues of the influence of urban structures on microclimate and thermal comfort in the Metropolitan Area of Lodz.

The research thesis assumed the existence of a relationship between the development form and the effectiveness of implemented adaptation strategies. A comprehensive analysis of the experimental and numerical data as well as current state-of-the-art achievements was conducted with the aim of its verification. The analysis allowed to formulate the following general conclusions:

1. In order to assess the complex physical phenomena occurring in urban areas, it is necessary to determine the characteristic development forms for a given area.

This study attempts to characterize the typical development forms in the Metropolitan Area of Lodz. For this purpose, the author proposed her own method based on the use of Geographic Information Systems. At first, information was obtained from the digital databases of state institutions involved in the city's spatial planning (the Surveying Centre). They were used to determine the structure's compactness, percentage of built-up area, side wall area of buildings, building height, Sky View Factor (SVF), and height-to-width ratio (AR). The street canyon and forecourt were considered typical forms found within the Metropolitan Area. Due to the historical nature of the area, it was necessary to obtain additional information from the archives (National Archives, City Conservator Office, and Regional Conservator Office). On their basis, the thickness of building object partitions was determined, and building materials occurring in the Metropolitan Area were characterized. Although this approach is not used in the literature, it was implemented to represent the building structure as close to reality as possible. The result was the creation of geometric models for typical forms - a street canyon and an urban forecourt. The mapping of typical structures of the Metropolitan Area of Lodz taking into account detailed material characteristics was of key importance for the quality of analyses conducted.

2. Analyses of microclimatic conditions can be carried out using numerical simulations. If appropriate initial conditions are adopted, it is possible to evaluate the complex physical processes occurring in the city in a relatively short time. The key issue is the mapping of development structure, as well as determining the input meteorological conditions prevailing in the area.

Based on the author's research, it can be concluded that numerical methods are an alternative to time-consuming field studies. They allow assessing the microclimatic conditions in public spaces. Moreover, they enable to take into account different variants of transformations of urban development structure and to choose an optimal solution at the project stage.

3. In the field of urban climatology it is common practice to use information from meteorological stations as input data in simulation studies. Usually they are located in suburban areas, sometimes a dozen or so kilometers away from the study area. Such approach is undoubtedly advantageous due to easiness of data acquisition, but it is burdened with some errors. It does not take into account the complex relations between the structure of buildings and microclimate. It is particularly important in the case of air flow.

The urban layout structure affects the flow attenuation, which should be taken into account in simulation studies. In order to make the assumed initial conditions correspond with the real anemological conditions, an original method was proposed in this paper, which enables the airflow to be estimated on the basis of information obtained from the nearest meteorological station Lodz-Lublinek. Based on the Simiu relation, the wind speed profile at the inlet of the computational domain was modified.

4. Typical meteorological years, which are a commonly used type of input information for numerical simulations, represent the average microclimatic conditions prevailing in the considered geographical area. They are developed on the basis of long-term measurement data, which are most often obtained from suburban meteorological stations. The compiled dataset, which is publicly available, was created on the basis of information from 1971-2000. This means that the research concerns conditions which have been modified due to ongoing climatic changes. Therefore, the author has developed an updated climate database based on information for 2004-2015, which has been used to assess the effectiveness of selected adaptation strategies implemented in the areas of typical urban forms of the Metropolitan Area of Lodz.
5. The effectiveness of adaptation strategies depends on the climatic zone, spatial management, as well as the implemented solution. Therefore, the main aim of this study was to estimate the impact of selected adaptation strategies on microclimatic conditions and human thermal comfort. Their impact on the street canyon and urban forecourt was considered. Two orientations were taken into account, i.e. east-west and north-south. It was based on the characteristic urban layout of the city (checkerboard plan).

The study showed that the effectiveness of blue-green adaptation strategies varied. The most effective solutions were found to be:

- in canyons with an east-west orientation - (1) high greenery (reduced outdoor air temperature of 0.81°C, floor temperature of 1.81°C, and building wall temperature of 8°C) and (2) bioretention planters (reduced ambient temperature of 2.52°C);
- in canyons with a north-south orientation - (1) high greenery (reduced ambient air temperature - 0.72°C, floor temperature - 2.23°C, and building wall temperature - 8°C), and (2) bioretention planters (0.91°C);
- in urban forecourts with an east-west orientation - (1) green roof (reduced outdoor air temperature - 0.44°C, roof slope temperature - 36°C);

- in urban forecourts with a north-south orientation - green roof (reduced outdoor air temperature - 0.31°C, roof slope temperature - 36°C).

The analyses showed that the key factor was the air flow in the areas of typical building forms of the Metropolitan Area. The wind flow was assumed to be from the eastern sector. Therefore, it was noticed that the impact of adaptation strategies was intensified within the forms with east-west orientation. Accordingly, it can be assumed that properly designed development structure, which will ensure proper air flow, will contribute to the improvement of microclimatic conditions and thermal comfort in highly urbanized areas.

6. The final stage was to investigate the impact of green roofs and living facades on the indoor thermal conditions of buildings. The study evaluated adaptive strategies implemented on existing as well as modernized buildings. The effectiveness of selected solutions was dependent on the construction of building envelope. In case of existing buildings, which were not insulated, the reduction of comfort index, which was the operative temperature, was on the level of 0.28°C (Green Roof scenario), 2.41°C (Green Wall scenario). The adaptation of natural strategies on modernized buildings, adapted to current legal requirements, had a lower effectiveness (0.05°C (Green Roof scenario), 0.70°C (Green Wall scenario)).

The research results allow to formulate a conclusion that the assumed **research thesis has been verified in a positive way**. The research procedure provided an opportunity to assess the effectiveness of adaptation strategies in the specific development systems of the Metropolitan Area of Lodz. As a result, the assumed application objective was achieved. Recommendation cards were developed as planning guidelines for the most effective adaptation solutions.

This study can be used in the decision-making processes, i.e. creation of municipal climate change adaptation plans, revitalization programs, or local spatial development plans. The recommendations can provide guidance that will contribute to the improvement of the quality of life of people living in cities.

## **10.2. Recommendations for future research**

In order to advance the current knowledge, and to support and facilitate the urban planners and municipal authorities application of adaptation strategies the following recommendations may be put forward:

- It is advisable to conduct detailed studies on the influence of different plant species on the microclimate modification in specific seasons. These would include both real-scale measurements (for existing solutions) and laboratory studies to determine physical parameters of plants such as: Leaf Area Index, emissivity/reflectivity of foliage, stomatal resistance. The analyses results would allow to develop a catalog of plants adapted to specific urban conditions (resistant to soil and air pollution, with low soil and humidity requirements, low allergenic potential). This would contribute to the modification of solutions currently available in the Envi-met software database.
- Include the impact of air pollution in adaptation measures. Determination of the effectiveness of selected solutions with respect to immission reduction.
- Identification of local climate zones within the city. Delineate areas with similar physical characteristics, such as terrain roughness class, development structure compactness, percentage of impervious surface, biologically active area, or albedo of building materials. For such separated zones basic microclimate parameters should be determined. These parameters could be then used to calculate correction coefficients allowing modification of data from measurement stations. This would result in taking into account conditions similar to the real ones.
- Further research on the human body's response to thermal and wind discomfort conditions involving measurements and interviews with space users is indicated. As previous studies have shown, geosocial factors related to the adaptation level to climatic conditions have a very significant impact on human comfort in the outdoor environment. Even within European cities, variation in the perception of similar thermal conditions has been found. Therefore, it is important to identify the residents' actual perceptions of a particular city.
- According to the author's research, air flow significantly influences the effectiveness of adaptation solutions. Therefore, for zones with complex development structures, additional airflow analyses should be conducted using numerical simulations or wind tunnel.
- Due to the fact that the effectiveness of adaptation solutions depends on many factors, it would be interesting to use multi-criteria optimization aiming to determine the optimal adaptation strategy for a specific urban space.

## LITERATURE

### *Publications*

1. Auliciems A. *Human Bioclimatology: An Introduction*. A. Auliciems [in:] *Human Bioclimatology: Advances in Bioclimatology*. Springer: Berlin, Germany, 1998.
2. Barden H. *Simulationsmodell für den Wasser-, Energie-, und Stoffhaushalt in Pflanzenbeständen*. Leibniz Universität Hannover Institut für Meteorologie und Klimatologie: Hannover, Germany, 1982.
3. Bruse M. *Development of a microscale model for a calculation of surface temperature in structured terrain*. Institute for Geography, University of Bochum: Bochum, Germany, 1995.
4. Fanger P. O. *Thermal comfort*. Danish Technical Press: Copenhagen, Denmark, 1970.
5. Flaga A. *Inżynieria wiatrowa. Podstawy i zastosowania*. Arkady: Warsaw, Poland, 2008. ISBN: 9788321345260.
6. Hegger M., Fuchs M., Stark T., Zeumer M. *Energy Manual, Sustainable Architecture*. Birkhauser, Basel-Boston-Berlin, 2008. ISBN: 978-3-7643-8764-8.
7. Huttner S. *Further development and application of the 3D microclimate simulation ENVI-met*. Johan Gutenberg University of Mainz: Mainz, Germany, 2012.
8. Huttner S., Bruse M., Dostal P. *Using ENVI-met to simulate the impact of global warming on the microclimate in central European cities*. Mayer H., Matzarakis A. [in:] *Berichte des Meteorologischen Instituts der Albert-Ludwigs-Universität*: Freiburg, Germany, 2008.
9. Iwaszuk E., Rudik G., Duin L., Mederake L., McKenna D., Naumann S., Wagner I. *Błękitno-zielona infrastruktura dla łagodzenia zmian klimatu w miastach*. Ecologic Institute & Fundacja Sendzimira: Berlin-Cracow, Germany-Poland 2019. ISBN 978-83-62168-11-8.
10. Jacobs C. M. J. *Direct Impact of atmospheric CO2 enrichment in regional transpiration*. Wageningen Agricultural University: Wageningen, the Netherlands, 1994.
11. Kicińska B., Wawer J. *Wpływ urbanizacji na warunki klimatyczne w Warszawie*. Błażejczyk K. [in:] *Klimat Warszawy i miejscowości strefy podmiejskiej*. University of Warsaw Press: Warsaw, Poland 2010. ISBN 978-83-89502-09-4.
12. Klemm K. *Kompleksowa ocena warunków mikroklimatu w luźnych i zwartych strukturach urbanistycznych*. Polish Academy of Sciences: Warsaw, Poland 2011. ISBN 978-83-89687-66-1.

13. Kłysik K. *Spatial structure of the urban heat island in Łódź*. Folia Geographica Physica. Acta Universitatis Lodziensis 1998, 3, 385-391.
14. Laskowski L. *Wybrane zagadnienia fizyki miasta*. Central Information Center for Construction: Warsaw, Poland 1987.
15. Lewińska J. *Klimat miasta, zasoby, zagrożenia, kształtowanie*. Institute of Spatial and Communal Management: Cracow, Poland 2000. ISBN: 978-8-3868-4795-2.
16. Oke T. R. *Boundary Layer Climates*. Taylor & Francis: New York, United States of America 1987. ISBN 0-203-40721-0.
17. Parsons K. *Human thermal environments. The effects of hot, moderate and cold environments on human health, comfort and performance*. Taylor & Francis: London and New York, 2003.
18. Santamouris M. *Appropriate material for the urban environment*. M. Santamouris (ed.) in: *Energy and Climate in the Urban Environment*, James & James (Science) Publishers Ltd, London, England 2000, 160-182.
19. Sikora S. *Bioklimat Wrocławia*. Scientific Dissertations of the Institute of Geography and Regional Development of the University of Lodz: Wrocław, Polska, 2008.
20. Toudert F. A. *Dependence of Outdoor Thermal Comfort on Street Design in Hot and Dry Climate*. University of Freiburg: Freiburg, Germany, 2005.
21. Zielonko-Jung K. *Kształtowanie przestrzenne architektury ekologicznej w strukturze miasta*. Scientific Works of the Warsaw University of Technology. Architecture Series: Warsaw, Poland 2013. ISSN 1896-1630.
22. Żurański J. A. *Wpływ warunków klimatycznych i terenowych na obciążenie wiatrem konstrukcji budowlanych*. Scientific Work of the Building Research Institute: Warsaw, Poland 2005.

#### *Scientific Journals*

1. Abdelmonem M. G., Mushatat S., Ibrahim R. I. *The Role of Urban Pattern Indicators for Sustainable Urban Forms in the Developed Countries. A Pragmatic Evaluation of Two Sustainable Urban Contexts*. Journal for Engineering Sciences 2019, 6(2), 65-75.
2. Aboelata A., Sadoudi S. *Evaluating the effect of trees on UHI mitigation and reduction of energy usage in different built up areas in Cairo*. Building and Environment 2020, 168, 1-13.



3. Acero J. A., Herranz-Pascual K. *A comparison of thermal comfort conditions in four urban spaces by means of measurements and modelling techniques*. Building and Environment 2015, 93, 245-257.
4. Acero J. A., Koh E. J. Y., Li X. X., Ruefenacht L. A., Pignatta G., Norford L. K. *Thermal impact of the orientation and height of vertical greenery on pedestrian in a tropical area*. Building Simulation 2019, 12, 973-984.
5. Asaeda T., Ca V. T. *The subsurface transport of heat and moisture and its effects on the environment: a numerical model*. Boundary-Layer Meteorology 1993, 65, 159-179.
6. Akbari H., Cartalis C., Kolokotsa D., Muscio A., Pisello A. L., Rossi F., Santamouris M., Synnefa A., Wong N. H., Zinzi M. *Local Climate Change and Urban Heat Island Mitigation Techniques - The State of the Art*. Journal of Civil Engineering and Management 2016, 22(1), 1-16.
7. Akbari H., Pomerantz M., Taha H. *Cool surfaces and shade trees to reduce energy use and improve air quality in urban areas*. Solar Energy 2001, 70(3), 295-310.
8. Alexandri E., Johnes P. *Temperature decreases in an urban canyon due to green walls and roofs in diverse climates*. Building and Environment 2008, 43(4), 480-493.
9. Aljawabra F., Nikolopoulou M. *The influence of hot arid climate on the use of outdoor urban spaces and thermal comfort: do cultural and social backgrounds matter?*. Intel technology journal 2010, 2(3), 1-20.
10. Arsenović D., Savić S., Lužanin Z., Radić I., Milošević D., Arsić M. *Heat-related Mortality as an Indicator of Population Vulnerability in a Mid-sized Central European City (Novi Sad, Serbia, summer 2015)*. Geographica Pannonica 2019, 23(4), 204-215.
11. Assimakopoulos M. N., De Masi R. F., Rossi F., Papadaki D., Ruggiero S. *Green Wall Design Approach Towards Energy Performance and Indoor Comfort Improvement: A Case Study in Athens*. Sustainability 2020, 12(3772), [1-23].
12. Ayyad Y. N., Sharples S. *Envi-MET validation and sensitivity analysis using field measurements in a hot arid climate*. IOP Conference Series: Earth and Environmental Science 2019, 329(012040), [1-9].
13. Bahi H., Rhinane H., Bensalmia A., Fehrenbach U., Scherer D. *Effects of Urbanization and Seasonal Cycle on the Surface Urban Heat Island Patterns in the Coastal Growing Cities: A Case Study of Casablanca, Morocco*. Remote Sensing 2016, 8, 829.
14. Battista, G., Basilicata, C., Mauri, L. *Green Roof Effects in a Case Study of Rome (Italy)*. Energy Procedia 2016, 101, 1058-1063.

15. Bauer T. *Interaction of Urban Heat Island Effects and Land - Sea Breezes during a New York City Heat Event*. Journal of Applied Meteorology and Climatology 2020, 59, 477-495.
16. Becker S., Potchter O., Yaakov Y. *Calculated and observed human thermal sensation in an extremely hot and dry climate*. Energy and Buildings 2003, 35, 747-756.
17. Bernard J., Bocher E., Gwendall P., Palominos S. *Sky View Factor Calculation in Urban Context: Computational Performance and Accuracy Analysis of Two Open and Free GIS Tools*. Climate, 2018, 6(3), [1-24].
18. Błażejczyk K., Broede P., Fiala D., Havenith G., Holmér I., Jendritzky G., Kampmann B., Kunert A. *Nowy wskaźnik oceny warunków klimatoterapii uzdrowiskowej (UTCI)*. Balneologia Polska 2009, 4(188), 313-321.
19. Bruse M., Flerer H. *Simulating surface-plant-air interactions inside urban environments with a three dimensional numerical model*. Environmental Modelling and Software 1998, 13(3-4), 373-384.
20. Businger J. A., Wyngaard J. C., Izumi Y., Bradley E. F. *Flux-Profile relationships in the atmospheric surface layer*. Journal of the Atmospheric Sciences 1971, 28(2), 181-189.
21. Chatzidimitriou A., Yannas S. *Microclimate development in open urban spaces: The influence of form and materials*. Energy and Buildings 2015, 108, 156-174.
22. Chen L., Wen Y., Zhang L., Xiang W. N. *Studies of thermal comfort and space use in an urban park square in cool and cold seasons in Shanghai*. Building and Environment 2015, 94, 644-653.
23. Clapp R. B., Hornberger G. *Empirical equations for some soil hydraulic properties*. Water Resource Research 1978, 14(4), 601-604.
24. Coccolo S., Kampf J., Scartezzini J. L., Pearlmutter D. *Outdoor human comfort and thermal stress : A comprehensive review on models and standards*. Urban Climate 2016, 18, 33-57.
25. Cohen P., Potchter O., Matzarakis A. *Human thermal perception of Coastal Mediterranean outdoor urban environments*. Applied Geography 2013, 37, 1-10.
26. Crawley D. B. *Which Weather Data Should You Use for Energy Simulations of Commercial Buildings?*. ASHRAE Transactions 1998, 2, 1-18.
27. Da Silva F. T., De Alvarez C. E. *An integrated approach for ventilation's assessment on outdoor thermal comfort*. Building and Environment 2015, 87, 59-71.

28. Darbani E. S., Parapari D. M., Boland J., Sharifi E. *Impacts of urban form and urban heat island on the outdoor thermal comfort: a pilot study on Mashhad*. International Journal of Biometeorology 2021, 65, 1101-1117.
29. De B., Mukherjee M. *Optimisation of canyon orientation and aspect ratio in warm-humid climate: Case of Rajarhat Newtown, India*. Urban Climate 2018, 24, 887-920.
30. Deardorff R. W. *Efficient prediction of ground surface temperature and moisture with inclusion of a layer of vegetation*. Journal of Geophysical Research 1987, 83, 1189-1903.
31. Deng J., Wong N. H. *Impact of urban canyon geometries on outdoor thermal comfort in central business districts*. Sustainable Cities and Society 2020, 53(101966), [1-18].
32. Dian C., Pongrácz R., Dezső Z., Bartholy J. *Annual and monthly analysis of surface urban heat island intensity with respect to the local climate zones in Budapest*. Urban Climate 2020, 31(100573), [1-16].
33. Djedjig R., Bozonnet E., Belarbi R. *Integration of a green envelope model in a transient building*. In Proceedings of the 13th Conference of International Building Performance Simulation Association, Chambéry, France, 26-28 August 2013.
34. Duarte D. H. S., Shinzato P., Santos Gusson C., Abrahão Alves C. *The impact of vegetation on urban microclimate to counterbalance built density in a subtropical changing climate*. Urban Climate 2015, 14, 224-239.
35. Eliasson I., Knez I., Westerberg U., Thorsson S., Lindberg F. *Climate and behaviour in a Nordic city*. Landscape and Urban Planning 2007, 82, 72-84.
36. Elnabawi M. H., Hamza N., Dudek S. *Thermal perception of outdoor urban spaces in the hot arid region of Cairo, Egypt*. Sustainable Cities and Society 2016, 22, 136-145.
37. Eludoyin O. M., Adelekan I. O. *The physiologic climate of Nigeria*. International Journal of Biometeorology, 2013, 57(2), 241-264.
38. Equere V., Mirzaei P. A., Riffat S. *Definition of a new morphological parameter to improve prediction of urban heat island*. Sustainable Cities and Society 2020, 56, 1-18.
39. Eumorfopoulou E., Aravantinos D. *The contribution of a planted roof to the thermal protection of buildings in Greece*. Energy and Buildings 1998, 27, 29-36.
40. Fang Z., Lin Z., Mak C. M., Niu J., Tse K. *Investigation into sensitivities of factors in outdoor thermal comfort indices*. Building and Environment 2018, 128, 129-142.
41. Fanger P. O. *Assessment of man's thermal comfort in practice*. British Journal of Industrial Medicine 1973, 30(4), 313-24.

42. Ferrari A., Kubilay A., Derome D., Carmeliet J. *The use of permeable and reflective pavements as a potential strategy for urban heat island mitigation*. Urban Climate 2020, 31(100534), [1-25].
43. Fischereit J., Schlünzen K. H. *Evaluation of thermal indices for their applicability in obstacle-resolving meteorology models*. International Journal of Biometeorology 2018, 62, 1887-1900.
44. Forouzandeh A. *Numerical modeling validation for the microclimate thermal condition of semi-closed courtyard spaces between buildings*. Sustainable Cities and Society 2018, 36, 327-345.
45. Fortuniak K., Pawlak W., Podstawczyńska A., Siedlecki M., Wibig J., Wilk S. *Łódzkie Badania Klimatu Miasta*. Acta Geographica Lodzensis 2019, 108, 35-49.
46. Freitas C. R., Grigorieva E. A. *A comparison and appraisal of a comprehensive range of human thermal climate indices*. International Journal of Biometeorology 2017, 61, 487-512.
47. Gargari C., Bibbiani C., Fantozzi F., Campiotti C. A. *Simulation of the thermal behaviour of a building retrofitted with a green roof: optimization of energy efficiency with reference to Italian climatic zones*. Agriculture and Agricultural Science Procedia 2016, 8, 628-636.
48. Geletič J., Lehnert M., Savić S., Milošević D. *Inter-/intra-zonal seasonal variability of the surface urban heat island based on local climate zones in three central European cities*. Building and Environment 2019, 156, 21-32.
49. Ghaffarianhoseini A., Berardi U., Ghaffarianhoseini A. *Thermal performance characteristics of unshaded courtyards in hot and humid climates*. Building and Environment 2015, 87, 154-168.
50. Giuseppe E., Ulpiani G., Cancellieri C., Perna C., D'Orazio M., Zinzi M. *Numerical modelling and experimental validation of the microclimatic impacts of water mist cooling in urban areas*. Energy and Buildings 2021, 231(110638), [1-17].
51. Goggins W. B., Chan E. Y. Y., Ng E., Ren C., Chen L. *Effect Modification of the Association between Short-term Meteorological Factors and Mortality by Urban Heat Islands in Hong Kong*. PLoS ONE 2012, 7(6), [1-7].
52. Grudzińska M., Jakusik E. *Typowy Rok Meteorologiczny i późniejsze dane klimatyczne jako czynniki kształtujące zapotrzebowanie na energię*. The Construction Review 2016, 3, 44-50.

53. Hamada, S., Ohta, T. *Seasonal variations in the cooling effect of urban green areas on surrounding urban areas*. Urban Forestry & Urban Greening 2010, 9(1), 15-24.
54. Hart M. A., Sailor D. J. *Quantifying the influence of land-use and surface characteristics on spatial variability in the urban heat island*. Theoretical and Applied Climatology 2009, 95, 397-406.
55. Hashim N. H. M., Tan K. W., Ling Y. *Determination of Thermal Comfort for Social Impact Assessment: Case Study in Kota Damansara, Selangor, Malaysia*. American Journal of Applied Sciences 2016, 13(11), 1156-1170.
56. Hathway E. A., Sharples S. *The interaction of rivers and urban form in mitigating the Urban Heat Island effect: a UK case study*. Building and Environment 2012, 58, 14-22.
57. Hedquist B. C., Brazel A. J. *Seasonal variability of temperatures and outdoor human comfort in Phoenix, Arizona, U.S.A*. Building and Environment 2014, 72, 377-388.
58. Herath H. M. P. I. K., Halwatura R. U., Jayasinghe G. Y. *Evaluation of green infrastructure effects on tropical Sri Lankan urban context as an urban heat island adaptation strategy*. Urban Forestry & Urban Greening 2018, 29, 212-222.
59. Hess M., Leśniak B., Olecki Z., Rauczyńska-Olecka D. *Wpływ krakowskiej aglomeracji miejsko-przemysłowej na promieniowanie słoneczne dochodzące do powierzchni Ziemi*. Scientific Journals of the Jagiellonian University. Geographical Research 1980, 51, 7-73.
60. Hien W. N., Ignatius M., Eliza A., Jusuf S. K., Samsudin R. *Comparison of STEVE and ENVI-met as temperature prediction models for Singapore context*. International Journal of Sustainable Building Technology and Urban Development 2012, 3, 197-209.
61. Hirashima S. Q. S., De Assis E. S., Nikolopoulou M. *Daytime thermal comfort in urban spaces: A field study in Brazil*. Building and Environment 2016, 107, 245-253.
62. Hoelscher M., Nehls T., Jänicke B., Wessolek G. *Quantifying cooling effects of façade greening: Shading, transpiration and insulation*. Energy and Buildings 2016, 114, 283-290.
63. Hogrefe C., Lynn B., Civerolo K., Ku J. *Simulating changes in regional air pollution over the Eastern United States due to changes in global and regional climate and emissions*. Journal of Geophysical Research Atmospheres 2004, 109(22), 1-13.
64. Hong J., Hong J., Kwon E. E., Yoon D. K. *Temporal dynamics of urban heat island correlated with the socioeconomic development over the past half-century in Seoul, Korea*. Environmental Pollution 2019, 254, 1-9.

65. Höppe P. *The physiological equivalent temperature – a universal index for the biometeorological assessment of the thermal environment*. International Journal of Biometeorology 1999, 43, 71-75.
66. Huang J., Zhou C., Zhuo Y., Xu L., Jiang Y. *Outdoor thermal environments and activities in open space: An experiment study in humid subtropical climates*. Building and Environment 2016, 103, 238-249.
67. Hwang R. L., Lin T. P., Cheng M. J., Lo J. H. *Adaptive comfort model for tree-shaded outdoors in Taiwan*. Building and Environment 2010, 45(8),1873-1879.
68. Jacobs C., Klok L., Bruse M., Cortesão J., Lenzholzer S., Kluck J. *Are urban water bodies really cooling?*. Urban Climate 2020, 32 (100607), [1-14].
69. Jänicke B., Meier F., Hoelscher M. T., Scherer D. *Evaluating the Effects of Façade Greening on Human Bioclimate in a Complex Urban Environment*. Advances in Meteorology 2015, 2015(747259), [1-15].
70. Jendritzky G., Nübler W. *A model analyzing the urban thermal environment in physiologically significant terms*. Meteorology and Atmospheric Physics 1981, 29, 313-326.
71. Jihad A., Tahiri M. *Modeling the urban geometry influence on outdoor thermal comfort in the case of Moroccan microclimate*. Urban Climate 2016, 16, 25-42.
72. Jin H., Shao T., Zhang R. *Effect of water body forms on microclimate of residential district*. Energy Procedia 2017, 134, 256-265.
73. Karimi Afshar N., Karimian Z., Doostan R., Habibi Nokhandan M. *Influence of planting designs on winter thermal comfort in an urban park*. Journal of Environmental Engineering and Landscape Management 2018, 26(3), 232-240.
74. Kántor N. *Differences between the evaluation of thermal environment in shaded and sunny position*. Hungarian Geographical Bulletin 2016, 65, 139-153.
75. Kántor N., Egerhazi L., Unger J. *Subjective estimation of thermal environment in recreational urban spaces - part I: investigations in Szeged, Hungary*. International Journal of Biometeorology 2012, 56, 1075-88.
76. Kántor N., Unger J., Gulyas A. *Human bioclimatology evaluation with objective and subjective approaches on the thermal conditions of a square*. Acta Climatologica et Chorologica 2007, 40, 47-58.
77. Ketterer C., Matzarakis A. *Comparison of different methods for the assessment of the urban heat island in Stuttgart, Germany*. International Journal of Biometeorology 2015, 59(9), 1299-1309.

78. Khotbehsara E. M., Daemei A. B., Malekjahan F. A. *Simulation study of the eco green roof in order to reduce heat transfer in four different climatic zones*. Results in Engineering 2019, 2(100010), [1-8].
79. Knez I., Thorsson S. *Influences of culture and environmental attitude on thermal, emotional and perceptual evaluations of a public square*. International Journal of Biometeorology 2006, 50(5), 258-68.
80. Knowlton K., Rosenthal J. E., Hogrefe C., Lynn B. *Assessing Ozon-related Health Impacts Under a Changing Climate*. Environmental Health Perspectives 2004, 112(15), 1557-1563.
81. Kotharkar R., Ramesh A., Bagade, A. *Urban Heat Island studies in South Asia: A critical review*. Urban Climate 2018, 24, 1011-1026.
82. Kováts R. S., Hajat S. *Heat Stress and Public Health: A Critical Review*. Annual Review of Public Health 2008, 29(1), 41-55.
83. Kovács A., Unger J., Gál C. V., Kántor N. *Adjustment of the thermal component of two tourism climatological assessment tools using thermal perception and preference surveys from Hungary*. Theoretical and Applied Climatology 2016, 125, 113-130.
84. Köhler M., Kaiser D. *Evidence of the Climate Mitigation Effect of Green Roofs - A 20-Year Weather Study on an Extensive Green Roof (EGR) in Northeast Germany*. Buildings 2019, 9(7), 157, [1-18].
85. Krüger E., Minella F., Matzarakis A. *Comparison of different methods of estimating the mean radiant temperature in outdoor thermal comfort studies*. International Journal of Biometeorology 2014, 58(8), 1727-1737.
86. Krüger E. L., Tamura C. A., Bröde P., Schweiker M., Wagner A. *Short- and long-term acclimatization in outdoor spaces: Exposure time, seasonal and heatwave adaptation effects*. Building and Environment 2017, 116, 17-29.
87. Kumar V. *Modelling and simulation of the thermal performance of a passive roof*. International Journal of Mechanical Engineering and Technology (IJMET) 2017, 8(6), 510-516.
88. Lai D., Zhou C., Huang J., Jiang Y., Long Z., Chen Q. *Outdoor space quality: A field study in an urban residential community in central China*. Energy and Buildings 2014, 68, 713-720.
89. Lam C. K. C., Loughnan M., Tapper N. *Visitors' perception of thermal comfort during extreme heat events at the Royal Botanic Garden Melbourne*. International Journal of Biometeorology 2018, 62, 97-112.

90. Launder B., Spalding D. B. *The numerical computation of turbulent flow*. Computer Methods in Applied Mechanics and Engineering 1974, 3, 269-289.
91. Lee H., Mayer H. *Solar elevation impact of the heat stress mitigation of pedestrians on tree-lined sidewalks of E-W street canyons - Analysis under Central European heat wave conditions*. Urban Forestry & Urban Greening 2021, 58(126905), [1-12].
92. Lee H., Mayer H. *Validation of the mean radiant temperature simulated by the RayMan software in urban environments*. International Journal of Biometeorology 2016, 60, 1775-1785.
93. Lee H., Mayer H., Chen L. *Contribution of trees and grasslands to the mitigation of human heat stress in a residential district of Freiburg, Southwest Germany*. Landscape and Urban Planning 2016, 148, 37-50.
94. Lenzholer S., Kohl J. *Immersed in microclimatic space: Microclimate experience and perception of spatial configuration in Dutch squares*. Landscape and Urban Planning 2010, 95(1-2), 1-15.
95. Li K., Zhang Y., Zhao L. *Outdoor thermal comfort and activities in the urban residential community in a humid subtropical area of China*. Energy and Buildings 2016, 133, 498-511.
96. Li Z., Chow D. H. C., Yao J., Zheng X., Zhao W. *The effectiveness of adding horizontal greening and vertical greening to courtyard areas of existing buildings in the hot summer cold winter region of China: A case study for Ningbo*. Energy and Buildings 2019, 196, 227-239.
97. Lin T. P. *Thermal perception, adaptation and attendance in a public square in hot and humid regions*. Building and Environment 2009, 44, 2017-2026.
98. Lin T., Dear R., Hwang R. *Effect of thermal adaptation on seasonal outdoor thermal comfort*. International Journal of Climatology 2011, 31, 302-312.
99. Lin T. P., Matzarakis A. *Tourism climate and thermal comfort in Sun Moon Lake, Taiwan*. International Journal of Biometeorology 2008, 52, 281-290.
100. Lin T. P., Yang S. R., Matzarakis A. *Customized rating assessment of climate suitability (CRACS): climate satisfaction evaluation based on subjective perception*. International Journal of Biometeorology 2015, 59(12), 1825-1837.
101. Lis A. *Temperatura ekwiwalentna i operatywna w ocenie środowiska wnetrz*. Scientific Journals of the Częstochowa University of Technology. Civil Engineering 2015, 21(171), 183-189.



102. Liu J., Chen J. M., Black T. A., Novak M. D. *E-ε modelling of turbulent air flow downwind of a model forest edge*. *Boundary-Layer Meteorology* 1996, 77, 21-44.
103. Liu W., Zhang Y., Deng Q. *The effects of urban microclimate on outdoor thermal sensation and neutral temperature in hot-summer and cold-winter climate*. *Energy and Buildings* 2016, 128, 190-197.
104. Liu Z., Cheng W., Jim C. Y., Morakinyo T. E., Shi Y., Ng E. *Heat mitigation benefits of urban green and blue infrastructures: A systematic review of modeling techniques, validation and scenario simulation in ENVI-met V4*. *Building and Environment* 2021, 200(107939), [1-15].
105. Louafi S., Abdou S., Reiter S. *Effect of vegetation cover on thermal and visual comfort of pedestrians in urban spaces in hot and dry climate*. *Nature and Technology* 2017, 17, 30-41.
106. Mabdeh S., Al Radaideh T., Hiyari M. *Enhancing thermal comfort of residential buildings through dual functional passive system (solar-wall)*. *Journal of Green Building* 2020, 16(2), 139-161.
107. Mahmoud A. H. A. *Analysis of the microclimatic and human comfort conditions in an urban park in hot and arid regions*. *Building and Environment* 2011, 46, 2641-2656.
108. Makaremi N., Salleh E., Jaafar M. Z., Ghaffarian Hoseini A. *Thermal comfort conditions of shaded outdoor spaces in hot and humid climate of Malaysia*. *Building and Environment* 2012, 48, 7-14.
109. Maras I., Schmidt T., Paas B., Ziefle M., Schneider C. *The impact of human-biometeorological factors on perceived thermal comfort in urban public places*. *Meteorologische Zeitschrift* 2016, 25, 407-420.
110. Martilli A., Krayenhoff S., Nazarian N. *Is the Urban Heat Island intensity relevant for heat mitigation studies?* *Urban Climate* 2020, 31(100541), [1-4].
111. Martinelli L., Matzarakis A. *Influence of height/width proportions on the thermal comfort of courtyard topology for Italian climate zones*. *Sustainable Cities and Society* 2017, 29, 97-106.
112. Mellor G. L., Yamada T. *A simulation of the Wangara atmospheric boundary layer data*. *Journal of the Atmospheric Sciences* 1975, 32, 2309-2329.
113. Metje N., Sterling M., Baker C. J. *Pedestrian comfort using clothing values and body temperatures*. *Journal of Wind Engineering and Industrial Aerodynamics* 2008, 96(4), 412-435.

114. Middel A., Chhetri N., Quay R. *Urban forestry and cool roofs: Assessment of heat mitigation strategies in Phoenix residential neighborhoods*. Urban Forestry & Urban Greening 2015, 14(1), 178-186.
115. Middel A., Häb K., Brazel A. J., Martin C. A., Guhathakurta S. *Impact of urban form and design on mid-afternoon microclimate in Phoenix Local Climate Zones*. Landscape and Urban Planning 2014, 122, 16-28.
116. Middel A., Selover N., Hagen B., Chhetri N. *Impact of shade on outdoor thermal comfort - a seasonal field study in Tempe, Arizona*. International Journal of Biometeorology 2017, 60(12), 1849-1861.
117. Morakinyo T. E., Kalani K. W. D., Dahanayake C., Ng E., Chow C. L. *Temperature and cooling demand reduction by green-roof types in different climates and urban densities: A co-simulation parametric study*. Energy and Buildings 2017, 145(15), 226-237.
118. Morakinyo T. E., Lam Y. F. *Simulation study on the impact of tree-configuration, planting pattern and wind condition on street-canyon's micro-climate and thermal comfort*. Buildings and Environment 2016, 103, 262-275.
119. Narowski P. *Metody wyznaczania typowych lat meteorologicznych TMY2, WYEC2, oraz według normy EN ISO 15927-4*. District heating, Heating, Ventilation 2014, 45(12), 479-485.
120. Nastran M., Kobal M., Eler K. *Urban heat islands in relation to green land use in European cities*. Urban Forestry & Urban Greening 2019, 37, 33-41.
121. Ng E., Chen L., Wang Y., Yuan C. *A study on the cooling effects of greening in a high-density city: An experience from Hong Kong*. Building and Environment 2012, 47, 256-271.
122. Ng E., Cheng V. *Urban human thermal comfort in hot and humid Hong Kong*. Energy and Buildings 2012, 55, 51-65.
123. Niachou A., Papakonstantinou K., Santamouris M., Tsangrassoulis A., Mihalakakou G. *Analysis of the green roof thermal properties and investigation of its energy performance*. Energy and Buildings 2001, 33, 719-729.
124. Nikolopoulou M., Baker N., Steemers K. *Thermal comfort in outdoor urban spaces: understanding the human parameter*. Solar Energy 2001, 70(3), 227-235.
125. Oke T. R. *Canyon geometry and the nocturnal urban heat island. Comparison of scale model and field observations*. Journal of Climatology 1981, 1(3), 237-254.

126. Oliveira S., Andrade H. *An initial assessment of the bioclimatic comfort in an outdoor public space in Lisbon*. International Journal of Biometeorology 2007, 52, 69-84.
127. Ouyang W., Morakinyo T. E., Ren C., Ng E. *The cooling efficiency of variable greenery coverage ratios in different urban densities: A study in subtropical climate*. Building and Environment 2020, 174(106772), [1-13].
128. Pantavou K., Chatzi E., Theoharatos G. *Case study of skin temperature and thermal perception in a hot outdoor environment*. International Journal of Biometeorology 2014, 58, 1163-73.
129. Peng L. L. H., Jim C. Y. *Green-Roof Effects on Neighborhood Microclimate and Human Thermal Sensation*. Energies 2013, 6, 598-618.
130. Pielke R. A. *Mesoscale meteorological modelling*. Academic Press: Orlando, the United States of America, 1984.
131. Potchter O., Cohen P., Lin T., Matzarakis A. *Outdoor human thermal perception in various climates: a comprehensive review of approaches, methods and quantification*. Science of the Total Environment 2018, 631-632, 390-406.
132. Ragab A., Abdelrady A. *Impact of green roofs on energy demand for cooling in Egyptian buildings*. Applied Sciences 2020, 12(14), 1-13.
133. Ragheb A. A., El-Darwish I. I., Ahmed S. *Microclimate and human comfort consideration in planning a historic urban quarter*. International Journal of Sustainable Built Environment 2016, 5(1), 156-167.
134. Ramírez-Aguilar E. A., Souza L. C. L. *Urban form and population density: Influences on Urban Heat Island intensities in Bogotá, Colombia*. Urban Climate 2019, 29(100497), [1-19].
135. Ratti C., Raydan D., Steemers K. *Building form and environmental performance: archetypes, analysis and an arid climate*. Energy and Buildings 2003, 35(1), 49-59.
136. Resler J., Eben K., Geletič J., Krč P., Rosecký M., Sühling M., Belda M., Fuka V., Halenka T., Huszár P., Karlický J., Benešová N., Ďoubalová J., Honzáková K., Keder J., Nápravníková Š., Vlček O. *Validation of the PALM model system 6.0 in real urban environment; case study of Pragu-Djevice, Czech Republic*. Geoscientific Model Development 2020, 14, 4797-4842.
137. Rodríguez L. R., Ramos J. S., de la Flor F. J. S., Domínguez S. A. *Analyzing the urban heat Island: Comprehensive methodology for data gathering and optimal design of mobile transects*. Sustainable Cities and Society 2020, 55(102027), [1-18].

138. Rodríguez-Algeciras J., Tablada A., Chaos-Years M., De la Paz G., Matzarakis A. *Influence of aspect ratio and orientation on large courtyard thermal conditions in the historical centre on Camagüey-Cuba*. *Renewable Energy* 2018, 125, 840-856.
139. Rui L., Buccolieri R., Gao Z., Gatto E., Ding W. *Study of the effect of green quantity and structure on thermal comfort and air quality in an urban-like residential district by ENVI-met modelling*. *Building Simulation* 2019, 12, 183-194.
140. Ruddy M., Scott D. *Bioclimatic comfort and the thermal perceptions and preferences of beach tourists*. *International Journal of Biometeorology* 2015, 59, 37-45.
141. Sailor D. J. *A green roof model for building energy simulation programs*. *Energy and Buildings* 2008, 40, 1466-1478.
142. Saiz S., Kennedy K., Bass B., Pressnail K. *Comparative Life Cycle Assessment of Standard and Green Roofs*. *Environmental Science & Technology* 2006, 40, 4312-4316.
143. Salata F., Golasi I., De Lieto Vollaro R., De Lieto Vollaro A. *Outdoor thermal comfort in the Mediterranean area. A transversal study in Rome, Italy*. *Building and Environment* 2016, 96, 46-61.
144. Salvati A., Roura H. C., Cecere C. *Microclimatic response of urban form in the Mediterranean context*. In *Proceedings of Twenty-Second International Seminar on Urban Form, Rome, Italy, 23-26 September 2015*.
145. Sangkertadi S., Syafriny R. *New equation for estimating outdoor thermal comfort in humid tropical environment*. *European Journal of Sustainable Development Research* 2014, 3(4), 43-52.
146. Scharf B., Kraus F. *Green Roofs and Greenpass*. *Buildings* 2019, 9(205), [1-26].
147. Schnell I., Potchter O., Yaakov Y., Epstein Y., Brener S., Hermesh H. *Urban daily life routines and human exposure to environmental discomfort*. *Environmental monitoring and assessment* 2012, 184, 4575-90.
148. Shaheen A. M. A., Sabry H. M. K., El Dessoqy Faggal A. A. *Double Skin Green Façade in Workplace for Enhancing Thermal Performance in Greater Cairo*. *Engineering Research Journal* 2020, 168, A1-A12.
149. Shahraiyni H. T., Sodoudi S., El-Zafarany A., Seoud T. A., Ashraf H., Krone K. *A Comprehensive Statistical Study on Daytime Surface Urban Heat Island during Summer in Urban Areas, Case Study: Cairo and Its New Towns*. *Remote Sensing* 2016, 8(643), [1-20].
150. Sharifi A. *Resilient urban forms: A review of literature on streets and street networks*. *Building and Environment* 2019, 147, 171-187.

151. Shooshtarian S., Rajagopalan P. *Study of thermal satisfaction in an Australian educational precinct*. Building and Environment 2017, 123, 119-132.
152. Shooshtarian S., Ridley I. *The effect of individual and social environments on the users thermal perceptions of educational urban precincts*. Sustainable Cities and Society 2016, 26, 119-133.
153. Sievers U., Mayer I., Zdunkowski W. G. *Numerische Simulation des urbanen Klimas mit einem zweidimensionalen Modell*. Meteorologische Rundschau 1987, 40, 40-52.
154. Silva H., Fillpot B. S. *Modeling nexus of urban heat island mitigation strategies with electricity/power usage and consumer costs: A case study for Phoenix, Arizona, USA*. Theoretical and Applied Climatology 2018, 131, 661-669.
155. Simiu, E. *Equivalent statistic wind load for tall building design*. In Proceedings of the 4th International Conference on Wind Effects on Buildings and Structures, Heathrow, UK, 8-12 September 1975.
156. Simwanda M., Ranagalage M., Estoque R. C., Murayama Y. *Spatial Analysis of Surface Urban Heat Islands in Four Rapidly Growing African Cities*. Remote Sensing 2019, 11, 1645.
157. Sözen İ., Oral G. K. *Outdoor thermal comfort in urban canyon and courtyard in hot arid climate: A parametric study based on the vernacular settlement of Mardin*. Sustainable Cities and Society 2019, 48(101398), [1-15].
158. Spagnolo J., de Dear R. J. *A Field Study of Thermal Comfort in Outdoor and Semi-Outdoor Environments in Subtropical Sydney Australia*. Building and Environment 203, 38, 721-738.
159. Srivanit M., Hokao K. *Evaluating the cooling effects of greening for improving the outdoor thermal environment at an institutional campus in the summer*. Building and Environment 2013, 66, 158-172.
160. Steeneveld G. J., Koopmans S., Heusinkveld B. G., Theeuwes N. E. *Refreshing the role of open water surfaces on mitigating the maximum urban heat island effect*. Landscape and Urban Planning 2014, 121, 92-96.
161. Stull R. *A convective transport theory for surface fluxes*. Journal of the Atmospheric Sciences 1994, 51(1), 3-22.
162. Sugawara H., Takamura T. *Surface Albedo in Cities: Case Study in Sapporo and Tokyo, Japan*. Boundary-Layer Meteorology 2014, 153, 539-553.

163. Szymanowski M., Kryza M. *Local regression models for spatial interpolation of urban heat island - An example from Wrocław, SW Poland*. Theoretical and Applied Climatology 2012, 108, 53-71.
164. Takács Á., Kiss M., Hof A., Tanács A., Gulyás A., Kántor N. *Microclimate modification by urban shade trees - an integrated approach to aid ecosystem service based decision-making*. Procedia Environmental Sciences 2016, 32, 97-109.
165. Teshnehdel S., Akbari H., Giuseppe E., Brown R. D. *Effect of tree cover and tree species on microclimate and pedestrian comfort in a residential district in Iran*. Building and Environment 2020, 178(106899), [1-12].
166. Thorsson S., Honjo T., Lindberg F., Eliasson I., Lim E. M. *Thermal Comfort and Outdoor Activity in Japanese Urban Public Places*. Environment and Behavior 2007, 39, 660-684.
167. Thorsson S., Lindqvist M., Lindqvist S. *Thermal bioclimatic conditions and patterns of behaviour in an urban park in Goteborg, Sweden*. International Journal of Meteorology 2004, 48(3), 149-156.
168. Tjernström M. *Some tests with a surface energy balance scheme including a bulk parametrization for a vegetation in a mesoscale model*. Boundary-Layer Meteorology 1989, 48(1), 33-68.
169. Tsoka S., Leduc T., Rodler A. *Assessing the effects of urban trees on building cooling energy needs: The role of foliage density and planting pattern*. Sustainable Cities and Society 2021, 65(102633), [1-16].
170. Tung C. H., Chen C. P., Tsai K. T., Kántor N., Hwang R. L., Matzarakis A., Lin T. P. *Outdoor thermal comfort characteristics in the hot and humid region from a gender perspective*. International Journal of Biometeorology 2014, 58, 1927-39.
171. Umezaki A. S., Ribeiro F. N. D., Oliveira A. P., Soares J., Miranda R. M. *Numerical characterization of spatial and temporal evolution of summer urban heat island intensity in São Paulo, Brazil*. Urban Climate 2020, 32, 1-12.
172. Van Hove L. W. A., Jacobs C. M. J., Heusinkveld B. G., Elbers J. A., van Driel B. L., Holtslag A. A. M. *Temporal and spatial variability of urban heat island and thermal comfort within the Rotterdam agglomeration*. Building and Environment 2015, 83, 91-103.
173. Veena K., Parammasivam K. M., Venkatesii T. N. *Urban Heat island studies: Current status in India and a comparison with the International studies*. Journal of Earth System Science 2020, 129(85), 1-15.

174. Völker S., Baumeister H., Classen T., Hornberg C., Kistemann T. *Evidence for the temperature-mitigating capacity of urban blue space - a health geographic perspective*. *Erdkunde* 2013, 67, 355-371.
175. Wang Y., Akbari H. *Effect of Sky View Factor on Outdoor Temperature and Comfort in Montreal*. *Environmental Engineering Science* 2014, 31(6), 272-287.
176. Wang Y., De Groot R., Bakker F., Wörtche H., Leemans R. *Thermal comfort in urban green spaces: a survey on a Dutch university campus*. *International Journal of Biometeorology* 2017, 6, 87-101.
177. Wang W., Zhou W., Ng E. Y. Y., Xu Y. *Urban heat islands in Hong Kong: Statistical modelling and trend detection*. *Natural Hazards* 2016, 83, 885-907.
178. Wieringa J. *Updating the Davenport roughness classification*. *Journal of Wind Engineering and Industrial Aerodynamics* 1992, 41-44, 357-368.
179. Willmott C. J. *On the validation on models*. *Physical Geography* 1981, 2(2), 184-194.
180. Wilson J. D. *A second-order closure model for flow through vegetation*. *Boundary-Layer Meteorology* 1988, 42, 371-392.
181. Wong N. H., Chen Y., Ong C. L., Sia A. *Investigation of thermal benefits of rooftop garden in the tropical environment*. *Energy and Buildings* 2003, 35, 35-364.
182. Wong N. H., Kwang T. A. Y., Chen Y., Sekar Y. K., Tan P. Y., Chan D. *Thermal evaluation of vertical greenery systems for building walls*. *Building and Environment* 2010, 45(3), 663-672.
183. Wu Z., Chen L. *Optimizing the spatial arrangement of trees in residential neighbourhoods for better cooling effects: Integrating modelling with in-situ measurements*. *Landscape and Urban Planning* 2017, 167, 463-472.
184. Wu X., Wang G., Yao R., Wang L., Yu D., Gui X. *Investigating Surface Urban Heat Islands in South America Based on MODIS Data from 2003-2016*. *Remote Sensing* 2019, 11, 1212.
185. Xi T., Li Q., Mochida A., Meng Q. *Study on the outdoor thermal environment and thermal comfort around campus clusters in subtropical urban areas*. *Building and Environment* 2012, 52, 162-170.
186. Yahia M. W., Johansson E. *Urban microclimate and thermal comfort in outdoor spaces in hot dry Damascus*. In *Proceedings of 8th International Conference on Urban Climate (ICUC-8)*, Ireland, Dublin, 6-10 August 2012.

187. Yamada T. *A numerical study of turbulent airflow in and above a forest canopy*. Journal of the Meteorological Society of Japan 1982, 60, 439-454.
188. Yan H., Wu F., Dong L. *Influence of a large urban park on the local urban thermal environment*. Science of The Total Environment 2018, 662-663, 882-891.
189. Yang X., Peng L. L. H., Jiang Z., Chen Y., Yao L., He Y., Xu T. *Impact of urban heat island on energy demand in buildings: Local climate zones in Nanjing*. Applied Energy 2020, 260, 1-13.
190. Yang W., Wong N. H., Jusuf S. K. *Thermal comfort in outdoor urban spaces in Singapore*. Building and Environment 2013, 59, 426-435.
191. Zeng Y., Dong L. *Thermal human biometeorological conditions and subjective thermal sensation in pedestrian streets in Chengdu, China*. International Journal of Biometeorology 2015, 59, 99-108.
192. Zhang L., Deng Z., Liang L., Zhang Y., Meng Q., Wang J., Santamouris M. *Thermal behavior of a vertical green façade and its impact on the indoor and outdoor thermal environment*. Energy and Buildings 2019, 204(109502), [1-14].
193. Zhang Y., Murray A. T., Turner B. L., II. *Optimizing green space locations to reduce daytime and nighttime urban heat island effects in Phoenix, Arizona*. Landscape and Urban Planning 2017, 165, 162-171.
194. Zhao L., Zhou X., Li L., He S., Chen S. *Study on outdoor thermal comfort on a campus in a subtropical urban area in summer*. Sustainable Cities and Society 2016, 22, 164-170.
195. Zhou Z., Chen H., Deng Q., Mochida A. *A Field Study of Thermal Comfort in Outdoor and Semi-outdoor Environments in a Humid Subtropical Climate City*. Journal of Asian Architecture and Building Engineering 2013, 12(1), 73-79.

#### *Legal documents*

1. ASHRAE. *Standard 55 - Thermal environmental conditions for human occupancy*. American Society of Heating, Refrigeration and Air Conditioning Engineers: Atlanta, GA, USA, 2014.
2. *Directive 2002/91/EC of the European Parliament and of the Council of 16 December 2002 on the energy performance of buildings* (Journal of Laws UE L1, 2003).
3. *Directive (EU) 2018/844 of the European Parliament and of the Council of 30 May 2018 amending Directive 2010/31/EU on the energy performance of buildings and Directive*



- 2012/27/EU on energy efficiency (Text with EEA relevance)(Journal of Laws UE L, 2018).
4. Frankenstein S., Koenig G. *Fast all-season soil strength (FASST)*. U.S. Army Engineer Research and Development Center, Cold Regions Research and Engineering Laboratory (ERDC/CRREL), Special Report SR-04-01: Washington, United States of America 2004.
  5. Frankenstein S., Koenig G. *FASST Vegetation Models*. U.S. Army Engineer Research and Development Center, Cold Regions Research and Engineering Laboratory (ERDC/CRREL), Technical Report TR-04-25: Washington, United States of America 2004.
  6. *Green Paper from the Commission to the Council, the European Parliament, the European Economic and Social Committee and the Committee of the Regions - Adapting to climate change in Europe - options for EU action*, 2007.
  7. *Paris Agreement - UN Framework Convention on Climate Change* (Journal of Laws UE L 282, 2016).
  8. *PN-ISO 7726:2001 - Ergonomics of the thermal environment - Instruments for measuring physical quantities*. The Polish Committee for Standardization: Warsaw, Poland, 2001.
  9. *PN-ISO 15927-4:2005 - Hygrothermal performance of buildings - Calculation and presentation of climatic data - Part 4: Hourly data for assessing the annual energy use for heating and cooling*. The Polish Committee for Standardization: Warsaw, Poland, 2005.
  10. *PN-EN ISO 7730:2006 - Ergonomics of the thermal environment - Analytical determination and interpretation of thermal comfort using calculation of the PMV and PPD indices and local thermal comfort criteria*. The Polish Committee for Standardization: Warsaw, Poland, 2006.
  11. *PN-EN ISO 13790:2008 - Energy performance of buildings - Calculation of energy use for space heating and cooling*. The Polish Committee for Standardization: Warsaw, Poland, 2008.
  12. *PN-EN 16798 - 1:2019-06 - Energy performance of buildings - Ventilation of buildings - Part 1: Indoor environment input parameters for design and assessment of energy performance of buildings with respect to indoor air quality, thermal environment, lighting and acoustics - Module M1-6*. The Polish Committee for Standardization: Warsaw, Poland, 2019.

13. *Regulation Of The Minister Of Infrastructure Of 12 April 2002 On Technical Conditions, Which Should Correspond To The Buildings And Their Location* (Journal of Laws 2002, number 75, item 690).
14. *Regulation of 6 November 2008 on the methodology for calculation of energy performance of buildings constituting an independent technical and utilitarian entity, as well as the method of preparation and examples of their energy performance certificates* (Journal of Laws 2008, number 201, item 1240, as amended).
15. *Resolution no. XL/1074/17 of the City Council of Lodz of 11 January 2017 on the Adoption of a Local Spatial Development Plan for Part of the City of Lodz Located in the Area of Włókniarzy Avenue and the Following Streets: Andrzeja Struga and Łąkowa* (the Plan no. 92).
16. *Resolution no. XLVIII/1227/17 of the City Council of Lodz of 10 May 2017 on the Adoption of a Local Spatial Development Plan for Part of the City of Lodz Located in the Area of Marszałka Józefa Piłsudskiego Avenue and the Following Streets: Piotrkowska, Nawrot and Henryka Sienkiewicza* (the Plan no. 97).
17. *Resolution no. XLVIII/1228/17 of the City Council of Lodz of 10 May 2017 2017 on the Adoption of a Local Spatial Development Plan for Part of the City of Lodz Located in the Area of Tadeusza Kościuszki and Adama Mickiewicza Avenue and the Following Streets: Andrzeja Struga and Piotrkowska* (the Plan no. 98).
18. *Resolution no. VI/211/19 of the City Council of Lodz of 6 March 2019 on the Adoption of a Local Spatial Development Plan for Part of the City of Lodz Located in the Area of Tadeusz Kościuszki Avenue and the Following Streets: 6 Sierpnia, Generała Lucjana Żeligowskiego, św. Jerzego, Cmentarna, Legionów, Zachodnia and Wólczańska* (the Plan no. 118).
19. *White Paper. Completing the Internal Market: White Paper From the Commission to the European Council*, 1985.
20. Williams K. *Urban form and infrastructure: a morphological review*. Foresight, Government Office for Science [in:] *Future of cities: working paper*. Foresight, Government Office for Science, the UK, 2014.

### *Netography*

European Commission. The European Commission's science and knowledge service. *Projection of Economic impacts of climate change in Sectors of the EU based on bottom-up Analysis (PESETA)*. Source: <https://ec.europa.eu/jrc/en/peseta-iv>

Environmental Protection Agency. *Heat Island Compendium*. Source: <https://www.epa.gov/heat-islands/heat-island-compendium>

European Commission. *European Green Deal, Aspiration to be the first climate neutral continent*. Source: [https://ec.europa.eu/info/strategy/priorities-2019-2024/european-green-deal\\_pl](https://ec.europa.eu/info/strategy/priorities-2019-2024/european-green-deal_pl)

European Commission. *Climate and Energy Policy Framework to 2030. Climate action, 2020*. Source: [https://ec.europa.eu/clima/eu-action/climate-strategies-targets/2030-climate-energy-framework\\_pl](https://ec.europa.eu/clima/eu-action/climate-strategies-targets/2030-climate-energy-framework_pl)

Ministry of Environment of Poland, Department of Sustainable Development and International Cooperation. *CLIMADA. Adapting to climate change*. Source: <http://klimada.mos.gov.pl>

United Nations Population Division. *World Urbanization Prospects: 2018 Revision. Urban population (% of total population)*. Source: <https://data.worldbank.org/indicator/SP.URB.TOTL.IN.ZS>

#### *Data*

*Publicly available measurement and observation data* (<https://danepubliczne.imgw.pl>)

## List of figure captions

<b>Figure 2.1. a.</b> Structure of the atmospheric boundary layer over the city (a) mesoscale; abbreviations: PBL - planetary boundary layer, UBL - urban boundary layer, SL - surface layer).....	- 7 -
<b>Figure 2.1. b-c.</b> Structure of the atmospheric boundary layer over the city (b) local scale; c) microscale; abbreviations: UBL - urban boundary layer, SL - surface layer, RL - friction layer, UCL - roof layer).....	- 8 -
<b>Figure 2.2.</b> Wind profiles.....	- 11 -
<b>Figure 2.3.</b> Breeze circulation over the city .....	- 12 -
<b>Figure 2.4.</b> ASROS center in Fukuoka.....	- 15 -
<b>Figure 2.5.</b> Green roof, Lake Toxaway, NC.....	- 16 -
<b>Figure 2.6.</b> Green wall systems (left - Residential Green Wall, Canaletto, 259 City Road, London; right - Cairo, Egypt).....	- 17 -
<b>Figure 2.7.</b> Potsdamer Platz retention pond.....	- 17 -
<b>Figure 2.8.</b> Bioretention basin at Water Street in Plymouth Center, Massachusetts.....	- 17 -
<b>Figure 2.9.</b> Infiltration trench in Paso Robles, United States .....	- 17 -
<b>Figure 2.10.</b> Bioretention planters in El Cerrito, United States.....	- 17 -
<b>Figure 3.1.</b> Model domain in the ENVI-met application.....	- 38 -
<b>Figure 4.1.</b> Parameters used to determine the Aspect Ratio for asymmetric canyons ..	- 55 -
<b>Figure 4.2.</b> Sky View Factor.....	- 56 -
<b>Figure 4.3.</b> Wall parameters of a building characterized by the Metropolitan Area in Lodz .....	- 60 -
<b>Figure 4.4.</b> Roofing parameters of a building characterized by the Metropolitan Area in Lodz.....	- 60 -
<b>Figure 4.5.</b> The model of the typical canyon in the Metropolitan Area in Lodz.....	- 60 -
<b>Figure. 4.6.</b> Morphological parameters necessary to calculate average building height and site coverage ratio.....	- 62 -
<b>Figure 4.7.</b> Morphological parameters necessary to calculate façade to site ratio .....	- 63 -
<b>Figure 4.8.</b> The model of the typical forecourt in the Metropolitan Area in Lodz.....	- 65 -

<b>Figure 5.1.</b> Frequency of air temperatures for each weather period (Typical Meteorological Year).....	<b>- 69 -</b>
<b>Figure 5.2.</b> Frequency of solar radiation for each weather period (Typical Meteorological Year).....	<b>- 69 -</b>
<b>Figure 5.3.</b> Frequency of relative humidity for each weather period (Typical Meteorological Year).....	<b>- 70 -</b>
<b>Figure 5.4.</b> Frequency of individual wind speed values at 10 m height for each weather period (Typical Meteorological Year).....	<b>- 71 -</b>
<b>Figure 5.5.</b> Frequency of individual wind directions for each weather period (Typical Meteorological Year) .....	<b>- 74 -</b>
<b>Figure 6.1.</b> Geometry of considered urban forms (left column - canyons; right column - forecourts) .....	<b>- 77 -</b>
<b>Figure 6.2.</b> Air temperature in canyons with east-west orientation (top left - at north facade (E-WN); top right - at south facade (E-WS), <b>3 pm</b> ; bottom left - at north facade (E-WN), bottom right - at south facade (E-WS), <b>3 am</b> ).....	<b>- 78 -</b>
<b>Figure 6.3.</b> Surface temperature in canyons with east-west orientation (left - at north facade (E-WN); right - at south facade (E-WS)) .....	<b>- 79 -</b>
<b>Figure 6.4.</b> Airflow in canyons with east-west orientation (left - at north facade (E-WN); right - at south facade (E-WS)) .....	<b>- 80 -</b>
<b>Figure 6.5.</b> Air temperature in canyons with north-south orientation (upper left - at east facade (N-SE); upper right - at west facade (N-SW), <b>3 pm</b> ; lower left - at east facade (N-SE), lower right - at west facade (N-SW), <b>3 am</b> ).....	<b>- 81 -</b>
<b>Figure 6.6.</b> Surface temperature in canyons with north-south orientation (left - at east facade (N-SE); right - at west facade (N-SW)).....	<b>- 82 -</b>
<b>Figure 6.7.</b> Airflow in canyons with north-south orientation (left - at east facade (N-SE); right - at west facade (N-SW)) .....	<b>- 83 -</b>
<b>Figure 6.8.</b> PET in canyons with east-west orientation (top left - at north facade (E-WN); top right - at south facade (E-WS), <b>3 pm</b> ; bottom left - at north facade (E-WN), bottom right - at south facade (E-WS), <b>3 am</b> ).....	<b>- 84 -</b>

<b>Figure 6.9.</b> PET in canyons with north-south orientation (top left - at east facade (N-SE); top right - at west facade (N-SW), <b>3 pm</b> ; bottom left - at east facade (N-SE), bottom right - at west facade (N-SW), <b>3 am</b> ).....	<b>- 86 -</b>
<b>Figure 6.10.</b> Air temperature in forecourts with east-west orientation (left - at the north facade (E-WN), <b>3 pm</b> ; right - at the north facade (E-WN), <b>3 am</b> ).....	<b>- 87 -</b>
<b>Figure 6.11.</b> Surface temperature in forecourts with east-west orientation (left - by north facade (E-WN); right - by south facade (E-WS)).....	<b>- 88 -</b>
<b>Figure 6.12.</b> Air temperature in forecourts with north-south orientation (left - at the eastern facade (N-SE), <b>3 pm</b> ; right - at the eastern facade (N-SE), <b>3 am</b> ).....	<b>- 89 -</b>
<b>Figure 6.13.</b> Pavement temperature in forecourts with north-south orientation (left - at east facade (N-SE); right - at west facade (N-SW)) .....	<b>- 89 -</b>
<b>Figure. 6.14.</b> Effect of building structure on thermal comfort in the east-west oriented forecourt (upper left - E-WN, upper right - E-WS, <b>3 pm</b> ; bottom left - E-WN, bottom right - E-WS, <b>3 am</b> ) .....	<b>- 90 -</b>
<b>Figure. 6.15.</b> Effect of building structure on thermal comfort in the north-south oriented forecourt (upper left - N-SE, upper right - N-SW, <b>3 pm</b> ; bottom left - N-SE, bottom right - N-SW, <b>3 am</b> ) .....	<b>- 91 -</b>
<b>Figure 7.1.</b> Green scenarios in the canyons .....	<b>- 93 -</b>
<b>Figure 7.2.</b> The construction of the green roof.....	<b>- 95 -</b>
<b>Figure 7.3.</b> The construction of the green wall.....	<b>- 95 -</b>
<b>Figure 7.4.</b> Location of E-WN and E-WS measurement points in the street canyon....	<b>- 97 -</b>
<b>Figure 7.5.</b> Impact of green roofs on thermal conditions of the east-west oriented canyon... ..	<b>- 97 -</b>
<b>Figure 7.6.</b> Impact of green walls on thermal conditions of the east-west oriented canyon.. ..	<b>- 98 -</b>
<b>Figure 7.7.</b> Location of E-WN-T and E-WS-T measurement points in the street canyon.... ..	<b>- 99 -</b>
<b>Figure 7.8.</b> Impact of tall greenery on thermal conditions in the east-west oriented canyon (left column - E-WN-T; right column - E-WS-T).....	<b>- 100 -</b>
<b>Figure 7.9.</b> Location of N-SW and N-SE measurement points in the street canyon...-	<b>101 -</b>

<b>Figure 7.10.</b> Impact of green roofs on thermal conditions in the north-south oriented canyon area .....	- 102 -
<b>Figure 7.11.</b> Impact of green walls on thermal conditions in the north-south oriented canyon area .....	- 102 -
<b>Figure 7.12.</b> Location of N-SW-T and N-SE-T measurement points in street canyon.....	- 103 -
<b>Figure 7.13.</b> Impact of tall greenery on thermal conditions of the north-south oriented canyon .....	- 104 -
<b>Figure 7.14.</b> Impact of green solutions on thermal comfort in the east-west oriented canyon (upper left - E-WN, upper right - E-WS, <b>3 pm</b> ; bottom left - E-WN, bottom right - E-WS, <b>3 am</b> ) .....	- 105 -
<b>Figure 7.15.</b> Impact of green solutions on thermal comfort in the north-south oriented canyon (upper left - N-SE, upper right - N-SW, <b>3 pm</b> ; bottom left - N-SE, bottom right - N-SW, <b>3 am</b> ) .....	- 107 -
<b>Figure 7.16.</b> Green scenarios in the forecourts .....	- 108 -
<b>Figure 7.17.</b> Location of E-WN and E-WS measurement points in the urban forecourt.....	- 110 -
<b>Figure 7.18.</b> Impact of green roofs on thermal conditions of the east-west (E-WN) oriented urban forecourt .....	- 110 -
<b>Figure 7.19.</b> Impact of green walls on thermal conditions of the east-west (E-WN) oriented urban forecourt.....	- 111 -
<b>Figure 7.20.</b> Location of N-SW and N-SE measurement points in the urban forecourt.....	- 112 -
<b>Figure 7.21.</b> Impact of green roofs on thermal conditions of the north-south (N-SE) oriented urban forecourt .....	- 113 -
<b>Figure 7.22.</b> Impact of green walls on thermal conditions of the north-south (N-SE) oriented urban forecourt.....	- 114 -
<b>Figure 7.23.</b> Impact of green solutions on thermal comfort in the east-west oriented forecourt (upper left - E-WN, upper right - E-WS, <b>3 pm</b> ; bottom left - E-WN, bottom right - E-WS, <b>3 am</b> ) .....	- 115 -

<b>Figure 7.24.</b> Impact of green solutions on thermal comfort in the north-south oriented forecourt (upper left - N-SE, upper right - N-SW, <b>3 pm</b> ; bottom left - N-SE, bottom right - N-SW, <b>3 am</b> ) .....	- 116 -
<b>Figure 7.25.</b> Blue solutions introduced in the canyons.....	- 117 -
<b>Figure 7.26.</b> The potential constructions of bioretention planters.....	- 118 -
<b>Figure 7.27.</b> Location of E-WN, E-WA, and E-WS measurement points in the street canyon .....	- 119 -
<b>Figure 7.28.</b> Impact of blue solutions on thermal conditions in the east-west oriented canyon (left column - E-WN; right column - E-WA).....	- 119 -
<b>Figure 7.29.</b> Location of N-SW, N-SA, and N-SE points in a street canyon .....	- 120 -
<b>Figure 7.30.</b> Impact of blue solutions on thermal conditions in the north-south oriented canyon (left column - N-SE, <b>3 pm</b> ; right column - N-SE, <b>3 am</b> ).....	- 121 -
<b>Figure 7.31.</b> Impact of blue infrastructure on thermal comfort in the east-west oriented canyon (upper left - E-WN, upper right - E-WS, <b>3 pm</b> ; bottom left - E-WN, bottom right - E-WS, <b>3 am</b> ).....	- 122 -
<b>Figure 7.32.</b> Impact of blue infrastructure on thermal comfort in the north-south oriented canyon (upper left - N-SE, upper right - N-SW, <b>3 pm</b> ; bottom left - N-SE, bottom right - N-SW, <b>3 am</b> ) .....	- 123 -
<b>Figure 7.33.</b> Blue solutions introduced in urban forecourts. ....	- 124 -
<b>Figure 7.34.</b> The construction scheme of water reservoir .....	- 125 -
<b>Figure 7.35.</b> Location of E-WN and E-WS measurement points in the forecourt .....	- 125 -
<b>Figure 7.36.</b> Impact of blue solutions on thermal conditions in the east-west oriented forecourt .....	- 126 -
<b>Figure 7.37.</b> Location of N-SW and N-SE measurement points in the urban forecourt.....	- 126 -
<b>Figure 7.38.</b> Impact of blue solutions on thermal conditions in the north-south oriented forecourt (left column - N-SE, <b>3 pm</b> ; right column - N-SE, <b>3 am</b> ) .....	- 127 -
<b>Figure 7.39.</b> Impact of blue infrastructure on thermal comfort in the east-west oriented forecourt (left - E-WN, <b>3 pm</b> ; right - E-WN, <b>3 am</b> ).....	- 128 -



<b>Figure 7.40.</b> Impact of blue infrastructure on thermal comfort in the north-south oriented forecourt (left - N-SE, 3 pm; right - N-SE, 3 am).....	<b>128</b>
<b>Figure 7.41.</b> Impact of selected adaptation strategies on human thermal sensations in outdoor environments - street canyons.....	<b>138</b>
<b>Figure 7.42.</b> Impact of selected adaptation strategies on human thermal sensation in outdoor environments - urban forecourts.....	<b>143</b>
<b>Figure 8.1.</b> The living room parameters used to create the prototype .....	<b>147</b>
<b>Figure 8.2.</b> The living room model of a residential building in the Metropolitan Area of Lodz.....	<b>147</b>
<b>Figure 8.3.</b> The construction of green roof - RTR2021/GR scenario.....	<b>148</b>
<b>Figure 8.4.</b> The construction of green wall - WTR2021/GR scenario .....	<b>148</b>
<b>Figure 8.5.</b> Simplified representation of the energy balance in the passive construction.....	<b>149</b>
<b>Figure 8.6.</b> Operative temperature (scenarios related to roof structure modification) -	<b>154</b>
<b>Figure 8.7.</b> Operative temperature (scenarios related to modification of living space wall structures) .....	<b>156</b>
<b>Figure 9.1.</b> Air temperature in east-west oriented canyons (the left column), in north-south oriented canyons (the right column), during the warmest day of the Typical Meteorological Year (05.07.2015).....	<b>158</b>
<b>Figure 9.2.</b> PET in east-west oriented canyons (the left column), in north-south oriented canyons (the right column), during the warmest day of the Typical Meteorological Year (05.07.2015) .....	<b>159</b>
<b>Figure 9.3.</b> Air temperature in east-west oriented urban forecourts (the left column), in north-south oriented urban forecourts (the right column), during the warmest day of the Typical Meteorological Year (05.07.2015) .....	<b>161</b>
<b>Figure 9.4.</b> PET in east-west oriented urban forecourts (the left column), in north-south oriented urban forecourts (the right column), during the warmest day of the Typical Meteorological Year (05.07.2015) .....	<b>162</b>
<b>Figure 9.5.</b> Adaptation measures in the east-west oriented canyon (1. green roof, 2. green wall, 3. tall greenery, 4. bioretention planter) .....	<b>167</b>

<b>Figure 9.6.</b> Adaptation measures in the north-south oriented canyon (1. green roof, 2. green wall, 3. tall greenery, 4. bioretention planter) .....	- 169 -
<b>Figure 9.7.</b> Adaptation measures - east-west oriented urban forecourt (1. green roof, 3. blue-green infrastructure) .....	- 171 -
<b>Figure 9.8.</b> Adaptation measures - east-west oriented urban forecourt (1. green roof, 2. green wall, 3. blue-green infrastructure) .....	- 171 -
<b>Figure 9.9.</b> Adaptive measures - north-south oriented urban forecourt (1. green roof, 3. blue infrastructure) .....	- 172 -
<b>Figure 9.10.</b> Adaptive measures - north-south oriented urban forecourt (1. green roof, 2. green wall, 3. blue infrastructure).....	- 173 -

**List of table captions**

<b>Table 2.1.</b> Albedo of city element. ....	- 10 -
<b>Table 2.2.</b> Relationship of meteorological parameters and physical factors according to MEMI model .....	- 22 -
<b>Table 2.3.</b> Thermal comfort indices used in environment studies .....	- 24 -
<b>Table 2.4.</b> PMV scale.....	- 27 -
<b>Table 2.5.</b> PET index scale .....	- 28 -
<b>Table 2.6.</b> UTCI index scale .....	- 30 -
<b>Table 2.7.</b> ASHRAE-55 Thermal Sensation Vote scale (TSV).....	- 31 -
<b>Table 2.8.</b> Broadened Thermal Sensation Vote scale (TSV).....	- 31 -
<b>Table 3.1.</b> Chosen model components .....	- 36 -
<b>Table 3.2.</b> Material parameters .....	- 37 -
<b>Table 3.3.</b> Quantitative chosen measures of the performance of the ENVI-met.....	- 52 -
<b>Table 4.1.</b> Development parameters in the Metropolitan Area.....	- 58 -
<b>Table 4.2.</b> Morphological parameters of development in the Metropolitan Area .....	- 64 -
<b>Table 5.1.</b> Typical Meteorological Year .....	- 68 -
<b>Table 5.2.</b> Wind speeds in the suburban area and their values in the Metropolitan Area.....	- 73 -

<b>Table 5.3.</b> The warmest day of a Typical Meteorological Year. ....	<b>- 75 -</b>
<b>Table 7.1.</b> Impact of green roofs on air temperature in canyons. ....	<b>- 131 -</b>
<b>Table 7.2.</b> Impact of green walls on air temperature in canyons .....	<b>- 132 -</b>
<b>Table 7.3.</b> Impact of trees on air temperature in canyons.....	<b>- 134 -</b>
<b>Table 7.4.</b> Impact of blue infrastructure on air temperature in canyons.....	<b>- 136 -</b>
<b>Table 7.5.</b> Impact of green roofs on air temperature in urban forecourts.....	<b>- 140 -</b>
<b>Table 7.6.</b> Impact of green walls on air temperature in urban forecourts.....	<b>- 141 -</b>
<b>Table 7.7.</b> Impact of blue infrastructure on air temperature in urban forecourts.....	<b>- 142 -</b>
<b>Table 8.1.</b> Parameters of computational models of the applied adaptation strategies (roof). .....	<b>- 151 -</b>
<b>Table 8.2.</b> Parameters of computational models of the applied adaptation strategies (outer wall).....	<b>- 152 -</b>
<b>Table 9.1.</b> Study of the influence of green roof construction on the thermal comfort of building occupants.....	<b>- 164 -</b>
<b>Table 9.2.</b> Study of the influence of green wall construction on the thermal comfort of building occupants.....	<b>- 165 -</b>

## Appendixes

**Appendix 1.** Statistical distribution of air temperature (Typical Meteorological Year).

AIR TEMPERATURE				
RANGE	NUMBER OF HOURS	FREQUENCY	CUMULATIVE NUMBER OF HOURS	CUMULATED FREQUENCY
<b>SPRING</b>				
(-5.00) °C - 0.00 °C	11	1,39	11	1,39
0.00 °C - 5.00 °C	158	19,95	169	21,34
5.00 °C - 10.00 °C	318	40,15	487	61,49
10.00 °C - 15.00 °C	205	25,88	692	87,37
15.00 °C - 20.00 °C	82	10,35	774	97,73
20.00 °C - 25.00 °C	16	2,02	790	99,75
25.00 °C - 30.00 °C	2	0,25	792	100,00
<b>SUMMER</b>				
0.00 °C - 5.00 °C	2	0,06	2	0,06
5.00 °C - 10.00 °C	44	1,26	46	1,32
10.00 °C - 15.00 °C	329	9,45	375	10,78
15.00 °C - 20.00 °C	1151	33,07	1526	43,85
20.00 °C - 25.00 °C	1095	31,47	2621	75,32
25.00 °C - 30.00 °C	602	17,30	3223	92,61
30.00 °C - 35.00 °C	209	6,01	3432	98,62
35.00 °C - 40.00 °C	48	1,38	3480	100,00
<b>AUTUMN</b>				
0.00 °C - 5.00 °C	20	1,74	20	1,74
5.00 °C - 10.00 °C	178	15,45	198	17,19
10.00 °C - 15.00 °C	511	44,36	709	61,55
15.00 °C - 20.00 °C	306	26,56	1015	88,11
20.00 °C - 25.00 °C	97	8,42	1112	96,53
25.00 °C - 30.00 °C	40	3,47	1152	100,00
<b>WINTER</b>				
(-15.00) °C - (-10.00) °C	1	0,03	1	0,03
(-10.00) °C - (-5.00) °C	112	3,33	113	3,36
(-5.00) °C - 0.00 °C	240	7,14	353	10,51
0.00 °C - 5.00 °C	960	28,57	1313	39,08
5.00 °C - 10.00 °C	1350	40,18	2663	79,26
10.00 °C - 15.00 °C	528	15,71	3191	94,97
15.00 °C - 20.00 °C	137	4,08	3328	99,05
20.00 °C - 25.00 °C	29	0,86	3357	99,91
30.00 °C - 35.00 °C	3	0,09	3360	100,00

**Appendix 2.** Statistical distribution of global solar radiation (Typical Meteorological Year).

GLOBAL SOLAR RADIATION				
RANGE	NUMBER OF HOURS	FREQUENCY	CUMULATIVE NUMBER OF HOURS	CUMULATED FREQUENCY
<b>SPRING</b>				
0 - 100 W/m <sup>2</sup>	469	59,22	469	59,22
100 - 200 W/m <sup>2</sup>	78	9,85	547	69,07

**Appendix 2.** Continuation.

<b>GLOBAL SOLAR RADIATION</b>				
<b>RANGE</b>	<b>NUMBER OF HOURS</b>	<b>FREQUENCY</b>	<b>CUMULATIVE NUMBER OF HOURS</b>	<b>CUMULATED FREQUENCY</b>
<b>SPRING</b>				
200 - 300 W/m <sup>2</sup>	50	6,31	597	75,38
300 - 400 W/m <sup>2</sup>	41	5,18	638	80,56
400 - 500 W/m <sup>2</sup>	52	6,57	690	87,12
500 - 600 W/m <sup>2</sup>	43	5,43	733	92,55
600 - 700 W/m <sup>2</sup>	40	5,05	773	97,60
700 - 800 W/m <sup>2</sup>	19	2,40	792	100,00
<b>SUMMER</b>				
0 - 100 W/m <sup>2</sup>	1830	52,59	1830	52,59
100 - 200 W/m <sup>2</sup>	341	9,80	2171	62,39
200 - 300 W/m <sup>2</sup>	295	8,48	2466	70,86
300 - 400 W/m <sup>2</sup>	256	7,36	2722	78,22
400 - 500 W/m <sup>2</sup>	220	6,32	2942	84,54
500 - 600 W/m <sup>2</sup>	236	6,78	3178	91,32
600 - 700 W/m <sup>2</sup>	158	4,54	3336	95,86
700 - 800 W/m <sup>2</sup>	108	3,10	3444	98,97
800 - 900 W/m <sup>2</sup>	34	0,98	3478	99,94
900 - 1000 W/m <sup>2</sup>	2	0,06	3480	100,00
<b>AUTUMN</b>				
0 - 100 W/m <sup>2</sup>	889	77,17	889	77,17
100 - 200 W/m <sup>2</sup>	108	9,38	997	86,55
200 - 300 W/m <sup>2</sup>	65	5,64	1062	92,19
300 - 400 W/m <sup>2</sup>	48	4,17	1110	96,35
400 - 500 W/m <sup>2</sup>	38	3,30	1148	99,65
500 - 600 W/m <sup>2</sup>	4	0,35	1152	100,00
<b>WINTER</b>				
0 - 100 W/m <sup>2</sup>	2874	85,54	2874	85,54
100 - 200 W/m <sup>2</sup>	270	8,04	3144	93,57
200 - 300 W/m <sup>2</sup>	106	3,15	3250	96,73
300 - 400 W/m <sup>2</sup>	51	1,52	3301	98,24
400 - 500 W/m <sup>2</sup>	42	1,25	3343	99,49
500 - 600 W/m <sup>2</sup>	17	0,51	3360	100,00

**Appendix 3.** Statistical distribution of relative humidity (Typical Meteorological Year).

<b>RELATIVE HUMIDITY</b>				
<b>RANGE</b>	<b>NUMBER OF HOURS</b>	<b>FREQUENCY</b>	<b>CUMULATIVE NUMBER OF HOURS</b>	<b>CUMULATED FREQUENCY</b>
<b>SPRING</b>				
20% - 30%	32	4,04	32	4,04
30% - 40%	93	11,74	125	15,78
40% - 50%	91	11,49	216	27,27
50% - 60%	84	10,61	300	37,88
60% - 70%	90	11,36	390	49,24

**Appendix 3.** Continuation.

<b>RELATIVE HUMIDITY</b>				
<b>RANGE</b>	<b>NUMBER OF HOURS</b>	<b>FREQUENCY</b>	<b>CUMULATIVE NUMBER OF HOURS</b>	<b>CUMULATED FREQUENCY</b>
<b>SPRING</b>				
70% - 80%	118	14,90	508	64,14
80% - 90%	140	17,68	648	81,82
90% - 100%	144	18,18	792	100,00
<b>SUMMER</b>				
20% - 30%	3	0,11	3	0,11
30% - 40%	78	2,81	81	2,92
40% - 50%	242	8,72	323	11,64
50% - 60%	458	16,51	781	28,15
60% - 70%	507	18,28	1288	46,43
70% - 80%	422	15,21	1710	61,64
80% - 90%	484	17,45	2194	79,09
90% - 100%	580	20,91	2774	100,00
<b>AUTUMN</b>				
40% - 50%	1	0,14	1	0,14
50% - 60%	38	5,31	39	5,45
60% - 70%	63	8,81	102	14,27
70% - 80%	84	11,75	186	26,01
80% - 90%	204	28,53	390	54,55
90% - 100%	325	45,45	715	100,00
<b>WINTER</b>				
30% - 40%	5	0,26	5	0,26
40% - 50%	26	1,35	31	1,61
50% - 60%	67	3,48	98	5,08
60% - 70%	100	5,19	198	10,27
70% - 80%	253	13,12	451	23,39
80% - 90%	568	29,46	1019	52,85
90% - 100%	909	47,15	1928	100,00

**Appendix 4.** Statistical distribution of wind speed at a height of 10 m (Typical Meteorological Year).

<b>WIND SPEED AT A HEIGHT OF 10 M</b>				
<b>RANGE</b>	<b>NUMBER OF HOURS</b>	<b>FREQUENCY</b>	<b>CUMULATIVE NUMBER OF HOURS</b>	<b>CUMULATED FREQUENCY</b>
<b>SPRING</b>				
0 m/s - 1 m/s	108	13,64	108	13,64
1 m/s - 2 m/s	108	13,64	216	27,27
2 m/s - 3 m/s	144	18,18	360	45,45
3 m/s - 4 m/s	182	22,98	542	68,43
4 m/s - 5 m/s	136	17,17	678	85,61
5 m/s - 6 m/s	67	8,46	745	94,07
6 m/s - 7 m/s	32	4,04	777	98,11
7 m/s - 8 m/s	13	1,64	790	99,75
8 m/s - 9 m/s	1	0,13	791	99,87
9 m/s - 10 m/s	1	0,13	792	100,00

**Appendix 4.** Continuation.

<b>WIND SPEED AT A HEIGHT OF 10 M</b>				
<b>RANGE</b>	<b>NUMBER OF HOURS</b>	<b>FREQUENCY</b>	<b>CUMULATIVE NUMBER OF HOURS</b>	<b>CUMULATED FREQUENCY</b>
<b>SUMMER</b>				
0 m/s - 1 m/s	711	20,43	711	20,43
1 m/s - 2 m/s	721	20,72	1432	41,15
2 m/s - 3 m/s	689	19,80	2121	60,95
3 m/s - 4 m/s	547	15,72	2668	76,67
4 m/s - 5 m/s	386	11,09	3054	87,76
5 m/s - 6 m/s	208	5,98	3262	93,74
6 m/s - 7 m/s	134	3,85	3396	97,59
7 m/s - 8 m/s	53	1,52	3449	99,11
8 m/s - 9 m/s	28	0,80	3477	99,91
9 m/s - 10 m/s	2	0,06	3479	99,97
10 m/s - 11 m/s	1	0,03	3480	100,00
<b>AUTUMN</b>				
0 m/s - 1 m/s	201	17,45	201	17,45
1 m/s - 2 m/s	203	17,62	404	35,07
2 m/s - 3 m/s	238	20,66	642	55,73
3 m/s - 4 m/s	189	16,41	831	72,14
4 m/s - 5 m/s	141	12,24	972	84,38
5 m/s - 6 m/s	94	8,16	1066	92,53
6 m/s - 7 m/s	57	4,95	1123	97,48
7 m/s - 8 m/s	22	1,91	1145	99,39
8 m/s - 9 m/s	4	0,35	1149	99,74
9 m/s - 10 m/s	2	0,17	1151	99,91
10 m/s - 11 m/s	0	0,00	1151	99,91
11 m/s - 12 m/s	0	0,00	1151	99,91
12 m/s - 13 m/s	0	0,00	1151	99,91
13 m/s - 14 m/s	1	0,09	1152	100,00
<b>WINTER</b>				
0 m/s - 1 m/s	369	10,98	369	10,98
1 m/s - 2 m/s	482	14,35	851	25,33
2 m/s - 3 m/s	621	18,48	1472	43,81
3 m/s - 4 m/s	590	17,56	2062	61,37
4 m/s - 5 m/s	536	15,95	2598	77,32
5 m/s - 6 m/s	336	10,00	2934	87,32
6 m/s - 7 m/s	236	7,02	3170	94,35
7 m/s - 8 m/s	109	3,24	3279	97,59
8 m/s - 9 m/s	51	1,52	3330	99,11
9 m/s - 10 m/s	17	0,51	3347	99,61
10 m/s - 11 m/s	9	0,27	3356	99,88
11 m/s - 12 m/s	3	0,09	3359	99,97
12 m/s - 13 m/s	1	0,03	3360	100,00

**Appendix 5.** Wind direction statistical distribution (Typical Meteorological Year).

DIRECTION	RANGE	SPRING		SUMMER		AUTUMN		WINTER	
		NUMBER OF HOURS	FREQUENCY	NUMBER OF HOURS	FREQUENCY	NUMBER OF HOURS	FREQUENCY	NUMBER OF HOURS	FREQUENCY
N	0 °	51	6,44	220	6,32	103	8,94	157	4,67
	10 °	14	1,77	25	0,72	7	0,61	45	1,34
	20 °	29	3,66	32	0,92	2	0,17	33	0,98
NE	30 °	26	3,28	32	0,92	0	0,00	21	0,63
	40 °	23	2,90	29	0,83	3	0,26	19	0,57
	50 °	24	3,03	47	1,35	3	0,26	16	0,48
	60 °	27	3,41	61	1,75	4	0,35	27	0,80
E	70 °	22	2,78	57	1,64	2	0,17	42	1,25
	80 °	22	2,78	94	2,70	21	1,82	72	2,14
	90 °	32	4,04	124	3,56	62	5,38	186	5,54
	100 °	31	3,91	140	4,02	91	7,90	193	5,74
	110 °	19	2,40	98	2,82	47	4,08	114	3,39
SE	120 °	17	2,15	79	2,27	31	2,69	62	1,85
	130 °	7	0,88	85	2,44	24	2,08	55	1,64
	140 °	16	2,02	62	1,78	14	1,22	41	1,22
	150 °	8	1,01	46	1,32	13	1,13	31	0,92
S	160 °	7	0,88	47	1,35	27	2,34	33	0,98
	170 °	7	0,88	50	1,44	31	2,69	50	1,49
	180 °	14	1,77	54	1,55	28	2,43	80	2,38
	190 °	18	2,27	76	2,18	42	3,65	100	2,98
	200 °	19	2,40	61	1,75	32	2,78	104	3,10
SW	210 °	31	3,91	73	2,10	54	4,69	146	4,35
	220 °	17	2,15	112	3,22	83	7,20	169	5,03
	230 °	22	2,78	121	3,48	64	5,56	155	4,61
	240 °	23	2,90	144	4,14	61	5,30	176	5,24
W	250 °	26	3,28	172	4,94	78	6,77	255	7,59
	260 °	54	6,82	197	5,66	63	5,47	208	6,19
	270 °	44	5,56	210	6,03	47	4,08	186	5,54
	280 °	27	3,41	189	5,43	30	2,60	117	3,48
	290 °	19	2,40	159	4,57	25	2,17	116	3,45
NW	300 °	26	3,28	160	4,60	16	1,39	117	3,48
	310 °	17	2,15	110	3,16	14	1,22	69	2,05
	320 °	16	2,02	102	2,93	17	1,48	50	1,49
	330 °	9	1,14	88	2,53	7	0,61	42	1,25
N	340 °	16	2,02	66	1,90	2	0,17	35	1,04
	350 °	12	1,52	58	1,67	4	0,35	38	1,13



**Appendix 6.** Influence of green roofs on the thermals of the east-west canyon.

Air temperature in the canyon with an east-west orientation [°C]								
Height (m)	BC		GR		GR2		GR3	
	day	night	day	night	day	night	day	night
<b>E-WN</b>								
<b>1.5m</b>	34.65	17.53	34.62	17.52	34.23	18.16	34.18	18.16
<b>5.5m</b>	33.73	17.84	33.68	17.84	33.32	18.54	33.25	18.53
<b>15.5m</b>	32.67	19.70	32.54	19.67	32.17	20.38	32.04	20.34

**Appendix 7.** The influence of green walls on the thermal conditions of the canyon with an east-west orientation.

Air temperature in the canyon with an east-west orientation [°C]								
Height (m)	BC		W		W2		W3	
	day	night	day	night	day	night	day	night
<b>E-WN</b>								
<b>1.5m</b>	34.65	17.53	34.25	18.08	34.27	18.06	33.89	18.04
<b>5.5m</b>	33.73	17.84	33.33	18.46	33.35	18.43	33.12	18.49
<b>15.5m</b>	32.67	19.70	32.28	20.40	32.28	20.39	32.19	20.59

**Appendix 8.** The influence of high greenery on the thermal conditions in the canyon with an east-west orientation.

Air temperature in the canyon with an east-west orientation [°C]								
Height (m)	BC		T		T2		T3	
	day	night	day	night	day	night	day	night
<b>E-WN-T</b>								
<b>ST</b>	41.77	18.26	40.22	18.52	40.20	18.45	40.16	18.46
<b>1.5m</b>	34.65	17.53	34.02	18.34	33.99	18.23	33.89	18.19
<b>5.5m</b>	33.73	17.84	33.14	18.66	33.11	18.59	33.00	18.55
<b>15.5m</b>	32.67	19.70	32.20	20.36	32.18	20.39	32.14	20.37
<b>E-WS-T</b>								
<b>ST</b>	32.60	18.26	31.11	18.49	31.04	18.42	30.79	18.42
<b>1.5m</b>	33.54	17.49	32.88	18.32	32.84	18.20	32.73	18.16
<b>5.5m</b>	33.23	17.84	32.65	18.66	32.61	18.59	32.53	18.54
<b>15.5m</b>	32.60	19.71	32.12	20.37	32.11	20.41	32.07	20.40
<b>ST</b> – surface temperature [°C]								

**Appendix 9.** The influence of green roofs on the thermal conditions in the canyon with a north-south orientation.

Air temperature in the canyon with a north-south orientation [°C]								
Height (m)	BC		GR		GR2		GR3	
	day	night	day	night	day	night	day	night
N-SE								
1.5m	33.57	18.96	32.92	19.33	33.01	19.35	32.81	19.31
5.5m	33.43	18.93	32.70	19.26	32.83	19.29	32.61	19.25
15.5m	32.99	18.45	32.19	19.07	32.43	19.09	32.17	19.07

**Appendix 10.** The influence of green walls on the thermal conditions in the canyon with a north-south orientation.

Air temperature in the canyon with a north-south orientation [°C]								
Height (m)	BC		W		W2		W3	
	day	night	day	night	day	night	day	night
N-SE								
1.5m	33.57	18.96	33.22	19.28	33.22	19.28	33.33	19.26
5.5m	33.43	18.93	33.02	19.22	33.02	19.22	33.10	19.20
15.5m	32.99	18.45	32.45	19.06	32.45	19.06	32.49	19.07

**Appendix 11.** The influence of high greenery on the thermal conditions of the canyon with a north-south orientation.

Air temperature in the canyon with a north-south orientation [°C]								
Height (m)	BC		T		T2		T3	
	day	night	day	night	day	night	day	night
N-SE-T								
ST	39.65	18.92	38.31	18.69	38.30	18.71	38.20	18.74
1.5m	33.57	18.96	32.91	19.22	32.90	19.27	32.85	19.31
5.5m	33.43	18.93	32.79	19.25	32.77	19.33	32.74	19.23
15.5m	32.99	18.45	32.37	19.71	32.29	20.62	32.36	19.76
N-SW-T								
ST	35.46	18.95	33.42	18.65	33.39	18.65	33.23	18.67
1.5m	33.36	18.97	32.71	19.33	32.70	19.40	32.65	19.31
5.5m	33.27	18.96	32.64	19.42	32.62	19.55	32.59	19.41
15.5m	32.83	18.77	32.27	19.82	32.24	20.46	32.25	19.85
ST – surface temperature [°C]								

**Appendix 12.** Influence of green roofs on the thermals of the forecourt with an east-west orientation.

Air temperature in the forecourt with an east-west orientation [°C]								
Height (m)	BC		FGR		FGR2		FGR3	
	day	night	day	night	day	night	day	night
E-WN								
1.5m	32.71	19.62	32.40	19.62	32.39	19.62	32.27	19.61
5.5m	32.56	19.67	32.30	19.67	32.30	19.67	32.18	19.66
15.5m	32.15	20.15	32.02	20.15	32.02	20.15	31.89	20.14

**Appendix 13.** Influence of green walls on the thermals of the forecourt with an east-west orientation.

Air temperature in the forecourt with an east-west orientation [°C]								
Height (m)	BC		FW		FW2		FW3	
	day	night	day	night	day	night	day	night
E-WN								
1.5m	32.71	19.62	32.54	19.63	32.56	19.62	32.66	19.47
5.5m	32.56	19.67	32.44	19.69	32.46	19.68	32.55	19.56
15.5m	32.15	20.15	32.11	20.17	32.12	20.17	32.14	20.16

**Appendix 14.** Influence of green roofs on the thermals of the forecourt with a north-south orientation.

Air temperature in the forecourt with a north-south orientation [°C]								
Height (m)	BC		FGR		FGR2		FGR3	
	day	night	day	night	day	night	day	night
N-SE								
1.5m	32.68	19.04	32.55	18.86	32.53	18.85	32.37	18.81
5.5m	32.65	19.05	32.53	18.86	32.51	18.86	32.34	18.81
15.5m	32.48	19.14	32.37	19.00	32.37	19.00	32.20	18.96

**Appendix 15.** Influence of green walls on the thermals of the forecourt with a north-south orientation.

Air temperature in the forecourt with a north-south orientation [°C]								
Height (m)	BC		FW		FW2		FW3	
	day	night	day	night	day	night	day	night
N-SE								
1.5m	32.68	19.04	32.61	18.83	32.63	18.81	32.74	18.57
5.5m	32.65	19.05	32.58	18.84	32.60	18.82	32.70	18.59
15.5m	32.48	19.14	32.38	18.99	32.39	18.99	32.42	18.97

**Appendix 16.** The influence of blue solutions on the thermal conditions in the east-west orientation canyon.

Air temperature in the canyon with an east-west orientation [°C]						
Height (m)	BC		BP		BP2	
	day	night	day	night	day	night
<b>E-WN</b>						
1.5m	34.65	17.53	32.72	18.52	32.72	18.22
5.5m	33.73	17.84	32.58	18.89	32.58	18.71
15.5m	32.67	19.70	32.06	20.52	32.06	20.56
<b>E-WA</b>						
1.5m	34.64	17.37	33.62	18.45	33.62	18.10
5.5m	33.52	17.92	32.87	18.90	32.87	18.71
15.5m	32.61	20.09	32.07	20.60	32.07	20.72

**Appendix 17.** The influence of blue solutions on thermal conditions in the canyon with a north-south orientation.

Air temperature in the canyon with a north-south orientation [°C]						
Height (m)	BC		BP		BP2	
	day	night	day	night	day	night
<b>N-SE</b>						
1.5m	33.57	18.96	32.70	19.44	32.66	19.44
5.5m	33.43	18.93	32.63	19.55	32.59	19.55
15.5m	32.99	18.45	32.24	20.42	32.22	20.42
<b>N-SA</b>						
1.5m	33.46	18.98	32.79	19.44	32.75	19.44
5.5m	33.34	18.95	32.70	19.57	32.66	19.57
15.5m	32.89	18.65	32.26	20.55	32.24	20.55

**Appendix 18.** The influence of blue solutions on the thermal conditions in the forecourt with an east-west orientation.

Air temperature in the forecourt with an east-west orientation [°C]						
Height (m)	BC		WR		WR2	
	day	night	day	night	day	night
<b>E-WN</b>						
1.5m	32.71	19.62	32.67	19.58	32.65	19.57
5.5m	32.56	19.67	32.54	19.63	32.52	19.63
15.5m	32.15	20.15	32.14	20.10	32.13	20.09

**Appendix 19.** The influence of blue solutions on thermal conditions in the forecourt with a north-south orientation.

Air temperature in the forecourt with a north-south orientation [°C]						
Height (m)	BC		WR		WR2	
	day	night	day	night	day	night
N-SE						
1.5m	32.68	19.04	32.63	19.03	32.61	19.02
5.5m	32.65	19.05	32.61	19.04	32.59	19.03
15.5m	32.48	19.14	32.47	19.14	32.46	19.13